CR-115712

LMSC-D266204
1 MAR 1972

SHUTTLE

FINAL REPORT

IMPROVEMENT OF REUSABLE SURFACE INSULATION MATERIAL

Contract NAS9-12137

National Aeronautics and Space Administration
Manned Spacecraft Center

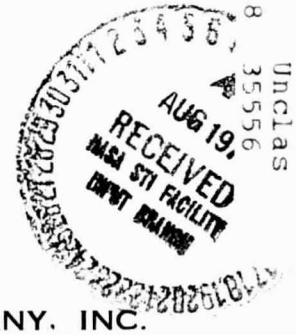

LOCKHEED MISSILES & SPACE COMPANY, INC.
A SUBSIDIARY OF LOCKHEED AIRCRAFT CORPORATION
SPACE SYSTEMS DIVISION • SUNNYVALE, CALIFORNIA

LMSC-D266204
1 MAR 1972

FINAL REPORT

IMPROVEMENT OF REUSABLE SURFACE INSULATION MATERIAL

Contract NAS9-12137

National Aeronautics and Space Administration
Manned Spacecraft Center

LOCKHEED MISSILES & SPACE COMPANY, INC.
A SUBSIDIARY OF LOCKHEED AIRCRAFT CORPORATION
SPACE SYSTEMS DIVISION • SUNNYVALE, CALIFORNIA

ABSTRACT/FOREWORD

This final report presents the results of NASA Contract NAS 9-12137, "Improvement of Reusable Surface Insulation Material," performed by Lockheed Missiles & Space Company, Inc., for the National Aeronautics and Space Administration, Manned Spacecraft Center, under the direction of the Materials Technology Branch of the Structures and Mechanics Division, I. K. Spiker, COR.

The objective of the contract was to improve the rigid surface insulation (RSI) system through the improvement of the LI-1500 material properties and the simplification of the RSI system. This program was coordinated with Contract NAS 9-12083 "Space Shuttle Thermal Protection System Development" for ensuring maximum mutual benefits to the shuttle TPS effort. The results generated for the contract effort are documented.

Through this contract, improvements have been made that impact the current TPS RSI design and are applicable to future designs. These improvements include: 2500°F-capability RSI systems, water-impervious surface coatings, establishment of a high-emittance coating constituent, development of a secondary water-reduction system, and achievement of a lower density (9 pcf) RSI material.

CONTENTS

Section		Page
	ABSTRACT/FOREWORD	iii
	ILLUSTRATIONS	vii
	TABLES	xi
1	INTRODUCTION	1.1-1
2	SUMMARY OF ACCOMPLISHMENTS	2-1
3	TECHNICAL PROGRAM	3-1
	3.1 Baseline Material For Comparison	3.1-1
	3.2 Study Requirements	3.2-1
	3.2.1 Material Analysis Techniques and Test Methods	3.2-6
	3.2.2 Study Results	3.2-13
	3.3 Development Requirements	3.3-1
	3.3.1 FI-600 Joint Closure Material	3.3-1
	3.3.2 Repair Technique for Coated LI-1500 Tile	3.3-4
	3.3.3 Elimination of Substrate Investigation	3.3-7
	3.3.4 Strengthening Attachment Interface	3.3-7
	3.3.5 Mechanical Attachment	3.3-10
	3.4 Coating Investigation	3.4-1
	3.4.1 Emissivity Investigations	3.4-3
	3.4.2 Integral Coating Investigation	3.4-27
	3.4.3 Improved Coating	3.4-40
	3.5 Moisture Reduction Technique and Vehicle Effects	3.5-1
	3.5.1 Investigation of Candidate Materials	3.5-2
	3.5.2 Selection of Material for Water Reduction	3.5-4
	3.6 Thermal Conductivity Investigations	3.6-1
	3.6.1 Infrared Transparency Reduction	3.6-1
	3.6.2 Lower Density Material	3.6-11

Section		Page
3.7	Material Property Determination	3.7-1
	3.7.1 LI-1500/0042 Material Properties	3.7-2
	3.7.2 LI-0900/0045 Material Properties	3.7-37
	3.7.3 LMSC RSI Batch-to-Batch Reproducibility	3.7-43

ILLUSTRATIONS

Figure		Page
1-1	Master Schedule	1.1-2
3-1	Program Overview	3-1
3.2-1	Thermal Expansion of Silica Materials	3.2-2
3.2-2	Thermal Expansion of Refractory Oxides	3.2-2
3.2.1.2-1	Test Setup – Furnace Testing of LI-1500 – Normal Atmosphere	3.2-12
3.2.2.1-1	Hot-Stage X-Ray Diffraction of Study Fiber Lots	3.2-15
3.2.2.1-2	Hot-Stage X-Ray Diffraction Study Lot 1213 Fiber	3.2-15
3.2.2.1-3	Fiber Characterization Influence of Thermal Exposure	3.2-17
3.2.2.1-4	Fiber Characterization Influence of Thermal Exposure	3.2-18
3.2.2.1-5	Fiber Characterization Influence of Thermal Exposure	3.2-19
3.2.2.1-6	Fiber Characterization Influence of Thermal Exposure	3.2-20
3.2.2.1-7	Fiber Characterization Influence of Thermal Exposure	3.2-21
3.2.2.1-8	Fiber Characterization Influence of Thermal Exposure	3.2-22
3.2.2.1-9	Effect of Isothermal Exposure at 2500 °F – Morphology Change Fiber Lot 2089	3.2-23
3.2.2.1-10	Effect of Isothermal Exposure at 2500° F – Morphology Change Fiber Lot 2089	3.2-23
3.2.2.1-11	Effect of Isothermal Exposure at 2500° F – Morphology Change Fiber Lot 2089	3.2-24
3.2.2.1-12	Effect of Isothermal Exposure at 2500° F – Morphology Change Fiber Lot 2089	3.2-24
3.2.2.1-13	Effect of Isothermal Treatment at 2200° F on Fiber Total Crystallinity, Fiber Lot 1213	3.2-27
3.2.2.1-14	Effect of Isothermal Treatment at 2200° F on Fiber Crystallinity, Fiber Lot 1213	3.2-28
3.2.2.1-15	Effect of Isothermal Treatment at 2300° F and 2500° F on Fiber Crystallinity, Fiber Lots 2089 and 2086	3.2-30
3.2.2.2-1	Effect of Isothermal Treatment on Total Crystallinity of LI-1500 Material (Fiber Lot 1213)	3.2-33

Figure		Page
3.2.2.2-2	The Effect of Isothermal Treatment on Crystallinity of LI-1500 (Improved Fiber Lot 2089)	3.2-34
3.2.2.3-1	Temperature Profile – Furnace Heated LI-1500 Model, 2 in. x 2 in. x 2 in.	3.2-36
3.2.2.3-2	Effect of Chemical Treatment (Fiber Lot 2086) – As Received, Left, and Acid, Right	3.2-43
3.3.1-1	FI-666 Joint Strip	3.3-3
3.3.1-2	Repair Sequence for Damaged RSI Tile	3.3-5
3.3.1.3-1	Flexural Properties as a Function of Density for LI-1500 Type Material – Resin Impregnated	3.3-9
3.3.1.3-2	Attachment Surface Strengthening Concept Evaluation Test	3.3-11
3.3.1.3-3	Test Results – Mechanical Fastener With Local Reinforcement	3.3-12
3.4.1-1	Effect of Emittance on Equilibrium Surface Temperature for a Given Heat Flux	3.4-5
3.4.1-2	Spectral Energy Distribution of Blackbody at Various Temperatures	3.4-6
3.4.1-3	Spectral Reflectance (at 75° F) of Three SiC/Borosilicate Coatings With Various Concentrations of SiC	3.4-17
3.4.1-4	Spectral Reflectance of Three SiC/Borosilicate Coatings With Various SiC Grit Sizes	3.4-18
3.4.1-5	Change in Spectral Reflectance of 0042 Coating After Exposure to 2,300° F at 10 Torr for 4 hr	3.4-19
3.4.1-6	Spectral Reflectance of Borosilicate Coatings at Three Temperatures	3.4-21
3.4.1-7	Comparative Spectral Reflectance: New 0042 and 0045 Versus Old 0025	3.4-23
3.4.1-8	Predicted Total Normal Emittance Values: New Coatings Versus Old 0025 as a Function of Temperature	3.4-24
3.4.1-9	Emissivity Constituent Materials (Exposed 4 hr at 2,300° F)	3.4-26
3.4.2-1	Integral Coatings Typical Density Gradients	3.4-28
3.4.2-2	Flexural Test Method	3.4-30
3.4.2-3	Flexural Properties as a Function of Density	3.4-30
3.4.2-4	SEM Photograph (500X & 2000X) Silica Densified LI-1500 Surface	3.4-39
3.4.3-1	Strain Relief Coating Surface Patterns	3.4-42
3.4.3-2	Texture Coating Study – Computer Modeling	3.4-43

Figure		Page
3.4.3-3	Variation of Coating Stress with Number of Coating Discontinuities	3.4-45
3.4.3-4	Thermal Expansion of Lithium-Aluminum Silicate Systems	3.4-49
3.4.3-5	Identical Coatings With and Without Dense Silica Substrate	3.4-51
3.4.3-6	System $Li_2OAl_2O_32SiO_2$ (Eucryptite) – SiO	3.4-53
3.4.3-7	Sintered-on Identification Marking	3.4-59
3.4.3-8	Borosilicate Coating After 4 hr, 2300° F at 10 Torr Vacuum	3.4-59
3.4.3-9	Photomicrographs of LI-0042 Surface Coating	3.4-60
3.4.3-10	Photomicrographs (100X) Illustrating Cross Section of LI-0042 Surface Coating	3.4-61
3.4.3-11	0042 Oversprayed With Coatings of Various Refractoriness	3.4-63
3.4.3-12	Cross-Section View of LI-0045 Coating (100X)	3.4-65
3.4.3-13	Photomicrographs (28X) of LI-0045 Coating After Isothermal Exposures at 2,500° F	3.4-66
3.5-1	Water Reduction Technique – Water Droplet Evaluation	3.5-6
3.5-2	Time/Temperature Water Repellency Evaluation	3.5-17
3.6.1-1	Optical System Schematic for Spectral Total Transmittance Measurements	3.6-2
3.6.1-2	Optical System Schematic for Spectral Normal Transmittance Measurements in Infrared	3.6-5
3.6.1-3	Spectral Transmittance of LI-1500 With Various Opacifiers (0.040-in. Thickness)	3.6-6
3.6.1-4	Influence of LI-1500 Thickness on Spectral Transmittance (Total)	3.6-8
3.6.1-5	Spectral Total Transmittance of Low-Density Fibrous Insulations at 0.160 in.	3.6-9
3.6.2-1	Shear-Loading Geometry	3.6-13
3.7.1-1	Sketch of Mechanical Property Test Specimens	3.7-2
3.7.1.1-1	Test Fixture for Tensile Tests of LI-1500 (Room Temperature and -150° F)	3.7-3
3.7.1.1-2	Test Fixture for Compression Tests of LI-1500	3.7-3
3.7.1.1-3	Shear Test Specimens and Mounting Plates	3.7-4
3.7.1.1-4	Schematic of Coating Test Apparatus	3.7-5
3.7.1.1-5	Oven Thermal Cycle for Thermal Degradation Tests	3.7-5
3.7.1.2-1	Comparison of Design Curves with Recent Thermal Conductivity Data	3.7-15

Figure		Page
3.7.1.2-2	Variation of LI-1500 Thermal Conductivity With Temperature and Pressure	3.7-15
3.7.2.2-1	LI-0900 Thermal Conductivity Test Data	3.7-40
3.7.4-1	Hot-Stage X-Ray Diffraction Analysis	3.7-45

TABLES

Table		Page
3.1-1	LI-1500 Baseline Material for Comparison	3.1-1
3.1-2	L-0025 Baseline Coating for Comparison	3.1-4
3.2-1	Densities of Common Forms of Silica	3.2-1
3.2.2.1-1	Chemical Analysis of Silica Fibers	3.2-14
3.2.2.2-1	Chemical Analyses – Baseline and Improved LI-1500	3.2-31
3.3.1-1	LI-1500 and FI-600 Thermal Conductivity Measurements	3.3-4
3.4.1-1	Radiant Energy Distributions for a Blackbody at Six Different Temperatures	3.4-7
3.4.1-2	High-Temperature, High-Emittance Pigment/Filler Candidates for LI-1500 Coatings	3.4-8
3.4.1-3	Emittance and Absorptance Values of Various Formulations (Excluding Silicon Carbides) From Room Temperature Reflectance Measurements at LMSC	3.4-12
3.4.1-4	Emittance and Absorptance Values of Various Silicon Carbide Systems From Room Temperature Measurements at LMSC Research Laboratory	3.4-16
3.4.2-1	Structural Comparison of Coating Concepts	3.4-32
3.4.2-2	Integral Coating Concept Evaluation	3.4-33
3.4.3-1	Thermal Expansion and Fusion Ranges for Various Glass Forming Compositions as Compared With Amorphous Silica	3.4-47
3.4.3-2	Lithium Aluminosilicate Frit (Patent 3,498,804)	3.4-50
3.4.3-3	Borosilicate Coatings	3.4-54
3.5-1	LI-1500 Moisture Reduction Technique Initial Materials Evaluation	3.5-5
3.5-2	Water Reduction Technique Materials Humidity Evaluation – (96% RH at RT)	3.5-7
3.5-3	LI-007 Moisture Reduction System Evaluation	3.5-9
3.7.1.1-1	Summary of Improved LI-1500 Mechanical Property Test Results	3.7-7

Table		Page
3.7.1.1-2	LI-1500 Insulation System Design Properties	3.7-9
3.7.1.2-1	Improved LI-1500/0042 System Thermosphysical Properties	3.7-10

Section 1
INTRODUCTION

The basic objective of this contract was to improve the Reusable Surface Insulation (RSI) system through the improvement of the LI-1500 material properties and the simplification of the RSI system. To accomplish the program objective, LMSC conducted investigations to study and analyze the constituent materials; to achieve improved thermal, physical, thermophysical, and other properties relatable to shuttle applications for the RSI and surface coating; and to evaluate the performance of the improved materials. The revised master schedule for this program is presented in Fig. 1-1.

The revised schedule reflects the program redirection after program midterm. This redirection included a two-month no-cost extension and relieved specific tasks such as the prototype panel deliverable requirements and continued investigation of the elimination of substrate phase. Prototype panels were fabricated from improved material systems and demonstrated under the companion TPS Program NAS 9-12083. The redirection was directed towards a greater effort in the areas of a lower density RSI system and improved surface coatings. The schedule extension allowed for a better time utilization to achieve the desired improvements and the evaluation of these improvements.

During this program, close coordination and surveillance was maintained with the Contract NAS 9-12083 Program for technical exchange to be of optimum mutual benefit for the overall shuttle TPS effort. Close coordination was also maintained with LMSC's material suppliers and with the Fiber Improvement Program (NAS 3-15566) to ensure that any forthcoming material improvements would immediately benefit this program.

The contract objectives have been satisfied through the investigations and analysis conducted, and by fabrication and evaluation of test specimens. Improvements have been accomplished that have provided a significant impact to current TPS RSI design as well

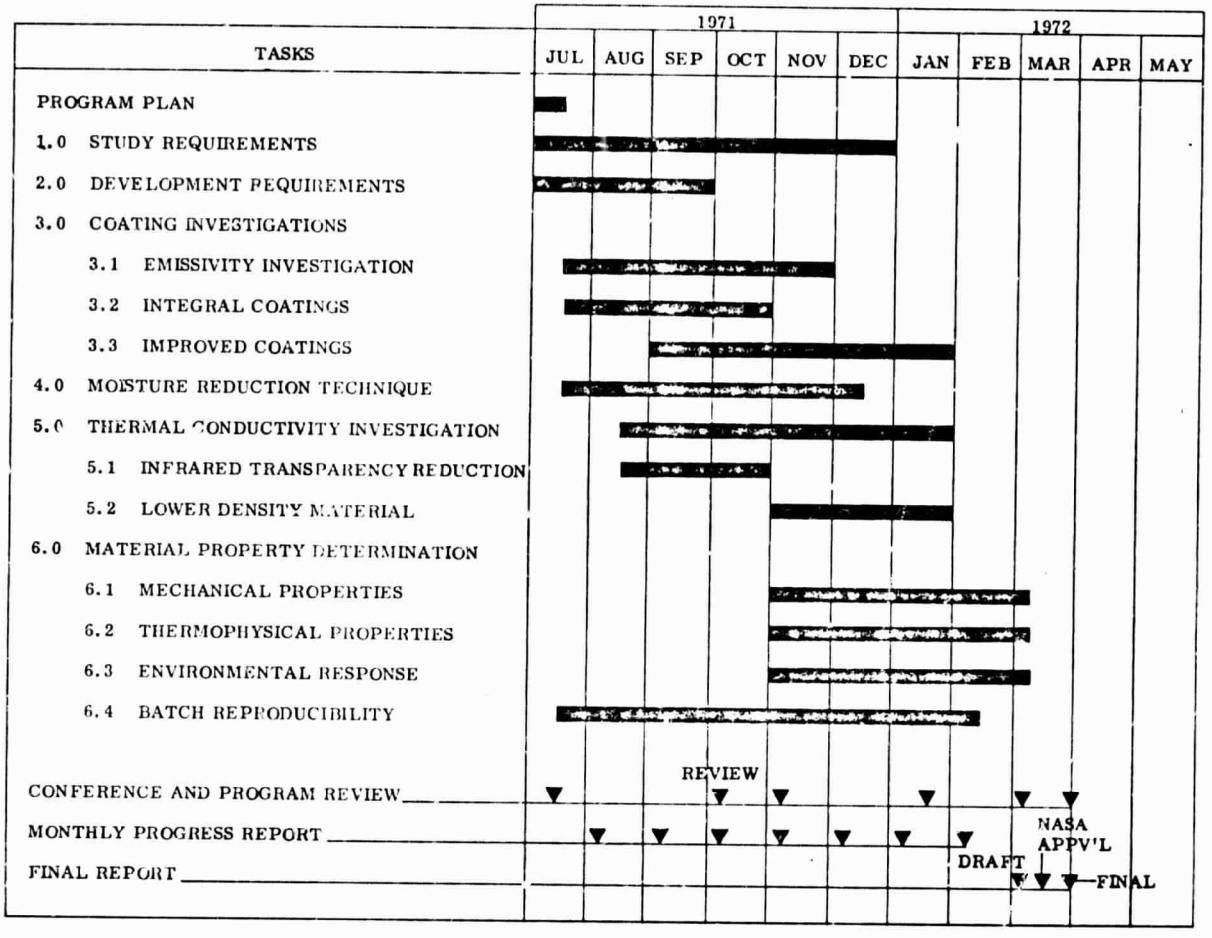

Fig. 1-1 Master Schedule

as for further future design considerations. Feasibility for other significant improvements has been shown along with identification of potential fruitful areas for such investigations.

This report was prepared by R. M. Beasley, Y. D. Izu, H. Nakano, E. Gzowski, L. Shoff, and A. Pechman.

Section 2

SUMMARY, CONCLUSIONS, AND RECOMMENDATIONS

2.1 SUMMARY OF ACCOMPLISHMENTS

(1) Characterized fiber and composite materials, increased understanding of factors influencing morphology.

(2) Evaluated the effect of candidate study materials on the LI-1500 material system.

(3) Characterized improved fiber in time for utilization on Contract NAS 9-12083.

(4) Achieved an improved LI-1500 (15 pcf) basic material with an improved borosilicate/SiC coating (LI-0012) in time for utilization in Contract NAS 9-12083.

(5) Screened and evaluated emissivity materials and established silicon carbide as a compatible high emittance (0.9) coating constituent.

(6) Screened and evaluated secondary water-reduction techniques and materials and established the LI-007 system as an effective hydrophobic water-repellant addition.

(7) Achieved an improved low-density RSI material system LI-0900 (9 pcf) with equivalent thermal capability and usable mechanical properties for shuttle TPS application.

(8) With processing adjustments, achieved a further improved borosilicate/SiC coating system (LI-0045) with equivalent thermal capabilities and water-impervious characteristics after 2500°F exposures.

(9) Obtained physical, mechanical, thermophysical, and environmental property data for the improved RSI material systems.

(10) Adopted a low-density, resilient FI-600 material with a specially developed impervious, high-emittance coating (L-0066) in time to provide weight savings and assembly simplification for NAS 9-12083 prototype hardware.

2.2 CONCLUSIONS AND RECOMMENDATIONS

It is concluded that phase transformation of silica RSI is not a problem as previously anticipated. It was determined that a significant amount of devitrification can be tolerated in both the coating and fiber composite. It was demonstrated that the rates for crystallization of LI-1500 can be sufficiently suppressed to be beyond the intended limits for use. Further, the improvements demonstrated during this program represent major simplifications for the RSI system by including superior coatings, direct attachment capabilities, and reduced weight. All of the improvements were determined to be repeatable.

It is recommended that the improvements demonstrated as feasible should be incorporated into the system design contracts for intensive development and evaluation. Also, the improvement activities started by this program should be continued with particular attention to study requirements of the factors which influence mechanical properties, further reductions in density and thermal conductivity, simplification of coating and attachment techniques, and reduced cost systems related to actual design property characteristic requirements.

Section 3
TECHNICAL PROGRAM

The primary objective of the technical program was to improve material properties and to simplify the Reusable Surface Insulation (RSI) system. The improvement of the RSI material was to better the properties of the previously selected baseline LI-1500 and surface coating system (Section 3.1). A three-phase technical approach was planned and conducted for the material improvement program. The triangular flow diagram of the program overview is illustrated in Fig. 3-1. The three tasks were closely interrelated and coordinated, and required mutual technical exchange for successful program completion. In addition, equally close coordination was maintained with the companion TPS Development Contract NAS 9-12083, and technical advances realized were immediately factored into the overall LMSC TPS effert. The program is illustrated in Fig. 3-1, and the results of the investigations are presented in the following sections.

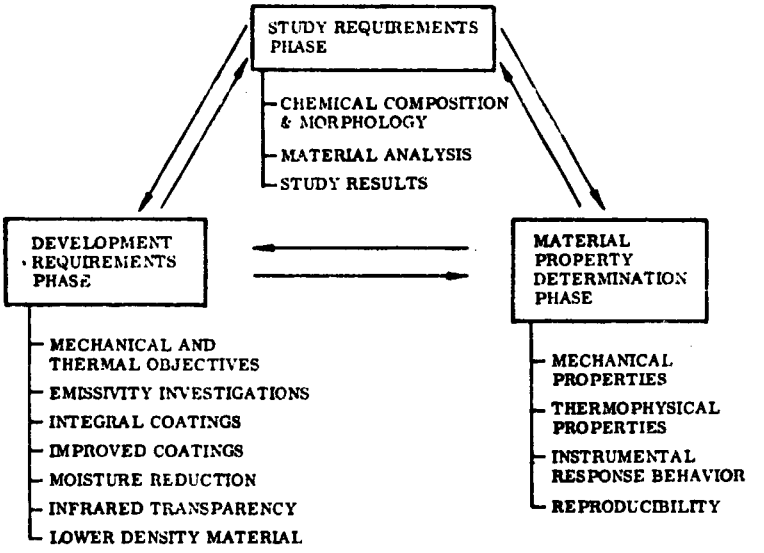

Fig. 3-1 Program Overview

3.1 BASELINE MATERIAL FOR COMPARISON

For this improvement of the RSI, the baseline material for comparison by direction was LI-1500 material similar to Tile No. TT-14B which was produced under NASA/MSC Contract No. NAS 9-11222 and evaluated in detail by Battelle Memorial Institute (NAS 9-10853). The baseline silica-fiber material for this LI-1500 tile was identified as Johns-Mansville Sales Corporation Fiber Lot No. 1213. The baseline surface coating system identified as LI-0025 was a borosilicate composition with chromia as the added emissivity agent. Table 3.1-1 and Table 3.1-2 show properties available for the LI-1500 baseline materials.

Table 3.1-1

LI-1500 BASELINE MATERIAL FOR COMPARISON

Chemical		LI-1500	
		(1)	(2)
	Fiber		
Percent SiO_2	98.58	~99	99.18
Percent Ash	1.42	~1	0.82
Crystallinity	Amorphous	–	Cristobalite 22% Quartz 4%
Mechanical (LI-1500)		**(1)**	**(3)**
Flexural Strength (psi)			
As processed		143-173	82-98
5 cycles at 1900° F		141-149	–
5 cycles at 2100° F		140-158	–
5 cycles at 2300° F		78-88	–
Flexural Modulus (10^3 psi)			
As processed		31-62	37-45
5 cycles at 1900°F		27-61	–
5 cycles at 2100°F		32-73	–

(1) Data source – Battelle (NAS 9-10853)
(2) Data source – LMSC (NAS 9-12137)
(3) Data source – LMSC (NAS 9-11222)

Table 3.1-1 (Cont)

Mechanical (LI-1500)	LI-1500	
	(1)	(3)
Flexural Strength (psi) with 0025 coating		
As processed	135-156	-
5 cycles at 1900°F	169-180	-
5 cycles at 2100°F	200-208	-
Flexural Modulus (10^3 psi) with 0025 coating		
As processed	30-88	-
5 cycles at 1900°F	32-91	-
5 cycles at 2100°F	28-104	-
Tensile Strength (psi)		
As prccessed	91-104	31-108
5 cycles at 1900°F	78	-
5 cycles at 2100°F	52-122	-
5 cycles at 2300°F	52-69	-
Tensile Modulus (10^3 psi)		
As processed	84-120	42-94
5 cycles at 1900°F	60	-
5 cycles at 2100°F	72-75	-
5 cycles at 2300°F	57-60	-
Tensile Strength (psi) with 0025 coating	61-79	-
Tensile Modulus (10^3 psi) with 0025 coating	104-111	-
Compressive Strength (psi)		
Transverse	-	38-43
Parallel		138-170

See footnotes on first page of table.

Table 3.1-1 (Cont)

Mechanical (LI-1500)	LI-1500	
	(1)	(3)
Compressive Modulus (10^3 psi)		
Transverse	-	4.6-4.95
Parallel	-	37-50
Shear Strength (psi)		
Transverse	-	12.5-25
Shear Modulus (10^3 psi)	-	1.0-1.4
Thermophysical Properties (LI-1500)	**LI-1500**	
Specific Heat (Btu/lb-°F)		
200°F	-	0.18
1000°F	-	0.28
2000°F	-	0.32
Thermal Expansion (in./in./°F)		
80°-1700°F		
Parallel	-	4.3×10^{-7}
Normal	$3\text{–}7 \times 10^{-7}$	2.7×10^{-7}
80°-2000°F		
Normal	$5\text{–}10 \times 10^{-7}$	-
Thermal Conductivity (Btu-in./ft^2-hr-°F)		
1 atm RT	-	0.35
500°F	0.31	-
1800°F	0.90	-
2000°F	-	1.56
Reduced pressure RT	-	0.17
2000°F	-	0.67

See footnotes on first page of table.

Table 3.1-2

L-0025 BASELINE COATING FOR COMPARISON

Thermophysical Properties	(1)	(2)
Total emittance	0.81 at 500°F 0.65 at 2000°F	0.85 at RT 0.63 at 2000°F
Solar absorptance	-	0.53-0.68
Thermal expansion (in./in. - °F)	-	2.0×10^{-7}
Mechanical Properties	**(1)**	**(2)**
Tensile		
Stress (psi)	-	600
Modulus (psi)	-	3.5×10^{6}
Compressive		
Stress (psi)	-	>600
Modulus (psi)	-	3.5×10^{6}
Flexural		
Stress (psi)	-	480
Modulus (psi)	-	0.96×10^{6}

(1) Data source - Battelle (NAS 9-10853)

(2) Data source - LMSC (NAS 9-11222)

3.2 STUDY REQUIREMENTS

Silica (SiO_2) exists as amorphous silica and as several crystalline species – i.e., quartz, cristobalite, and tridymite. Each form exhibits a different density and thermal expansion pattern. Table 3.2-1 shows the densities of these forms of silica.

Table 3.2-1

DENSITIES OF COMMON FORMS OF SILICA
(Room Temperature)

Quartz	2.65 (gm/cc)
Cristobalite	2.32
Tridymite	2.28
Amorphous	2.20

Figure 3.2-1 compares the thermal expansion characteristics of these forms. Silica was selected as the fiber for LI 1500 because of the low density, low thermal expansion, and low conductivity properties. The thermal expansion characteristics of amorphous silica are very low in comparison with other materials (Fig. 3.2-2). Amorphous silica is considered to be a superior material for rapid cyclic heating and cooling conditions. Complete transformation to cristobalite results in an undesirable upward shift in thermal expansion to a level similar to many ceramics such as mullite, silicon carbide, and alumina. Because of this, the LMSC objective always has been to start with amorphous silica and maintain that state over the longest combination of heating and time. It was first observed during investigations under LMSC-funded Independent Research and Development programs (IRAD) that the silica fibers show a considerable variation in crystallization characteristics when examined by hot-stage x-ray diffraction techniques. It also has been observed that some crystalline phases and change could be tolerated, but the limiting amount has not been established. Past tests conducted by

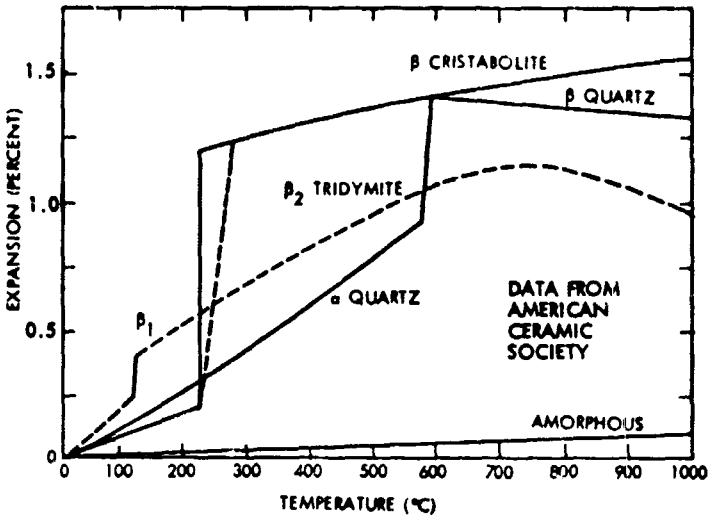

Fig. 3.2-1 Thermal Expansion of Silica Materials

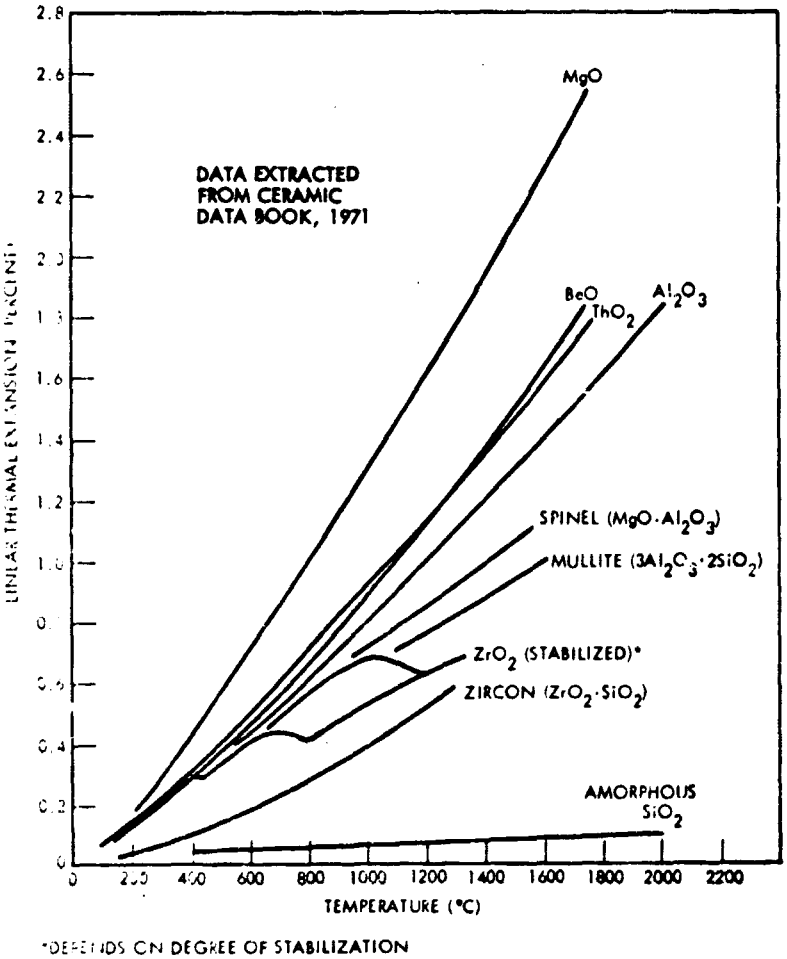

*DEPENDS ON DEGREE OF STABILIZATION

Fig. 3.2-2 Thermal Expansion of Refractory Oxides

LMSC, NASA, and USAF have shown that materials with a high crystalline content have performed successfully when tested under simulated flight conditions. For example, in a test conducted by NASA/Ames, a specimen which contained 20-percent crystalline phase was successfully arc-jet tested for nineteen 30-min cycles at 2300°F. At the conclusion of the 9.5 hr of test heating, the coating exhibited 33-percent crystalline content and the first 0.020 in. depth below the coating reached 37-percent crystalline content. In the initial screening of the fiber, this lot (1461) showed a substantial amount of crystallization below 2100°F as judged by hot-stage x-ray diffraction. Another specimen, TT 5-D,was tested by NASA/MSC successfully for 32 cycles of 10 min at 2300°F peak temperature. This specimen was fabricated from baseline Lot 1213.

After the MSC evaluations, a sample was removed from this specimen and analyzed by quantitative x-ray diffraction. The results were as follows:

Sample Location	Cristobalite (%)	Quartz (%)
Coating (LI 0025)	10	0
LI-1500, 0.000 to 0.020 below coating	26	6
LI-1500, 0.020 to 0.040 below coating	24	6

The specimen was then subjected to additional simulated entry trajectory cycles in the LMSC radiant heat facility. At the conclusion of these tests, no cracks were observed in the coating. It was re-examined by x-ray diffraction with the following results:

Sample Location	Cristobalite (%)	Quartz (%)
Coating (LI 0025)	23	0
LI-1500, 0.000 to 0.020 below coating	40	6
LI-1500, 0.020 to 0.040 below coating	31	8

Although these partially crystalline fiber composites demonstrated the capability of satisfactory performance in thermal tests, an improved compatible coated/insulation system was sought that would withstand the greatest number of re-entry cycles with

temperatures as high as 2500°F and remain impervious to water. This tendency toward devitrification (transformation to crystalline form) and the desire to minimize it placed severe limitations on the maximum processing temperature of the material and coating. In the quest of maintaining the amorphous state for the longest duration, hot-stage x-ray diffraction was used for screening raw materials. Chemistry and thermal performance tests also were considered in material selection. The use of these selection methods identified Lot 1213 as a superior fiber during the fulfilment of NASA Contract NAS 9-11222. A composite of this material (Tile No. TT14-B) was selected as the standard for comparison in the improvement activities in this program. This specific tile was selected because it was used in the evaluations conducted by Battelle Memorial Institute under contract to NASA/LMSC.

Prior to the start of this Material Improvement Program, LMSC investigated the influence of chemical composition (minor constituent levels) on the apparent onset of crystallization. This investigation resulted in meaningful data in terms of fiber requirements. The results of this investigation and evaluation of in-process fiber samples supplied by the vendor (on a proprietary basis) led to identification of the points of entry for contaminants and loss of control. Recommendations were made for specific changes in the fiber making process to improve the quality.

This new material had just been received prior to this program (May 1971) and initial evaluation indicated significant changes in crystallization characteristics, thermal dimensional stability, thermal mechanical characteristics, and thermal shock sensitivity or cracking tendencies. Because of preliminary data acquisition, this fiber contained the first improvement made ready for the concurrent TPS Development Program, NAS-912083. This new material was used for all RSI production for that program.

The objectives of the study requirements task of this program seek to increase the understanding of the factors influencing the behavior of LI-1500 and to provide guidelines for the selection of materials for an improved coating/insulation system that will successfully withstand the range of environmental conditions that may be experienced during space shuttle missions.

There are several objectives as follows:

Characterize the baseline and improved study materials

- Examine chemical composition of starting fiber and fully processed material and its influence on material behavior.
- Examine thermal behavior of baseline and improved materials with respect to crystallization characteristics, thermal dimensional stability, thermal mechanical characteristics, and thermal shock sensitivity or cracking tendencies.
- Examine the differences in thermal behavior between normal and reduced oxygen pressure.
- Identify shifts in the material characteristics caused by candidate components for coatings and emissivity agents.

Establish guidelines for selection of candidate LI-1500/coating systems

Establish estimate of material flight life

Establish chemical limits for starting fiber material composition

3.2.1 Material Analysis Techniques and Test Methods

The methods utilized in conducting the studies of fiber characteristics and LI-1500 material system included the following.

Chemical Analysis

Chemical analysis was used to establish the purity of the baseline and improved materials. It was also used in chemical treatment studies to determine whether fibers could be improved by chemical treatment and whether varied treatments would selectively remove minor chemical constituents which may affect the behavior of the material. The following analyses were carried out:

1. The samples were placed in a 1742°F muffle furnace for 1 hr, cooled in a dessicator, and weighed. This procedure was repeated to constant weight of the ignited sample.
2. Silica. Gravimetric method before and after acid treatment.
   a. The ignited sample above was then treated with nitric-hydrofluoric acid to volatilize silica as silicon tetrafluoride leaving unreacted residue. This also was done to constant weight; usually 3 to 4 treatments were necessary. The loss of material shown by weighing was called silica. Constant weight was defined as 15 min of heating at 932°F between acid treatments.
3. Ash. Gravimetric method after silica determinations.
   a. The residual material remaining after the silica determination was designated "ash". It also was based on an ignited basis.
4. Chemical analysis of ash. All values were in terms of ignited basis and were determined as follows:
   a. The sample was dissolved in 5 cc of concentrated HCl and made up to 25 cc in a volumetric flask.
      - Na, K, Ca, Mg were determined by flame photometry from an aliquot of the 25 cc. Beckman DU with flame attachment was used.
      - Fe was determined colorimetrically using the bipyridyl method (a red color is formed) on an aliquot of the dissolved ash.

b. An aliquot (usually remainder) of the dissolved ash was then evaporated to dryness and the rest of the metallics were examined by emission spectroscopy. An ARL 1.5-meter spectrograph using a 15-amp-DC arc between carbon electrodes was used. Comparison was obtained with a synthetic standard prepared from chemically pure salts. The standards were run on the same photographic film as the samples.

Elevated-Temperature X-Ray Diffraction (X-RD) Procedures for LI-1500 Evaluation

X-ray diffraction measurements on LI-1500 materials at elevated temperatures were performed on a Norelco wide angle x-ray diffractometer utilizing Ni filtered Cu Kα radiation at 40 kv and 20 Ma. The hot-stage (Materials Research Corporation Model X-86N-II) was aligned in the position of the conventional sample holder. After initial line-up, the sample was brought into contact with a line-up jig and secured for operation. Elevated temperature was attained with a 40-percent Rh-Pt ribbon heating element with a 13-percent RhPt-Pt thermocouple attached for temperature measurement.

Samples were prepared by pressing small amounts of the specimen material between stainless steel die faces by hand until a coherent specimen was formed approximately 10 mils thick. The specimen was cut to fit the heater element, placed on it, and a small drop of distilled water applied. It was usually necessary to spread the specimen over the element with the edge of a stainless spatula to ensure uniformity. After drying, the specimen was aligned in the hot stage.

X-ray diffractometer patterns were obtained by scanning over the main "amorphous" peak from 36 to 15°2θ in air at room temperature, 500°F, 1000°F, 1300°F, and in increments of 100°F thereafter until the cristobalite 101 diffraction line appeared to have stopped increasing in intensity or at a temperature of 2400°F - 2500°F. To ensure a long heater life, the temperature was never increased at a rate exceeding 482°F per minute and normally much slower than that at temperatures below 1300°F. In general, the specimen remained at each temperature for at least 20 min before the cristobalite 101 line was measured. The area under this peak, and the quartz $10\bar{1}1$ line when

present was obtained from the product of peak intensity minus background and the width at half maximum. This figure was plotted against temperature to produce the devitrification curve for the material.

The cristobalite values from this data are not quantitative because variations in sample density and thickness are uncontrollable and heating schedules were not adhered to. Temperature gradients which may occur in the specimen were considered insignificant in the observation of devitrification, because the specimen thickness is such that greater than 99 percent of the diffracted intensity can be detected. Although no devitrification has been observed at temperatures below 1300°F, the scans at room temperature, 500°F, and 1000°F are made to check for anomalies in sample configuration, heating, and intensity during the initial stages of the run.

The hot-stage x-ray technique was used extensively in the preliminary screening tests. It has proven valuable in characterizing materials with major differences in thermal response. However, the techniques are not sufficiently developed to provide complete quantitative data.

Although the hot-stage x-ray diffraction procedure is still valuable as an analytical tool, the room temperature quantitative x-ray diffraction analysis procedure is more economical for precise evaluation of materials.

Quantitative X-Ray Diffraction Analysis

Integrated intensity measurements obtained from the (101) lines of quartz and cristobalite were used to determine the concentration of these phases in LI-1500 materials by comparison to 100 percent standards according to the following procedure:

1. Sample Preparation:

   The entire sample was ground in a sapphire mortar and mixed until smooth. No screening of the specimen was done. Fractioned samples were taken with a sample splitter to avoid preferential segregation of the phases. The material was then poured over the sample holder and worked down with the edge of a microscope slide until the excess was pushed aside. The remaining

material was pressed into the sample holder with the face of the slide and with hand pressure to provide a smooth surface. The sample holder used here was a 3 x 2.5 x 0.3-cm block of nylon phenolic with a 2.5 x 1.4 x 1-cm slot machined to accommodate the specimen.

2. X-ray Measurements:

All measurements were made on a General Electric XRD-5 diffractometer with V-filtered Cr Kα radiation. Scans were made from 42° 2θ to below 32° 2θ at .2° 2θ per minute, and chart speeds of 12 in./hr. This resulted in covering a region in which all forms of SiO_2 would be detected. The integrated intensities were obtained directly from the chart by measuring peak intensity above background and multiplying by the width at one half maximum. The integrated intensities were compared to those of the standard materials run under the same conditions. The results obtained were in weight percent.

The cristobalite standard used for quantitative analysis was prepared by Georgia Institute of Technology (GIT). The quartz standard was a Permaquartz block manufactured for the General Electric Company by the General Crystal Company, Burlington, Wisconsin.

Quantitative x-ray diffraction analysis was the primary tool used in characterizing the LI-1500 materials to identify changes in crystallinity as the result of thermal treatments and the interaction of materials at elevated temperatures.

It also was used to monitor the LI-1500 produced on Contract NAS 9-12083. The technique outlined, adapted from the procedure used at GIT, produced results in close agreement with GIT on the basis of samples analyzed at both locations. In addition, there was an interchange and coordination of information and test procedures with NASA/MSC and University of Washington.

Scanning Electron Microscopy (SEM)

A Cambridge steroscan 2 scanning electron microscope was used to examine the material and changes in the material after specific treatments. It was equipped with a universal stage and tensile cartridge. It has a resolution of better than 200 Å and a working range of 20-30,000x. An MRC evaporator was used for gold shadowing of specimens.

Differential Thermal Analysis (DTA)

A Stone DTA analyzer was used in an effort to determine material characteristics. However, this equipment was limited to temperatures of 1832°F maximum, and lacked the sensitivity for precise analysis. Differential thermal analysis techniques were discontinued after several attempts to obtain useful data by this technique.

Physical Measurements and Visual Observation

Physical changes in the material after specific treatments such as shrinkage and distortion were evaluated by direct measurement and by observing the appearance of the specimens.

Thermal Response

In addition to the hot-stage x-ray diffraction procedure, furnace testing was used as the primary method of inducing changes in the material to study characteristics.

Tests were conducted at atmospheric and at reduced pressures. The heat treatments covered a range of temperatures where amorphous silica would be expected to undergo transformation to crystalline matter. The effect of time on the characteristics was evaluated by extended isothermal treatment for periods of up to 48 hr. The effect of heating was studied by short-duration furnace exposures at elevated temperatures. The test temperatures were monitored and controlled to independent calibrated temperature recorders with the thermocouple junction directly above the test specimens. All fiber test specimens were prepared from blocks cast (without binder) to a density of 5.5 pcf to minimize variables from density differences. All of the blocks were prefired to 2000°F for 1 hr. Tests showed that all of the fibers under

investigation remained amorphous after this normalizing heat treatment. LI-1500 test specimens were prepared from fully processed blocks which were fabricated by the LMSC standard procedure in the LI-1500 production facility. The normal atmosphere isothermal testing was performed in a Blue M Rad-O-Glow laboratory furnace (Model RG 3000D-IV). This is a silicon carbide heated furnace capable of 2750°F continuous service. All specimens for each specific isothermal series were placed in the furnace at the beginning of the run after the furnace had reached equilibrium. They were placed on fired fused silica setters approximately two inches above the hearth to minimize hearth influence. The test setup is shown in Fig. 3.2.1.2-1. Samples were removed as required for selected exposure times. After isothermal treatment, the entire specimen was ground and sampled for qualitative x-ray diffraction analysis.

The reduced pressure isothermal tests were performed in reentry simulators consisting of cold-wall chambers that contain 4 in. diam. x 12 in. length thoria dispersed nickel open cylinders, inductively heated.

The specimens were confined to a space approximately 2 in. long in the hot zone to ensure uniform temperature. They were supported on LI-1500 or fused silica supports. Temperature control was by thermocouple directly above the specimens connected to a Data Trak Controller-Programmer capable of single or cyclic programmed heating rates.

The pressure was measured by a Dubrovin gauge and regulated by a controlled leak valve and throttling valve on the vacuum line.

It was necessary to use a different procedure for running the reduced pressure tests than that of the atmospheric furnace tests because the specimens had to be cooled and opened to air for removal. The specimens were heated at a uniform rate from room temperature. Total heat-up times for 2200°F, 2300°F, and 2500°F were 7, 8 and 10 min, respectively. The specimens were held at the peak temperature for the specified test time and were allowed to cool at reduced pressure to near room temperature. The initial cooling rate was very rapid, cooling to below 2000°F in 2 to 4 min, depending on test temperature, and to below 1800°F in 4 to 6 min. Total cool-down time was approximately 1-1/2 hr.

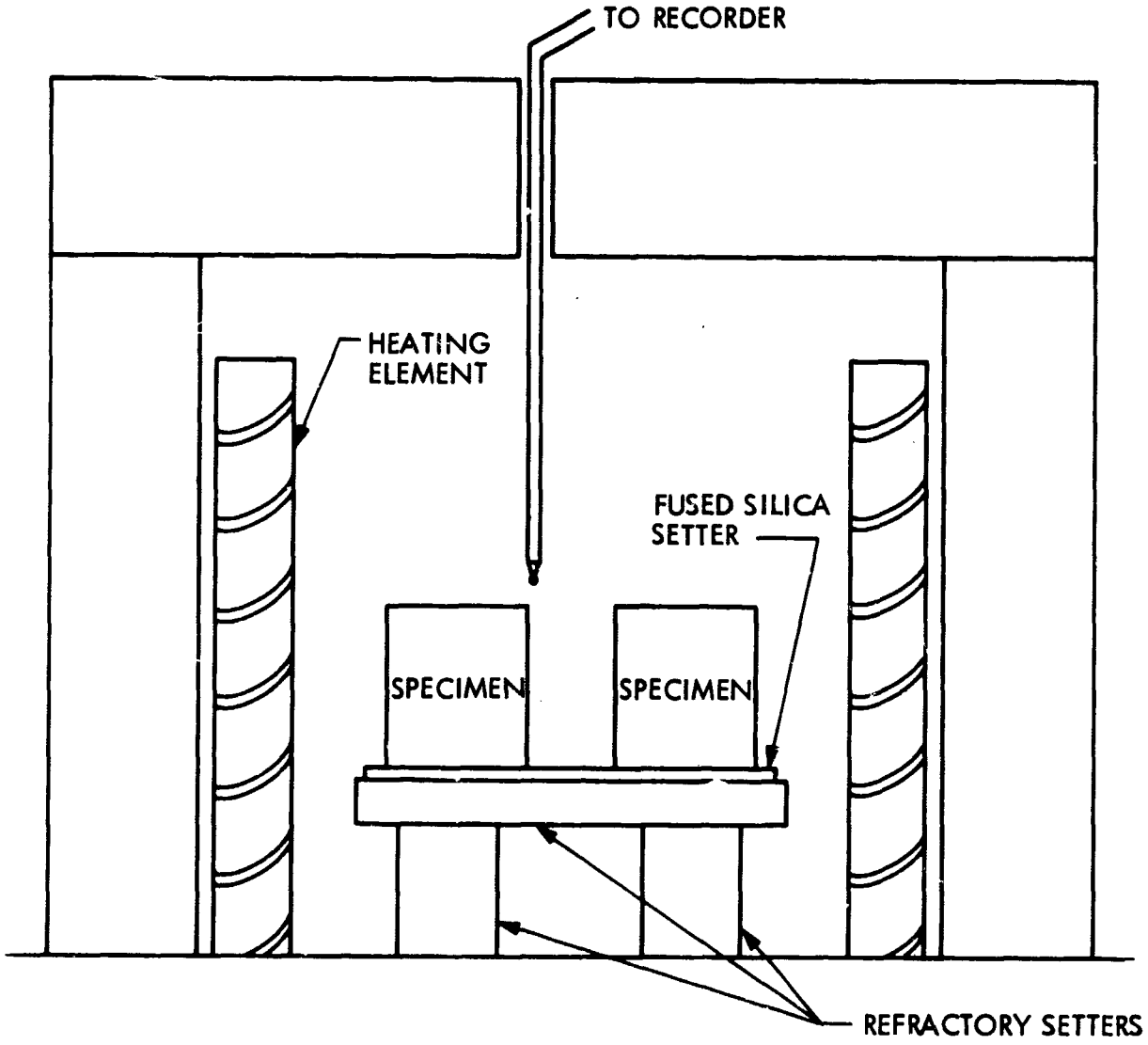

Fig. 3.2.1.2-1 Test Setup – Furnace Testing of LI-1500 – Normal Atmosphere

Screening of candidate materials for improved coatings, emittance, and opacification was also performed by furnace isothermal heating. Study material mixtures were thoroughly blended by grinding in a high purity alumina mortar. The test samples were placed into a covered fused silica crucible which had been prefired to 2300°F for 1 hr. To ensure high purity, the fused silica crucibles were processed and fabricated at LMSC specifically for this program use. The prepared samples were inserted directly into a furnace operating at the required test temperature and were allosed to soak for the required time. The transformation characteristics were evaluated by quantitative x-ray diffraction analysis.

3.2.2 Study Results

3.2.2.1 LI-1500 Fiber Characterization. The chemical compositions and crystallographic and thermal response characteristics of select silica fiber "lots" were evaluated as follows:

Fiber Materials (Johns-Manville)

- Lot No. 1213 – Baseline fiber material. Fiber lot material used in LI-1500 Tile No. TT-14B submitted under Contract NAS 9-11222.
- Lot No. 2089 – Fiber lot similar to production "lots" being utilized in the concurrent production for NAS 9-12083. Material produced by JM following LMSC-May 1971 recommended production processing.
- Lot No. 2086 – Only fiber lot in series 2083 through 2089 which exhibited a varying thermal response behavior. This particular lot was used in a study attempt to identify controlling chemical variables relatable to property characteristics.

Chemical Analysis

The chemical analyses of the three study fiber lots are presented in Table 3.2.2 1-1. As judged by the silica and ash contents, the lots (2086, 2089) produced at JM utilizing the LMSC-recommended process improvements exhibited increased purity.

Table 3.2.2.1-1
CHEMICAL ANALYSIS OF SILICA FIBERS

	LOT 1213	LOT 2086	LOT 2089
PERCENT SiO_2	98.58	99.52	99.62
PERCENT ASH	1.42	0.48	0.38
PERCENT Al_2O_3	0.29	0.073	0.053
B_2C_3	0.005	0.0001	0.0001
CaO	0.35	0.015	0.014
Cr_2O_3	0.0005	0.006	0.006
CuO	0.0001	0.003	0.002
Fe_2O_3	0.022	0.086	0.076
K_2O	0.020	0.0007	0.0015
MgO	0.55	0.025	0.024
MnO	TRACE	0.0006	0.0005
Na_2O	0.029	0.044	0.019
NiO	0.0001	0.0003	0.0003
TiO_2	0.044	0.042	0.036
ZrO_2	0.005	0.029	0.026
PbO	0.040	0.12	0.095
ZnO	0.017	0.003	-
Li_2O	-	0.0003	0.0003
Sb_2O_3	TRACE	0.002	0.003
SnO_2	0.0002	TRACE	TRACE
CoO	-	0.002	0.001
SrO	0.043	-	-

Thermal Response

The reduction of minor chemical constituents also improved the thermal response characteristics of the fibers. Figure 3.2.2.1-1 shows the varying crystallization characteristics of the study fiber lots as indicated by hot-stage x-ray diffraction analysis. Only the cristobalite curve is shown (neither the 2086 nor 2089 fiber showed any detectable quartz). The curves shown for Lots 2086 and 2089 "bracket" the patterns for all fibers used in the production of LI-1500 since May 1971. Figure 3.2.2.1-2 showing the 1213 hot-stage "X-RD" curve also shows quartz as a crystallization product. In the past, quartz was frequently indicated by hot-stage x-ray diffraction when screening candidate fiber lots for LI-1500 production.

Because the stability of glass is associated with very low fluidity[1], the reduction in the amount of impurities as evidenced in the silica contents in Table 3.2.2.1-1 had the

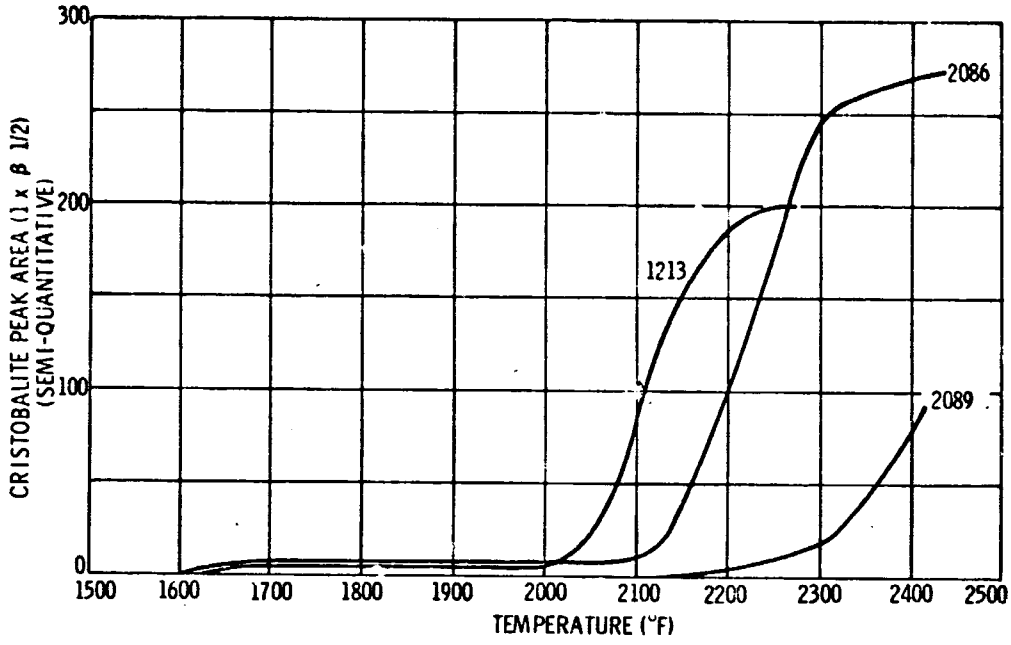

Fig. 3.2.2.1-1 Hot-Stage X-Ray Diffraction of Study Fiber Lots

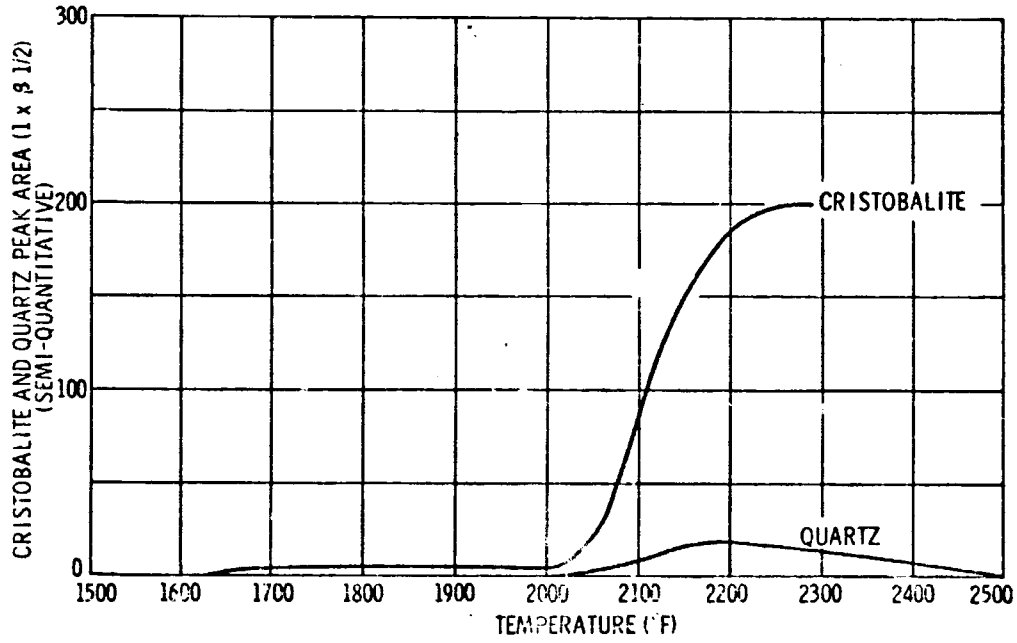

Fig. 3.2.2.1-2 Hot-Stage X-Ray Diffraction Study Lot 1213 Fiber

apparent effect of increasing the temperature/time for initiation of devitrification. The current fibers are lower in total alkali and alkaline earth oxides which lower the viscosity of glasses. Other investigators have observed that nucleation was promoted by specific contaminants. Ainslee et al.[2] and Wagstaff[4] noted that tap water residue which contains alkali and alkaline salts promotes nucleation of amorphous silica. Alkali salts[3,4] and sodium contamination from furnace components[5] have also been reported to promote nucleation.

A significant difference in the structural appearance of the fibers was observed after exposure to elevated temperatures. Specimens of the study fibers cast as 5.5 pcf composites were subjected to an exposure of 15 min at 2500°F in normal atmosphere. The thermally treated specimens were examined by "SEM" at the surface and at selected depths. The scanning electron photomicrographs (SEM) of the fiber specimens before and after thermal treatment are shown in Figs. 3.2.2.1-3 to 3.2.2.1-8. The as-received fibers of all lots were smooth in texture. Occasional particles of foreign matter similar to the one shown in Fig. 3.2.2.1-7 were evident in all fiber lots. However, Lot 2089 in general appeared to be the cleanest of the three lots. Figure 3.2.2.1-4 shows that the most significant change in fiber texture after thermal treatment occurred in the Lot 1213 fiber. The treated fibers are no longer smooth and have acquired an irregular surface. Fusion and/or amorphous silica flow appears to have started in the 2086 and 2089 fibers, but otherwise they appear unchanged. There was essentially little observable difference in fiber texture between the surface and interior of the specimens. There appears to be a correlation between devitrification and surface texture change of fibers upon exposure to high temperature.

SEM evaluation of 2089 fibers was conducted after extended isothermal exposure at 2500°F. The results in Figs. 3.2.2.1-9 to 3.2.2.1-12 show the appearance of the fibers at 2, 4, 8, and 16 hours, respectively. The broken appearance of the fibers resulted because the samples were taken at or very near the machined surface where the fibers also received the maximum thermal exposure. Fusion of the fibers was detectable at the 2-hr exposure. The smooth surface of the fibers was retained at the 2-hr and 4-hr exposures when the material was still amorphous. A definite change in

Fig. 3.2.2.1-3 Fiber Characterization Influence of Thermal Exposure
Fiber Lot 1213, As Received

Fig. 3.2.2.1-4 Fiber Characterization Influence of Thermal Exposure
Fiber Lot 1213, 2500°F 15 Minutes

Fig. 3.2.2.1-5 Fiber Characterization Influence of Thermal Exposure
Fiber Lot 2086, As Received

Fig. 3.2.2.1-6 Fiber Characterization Influence of Thermal Exposure
Fiber Lot 2086, 2500°F 15 Minutes

Fig. 3.2.2.1-7 Fiber Characterization Influence of Thermal Exposure
Fiber Lot 2089, As Received

Fig. 3.2.2.1-8 Fiber Characterization Influence of Thermal Exposure
Fiber Lot 2089, 2500°F 15 Minutes

Fig. 3.2.2.1-9 Effect of Isothermal Exposure at 2500°F – Morphology Change Fiber Lot 2089 (2 Hour)

Fig. 3.2.2.1-10 Effect of Isothermal Exposure at 2500°F – Morphology Change Fiber Lot 2089 (4 Hour)

5000X

Fig. 3.2.2.1-11 Effect of Isothermal Exposure at 2500°F – Morphology Change Fiber Lot 2089 (8 Hour)

5000X

Fig. 3.2.2.1-12 Effect of Isothermal Exposure at 2500°F – Morphology Change Fiber Lot 2089 (16 Hour)

fiber texture occurred between 4 and 8 hr during which time the material may have begun to transform. At 8 hr, the fibers lost the smooth surface and exhibited a rough texture. X-ray diffraction analysis of this specimen indicated a cristobalite content of 19 percent. The coarsening of texture was judged to be similar to that observed in the 1213 fibers after 15-min exposure. It was believed that the rough texture was evidence of crystalline transformation and growth which initiates on the surface. After 16 hr of continuous isothermal exposure, extensive fusion was evident and the identities of the individual fibers were almost lost. The x-ray diffraction analysis indicated 74 percent cristobalite.

The improved silica fibers typically exhibited the glassy behavior of absence of melting points but rather reductions of viscosity (softening point) with increasing temperatures and fusion with time. The amount of fusion evidenced in these evaluations was not noted in cyclic heating where temperatures were transient and shallow in depth. The retention of the glassy behavior of these fibers was borne out during the high temperature tensile tests described in this report, in which the LI-1500 went through a brittle/ductile transition with increasing temperature.

The morphological changes in the study fibers were investigated by quantitative x-ray diffraction analysis after isothermal treatment at selected temperatures and times. At 2200°F, the improved fibers (Lots 2086 and 2089) showed no evidence of crystalline transformation after continuous exposure through 32 hr. These findings were in conflict with the hot-stage x-ray diffraction studies which showed detectable cristobalite in 2089 fibers and a significant amount in 2086 fibers at 2200° F. Verification tests confirmed these initial isothermal results. The isothermal tests were conducted under closely controlled time and temperature conditions in a furnace which was certified to a maximum tolerance of ±10°F. Even so, it was found that the difficulty in exact duplication of data increased dramatically as test treatment times and temperatures were extended. The data appeared to become more a measure of the accumulated total of test variants, i.e., set-up, procedure, equipment contamination, etc, than an accurate reflection of material characteristics.

The techniques and procedures used in the two methods were reviewed and it was concluded that the hot-stage x-ray diffraction method was not as desirable for assessing fiber characteristics as the isothermal/quantitative x-ray diffraction technique. It lacked the utility to generate as meaningful data the development of go-no/go criteria for weight-percent crystalline determinations. This was particularly true after it was found that small amounts of transformation could be determined reproducibly by protecting the specimen in a closed silica crucible during isothermal treatment.

Fiber Lot 1213 readily devitrified at 2200° F. Figure 3.2.2.1-13 shows the transformation curves for total crystallinity in normal atmosphere and at reduced pressure. The results indicate that the transformation characteristics of this material are not significantly changed by firing at reduced pressure. This is not in agreement with findings of other investigators where atmospheric conditions (water, oxygen, etc.) were reported to increase the rate of crystobalite formation by at least an order of magnitude. The difference here may be attributable to background equipment and procedure contamination. In the other studies, the test specimens were sealed in quartz tubing containing the atmosphere of interest. (See Ref. 2.)

Baseline fiber Lot 1213 exhibited a high rate of quartz formation during the earlier stages of isothermal treatment. With continued exposure, the quartz was transformed to the more cristobalite form, as indicated by the curves shown in Fig. 3.2.2.1-14.

The 2089 fibers were exposed at 2300° F for periods up to 48 hr. The initial tests in both air and reduced pressure showed no transformation at 32 hr, and only 2-percent cristobalite after 48 hr under both conditions. However, a wide scatter in results was experienced during the verification runs. The same problem occurred during isothermal tests on fully processed LI-1500. It was found that this problem could be overcome by protecting the specimens in covered fused-silica crucibles fabricated by LMSC from extremely pure materials. Comparative tests at 2300°F for 48 hr in a "dirty" furnace showed that an exposed specimen exhibited 75-percent cristobalite, while the covered specimen heated at the same time showed no detectable crystal phase had been developed. The results obtained for covered specimens were found to be repeatable.

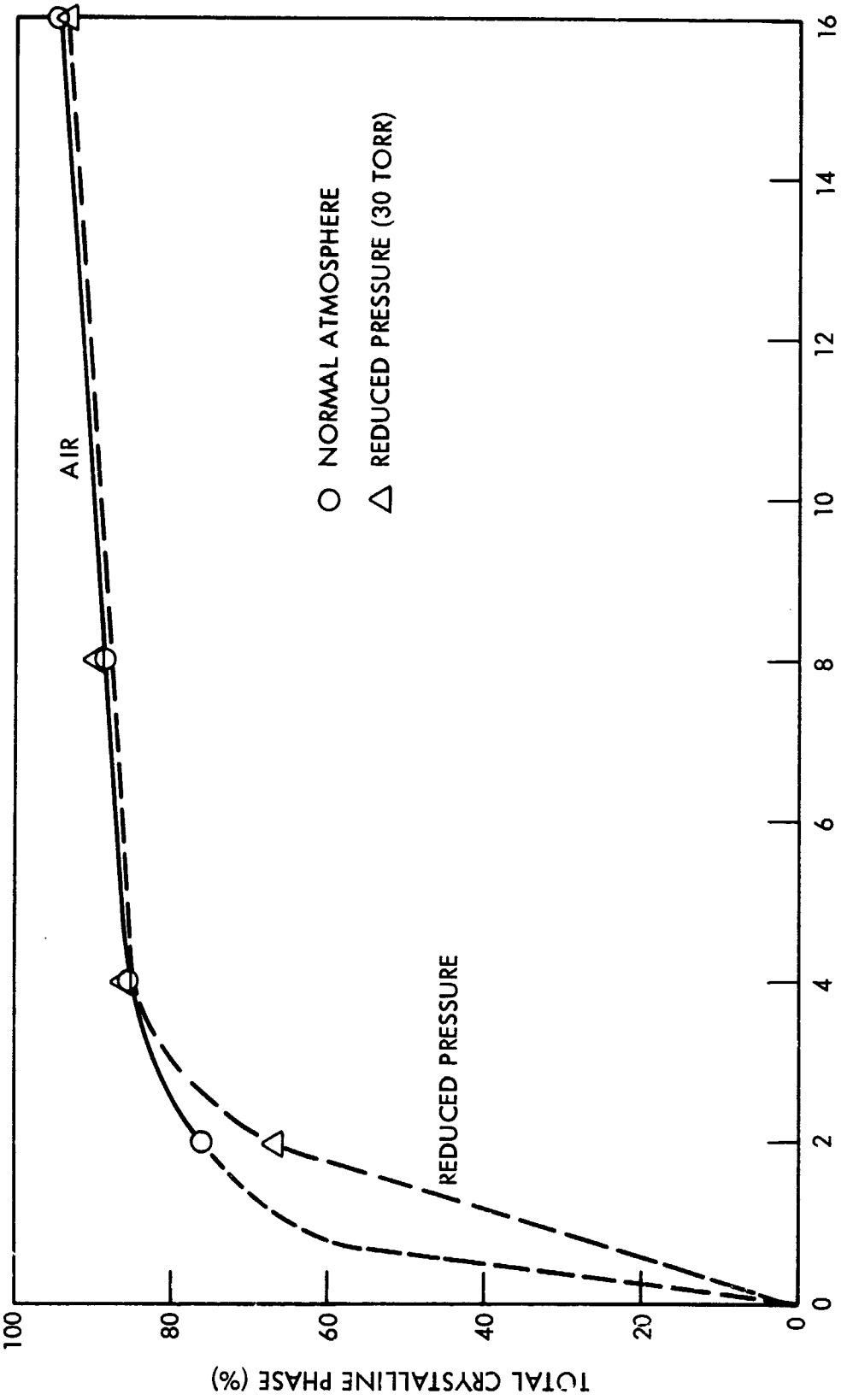

Fig. 3.2.2.1-13 Effect of Isothermal Treatment at 2200°F on Fiber Total Crystallinity, Fiber Lot 1213

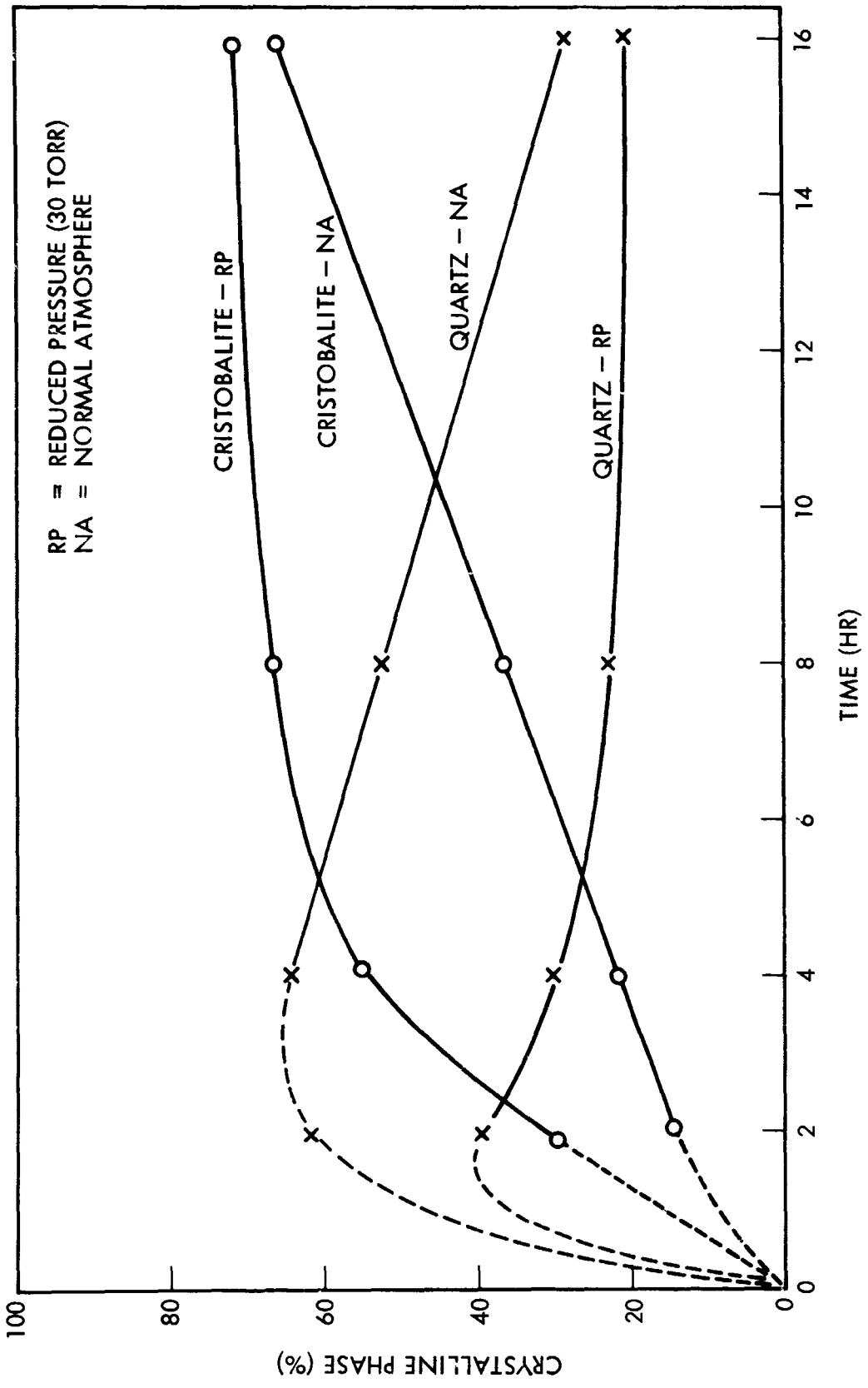

Fig. 3.2.2.1-14 Effect of Isothermal Treatment at 2200°F on Fiber Crystallinity, Fiber Lot 1213

The isothermal tests show that silica fiber currently used for the fabrication of LI-1500 is superior to those materials previously available with respect to resistance to crystalline transformation. Thermal treatment at reduced pressure had been expected to show increased resistance to crystallization of silica. As previously indicated, the reasons for not detecting these dramatic differences with reduced pressure is probably the result of sampling, treatment techniques, and equipment. The problems previously described with influence from furnace contaminants in air firings probably existed in the reduced-pressure evaluations also. Other investigators have reported (Ref. 2) that reduced pressure has a diminishing effect on crystallization of silica. While LMSC investigations did not verify these earlier findings, it was established that, either in air or at reduced pressures, the incubation period prior to the onset of crystallization was in excess of the target equivalent of 100 space-shuttle missions with 2500°F peak temperature (NAS 9-12083 trajectory). This period might be equivalent to about 1400 missions with peak temperature of 2300°F. Figure 3.2.2.1-15 presents a summary of the transformation characteristic versus time at 2300°F and 2500°F for study of Fiber Lots 2086 and 2089.

3.2.2.2 Characterization of Processed LI-1500. The chemical composition and crystallographic and thermal response characteristics of LI-1500 were examined as follows.

Chemical Analysis. Table 3.2.2.2-1 shows typical chemical analyses of fully processed LI-1500 fabricated from baseline Lot 1213 and improved fiber material. The improved LI-1500 material was taken from the LI-1500 production line (fiber Lot No. 2085).

These data indicate that in processing the starting fibers into LI-1500 and incorporating the binder, the total minor constituent level was reduced in both the baseline and improved fibers. This increase in purity of the processed LI-1500 through the careful control of the process further promotes the stability of the material. Comparing the baseline with the improved LI-1500 as used in production for NAS 9-12083, it is

significant that the level of the total alkali and alkaline oxides is reduced from 0.50 percent to 0.14 percent. The oxides in these groups are generally the most active promoters of devitrification.

Throughout the development of LI-1500, careful attention has been paid to maintaining and improving the purity level of the composite. These efforts have resulted in extending the incubation period before the onset of rapid crystallization.

Thermal Response. The effects of thermal treatment on the morphology of both the baseline and improved materials were extensively studied. A panel fabricated from Fiber Lot 1213 was selected as a standard for comparison, representative of the LI-1500 produced under Contract NAS 9-11222, with the fiber lots selected by application

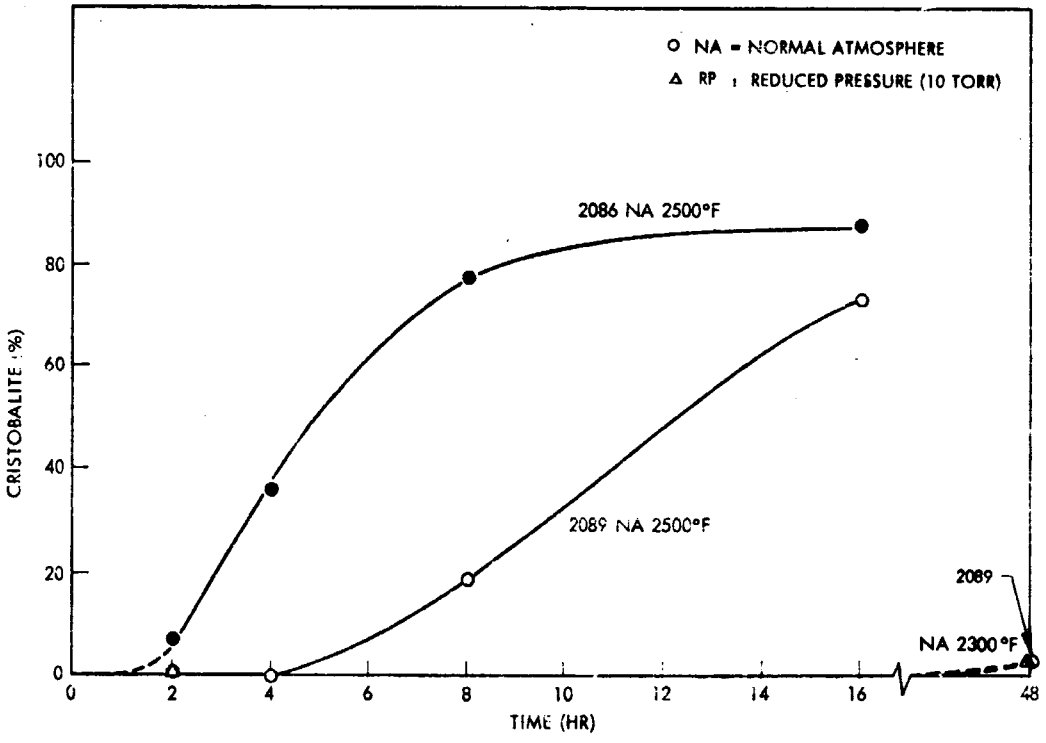

Fig. 3.2.2.1-15 Effect of Isothermal Treatment at 2300°F and 2500°F on Fiber Crystallinity, Fiber Lots 2089 and 2086

Table 3.2.2.2-1
CHEMICAL ANALYSES – BASELINE AND IMPROVED LI-1500

Compound	Baseline LI-1500, Fiber Lot 1213 (%)	Improved LI-1500, Fiber Lot 2085 (%)
SiO_2	99.18	99.73
Ash	0.82	0.27
Al_2O_3	0.178	0.042
B_2O_3	0.0002	Trace
CaO	0.090	0.0009
Cr_2O_3	0.039	0.011
CuO	0.024	0.008
Fe_2O_3	0.036	0.026
K_2O	0.0018	0.001
MgO	0.28	0.025
MnO	0.0001	0.0004
Na_2O	0.013	0.020
NiO	0.012	0.005
TiO_2	0.040	0.031
ZrO_2	0.026	0.025
PbO	0.041	0.052
ZnO	0.036	0.023
P_2O_5	Trace	
Ag_2O	Trace	
SnO_2	Trace	

of hot-stage x-ray diffraction data. The total crystalline content of the baseline LI-1500 was 26 percent by x-ray diffraction analysis after completion of processing. It comprised 22-percent cristobalite and 4-percent quartz. The dilution effect of the binder may be seen by comparing this crystalline content with that recorded for the basic

1213 fiber. This comparison indicates a tolerance for phase change when it is made, along with the consideration that this over-80-percent crystalline fiber performed perfectly in composite without a decay of results in 32 cycles for 10 min at 2300°F in NASA/MSC arc tests.

Isothermal treatments of the baseline material were conducted at 2200°F, 2300°F, and 2500°F. The summary of these results is shown in Fig. 3.2.2.2-1. As in previously reported results, no significant change appeared in the transformation characteristics when the material was treated at reduced pressure. The characteristics of the transformation curves are markedly different between the fiber and processed LI-1500. This can be attributed to the binder component and processing procedures which effectively retard the rate of crystal growth.

The transformation data for isothermally treated LI-1500 fabricated from the improved fibers were very similar to those recorded for the fiber alone. Initial runs up to 32 hr at 2200°F produced no detectable transformation. At 2300°F, runs were extended until detectable transformation occurred. At 48 hr in both air and reduced pressure, only 2-percent cristobalite was formed. Because this exposure might be equivalent to over 1400 missions, the phase stability of LI-1500 can be considered excellent for 2300°F use. Note that these results are the same as those obtained for starting fibers.

The transformation curves at 2500°F in Fig. 3.2.2.2-2 are almost identical for both air and reduced pressure. They are also very similar to the transformation characteristics of the starting fiber. The isothermal tests show that with the very low amount of transformation up to 4 hr, the material exhibits a margin of safety for surviving 100 missions at 2500°F peak temperature.

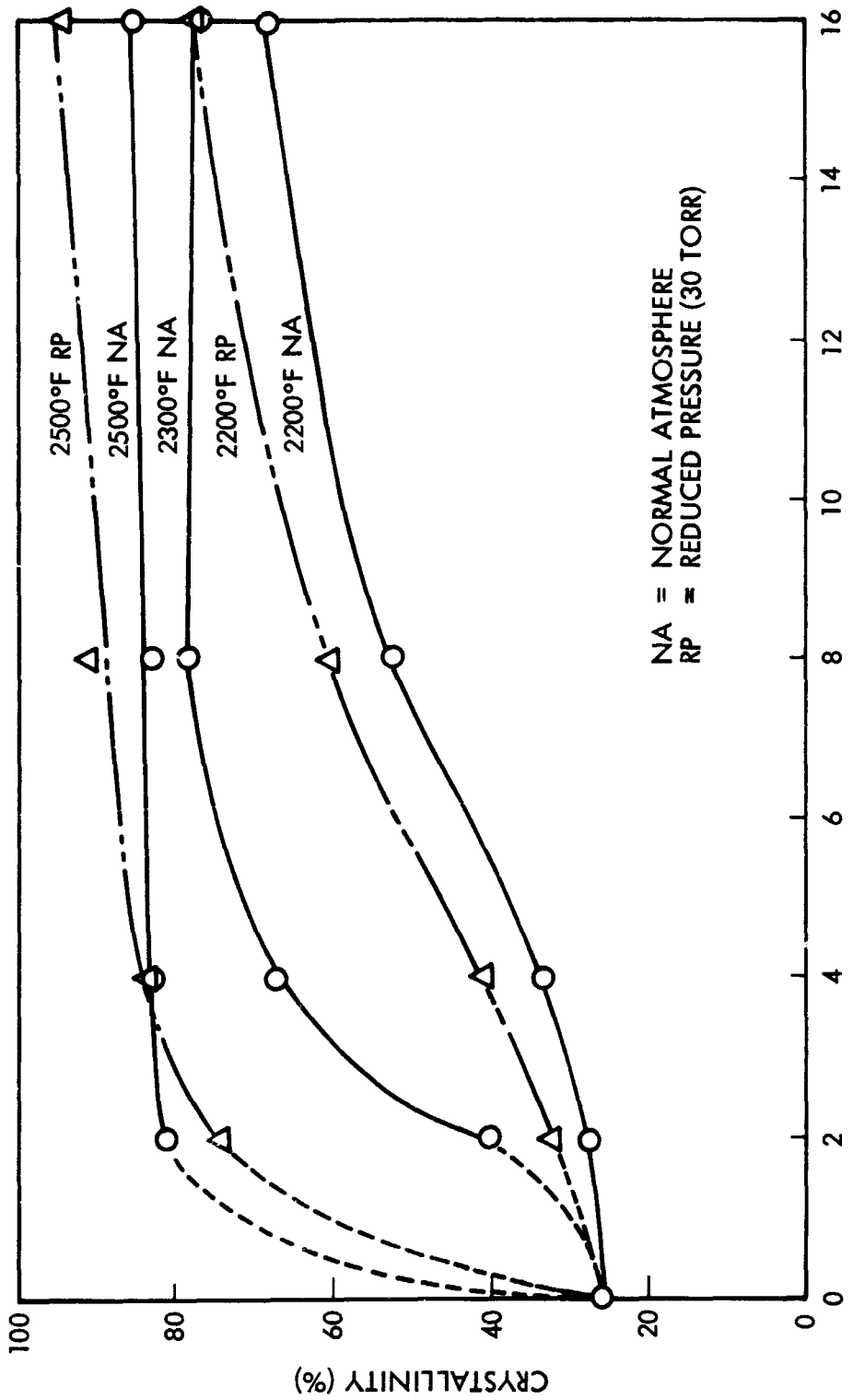

Fig. 3.2.2.2-1 Effect of Isothermal Treatment on Total Crystallinity of LI-1500 Material (Fiber Lot 1213)

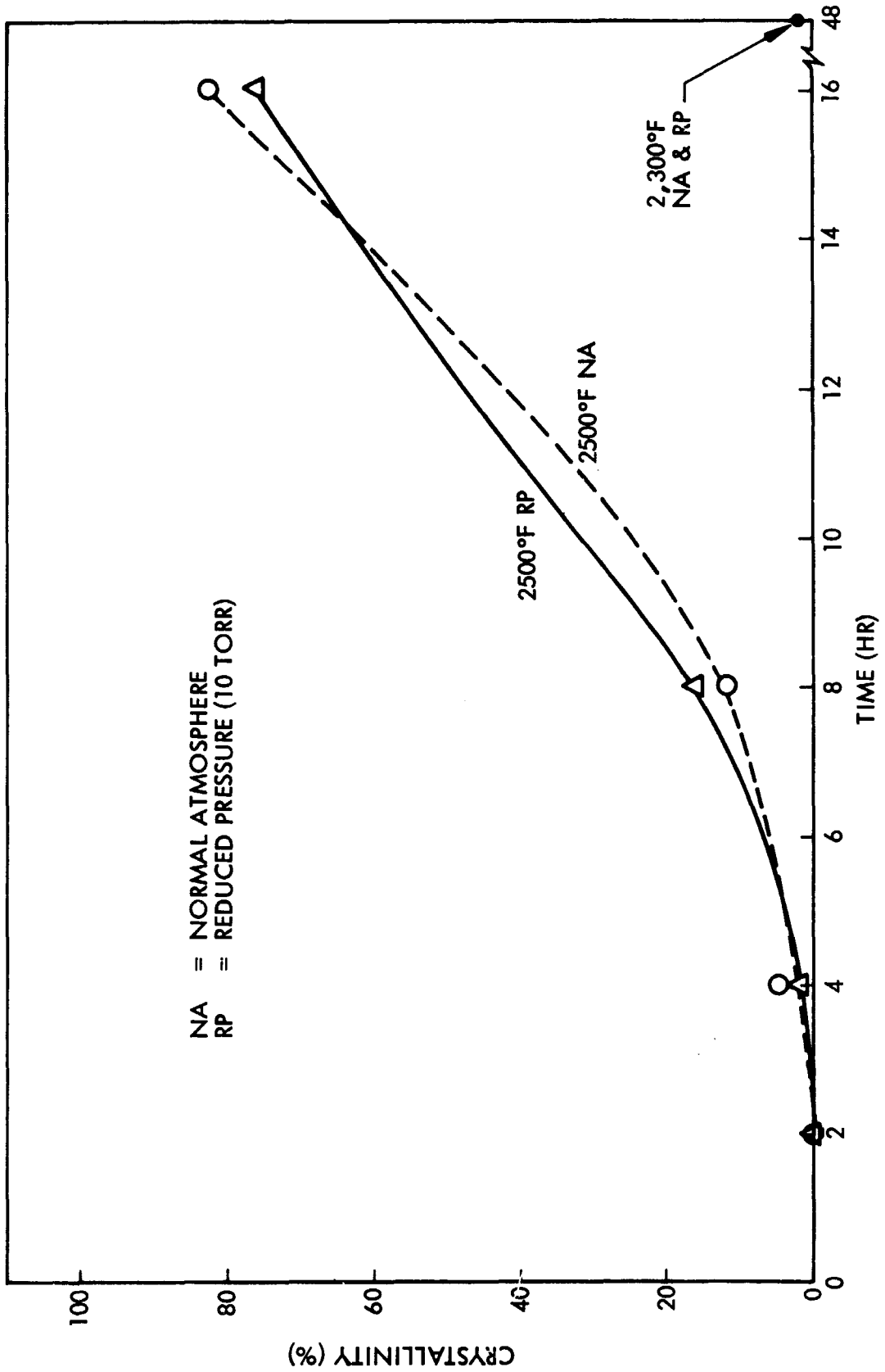

Fig. 3.2.2.2-2 The Effect of Isothermal Treatment on Crystallinity of LI-1500 (Improved Fiber Lot 2089)

3.2.2.3 Influence Treatments and Chemical Additives

Thermal Treatments. Fully processed LI-1500 was subjected to varied thermal heat treatments to examine the influence on shrinkage, crystallization, and density.

Direct furnace insertions at 2,300, 2,500 and 2,700° F were investigated, with varied sequences to determine the effect of multiple exposures at different temperatures. The noncrystalline LI-1500 will shrink in furnace exposures where heating is continuous from all sides and uniform throughout the composite structure. The following are typical results of isothermal furnace treatments.

Time at 2300° F (hr)	Additive Linear Shrinkage (%)			Crystalline (%)
	Length	Width	Thickness	
1	1.80	0.73	1.50	-0-
2	0.87	0.84	1.64	-0-
3	1.00	1.11	1.67	-0-

Furnace testing has little meaning with respect to determination of the thermal/dimensional stability which might be expected during cyclic flights. This is best evaluated by arc testing following simulated flight-heating projections. However, for economy, some evaluators have extended the hold time at peak test temperature to accumulate (during each cyclic exposure) total times representative of many flights – e.g., 32 cycles for 10 min may be considered representative of thermal material response of 160 flights with peak heating durations of 120 sec. Data from prolonged exposures should not be used to evaluate shrinkage or in-depth devitrification characteristics. The following may illustrate some of the differences between short-term heating and "soaking" exposures.

Figure 3.2.2.3-1 presents predicted heating with time through a 2-in. cube when inserted into a furnace operating at 2,500° F. It is evident that heating in a furnace – even for 5-min periods – is much more severe exposure than the material is expected to see in service due to in-depth heating.

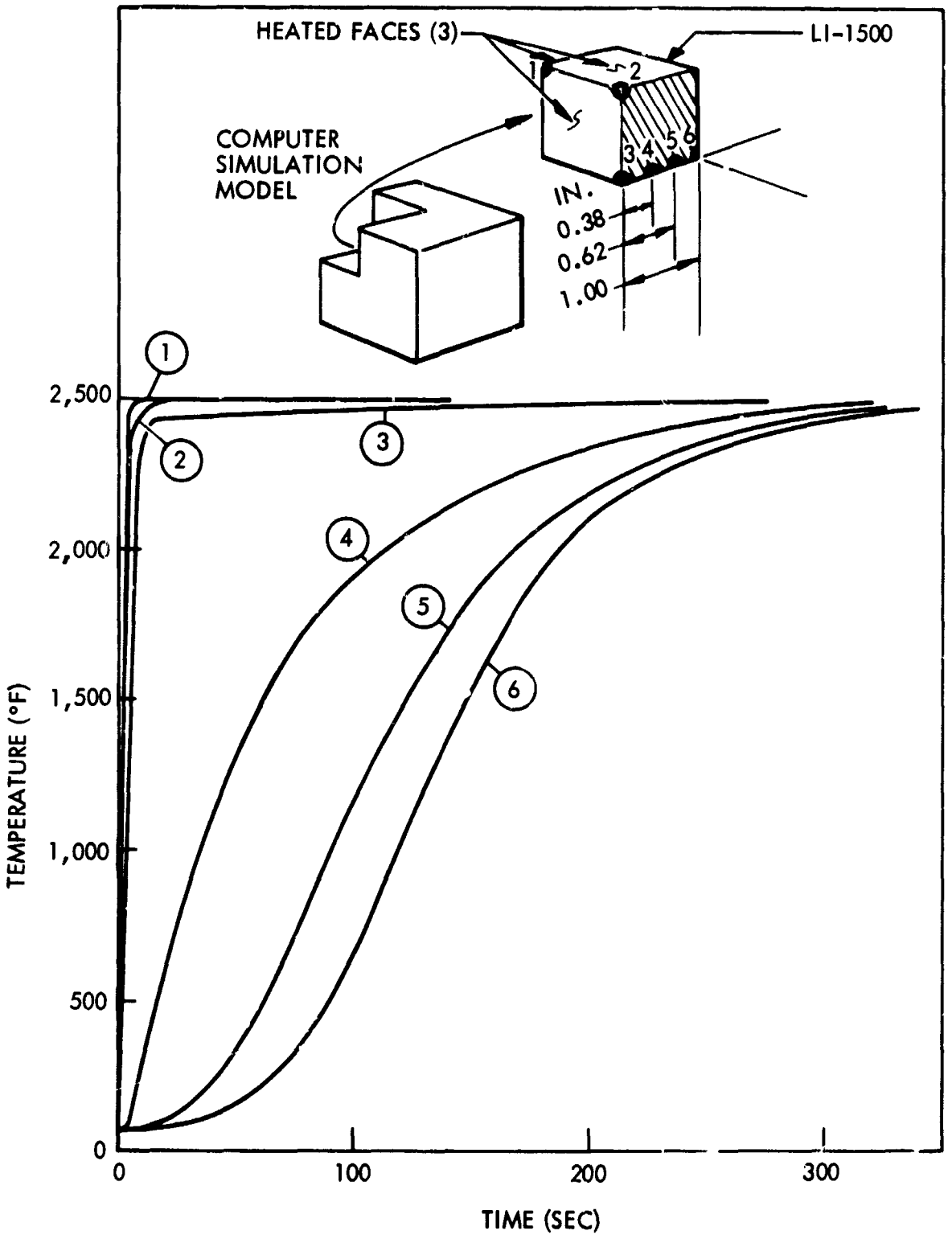

Fig. 3.2.2.3-1 Temperature Profile – Furnace Heated LI-1500 Model, 2 in. x 2 in. x 2 in.

Because the program NASA trajectory indicates a peak temperature of 2300° F for 120 sec, a 3-min furnace insertion (with an allowance of 1 min for the furnace to recover to set temperature) was used as more closely simulating peak surface conditions in evaluations comparing the shrinkage from short-cyclic and "soak" type heating. Seven 3-min cycles would approximate the equivalent surface exposure as one continuous 15-min cycle.

A total of fourteen 3-min insertions were performed at 2500°F. Seven 3-min insertions were performed at 2700° F. Comparative results between the 3-min and 15-min insertions were found to be as follows.

THE EFFECT OF LENGTH OF INSERTION TIME
ON
SHRINKAGE OF LI-1500 @ 2500° F

Temp. (° F)	Time (min)	No. of Cycles	Cumulative Linear Shrinkage (%)			Remarks
			Length	Width	Thickness	
2500	15	1	1.2	1.2	2.1	Measured at center of faces – slight distortion at corners.
2500	15	2	2.4	2.5	4.0	
2500	3	7	0.06	0.31	0.26	Measured at center of faces. Equivalent to surface exposure of one 15-min cycle.
2500	3	14	0.34	0.41	0.47	Same as above except two 15-min cycles.
2700	15	1	10.4	10.0	16.4	Measured at center of faces. Distorted severely at corners.

THE EFFECT OF LENGTH OF INSERTION TIME
ON
SHRINKAGE OF LI-1500 @ 2500° F

Temp. (° F)	Time (min)	No. of Cycles	Cumulative Linear Shrinkage (%)			Remarks
			Length	Width	Thickness	
2700	3	7	0.31	0.34	1.47*	*Thickness shrinkage is questionable because of moderate reaction of bottom with setter. Measured at center of faces. Equivalent to surface exposure of one 15-min cycle. Slightly distorted at corners due to longer term heating.

The results of the multiple 3-min insertion tests show that the shrinkage is decreased significantly when the insertion test procedure is modified to more closely approximate shallow heating service conditions. Note that the furnace insertion test with heating on all six faces is still more severe than would be encountered in service where only one face of a large surface is heated.

Continuous furnace exposure at high temperature may result in significantly higher shrinkage and edge distortion than multiple short exposures with equivalent length of temperature at the surface.

Another test was conducted in an effort to assess the thermal performance material in the advanced stages of use. For this study, the material (5-in. x 5-in. x 2.5-in. block) was pre-aged for seven cycles of 30 min each at 2,500° F in a furnace with all the adverse conditions of heating throughout the composite. The block was cooled to

C 3

room temperature between cycles. The total of 3.5-hr exposure exceeds the estimated 3.3 hr that the surface is expected to be exposed to peak temperatures during 100 reentry flights.

After thermal aging, two 3-in. x 3-in. x 1-in. thermal test models were extracted from the pre-aged block in a manner to yield test surfaces from the pre-aged surface and from the midplane surface. X-ray diffraction evaluation was performed on samples representative of the new test faces. The x-ray diffraction tests showed that no crystalline species were detectable either at the surface or midplane surfaces of the block after the multiple thermal aging exposures. Originally, it was planned to pre-age the material in a furnace environment to achieve a significant crystalline content. However, since the improved LI-1500 material does not readily convert to the crystalline species, it was decided to expose that material for a total time in the 2500° F furnace environments estimated to be equivalent to the exposure at peak temperatures for 100 reentry flights. The test surfaces of each model were coated with LI-0042 coating. The coated surface of Model TA-1 was at the original surface of the thermally aged block. The coated surface of Model TA-2 was at the midplane of the aged block. During the coating process, the models were subjected to two additional 2,500° F heat treatments of 15 min each.

The test models (TA-1 and TA-2) were subjected to nine simulated reentry cycles to a peak temperature of 2500° F and to two cycles at 2300° F peak temperature in the LMSC 24-in. by 24-in. Radiant Heat Facility. The temperature profile of the thermal cycle for these tests consisted of: (1) a 300-sec heatup to peak temperature, (2) a 150-sec hold at peak temperature, and (3) a 400-sec cool-down period.

No change in the LI-1500 or coating was apparent at the completion of the radiant heat testing. Measurement of the models showed that little shrinkage occurred. The shrinkage results for the models were as follows:

	TA-1 Shrinkage (%)	TA-2 Shrinkage (%)
Length	0.2	0.1
Width	0.1	-0-
Thickness	0.2	0.3

C.2

Penetrant dye inspection of the coated surfaces showed that the coating was impervious. No porosity and no cracks were evident.

In addition to the preceding checks, x-ray diffraction analysis was performed on sections of the coating and the base LI-1500 material after the radiant heat tests. The x-ray diffraction results for the coating indicated 14-percent and 8-percent crystallinity for TA-1 and TA-2, respectively. The base LI-1500 material showed no crystallinity. A sample of as-processed LI-0042 coating was analyzed concurrently for x-ray diffraction and showed 2-percent crystallinity. The absence of any crystallinity in the LI-1500 indicates that the 0042 coating system does not adversely influence the promotion of crystallinity in the base material. It is also important to note that the coating remains serviceable with a significant crystalline content.

Chemical Treatment of Starting Fibers. A study was made to determine whether chemical treatment of fully processed fibers might further increase purity and thereby improve thermal characteristics. The study also attempted to determine whether varying the chemical treatment would result in selective contaminant removal and perhaps identify the controlling variables relating to property characteristics.

Fiber Lot 2086,which originally exhibited high-shrinkage tnermal behavior, was selected for this study. Samples of the fiber were dispersed in each of three acid solutions with a 7-volume-percent concentration maintained at 80° C in a constant temperature water bath. The acids selected were HCl, H_2SO_4, and HNO_3. A portion of each dispersion was drawn at selected intervals of 1, 2, 4, 8, 16, and 168 hr and then thoroughly washed and dried. Silica and ash content were determined for each draw sample, and a chemical analysis was performed on the samples treated for 168 hr. Thermal behavior tests at 2,500° F were performed on cast cylindrical compacts from each treated sample. Measurements were performed before and after thermal exposure. For comparison, a specimen from as-received fibers also was tested.

The summary of the chemical and thermal evaluation of the chemically treated fibers is shown in the following table.

EFFECT OF SUPPLEMENTAL CHEMICAL TREATMENT ON SILICA FIBERS

Test Condition		Chemical		Thermal
		Silica Ignited Basis (%)	Ash (Minor Constituents) Ignited Basis (%)	Shrinkage, O.D. After 15 min At 2,500°F (%)
Lot 2086 Fibers As Received	(hr)	99.52	0.48	22.1
HCl Treated	- 1	99.58	0.42	9.3
	- 2	99.50	0.50	10.3
	- 4	99.53	0.47	9.3
	- 8	99.56	0.44	8.3
	- 16	99.55	0.45	8.6
	-168	99.55	0.45	8.2
H_2SO_4 Treated	- 1	99.59	0.41	9.3
	- 2	99.48	0.52	8.6
	- 4	99.53	0.47	9.3
	- 8	99.52	0.48	9.2
	- 16	99.55	0.45	8.9
	-168	99.55	0.45	9.0
HNO_3 Treated	- 1	99.59	0.41	8.7
	- 2	99.68	0.32	8.2
	- 4	99.52	0.48	7.3
	- 8	99.56	0.44	8.3
	- 16	99.58	0.42	7.6
	-168	99.62	0.38	7.3

Although an improvement in shrinkage characteristics was evidenced, the chemical treatment had little effect on the fiber purity. The reduction in ash content was slight. The results suggest that the HNO_3 treatment may have been slightly better. The range

in values can be attributed to variation in fiber chemistry and normal scatter in analytical technique.

The thermal treatment tests show a definite improvement in performance with respect to shrinkage. The greatest improvement occurred during the first hour of all treatments and might be attributed to removal of surface contaminants and "fines." This latter point is apparent in the scanning electron microscopy performed upon fired samples at 1000 x (Fig. 3.2.2.3-2). This examination by SEM after thermal treatment showed essentially no differences relative to the acids used. The results of this investigation suggest that the purity of the fully processed fiber cannot be significantly improved by chemical after-treatments.

The improvement in thermal processing-type behavior may be significant, but is apparently not related only to chemical changes. However, Fleming[8] and Dietzel[10] list the following metallic ions as influencing crystalline formation in decreasing order of effect: K, Na, Li, Ba, Pb, Ca, Fe^{+2}, Mg, Fe^{+3}, Al, Ti.

Metallic lead is a major problem in the Johns-Mansville fiber. When heated with silica, it melts and combines to form lead silicate glass with softening points approximating 1,400°F or lower. Tests show that a void 40 to 65 times the volume of the lead particle is formed in LI-1500 when fired to 2,000° −2,500° F. Specifically, a piece of lead metal 1 mm in diameter (0.5 mm^3) produced a void of at least 34-mm^3 volume.

Evaluation of Candidate Coating Constituents. The development of a dense, impervious coating for LI-1500 capable of withstanding multiple space-shuttle missions with peak temperatures to 2,500°F required a careful selection of materials. A principal objective in the coating development was to maintain a system with minimum devitrification characteristics.

The materials tested included potential emissivity adjusting agents and opacifying agents as well as the basic glass formers. The test results showing the morphological interreaction between material combinations provided a basis for formulating compatible coating compositions for LI-1500.

Fig. 3.2.2.3-2 Effect of Chemical Treatment (Fiber Lot 2086) – As Received, Left, and Acid, Right

A large number of materials were screened at 2,200°F. Cordierite- and spodumene-based materials were attractive because their low thermal expansion characteristics were compatible with LI-1500. Alone, these materials were stable. Mixed with an equal amount of silica and treated for 2 hr at 2,200°F, both materials produced 36-percent to 37-percent cristobalite. A number of commercial frits also resulted in excessive cristobalite formation. Alumina has been reported to have a lesser effect on crystallization than, for example, the alkali or alkaline earths. However, in 1-percent and 10-percent admixtures with silica, 24-percent and 62-percent cristobalite were formed at 2,200°F in 2 hr, respectively. Chromium oxide, which was used as the emissivity agent in the LI-0025 coating, when mixed equally with silica, produced 45-percent cristobalite in 15 hr exposure at 2,200°F. An equivalent amount of cristobalite was formed in 4 hr at 2,300°F, illustrating the dramatic influence of only 100°F increase in temperature. Cobalt oxide and silicon carbide were tested for the effect on morphology in contact with fused silica. Thermal treatment times for 2,300°F and 2,500°F were 4 hr and 2 hr, respectively. The results, including comparative results for chromium oxide, are as follows:

Mixture	Proportion	Temperature (°F)	Time (hr)	Percent Cristobalite
SiO_2 Test base	-	2300	4	ND*
SiO_2 Test base	-	2500	2	3-6
SiO_2 plus Cr_2O_3	1:1	2300	4	41
SiO_2 plus SiC	1:1	2300	4	2
SiO_2 plus SiC	1:1	2500	2	26
SiO_2 plus CoO	1:1	2300	4	3
SiO_2 plus CoO	1:1	2500	2	33

*ND - Not Detected. No quartz detected in any tests.

The tests indicated that though both SiC and CoO are less reactive than Cr_2O_3, an appreciable amount of devitrification occurs at 2,500°F with this silica test base. The testing was modified to more closely approximate the conditions in the coated structure. Mixtures of borosilicate test base (coatings) with candidate emissivity agents were tested at 2,500°F for 2 hr with the following results:

Mixture	Percent Cristobalite
Borosilicate test base	ND
Borosilicate plus SiC	ND
Borosilicate plus SiC plus CoO	39
Borosilicate plus CoO	55
Borosilicate plus CoO (High) plus Cr_2O_3	23
Borosilicate plus Cr_2O_3 (High) plus CoO	4
Borosilicate plus NiO	9
Borosilicate plus $NiO \cdot Cr_2O_3$ (spinel)	8
Borosilicate plus $FeTiO_5$	5
Borosilicate plus LI-1500 (ground)	3
Borosilicate plus LI-1500 plus SiC	5
LI-1500 (ground reference)	ND

The results of these tests showed that silicon carbide was the most logical candidate for the emissivity agent in a coat based upon borosilicates and that several others should be investigated. Cobalt oxide, showing a high reactivity, would be considered a poor choice at this time. Phase diagrams[9] show eutectic between CoO and SiO_2 at approximately 2,500°F indicating the probability of reaction between these materials. This material might be useful at lower temperatures than 2,500°F. Silicon carbide is relatively inert with silica and should be compatible at the intended service temperatures.

3.2.2.4 References

[1]D. Turnbull and M. H. Cohen, "Crystallization Kinetics and Glass Formation," Modern Aspects of the Vitreous State, p. 38-62, Butterworth and Co. Ltd. (1960)

[2]N. G. Ainslee, C. R. Morelock and D. Turnbull, "Devitrification Kinetics of Fused Silica. Symposium on Nucleation and Crystallization in Glasses and Melts, p. 97-107, American Ceramic Society (1962)

[3]F. E. Wagstaff, "Crystallization Kinetics of Internally Nucleated Vitreous Silica," Journal of American Ceramic Society, 51 (8) 449-452 (168)

[4]F. E. Wagstaff, Kinetics of the Crystallization of Vitreous Silica Thesis, Ph. D., Univ. of Utah, 1962 - University Microfilms, Ann Arbor, Michigan (1967)

[5]F. E. Wagstaff and K. J. Richards, "Kinetics of Crystallization of Stochiometric SiO_2 in H_2O Atmospheres, Journal of the American Ceramic Society 49 (3) 118-21 (1966)

[6]Oscar Knapp, "Devitrification and Thermal History," Glass Industry 40 (6) 307-326 (1959)

[7]J. D. MacKenzie, "Fusion of Quartz and Cristobalite," Journal of the American Ceramic Society 43 (12) 615-20 (1960)

[8]Georgia Institute of Technology, Engineering Experiment Station, Fused Silica Manual by J. D. Fleming, AEC Contract No. AT-(40-1)-2483, 1 Sept 1964

[9]D. P. Masse and Arnulf Muan, Trans. AIME, 233, 1448 (1965)

[10]A. Dietzel, Z. Elektrochem., 48, 9 (1942)

3.3 DEVELOPMENT REQUIREMENTS

Studies were conducted to determine the interrelationship of the various parameters of LI-1500 and surface coating materials. These studies, conducted under this program and Contract NAS 9-12083, influenced selection of development requirements for improving material and for simplifying the RSI system for shuttle applications.

A major concern in improving the combined baseline LI-1500 and surface coating system was the apparent incompatibility of the modulus and strength of the two constituents. These studies are described in more detail in the NAS 9-12083 Final Report (LMSC-D152738) and in Section 3.4. Various areas investigated to alleviate this incompatibility included effect of coating discontinuities, density gradients, densified LI-1500-to-coating interface, and other areas of coating investigations described in Section 3.4. A significant analysis conducted for the purpose of improving LI-1500/coating showed that the approach of locally densifying an interface region of the LI-1500 prior to application of the high-modulus ceramic surface coating was highly desirable. The analysis showed that such a system reduced the coating stress relative to the stress experienced by an add-on coating alone because of the closer match in elastic moduli at the coating/densified LI-1500 interface. This improvement objective was integrated into the coating investigation. Thermodynamic analyses performed on such densified designs indicated that the required increases in total thickness for a typical lower surface shuttle orbiter application were insignificant and within the accuracy of the original analysis utilizing the nondensified design.

The influence of the mechanical and thermal objectives analysis is reflected in various investigative and developmental material improvement phases of this program described in the remainder of this report. The development requirement studies conducted are also reflected in specific areas to improve and simplify the TPS RSI system.

3.3.1 FI-600 Joint Closure Material

Analysis of the shuttle TPS requirements indicated that the joint closure-strip areas (joint design selected by NAS 9-12083 program) of the TPS system will be exposed to a

maximum temperature of about 1,000° F. The joint strips are located well within the TPS system and will not be exposed to outer surface conditions. Thermal properties are of prime concern, with mechanical properties to be of an adequate magnitude for manufacturing and installation. For this particular application, a silica composite material of significantly lower density (5 to 6 lb/ft^3) was utilized. The surface area directly under the joint gap may be hard-surface-coated, but the material is intentionally resilient, which significantly aids manufacturing considerations in accommodating the fabrication tolerance at the joints of individual insulation tiles. The hardened surface is a borosilicate/silicon carbide coating formulation (LI-0066) developed for the FI-600 material, is impervious to water, and exhibits a high emissivity. The FI-600 joint strip material with the LI-0066 coating is shown in Fig. 3.3-1-1.

For thermal and acoustical verification, the FI-600 material was exposed to 1,400° F in a furnace for 16 hr and then fabricated into a joint model. This model was subjected to acoustic environments for a duration of 30 min with no observable damage or degradation of the FI-600 material. The evaluation is described in Section 3.7.3. Thermal conductivity measurements determined on a concurrent LMSC IRAD program for the FI-600 material indicate essentially equivalent properties when compared to the basic LI-1500 material. Preliminary results are presented in Table 3.3.1-1.

An analysis of the influence on total vehicle TPS weight was made utilizing the information gained from the fabrication (NAS 9-12083) of prototype panel No. 2 with LI-1500 tiles attached to aluminum substrate representing a primary structure. The completed prototype panel is shown in Fig. 3.3.1-1. The panel represents a 2 by 2 ft area of the shuttle TPS system. Weight considerations for this particular panel were as follows:

Weight of FI-666 Material	0.63 lb
Weight of Equivalent Volume of LI-1500	1.37 lb
Weight Savings per Square Foot Surface Area	0.19 lb

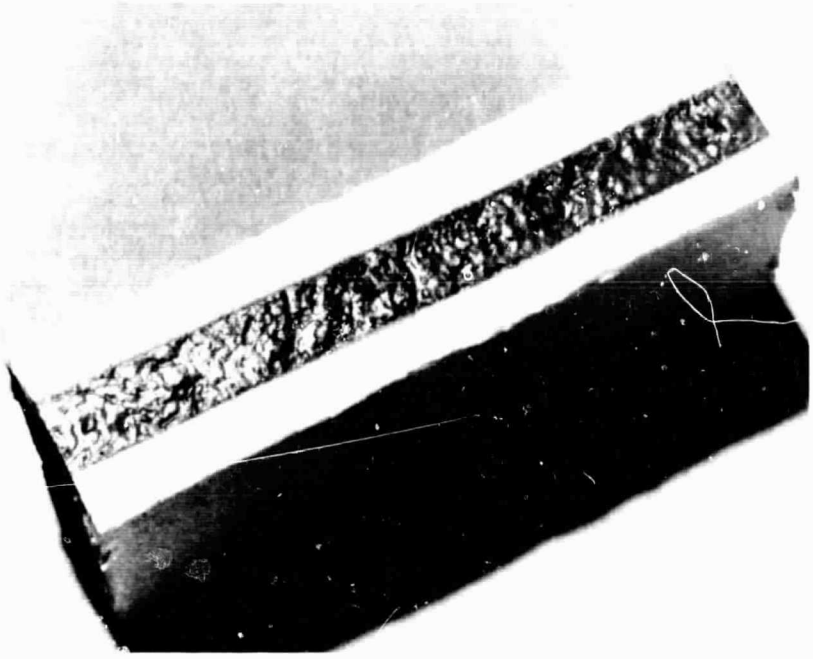

FI-600 Joint Strip With Coated Surface

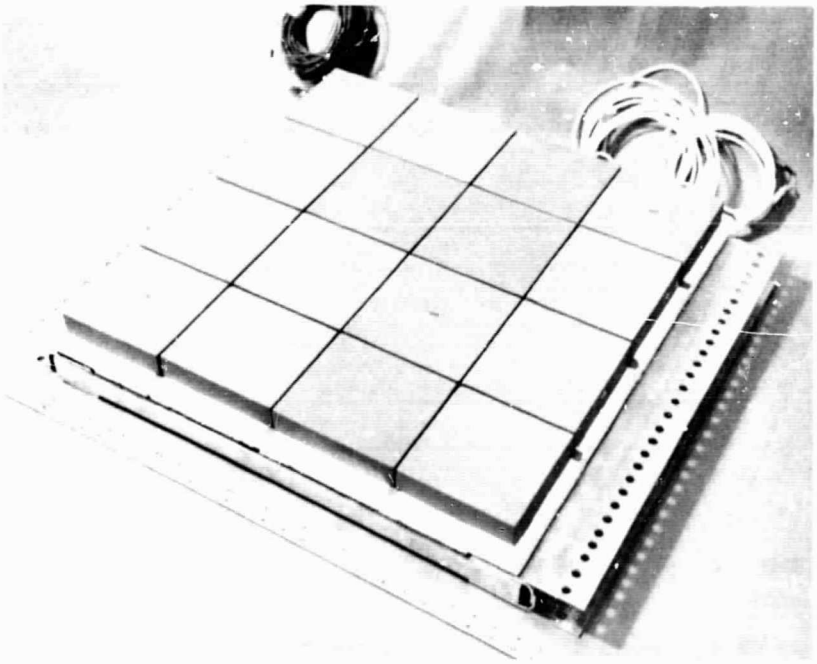

Prototype Panel No. 2 (NAS 9-12083) With FI-666 Joint Strips

Fig. 3.3.1-1 FI-666 Joint Strip

Table 3.3.1-1

LI-1500 AND FI-600 THERMAL CONDUCTIVITY MEASUREMENTS

Temp. (° F)	Pressure	Thermal Conductivity (Btu/in./ft^2-hr-° F)	
		FI-600	LI-1500
520	1 atm	0.48	0.45
1000	1 atm	0.83	0.70
1500	1 atm	1.16	1.15
520	1 mm Hg	0.108	0.25
1000	1 mm Hg	0.25	0.35
1500	1 mm Hg	0.42 (extrapolated)	0.47 - .55
520	10 mm Hg	0.30	–
1000	10 mm Hg	0.49	–
1500	10 mm Hg	0.82 (extrapolated)	–

Although the thickness of the FI-600 joint strip will vary with the thermal sizing of vehicle location and correspondingly influence the weights, a potential weight saving of 2,280 lb could be realized in a vehicle having 12,000 ft^2 of TPS surface area by direct substitution of FI-600 strips for the LI-1500 strips in current designs The savings would be even greater if the strips were sized specifically to take maximum advantage of this improvement.

3.3.2 Repair Technique for Coated LI-1500 Tile

Investigations were conducted to determine the feasibility of "in-field" repair of coated LI-1500 tiles. In-field repair techniques are needed when in-depth or similar damage occurs to the coated surface of the RSI tile assembled on the shuttle vehicle.

An in-field-type repair technique has been demonstrated. The results of using this technique are shown sequentially in Fig. 3.3.1-2. A 6 by 6 in. LI-1500/0042 coated tile damaged in-depth with the tip of a screwdriver is shown. The damaged area is

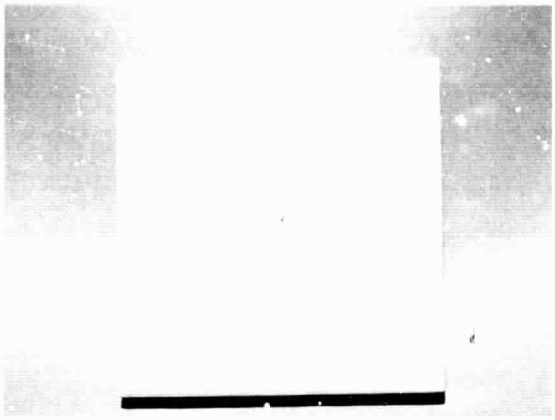

Damaged Tile

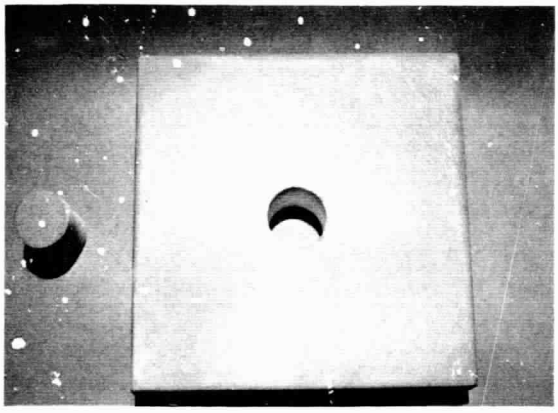

Tile With Damaged Section Removed
and Coated Repair Plug

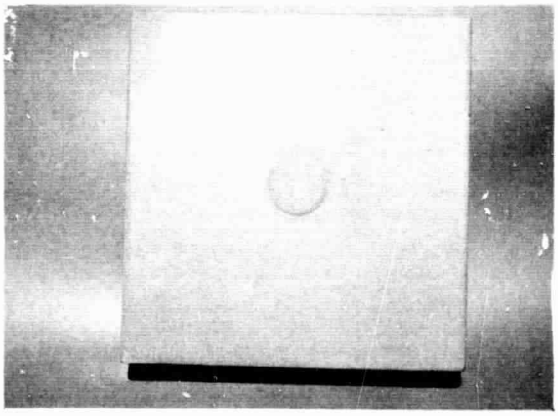

Repaired Tile

Fig. 3.3.1-2 Repair Sequence for Damaged RSI Tile

removed with a 1-in. hole saw utilizing a hand drill motor. An LI-0042 coated repair plug and the prepared tile are shown in the figure. The repaired tile with the plug in place and the coating re-applied for the final surface sealing is shown in the final photograph. A portable hand oxy-gas torch was used for the final coating re-application. No difficulty was experienced in cutting the coated tile or re-applying the coating. Exposure of the in-field repaired tile to a 2,500°F environment resulted in no visible detrimental effects.

For shuttle applications, several standard-size-diameter coated plugs could be prepared and stocked for immediate use. During in-field removal of the damaged tile sections, the cut would be made to match the required dimension of the particular standard stocked repair plugs. Repairs could be accomplished rapidly by this technique.

3.3.3 Elimination of Substrate Investigation

Design analysis conducted during this program and the companion NAS 9-12083 TPS Development indicated the desirability of improvement of the attachment concept. These desired areas of improvement included overall system simplification, strengthening of the RSI attachment interface, mechanical attachments, and considerations for strain isolation and reduction in system weight. The major effort for this phase of the program was redirected by NASA/MSC during contract midterm to be concentrated in the effort to achieve improved surface coatings and lower density RSI materials as described in Sections 3.4 and 3.6. However, certain laboratory investigations and analysis were conducted for the purpose of achieving technical data to aid future design considerations for improved attachment concepts. The results of the limited investigation and analysis conducted were as described in the following paragraphs.

3.3.4 Strengthening Attachment Interface

A limited investigation of various concepts to strengthen the LI-1500 RSI interface surface for improved attachment and strain isolation considerations was evaluated. These concepts included the strengthening of the LI-1500 by densification of the interface region with silica inorganic binder material and higher temperature capability organic resin systems and by use of reinforcement stiffeners such as wire screen and silica cloth.

The initial evaluation determined the apparent flexural properties as a function of density for the LI-1500 materials densified with the inorganic silica system and the organic resins. The use and results of the silica densification techniques to achieve varying densities and flexural properties are described in Section 3.4.2 supporting the integral coating study phase of the program. The test methods for apparent flexural property determinations were as described in Section 3.4.2. Three organic resin systems were selected for the evaluation for high temperature performance capabilities and for process compatibility with the LI-1500 material. These resin systems were:

- Dow Corning DC-805 silicone (phenylmethylpolysiloxane)
- Monsanto SC-1008 phenolic
- Monsanto Skybond 703 polyimide

The results of the tests are presented graphically in Fig. 3.3.1.3-1. For the preliminary evaluation, equivalent density (22 pcf) LI-1500/resin test specimens were prepared. The comparative flexural properties shown in the figure resulted in significantly higher strengths for the DC-805 resin system. No other work was done with the phenolic and polyimide resins during this program phase, and the DC-805 resin was used to obtain the flexural property-density relationship. Within the density range evaluated, the flexural properties increased linearly with the increase in density. Comparison of the LI-1500/DC-805 resin with the LI-1500/silica (Section 3.4.2) densified systems indicates a significantly higher flexural strength of an equivalent density basis for the resin than for the inorganic silica impregnated materials. At 30 pcf a 700-percent higher (1900 psi as compared with 270 psi) flexural strength is achieved with the resin system. Although the performance of the resin system must be maintained below the 600°F temperature range, the silica system performs successfully in regimes over 2,000°F. The higher mechanical properties of the resin system thought to be an indication of better load transfer capability may be advantageously utilized in future attachment design studies in interface areas where the lower temperatures are anticipated. The analysis of the influence of strengthening attachment interface surface density on the LI-1500 weight is presented in Fig. 3.3.1.3-2.

Two types of reinforcing stiffening concepts were evaluated for interface strengthening and strain isolation considerations. These were:

- Wire screen, 304 stainless, 16 mesh, 9 mil, 0.086 lb/ft^2
- "Quartz" cloth, "Astroquartz" style 582, 0.057 lb/ft^2

The wire screen was attached to LI-1500 specimen interface surfaces by adhesive bonding with the DC-805 resin and the RTV-560 silicone rubber. The flexural test specimens were prepared for test with the screen on the tension surface. The results are also presented in Fig. 3.3.1.3-1. The densities noted for these specimens are the overall densities of the 6-in. x 6-in. x 0.25-in. thick specimens. The DC-805 resin bonded system gave superior results when compared with the RTV-560 bonded system. Compared on the basis of equivalent densities, the screen/resin resulted in an approximate increase of 30 percent in apparent flexural strength over the LI-1500/DC-805

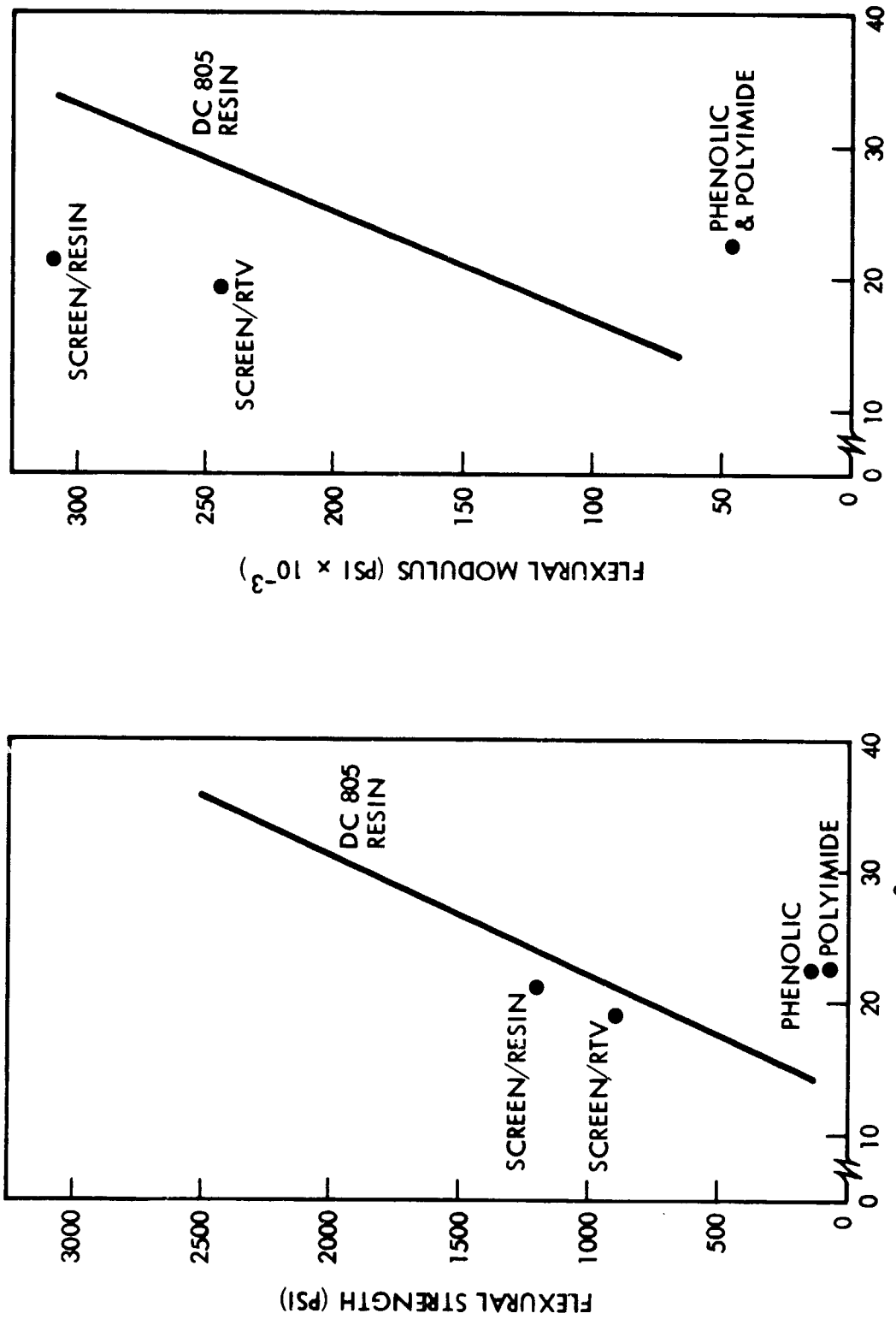

Fig. 3.3.1.3-1 Flexural Properties as a Function of Density for LI-1500-Type Material, Resin Impregnated

resin material. For comparison, the screen/resin concept thickness-density influence on the weight also is presented in Fig. 3.3.1.3-2.

The screen and cloth also were evaluated to obtain concept data for strain isolation considerations by bonding the reinforcement to the LI-1500 interface and loading in tension to failure through a smaller surface area pull tab. The test setup was as illustrated in Fig. 3.3.1.3-3. Both the RTV-560 and DC-805 adhesive bond systems were used. Results of the tests were as follows:

Reinforcement	Adhesive Bond	No. of Specimens Tested	Failure Load Avg. (lb)
"Quartz" Cloth	RTV-560	4	68
	DC-805	2	95
Wire Screen	RTV-560	2	74
	DC-805	4	104

All failures occurred in the LI-1500 material as shown in the photograph of the tested specimen in Fig. 3.3.1.3-3. Both the wire screen and the DC-805 resin exhibited their respective "stiffer" characteristics resulting in better load distribution and higher failure loads for this particular test.

3.3.5 Mechanical Attachment

Another strain isolation concept involved drilling and tapping of the LI-1500 material and the direct attachment through thread fasteners to the primary structure. Previous IRAD investigations demonstrated the machinability of the material (thread, joints, curvatures, etc.) and the strengthening of the material by addition of both organic and inorganic impregnants. A preliminary investigation was conducted to drill and tap the LI-1500 material, strengthen the threaded sections by organic and inorganic impregnants, and determine the pull-out force of this fastener concept. The DC-805 silicone resin was used as the organic impregnant. The threaded holes were readily machined into the LI-1500 material. For the organic impregnation, the resin was only applied locally to the threaded area and cured. Note that the weight of the resin added was approximately equal to the weight of the LI-1500 material removed from the threaded hole, thus achieving a zero net weight gain. The inorganic impregnation was applied throughout

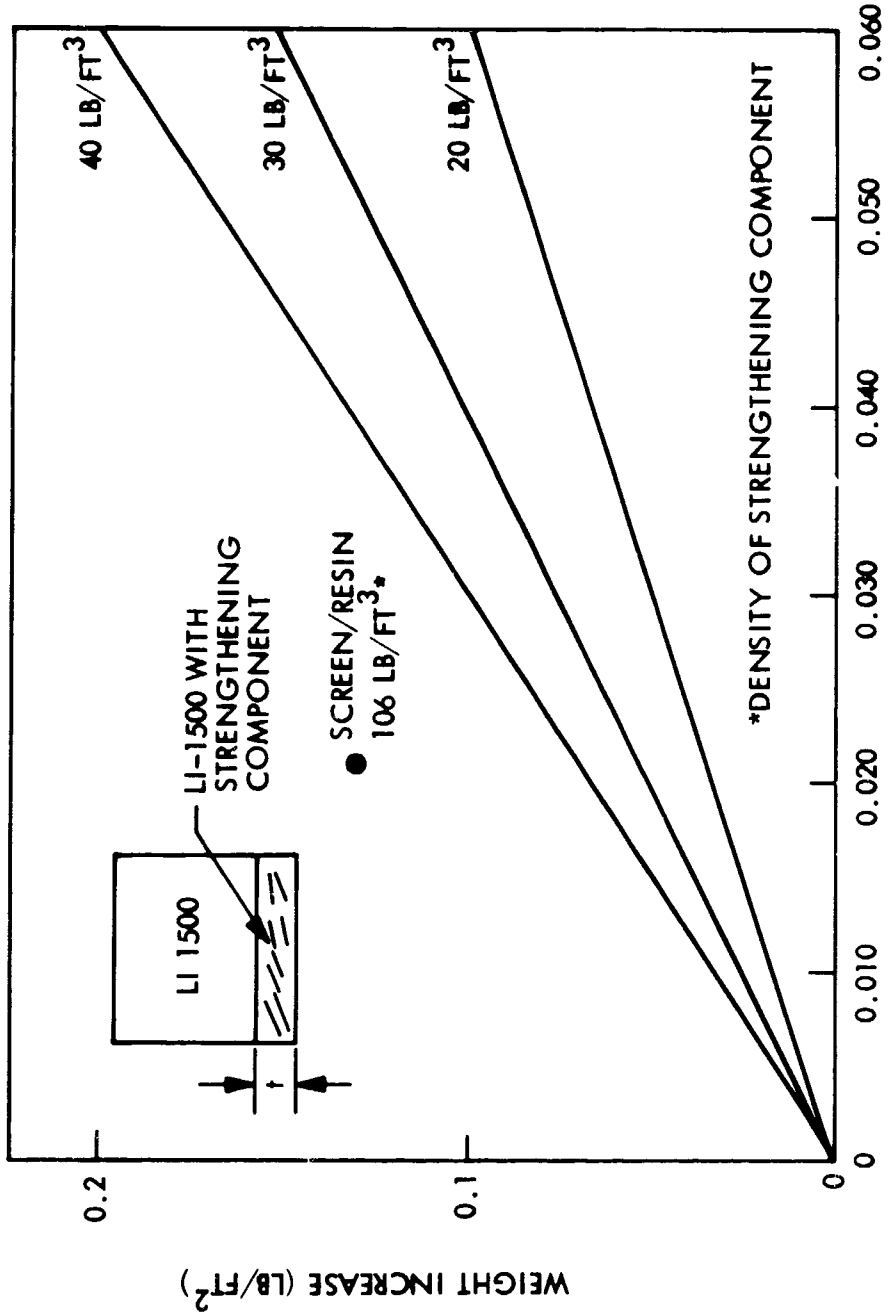

Fig. 3.3.1.3-2 Attachment Surface Strengthening Concept Evaluation Test

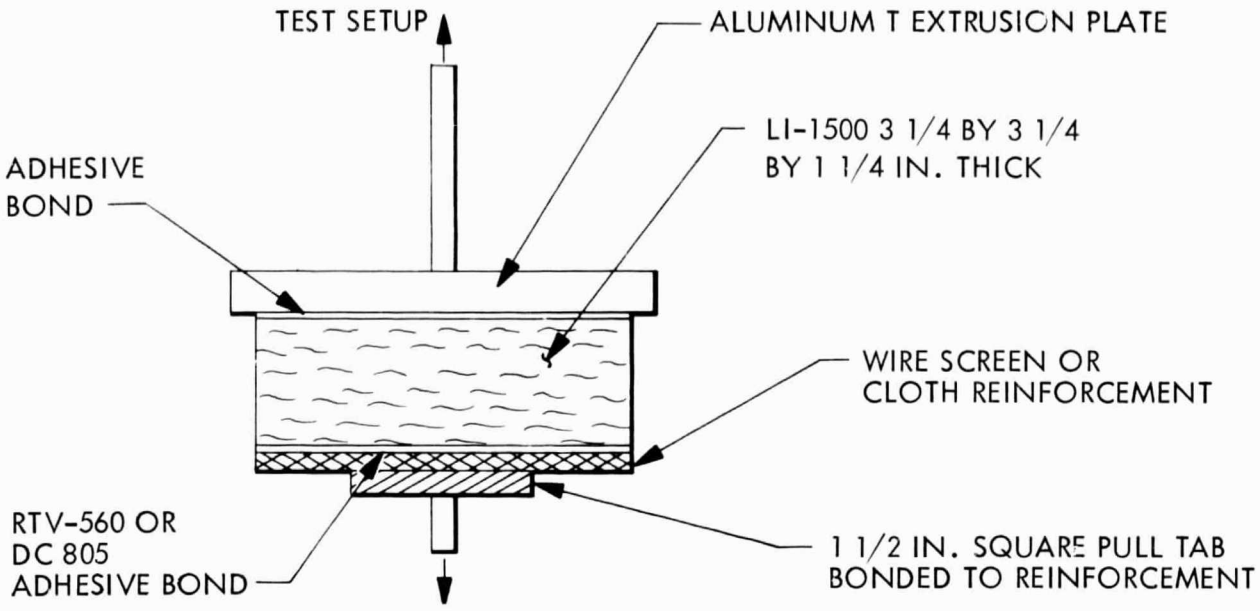

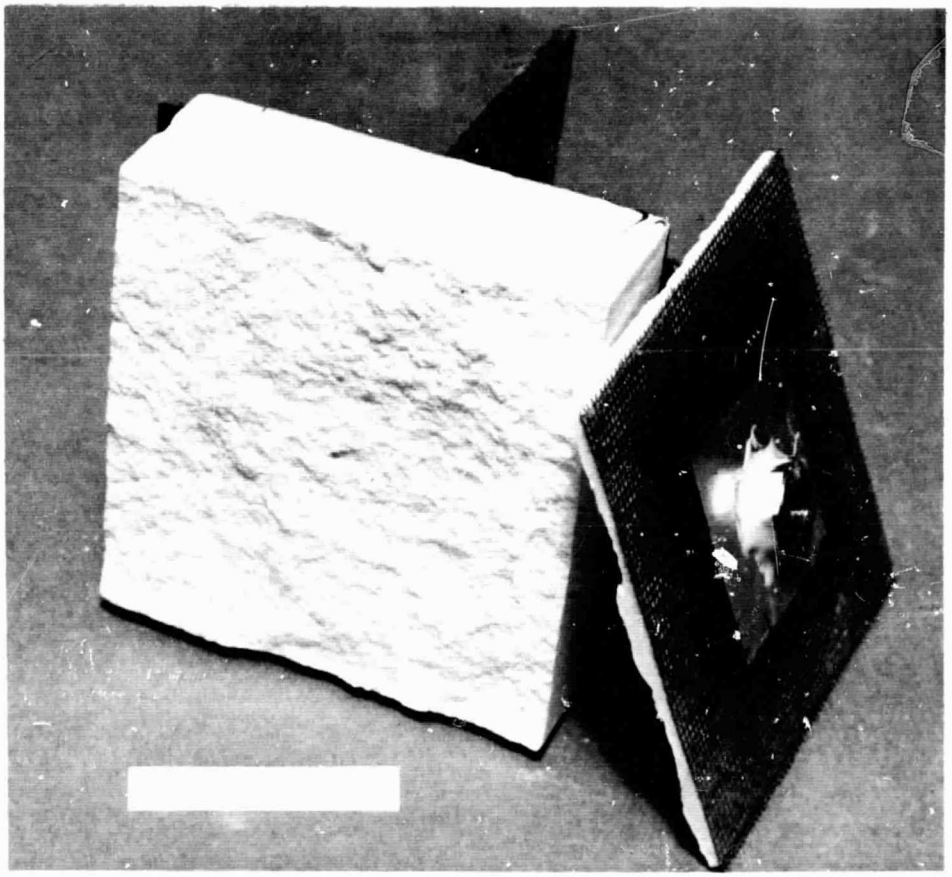

Fig. 3.3.1.3-3 Test Results – Mechanical Fastener With Local Reinforcement

the specimen, increasing the apparent bulk density of the LI-1500 specimens up to 27.5 lb/ft^3.

The test setup is illustrated in the following sketch.

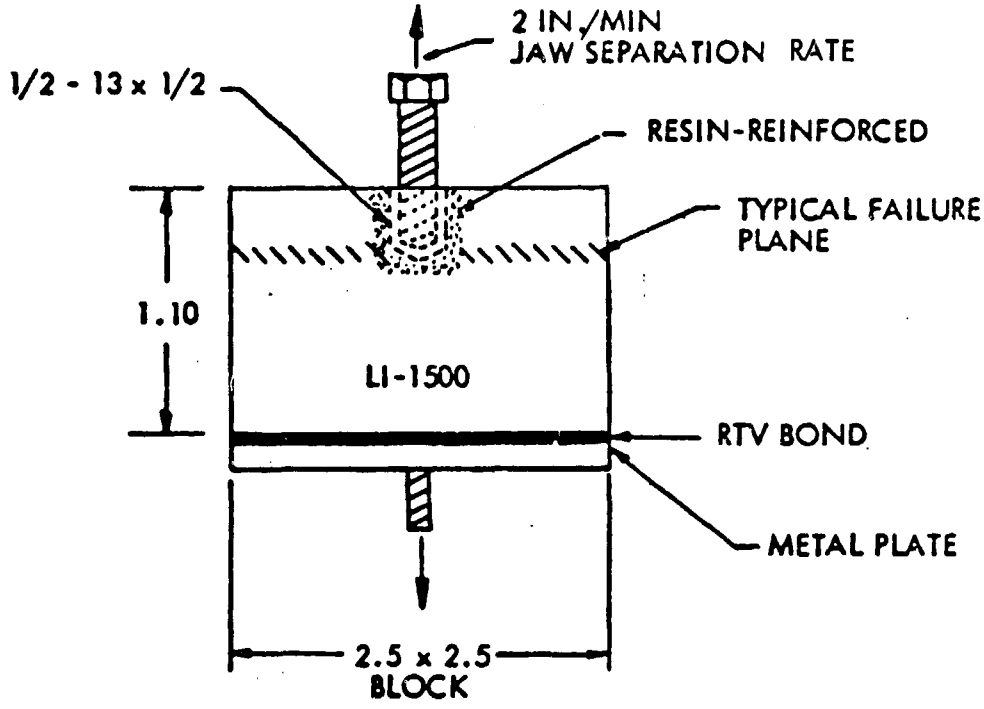

Results of the tests were as follows:

Reinforcement	No. of Specimens	Failure Load (lb)
DC-805 Resin	8	Avg. 31 Min. 29 Max. 40
Silica	2	125—127

All failure modes were similar; the typical failure plane is illustrated in the sketch. It is believed that significantly higher failure loads may be obtained

by use of higher resin concentrations. However, these preliminary results indicated that adequate strengths can be achieved by the LI-1500 with the mechanical fastener/local reinforcement concepts that may satisfy specific attachment design needs for the RSI system. Fabrication feasibility studies have shown that the threaded fasteners may be metallic, densified silica fibers, inorganically bonded oriented silica fibers, resin-impregnated silica fibers, elastomers, or a combination of any of these. Selection of any concept must be made with design considerations for both mechanical and thermal/physical property requirements for the particular application environment.

A consideration for RSI material attached by mechanical fasteners directly to a primary structure is the refurbishment or replacement of a particular tile as necessary. Various mechanical fastener concepts were presented and analyzed under Contract NAS 9-12083.* Of primary concern in many of the concepts is the ability to reach and work the fasteners from the external surface of the vehicle. To achieve this capability, a preliminary investigation was conducted utilizing the techniques developed for surface coating repair as described in Section 3.3. This technique demonstrated the capability of cleanly drilling through the 0042 coated LI-1500 tile, replacing the removed section with a pre-determined size coated plug, and resealing the plug-to-hole joint at the external surface with additional coating. The potential of "field" repair was also discussed (Section 3.3.2). The thermal response of this repair concept when exposed to reentry temperatures was presented in Section 3.3.1. For adaption to mechanical fastener attachment, the LI-1500 tiles may be predrilled with holes of applicable diameters located for specific fastener locations. After securing the fastener, the hole may be sealed by the techniques used for "field" repair. For removal or replacement of a particular tile, the "repair" technique may be used, i.e., drill-through to the fasteners, removal of the fastener, removal of the tile, replacement of the tile, securing of the fasteners, insertion of coated plugs, and final sealing. Specific location and/or type of fastener may be color coded by the plug coating containing a different emittance agent or with the permanent high temperature decal technique described in Section 3.4.3. With standardization of the drill holes, plugs of applicable dimensions may be stocked for immediate use. With this standardization and proper equipment, it is believed that the plug and reseal operation can be accomplished in minutes.

*Space Shuttle Thermal Protection System Development Final Report, LMSC-D152738.

A step-joint incorporated into the "repair" plug, to ensure that the thermal characteristics of the mounted tile are not degraded, is easily obtained.

Although much design and developmental work is needed before selection of the attachment systems most applicable for shuttle utilization, the LI-1500 RSI material system has the capability of modification and adaptability for specific shuttle TPS requirements.

3.4 COATING INVESTIGATION

The RSI material requires high temperature protective surface coatings which resist damage during installation and ground handling, prevents moisture intrusion, and exhibits the highest possible emissivity during shuttle orbit reentry. Requirements for the coating have evolved at LMSC over the past many years during evaluations of the LI-1500. For increased hardness, reduction of moisture pickup characteristics, and high surface emittance, an "add-on" ceramic coating was developed under IRAD programs. This ceramic coating was a borosilicate formulation with an admixture of chromium oxide for emittance purposes. This green coating was designated as "LI-0025" and served as a standard protection for the LI-1500 surface and was used in the TPS applications studies conducted under Contract NAS 9-11222 for NASA/MSC. During this contract it was determined that it would be necessary to improve the coating properties for the new anticipated shuttle requirements. The LI-0025 coating was utilized as the baseline material for comparison for this coating improvement investigation. The properties of the baseline coating material were previously presented in Section 3.1.

The objectives of the coating investigations were as follows:

- Conduct investigations to decrease modulus of coating and increase strain-to-failure by graded densification of the LI-1500 to provide an integral coating and/or placement of discontinuities in added coatings to provide strain relief.
- Improve emissivity of coatings by use of new emissivity agents, or more effective use of existing emissivity agents.
- Achieve water impervious coatings by modification of current coatings or development of new ceramic and/or overglaze coatings. Coating to remain water impervious after exposures of 2,300°F and 2,500°F.
- Improve the coating to achieve reuse capabilities of 100 space shuttle missions to 2,300°F and 2,500°F peak reentry heating.

- Develop application techniques necessary to coat tiles of relatively large surface areas as well as intricate geometries.
- Develop coating requirements with a minimal weight penalty to the overall RSI system.

SUMMARY OF ACCOMPLISHMENTS

- The investigations resulted in a borosilicate silicon carbide (SiO_2-B_2O_3-SiC) surface coating system identified as LI-0042 as the preliminary coating improvement. The 0042 coating successfully performed in cyclic heating environments of 2,500°F for 100 simulated shuttle missions.
- The 0042 coating retained its high emissivity characteristics after repeated thermal cycling environments, successfully performed in rain erosion environments, remained impervious to salt spray cyclic conditions, contributed a relatively low weight penalty to the overall RSI system.
- The LI-0042 coating exhibited reproducibility in application in over 100 test tiles fabricated for evaluation of Contract NAS 9-12083.
- Although water impervious after cyclic exposures to 2,300°F, the 0042 coating after continuous cyclic exposures at 2,500°F showed indications of some loss of its water impervious characteristics.
- A further improved coating for this program identified as LI-0045 was developed to be water impervious after cyclic heating to 2,500°F. The formulation and performance of this coating was essentially the same as that for the LI-0042 coating.
- Interim specifications and formulations for the LI-0042 and LI-0045 coatings have been prepared and are presented as an addendum to selective issues of this report for NASA/MSC.

3.4.1 Emissivity Investigations

The elevated temperature emittance of the baseline LI-0025 has been determined to range between a maximum of 0.70 and a minimum of 0.47 at 2,000° F (Ref. MSC-02567, LMSC-A984200). The values predicted for 2,500°F are lower. For lowering the surface peak temperature isotherms, the highest emissivity is desired.

As an illustration of the importance of emissivity, plots of hot-wall heat flux versus equilibrium temperature at various coating emittances are shown in Fig. 3.4.1-1. From these curves, it can be seen that the thermal performance of the RSI is highly dependent upon the surface emittance. For example, at hot-wall heat flux of 15 Btu/ft^2-sec, the equilibrium surface temperature for a coating emittance of 0.4 is 2,550°F, whereas for an emittance of 0.8 it is 2,050° F.

This portion of the effort was to select candidate emissivity agents which could be incorporated into the coating for improved emissivity properties without compromising other requirements such as elevated temperature stability and compatibility with the LI-1500 and coating system.

Emittance Behavior at Elevated Temperature. The total emittance of a nongray (spectrally selective) surface material or coating is usually temperature dependent and is determined by the spectral emittance characteristics of the surface at each temperature over a wavelength region. The spectral emittance property is also temperature dependent. However, for a thermally stable nonreactive surface, most of the changes that occur in total emittance with changing temperature can be attributed to changes in the wavelength region over which the spectral emittance values must be integrated. The wavelength interval of importance for each temperature is designated by the blackbody energy distribution curve (Planck's function) for that temperature (Fig. 3.4.1-2).

At high temperatures (i.e., >1500°F), the wavelength region of primary importance is the 1-micron to 5-micron region. For a coating to have a high total emittance at these temperatures, it must necessarily have a high average spectral emittance value at these wavelengths. This is illustrated by the spectral distribution curve in Fig. 3.4.1-2 which shows how the blackbody energy distribution peak shifts to shorter wavelengths with increasing temperature. The radiant energy distribution at various temperatures is shown in Table 3.4.1-1.

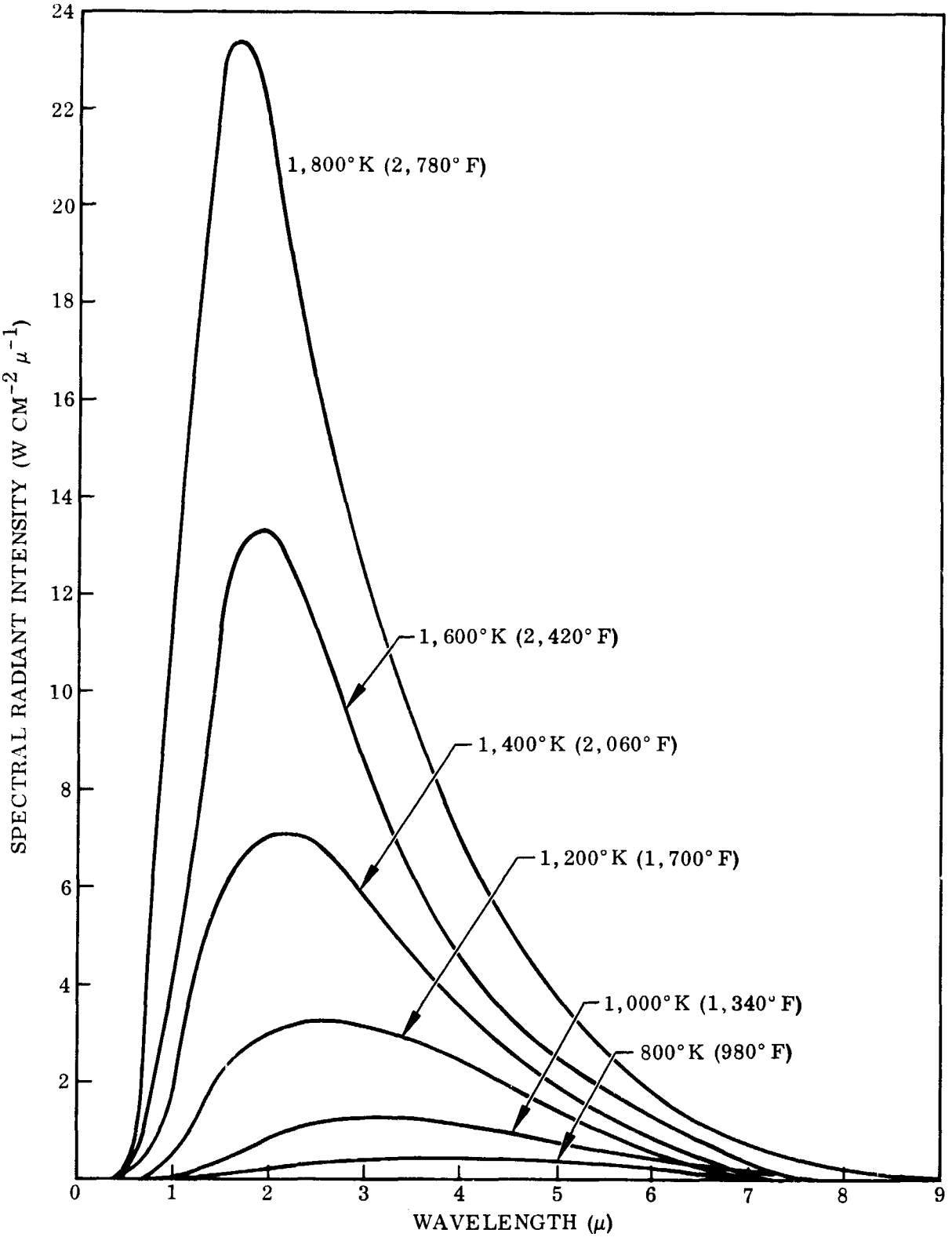

Fig. 3.4.1-2 Spectral Energy Distribution of Blackbody at Various Temperatures

Table 3.4.1-1

RADIANT ENERGY DISTRIBUTIONS FOR A BLACKBODY AT SIX DIFFERENT TEMPERATURES

Blackbody Temperature (°F)	Percentage of Total Blackbody Energy Radiated At Wavelengths Shorter Than —					
	$\lambda = 1\mu$	$\lambda = 2\mu$	$\lambda = 3\mu$	$\lambda = 4\mu$	$\lambda = 5\mu$	$\lambda = 6\mu$
70	0	0	0	0	1	27
500	0	0	2	9	20	68
1000	0	2	15	33	49	86
1500	0	10	33	55	69	93
2000	1	21	50	69	80	96
2500	2	34	63	78	87	98

At room temperature (70°F), the table indicates that only 1 percent of the total energy is radiated at wavelengths shorter than 5 microns. At 1,500°F, however, 69 percent of the energy radiated by a blackbody is at wavelengths shorter than 5 microns, and only 7 percent is radiated at wavelengths longer than 6 microns. At 2,500°F, more than 85 percent of the total energy is radiated at wavelengths between 1 and 5 microns. These illustrations show that it is quite possible for a coating to have a high total emittance at room temperature but to drop to a low emittance value at high temperatures because of the different spectral regions involved. For this reason, total emittance measurements at room temperature (e.g., emissometer readings) are of no value for indicating the high temperature emittance properties of a surface.

It also should be noted that more than 30 percent of the solar energy spectrum occurs at wavelengths longer than 1 micron. Therefore, it is impossible to obtain a coating which will have both a high temperature total emittance value and a low solar absorptance value.

High temperature emittance values can be predicted with some validity using room temperature spectral reflectance data. This approach is valid provided there is no reaction within the coating or between coating and substrate at the elevated temperature to yield some new species.

Potential Candidate Materials. Initial effort in this emissivity investigation was to rapidly screen potential candidate materials through literature.

The criteria used for initial selection were as follows:

- Total emittance greater than 0.7 at elevated temperatures (2,000-2,500°F).
- Elevated temperature oxidation stability.
- Reasonable expectation of compatibility with LI-1500.

References covered for this effort were Chemical Abstracts, 1966-70, "Thermo-Physical Properties of High Temperature Solid Materials," Y.S. Toukoukian, Editor, six volumes, Macmillan (1971); and several other bibliographies related to materials emittance and emittance measurements. A number of potentially useful materials were selected based upon apparent compatibility with LI-1500 coating requirements.

Based upon criteria listed above , and spectral emittance characteristics required of the high temperature emissivity agents, i.e., high emittance in the 1 to 5 micron range, several candidate materials were selected. These are listed together with pertinent data in Table 3.4.1-2. Data were not available for all materials at the temperature range of interest. In these cases, lower temperature information is presented.

From the list, chromium oxide, cobalt oxide, and silicon carbide were selected for immediate evaluation because they were readily available commercially and were stable at elevated temperatures of interest. Materials such as boron silicide with questionable availability and probable high cost and those with marginal emittance and oxidation stability at elevated temperatures were dropped from further consideration.

Other materials selected for further consideration were nickel oxide, silicon nitride, iron titanate, and nickel-chrome-spinel.

LMSC Spectral Reflectance Measurements. All of the candidate emissivity agents from the literature survey and those generated from the concurrent coating formulation study were evaluated for room temperature spectral reflectance properties.

Table 3.4.1-2

HIGH-TEMPERATURE, HIGH-EMITTANCE PIGMENT/FILLER CANDIDATES FOR LI-1500 COATINGS

Candidates	Formula	Density (g/cc)	Normal Spectral Emittance	Temperature °K(°F)	Ref.* Touloukian, 1967
Boron silicide	B_6Si	1.32	>0.8	1223 (1742)	V.6 p.377
Silicon carbide	SiC	2.32	>0.9	1358 (1985)	V.5 p.135
Silicon nitride	Si_3N_4	1.82	>0.75	1223 (1742)	V.5 p.553
Tantalum nitride	TaN	16.3	0.4 to 0.8, varies with preparation and atmosphere.	1648 (2507) and higher	V.5 p.569
Chromium oxide	Cr_2O_3	3.15	Two sets of data: 0.8 to 0.97 0.6 to 0.7	1273 (1832)	V.4(1) p.138
Nickel oxide	NIO	5.32	0.7 to 0.8	1273 (1832)	V.4(1) p.310
Ferrosoferric oxide	$FeO \cdot Fe_2O_3$	5.2	0.6 to 0.75	1273 (1832)	V.4(1) p.715
Lucalox ceramic	α-Al_2O_3 filled with MgO to control grain size		0.85 to 0.95	813 (1004)	V.4(1) p.32
$Al_2O_3 + Cr_2O_3$	50 Al_2O_3/50 Cr_2O_3 by weight	-	at 1-5 microns 0.6 ± 0.1	1273 (1832)	V.4(1) p.605
Al_2O_3 + NiO	50 Al_2O_3/50 NiO	-	at 1-5 microns 0.75 ± 0.05	1273 (1832)	V.4(1) p.609
$Cr_2O_3 + Y_2O_3$	50 Cr_2O_3/50 Y_2O_3, data same for 5, 10, 30 Y_2O_3	-	at 1-5 microns 0.7 ± 0.1	1273 (1832)	V.4(1) p.689
Aluminum silicate glass	Corning 1723A		normal total 0.85 ± 0.05	100 -1000° K (-460 to 1341)	V.4(2) p.1679
Chrome-magnesite firebrick	-	-	normal total 0.7 ± 0.1	1100 - 1800° K (1521 to 2781)	V.5 p.1039
Silica brick	"Silicrete"	-	normal total 0.7 ± 0.1	1100 - 1800° K (1521 to 2781)	V.5 p.1041
$Cr_2O_3 + MoSi_2$	50 Cr_2O_3/50 $MoSi_2$	-	1 - 5 microns 0.73 ± 0.06	1273 (1832)	V.5 p.769
Al phosphate on nickel* (water slurry)	-	-	hemispherical total 0.7 ± 0.1	407 - 874° K (273 to 934)	V.6(2) p.1429
Cobalt oxide on tantalum (plasma spray)	-	-	normal total 0.75 ± 0.05	1000 - 1600° K (1341 to 2421)	V.6(2) p.1373
Iron titanate on niobium (plasma spray)	-	-	hemispherical total 0.85 ± 0.05	650 - 1400° K (711 to 2061)	V.6(2) p.1385
Nickel chromie spinel* on niobium (plasma spray)	$NiO \cdot Cr_2O_3$	-	hemispherical total 0.87 ± 0.03	420 - 1400° K (297 to 2061)	V.6(2) p.1387
Rokide C on titanium (flame spray)	proprietary chromia	-	normal total 0.8 ± 0.05	1000 - 1500° K (1341 to 2241)	V.6(2) p.1345
$TiO_2 + Al_2O_3$ on molybdenum (plasma)	50 TiO_2/50 Al_2O_3	-	hemispherical total 0.9 ± 0.05	447 - 1000° K (345 to 1341)	V.6(2) p.1395

*Long term stability in air not reported

Measurements were made at wavelengths between 0.28μ and 25μ to indicate the spectral reflectance characteristics of the coatings (at room temperature) and to determine their solar absorptance (α_s); total normal emittance at room temperature (ϵ_{TN}) (70° F); and a prediction of their total emittance values at elevated temperatures.

Measurements were made with three different reflectometers:

1) A Cary Model 14 Spectrometer with an Integrating Sphere Reflectance attachment. This instrument measures the reflectance of opaque, room temperature surfaces at wavelengths between 0.28μ and 1.8μ. The resulting reflectance curves can then be used to determine α_s, assuming that the condition $\alpha_\lambda = 1 - R_\lambda$ is satisfied.

2) A Gier-Dunkle Model DB-100 Infrared Reflectometer. This instrument measures the total infrared reflectance of opaque, room temperature surfaces. Total room temperature emittance is inferred from the relationship $E_T = 1 - R_T$.

3) A Gier-Dunkle Model HC300 Heated Cavity Reflectometer (GDHC). This instrument is used in conjunction with a Perkin-Elmer Model 98 Monochromator, equipped with both NaCl and KBr prisms, to measure the near-normal spectral reflectance of opaque, room temperature (water-cooled) samples at wavelengths between 1.5μ and 25μ.

Three different methods of coating preparations were used and are as follows:

1) Spray Coating on Aluminum – This was used chiefly to obtain reflectance properties of a candidate material for use as emissivity agent. Specimens prepared in such a manner were easy to mount and cool in the heated cavity.

2) Coating Scraped Off LI-1500 – This was prepared by carefully scraping the LI-1500 with an X-Acto knife or sandpaper, but complete removal was difficult. Residual LI-1500 on the back – a good insulator – prevented, at times, efficient cooling in the heated cavity. This resulted in the detector reading both the reflectance and the emittance from the heated coating. Added together, these readings gave inordinately high reflectance value.

3) Coating cast as free film – To circumvent the problem of specimen heating in the cavity. This method was used on some specimens, but a flat disk was difficult to obtain. The edges tended to curl up. This concave surface resulted in some discrepancy between the readings of Cary and those of GDHC in the overlapping region between 1.5 μ and 1.8 μ. Where the discrepancy was large, the data from GDHC, which are considered more reliable in this region, were used.

Predicted total normal emittance values were obtained by numerically integrating the spectral emittance (1 - Rλ) curves over the appropriate region associated with the blackbody energy distribution curve for each temperature.

In Tables 3.4.1-3 and 3.4.1-4 are presented the solar absorption (α_s), total emittance at room temperature, and predicted emittance at various temperatures.

As indicated earlier, these predictions of emittance at elevated temperatures are based on the assumption that the spectral emittance characteristics are not temperature dependent. The main value of the table is in indicating total emittance trends that can be expected to occur with increasing temperature because of the nongray spectral emittance characteristics of the material as observed at room temperature.

Table 3.4.1-3 lists coatings of various emissivity agents, excluding silicon carbide. (Silicon carbide containing formulations will be discussed later.) The table shows that there are several emissivity agents that are potentially superior to the baseline chromium oxide at elevated temperature (2,000° F). These are cobalt oxide, iron titanate, mixed cobalt oxide – iron oxide – chromium oxide, nickel chrome spinel, and cobalt oxide – chromium oxide stain. When silicon carbide is included in this list, there are six emittance agents offering improved properties over the baseline Cr_2O_3.

The apparent discrepancy in the values of formulations containing nickel oxide is presumably caused by different oxidation states of nickel. In the formulation containing 50-percent nickel oxide, the specimen was fired to only 1,000° F, whereas on the other two

Table 3.4.1-3

EMITTANCE AND ABSORPTANCE VALUES OF VARIOUS FORMULATIONS
(EXCLUDING SILICON CARBIDES) FROM ROOM TEMPERATURE REFLECTANCE MEASUREMENTS AT LMSC

Coating Composition			Solar Absorptance	Total Emittance	Predicted Total Normal Emittance Values (°F)					
Emissivity Agent	Percent Used	Matrix	α_s	(DB-100)	70	500	1,000	1,500	2,000	2,500
Cr_2O_3	8	Borosilicate	0.69	0.89	0.86	0.85	0.79	0.71	0.67	0.60
CoO	8	Borosilicate	0.85	0.89	0.90	0.92	0.90	0.89	0.86	0.86
Si_3N_4	50	Silica	0.43	0.84	0.90	0.80	0.67	0.58	0.52	0.46
H_fO	50	Silica	0.32	0.82	0.86	0.73	0.60	0.51	0.44	0.38
Fe_2TiO_5	50	Silica	0.88	0.85	0.88	0.86	0.84	0.84	0.83	0.83
$CoO-Fe_2O_3-Cr_2O_3$	50	Silica	0.91	0.84	0.88	0.79	0.73	0.72	0.73	0.74
$NiO-Cr_2O_3$	50	Silica	0.94	0.88	0.91	0.88	0.86	0.86	0.87	0.88
$NiO-Cr_2O_3$	20	Borosilicate	0.87	0.84	0.86	0.87	0.86	0.84	0.83	0.82
$CoO-Cr_2O_3$ [a]	5	Borosilicate	0.70	0.83	0.74	0.78	0.73	0.69	0.66	0.66
$CoO-Cr_2O_3$ [b]	5	Borosilicate	0.69	0.85	0.86	0.88	0.89	0.88	0.86	0.85
NiO [c]	50	Silica	0.95	0.87	0.90	0.87	0.86	0.87	0.88	0.90
NiO [d]	5	Borosilicate	0.70	0.84	0.86	0.87	0.82	0.76	0.71	0.67
NiO [d]	20	Borosilicate	0.78	0.83	0.87	0.85	0.78	0.72	0.68	0.66

a. Low CoO
b. High CoO
c. Low Fired Coating (1,000°F)
d. High Fired Coating (2,500°F)

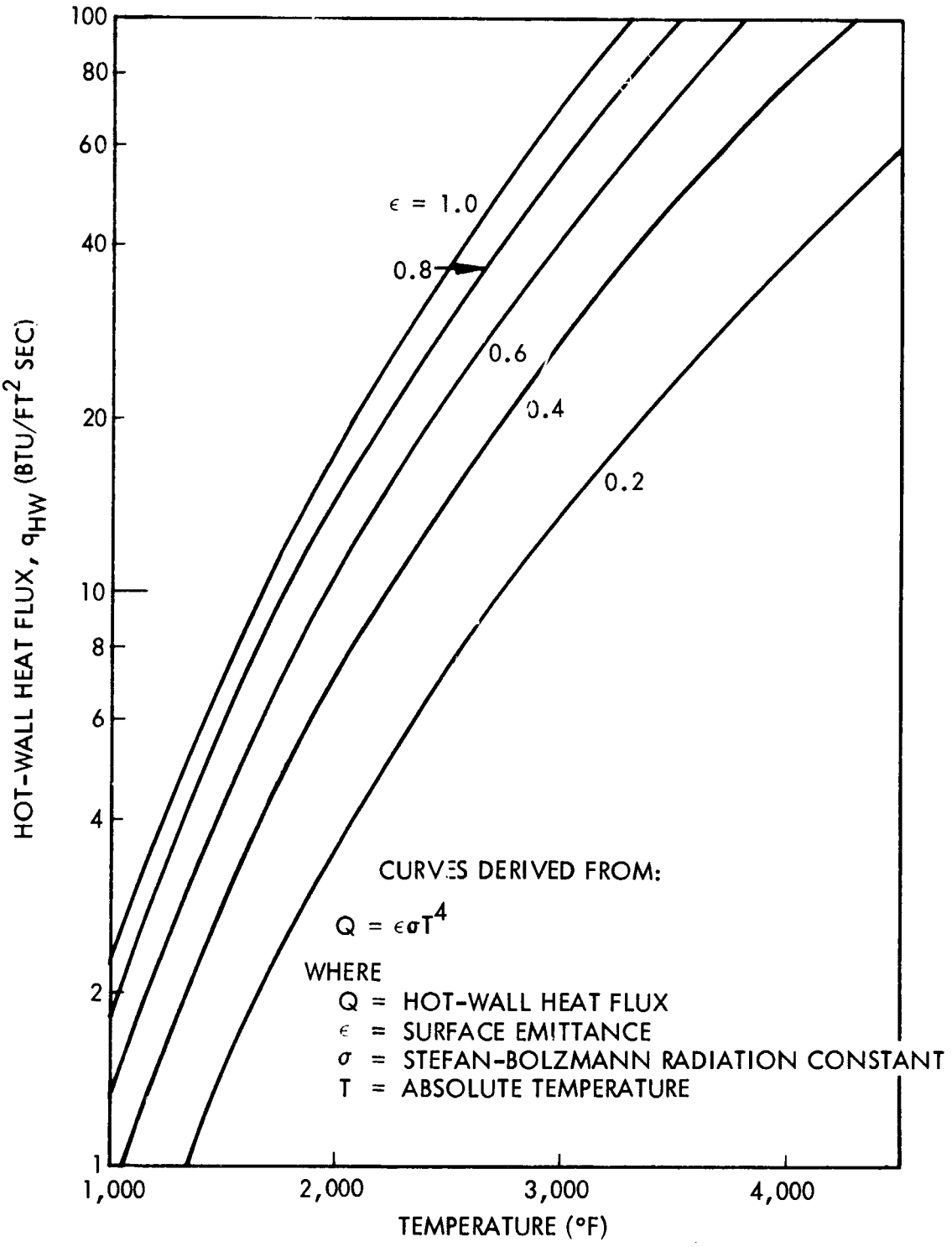

Fig. 3.4.1-1 Effect of Emittance on Equilibrium Surface Temperature for a Given Heat Flux

formulations, the coating was fired to 2,500°F. The differences also were noted visually as the low fired specimen was black whereas the high fired specimens were light green in color. From these results, nickel oxide is considered to be somewhat unstable at elevated temperatures.

The large differences in room temperature total emittance value between that of DB100 and that calculated from spectral reflectance data for cobalt oxide – chromia stain with low cobalt oxide content is probably caused by the insulating effect of the LI-1500 in the heated cavity.

Based on these results the emissivity agents in Table 3.4.1-2 are rated in the following order:

1. Cobalt Oxide – excellent emittance (0.90 ~ 0.86) up to 2,500°F, some reactivity with LI-1500 at peak temperatures - cobalt silicate detected
2. Cobalt Oxide - Chromia Stain with high CoO – excellent emittance up to 2,500°F, attractive blue color
3. Nickel Chrome Spinel ($NiO \cdot Cr_2O_3$) – excellent emittance, marginal opacity in borosilicate
4. Iron Titanate (Fe_2TiO_3) – excellent emittance, poor opacity in borosilicate
5. Cobalt Oxide - Iron Oxide Chromium Oxide Stain ($CoO - Fe_2O_3 - Cr_2O_3$) – good, better than Cr_2O_3
6. Nickel Oxide (NiO) – about same as Cr_2O_3 when high fired, questionable stability
7. Cobalt Oxide - Chromia Stain ($CoO - Cr_2O_3$) with low CoO – equal to Cr_2O_3
8. Silicon Nitride (Si_3N_4) – poor
9. Hafnium Oxide (HfO) – poor

Coatings with Silicon Carbide. As it was established early in the program that silicon carbide was the most effective emissivity agent for the LI-1500 RSI system, much of the work on emissivity was concentrated on this material. Pertinent data from reflectance measurements are presented in Table 3.4.1-4. (NOTE: Subsequent measurements at TRW indicated these values to be conservative.) The data in the table show the following:

(1) Concentration of silicon carbide may range from 4 percent to 50 percent in a borosilicate or silica matrix with very little effect on its excellent emittance properties. Figure 3.4.1-3 shows spectral reflectance of three borosilicate coatings with silicon carbide contents of 4, 5, and 10 percent. Note that the curves parallel and superimpose on each other. Relatively low reflectance in the wavelength region of 1μ to 5μ indicates that silicon carbide is a good emitter in this range. (NOTE: $1 - R_\lambda = \epsilon_\lambda$, which corresponds to the high radiant energy spectrum of the blackbody at elevated temperatures.) (See Fig. 3.4.1-2.)

(2) Silicon carbide particle size may vary from 600 to 1,200 grits with little effect, but fine particles size such as 7 μ are detrimental. As shown in Fig. 3.4.1-4, 7 μ silicon carbide shows considerable reflectance in the 1 μ to 5 μ range. Strictly from an emissivity consideration, it appears that coarser particles are better, but the practicality of producing a useful coating with such coarse grit obviates the use of such materials.

(3) Thermal and vacuum exposure equivalent to 120 cycles at perturbed area 2 has no effect on emittance properties As noted in Table 3.4.1-4, the predicted emittance of the 0042 coating at elevated temperatures remained unchanged after four hours exposure at 2,300°F, 10 Torr vacuum. The low emittance value of the exposed 0042 specimen may be attributable to the heating of the specimen in the heated cavity. This is indicated by the large differences in the room temperature values between that of DB-100 and that calculated (0.84 vs. 0.72). The spectral reflectance curve in Figure 3.4.1-5 shows that the exposed specimen is somewhat lower in reflectance in 1μ to 5μ range but higher reflectance in the 10μ to 19μ range is indicated. This apparently higher reflectance is probably the sum energy of inherent reflection and emittance caused by the heating.

(4) Overglaze may be applied over 0042 with no deleterious effect even after thermal exposure equivalent to 100 flights (4 hr at 2,300°F, 10 Torr vacuum).

(5) 0045 Coating (a variant of the LI-0042 coating for 2,500°F operation) has emittance properties equal to 0042.

Table 3.4.1-4

EMITTANCE AND ABSORPTANCE VALUES OF VARIOUS SILICON CARBIDE SYSTEMS FROM ROOM TEMPERATURE MEASUREMENTS AT LMSC RESEARCH LABORATORY

Coating Composition	Solar Absorptance α_s	Total Emittance (DB-100)	Predicted Total Normal Emittance Values (°F)					
			70	500	1,000	1,500	2,000	2,500
4% SiC in borosilicate	0.80	0.85	0.86	0.87	0.89	0.88	0.88	0.87
5% SiC in borosilicate (0042)	0.79	0.85	0.85	0.87	0.88	0.87	0.86	0.86
8% SiC in borosilicate	0.85	0.89	0.90	0.92	0.90	0.89	0.86	0.86
10% SiC in borosilicate	0.85	0.84	0.86	0.88	0.90	0.90	0.90	0.90
50% SiC in silica	0.85	0.85	0.88	0.89	0.90	0.91	0.90	0.90
600 grit SiC in borosilicate	0.86	0.86	0.87	0.89	0.90	0.92	0.92	0.92
1200 grit SiC in borosilicate	0.77	0.85	0.85	0.87	0.88	0.87	0.86	0.86
7μ SiC in borosilicate	0.69	0.84	0.83	0.85	0.84	0.82	0.80	0.78
0042 coating with clear borosilicate overglaze	0.80	0.89	0.84	0.87	0.89	0.88	0.87	0.87
0042 coating with overglaze after 4 hr at 2,300° F, 10 Torr, vacuum	0.81	0.84	0.85	0.87	0.88	0.87	0.87	0.86
0042 coating after 4 hr at 2,300° F, 10 Torr, vacuum	0.85	0.84	0.72	0.79	0.84	0.86	0.87	0.88
0045 coating	0.75	0.88	0.90	0.91	0.90	0.88	0.86	0.85

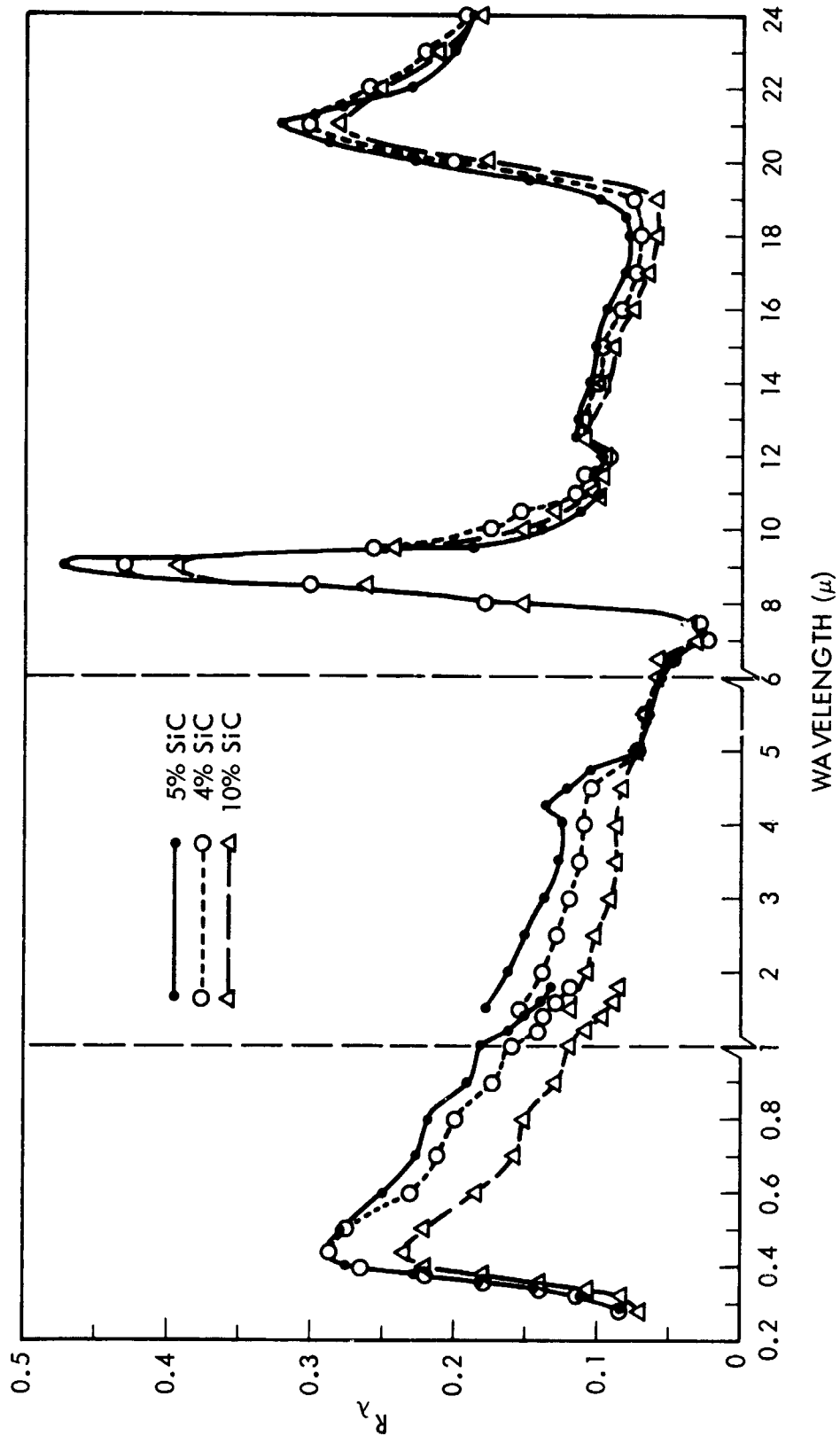

Fig. 3.4.1-3 Spectral Reflectance (at 75°F) of Three SiC/Borosilicate Coatings With Various Concentrations of SiC

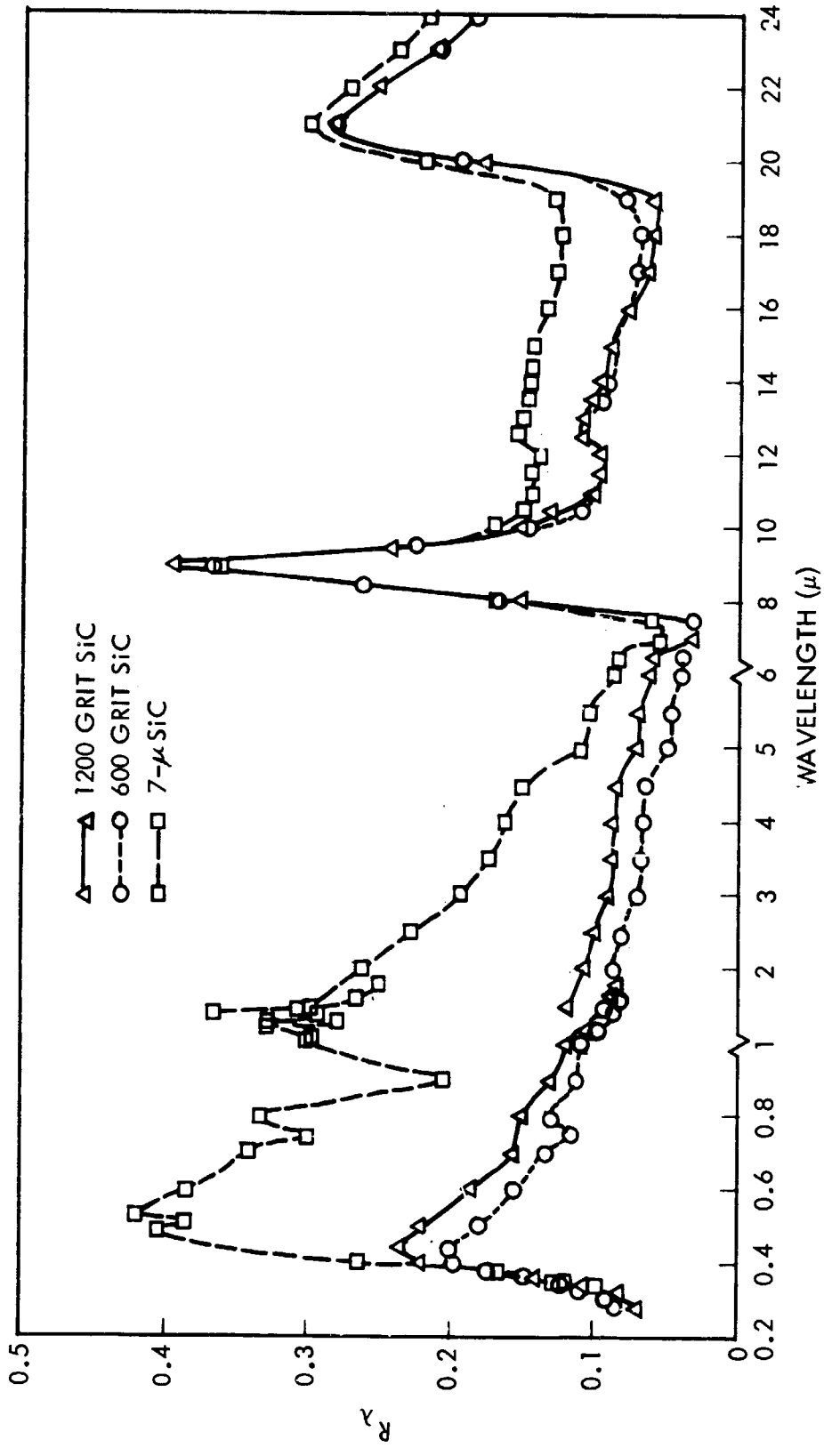

Fig. 3.4.1-4 Spectral Reflectance of Three SiC/Borosilicate Coatings With Various SiC Grit Sizes

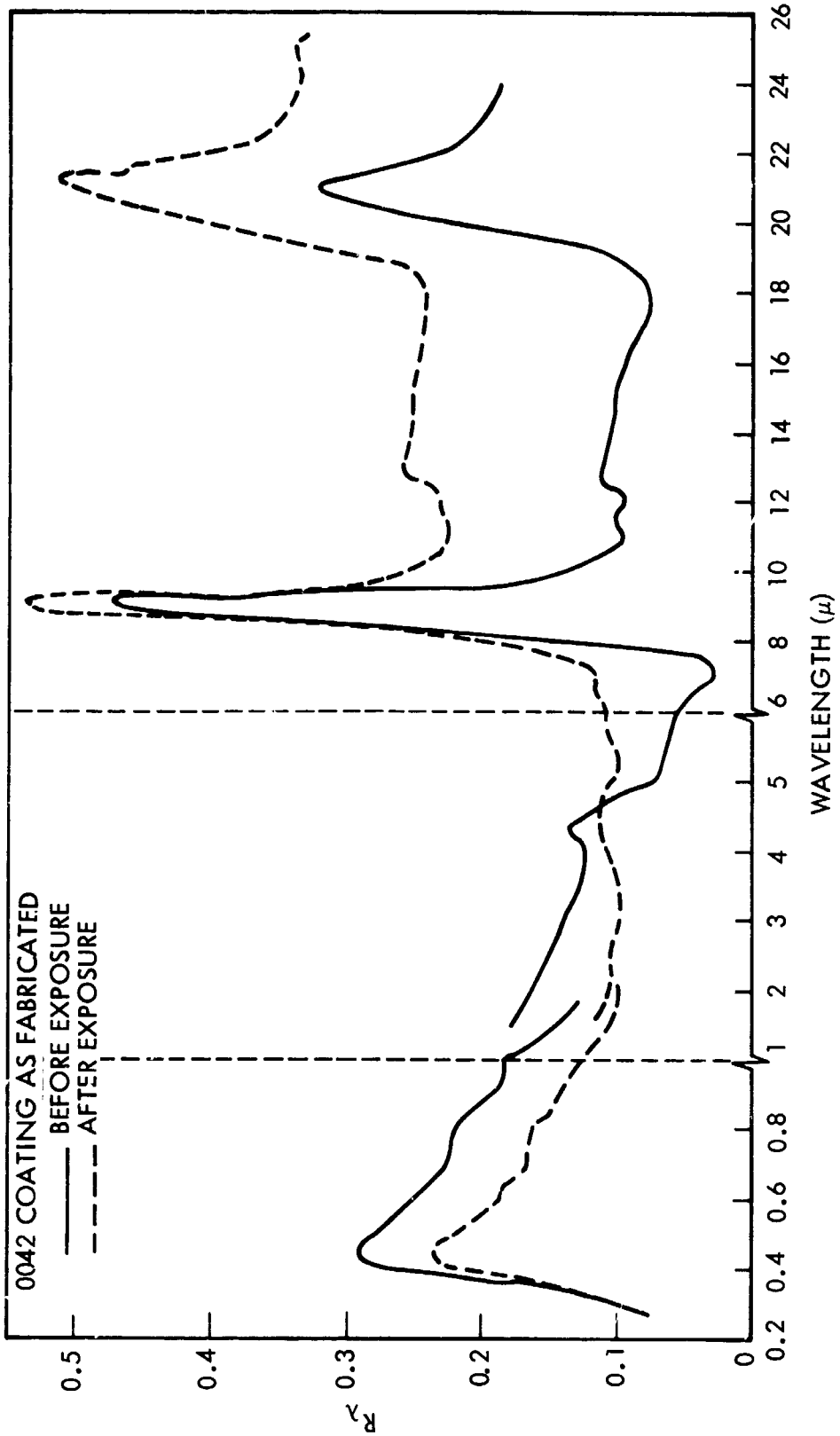

Fig. 3.4.1-5 Change in Spectral Reflectance of 0042 Coating After Exposure to 2,300°F at 10 Torr for 4 hr

Three coating formulations (considered at the time to be optimum in terms of emittance from LMSC room temperature reflectance data) were submitted to TRW Systems, Redondo Beach, California. Spectral reflectance measurements were made in air atmosphere at temperatures of 250, 930, 1,400, and 2,000°F. The spectral region covered was 0.9 to 25 microns. For these measurements, the specimens were backed with a platinum black surface (low reflectance). After the measurements, a polished platinum strip (high reflectance) was substituted to determine if the specimens were transparent by comparing the data at several wavelengths. The data between 1 and 5 microns at 280°F and 1,800°F showed no difference. Therefore, the reflectance data are considered valid as the specimens were not transparent.

The spectral reflectance data for the nominal 250°F, 930°F, and 2,000°F are presented in Fig. 3.4.1-6; data for 1,400°F are omitted for the sake of clarity. Note that the measurements at the three temperatures show the curves for the elevated temperature to be slightly higher in part, but essentially independent of temperature. Total normal emittance values computed at three temperatures using the reflectance data for the temperature are given below.

Temperature	70°F	1000°F	2000°F
Coating			
SiC in borosilicate matrix	0.89	0.93	0.93
CoO in borosilicate matrix	0.92	0.93	0.93
SiC + Cr_2O_3 in borosilicate matrix	0.88	0.91	0.89

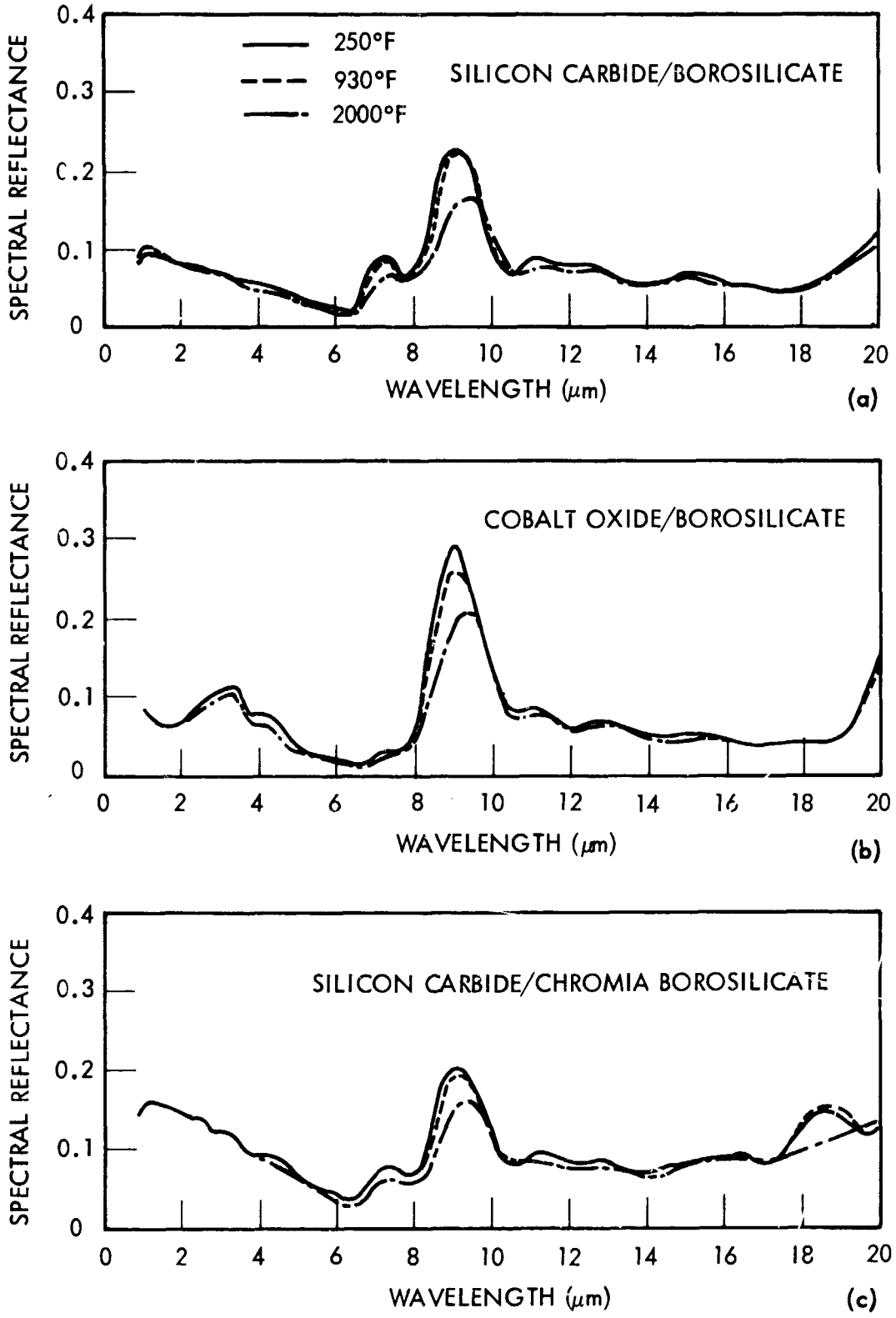

Fig. 3.4.1-6 Spectral Reflectance of Borosilicate Coatings at Three Temperatures

These data, taken from elevated reflectance measurements at TRW, confirm the same trend found at LMSC and also confirm the validity of the results, except that the LMSC values appear conservative. On both silicon carbide and cobalt oxide formulations, the TRW values are higher – 0.93 versus 0.86 for silicon carbide and 0.93 versus 0.86 for cobalt oxides.

Figure 3.4.1-7 shows spectral reflectance curves of three coatings – baseline 0025 chromia in borosilicate, new LI-0042 coating submitted under Contract NAS9-12083, and new improved 2,500° F resistant LI-0045 coating. These curves show that in the visible spectrum 0.4 μ–0.7 μ range, the 0025 has low reflectance, but in the near infrared between 0.8 μ and 3 μ there is a high reflectance plateau of 0.5–0.6 which is very damaging to its emissivity at elevated temperatures. There is another minor peak in the 3 μ to 4 μ range, but this is not as significant as the first one. Both silicon carbide formulations (LI-0042 and LI-0045) have a higher reflectance, 0.3, in the visible range, but the curve slopes down approximately linearly to less than 0.05 at 7μ range. Thus, its reflectance (or emittance) is low (or high) in the all important 1 to 5μ range. Note that the reflectance curves of LI-0042 and LI-0045 are very similar.

Figure 3.1.4-8 shows the temperature dependance of emittance of LI-0025 whereas the emittance of silicon carbide-borosilicate coatings LI-0042 and LI-0045 is independent of temperature and has a high value of 0.86 to 0.93.

Effect of Selected Emissivity Agents on Crystallinity of Basic Silica Fiber. In addition, evaluations were conducted to determine the possible effect of the emissivity material formulations on the crystallinity change of the silica fibers when exposed to elevated temperature. For this examination, a significantly high quantity of the individual emissivity agents as particulate oxide forms (Cr_2O_3, CoO and SiC) were impregnated into a cast filter cake of Lot 2089 fibers. Control specimens were exposed for 4 hr at 2,300°F and examined by x-ray diffraction techniques (utilizing Georgia Tech Standard) to determine crystalline phase changes. Morphology changes were examined by study techniques. The results after exposure for 4 hr at 2,300°F were as follows:

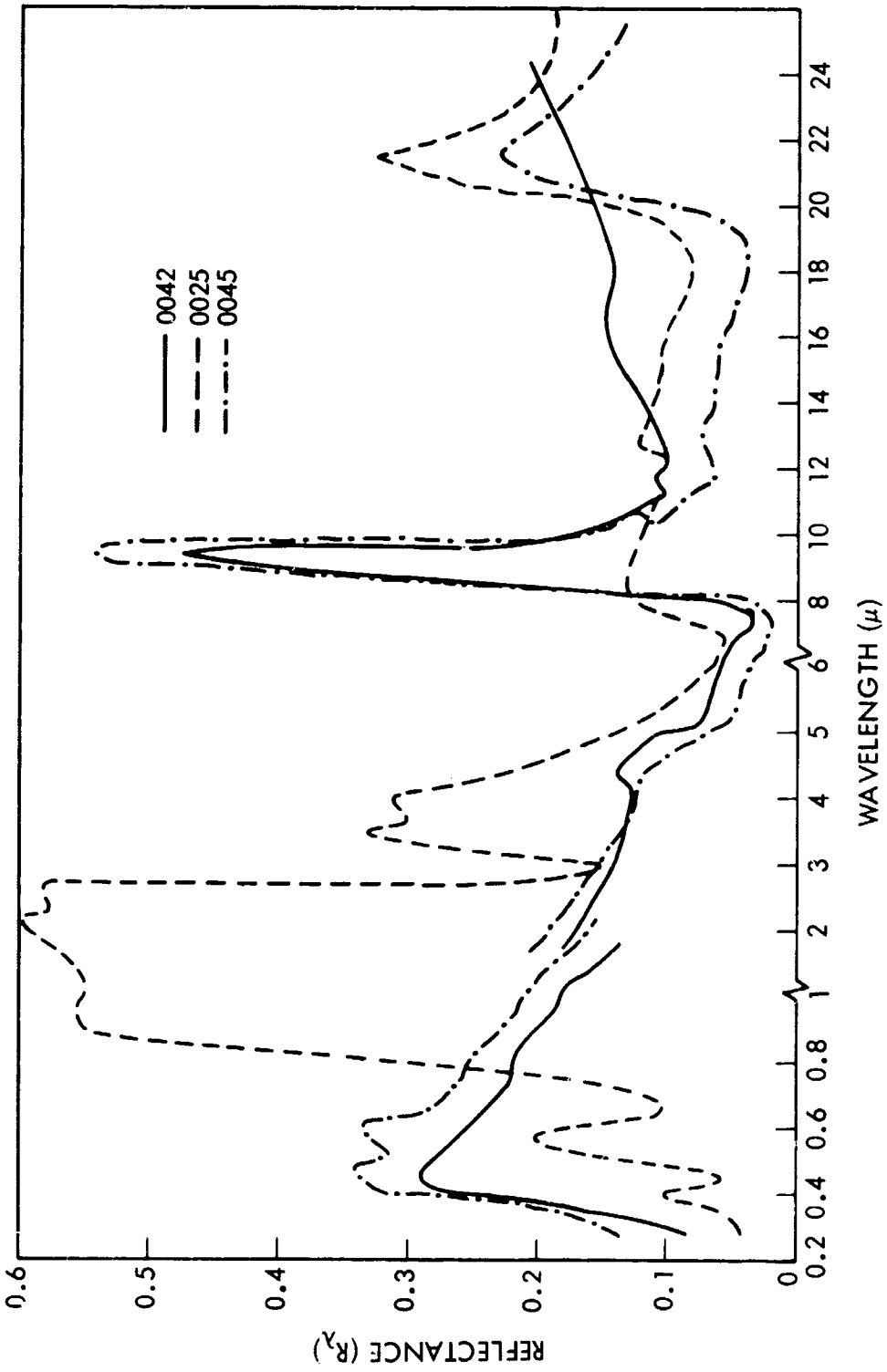

Fig. 3.4.1-7 Comparative Spectral Reflectance: New 0042 and 0045 Versus Old 0025

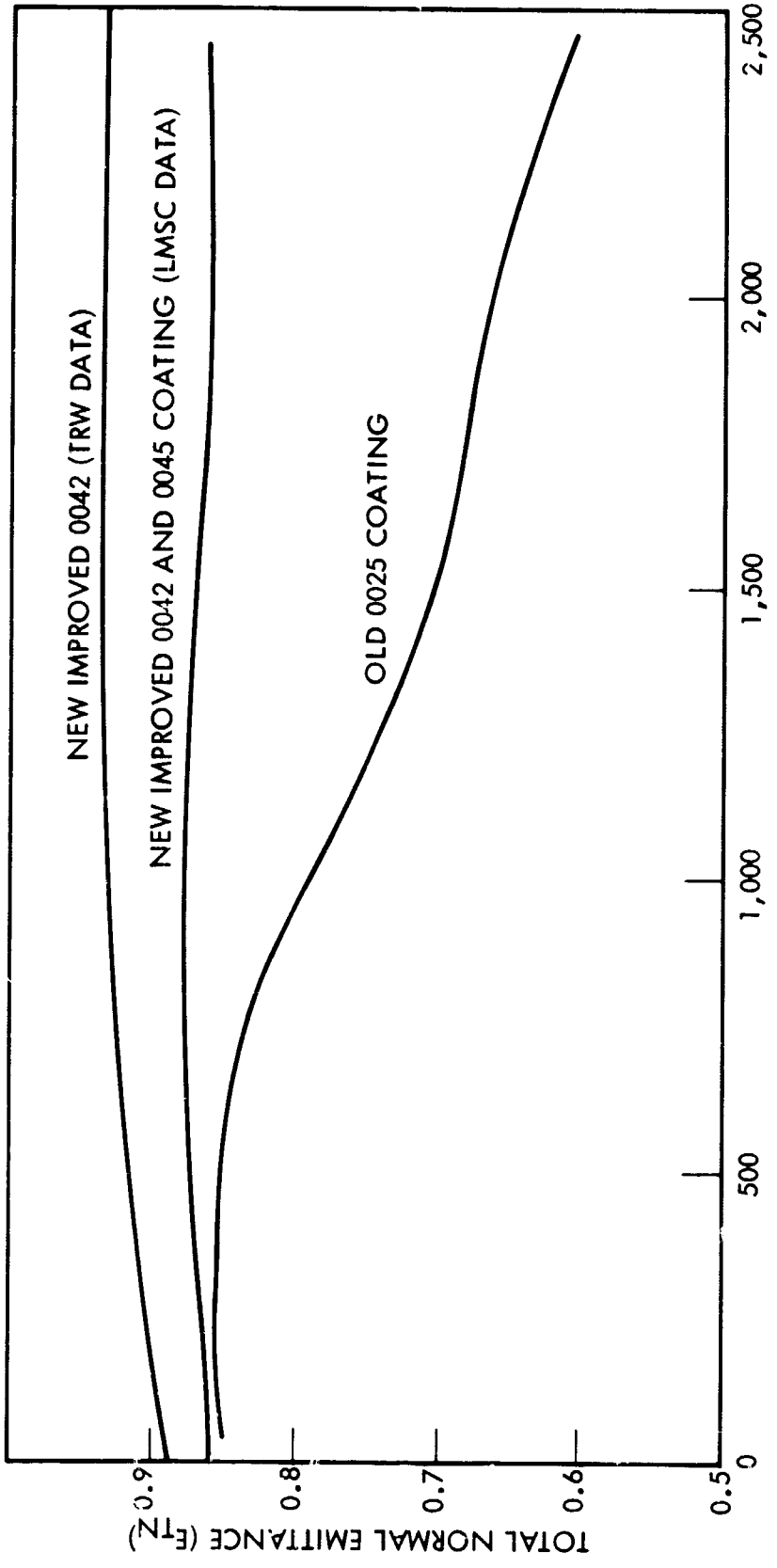

Fig. 3.4.1-8 Predicted Total Normal Emittance Values: New Coatings Versus Old 0025 as a Function of Temperature

	Crystallinity (%)
2089 Control	0
With Cr_2O_3	6
With CoO	3
With SiC	0

The SEM photographs for the CoO and Cr_2O_3 are presented in Fig. 3.1.4-9. Examination shows a very definite reaction of the CoO system with silica fibers while the fibers appear to be unaffected by the Cr_2O_3.

Later evaluation with lower concentration (approximately 4 percent) of the Cr_2O_3 materials showed very little or no promotion of crystallinity in the silica fibers, whereas some anomolous data was obtained on cobalt oxide. After exposure for 4 hr at 2,300°F, the x-ray diffraction data indicated the following:

	Crystallinity (%)
2089 Control	0
With Cr_2O_3 (particulate form)	0
With CoO (particulate form)	3
With CoO (solution form)	0
With SiC (particulate form)	0

COBALT OXIDE 5000X

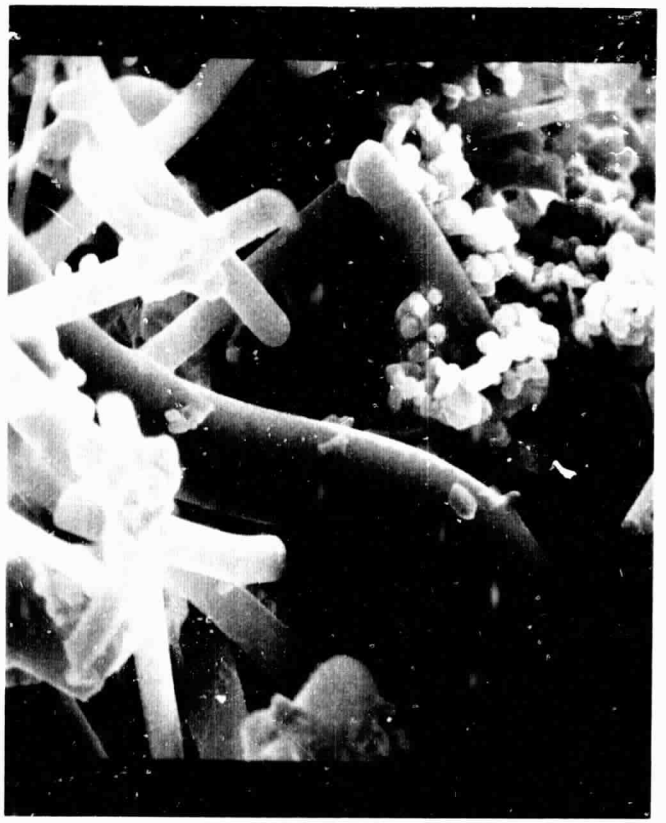

CHROMIA 5000X

Fig. 3.4.1-9 Emissivity Constituent Materials (Exposed 4 hr at 2,300° F)

3.4.2 Integral Coating Investigation

For an ideal RSI material system, an optimized compatibility of the lightweight insulation constituent with the surface coating material is desirable. Because of the specific requirements for each of the constituent materials, by necessity the surface coating is a hard, dense, impervious ceramic-type coating, while the insulation material is of extremely light weight exhibiting a highly controlled porous structure. When a ceramic type coating such as the LI-0025 is applied over a low-density insulation such as LI-1500, there occurs a significant mismatch in the mechanical properties at the interface of the two constituent materials. For example, the mismatch in tensile strength, elastic modulus, and strain-to-failure properties is by a factor of as much as 6X, 40X and 100X, respectively. Although the thermal expansion properties of the constituent materials are designed to be compatible, mechanical loads may be applied to the coating/insulation interface by steep temperature gradients and stresses transmitted from the primary structure during ascent and/or environments. Previous studies conducted under IRAD programs indicated that the integral coating approach offered a simple and effective means of achieving a compatible low modulus, high strain-to-failure RSI system. The integral coating approach was to form a gradual transition from the low-density insulation to the hard dense outer coating layer to attempt to avoid the problems associated with abrupt changes in material properties at the interfaces.

3.4.2.1 Density Gradient Integration. Utilizing techniques previously developed under IRAD programs, varying density gradients were obtained with the LI-1500 material by use of the silica impregnant solution. Typical density gradient profiles obtained by this method are shown in Fig. 3.4.2-1. The density profiles were measured by the incremental removal of the integral coating layers and calculating its average density for each increment removed. As shown in the figure, these density profiles were classified into two major types identified as linear and hyperbolic. By controlled silica solution concentration and impregnation applications, various density gradients were achieved and verified. It is obvious that the linear-type gradient, extending in-depth into the LI-1500 material, rapidly increases weight and does not seem attractive because of the weight penalty incurred.

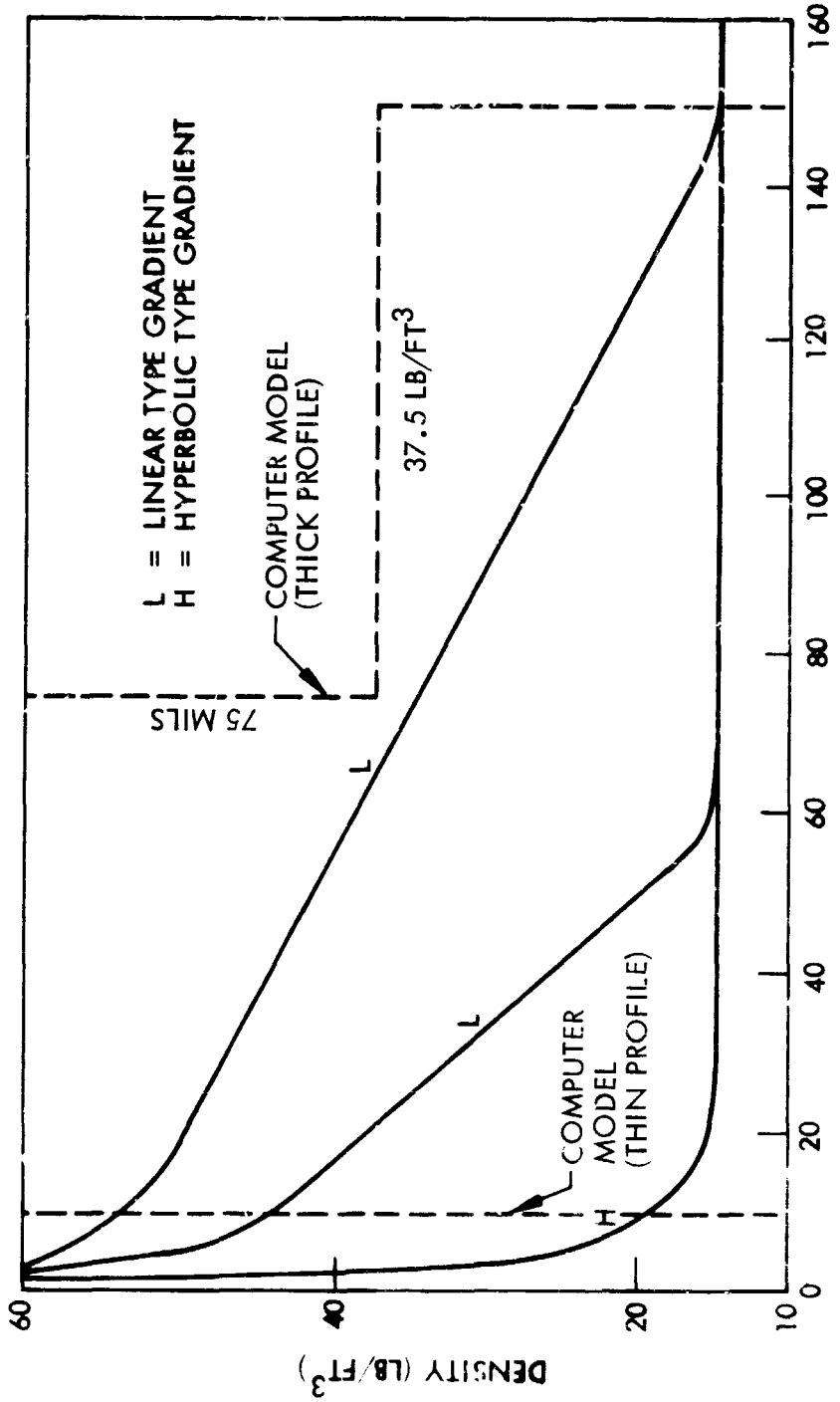

Fig. 3.4.2-1 Integral Coatings Typical Density Gradients

To determine the mechanical properties of the integral coating concept, specimens representing various increments of the densified coating layer were prepared. The LI-1500 material was machined into test bars 6 in.x 1 in.x 0.25 in.thick and were impregnated by silica addition to various densities up to 60 pcf. The flexural test method utilized was as illustrated in Fig. 3.4.2-2. By this method, no indentation or compression of the test materials was observed and good linearity in the load-deflection curve was obtained. The results of the flexural test evaluation are presented graphically in Fig. 3.4.2-3. These measurements of LI-1500 densified with silica indicated that both flexural break strength and flexural modulus increased proportionately with increasing density. Good uniformity of flexural properties was obtained on specimens of equal density by utilization of this test method. Further confirmation of this mechanical property versus density relationship was obtained by tensile property measurements of various densified LI-1500 specimens. The tensile evaluations resulted in the properties as shown below. Test specimens 1.5 in.wide by 0.25 in.thick and with a gauge length of 4.0 in.were utilized in these tests.

Densified LI-1500 (lb/ft^3)	Ultimate Tensile Stress (psi)	Modulus (psi)
58.9	265	238,000
58.3	155	267,000
46.3	168	250,000
45.2	171	161,000
44.4	131	192,000
29.8	101.0	116,000
28.1	88.9	142,000
27.6	91.6	135,500
16.6	74.7	68,200
14.7	77.3	91,900
14.5	72.2	69,500

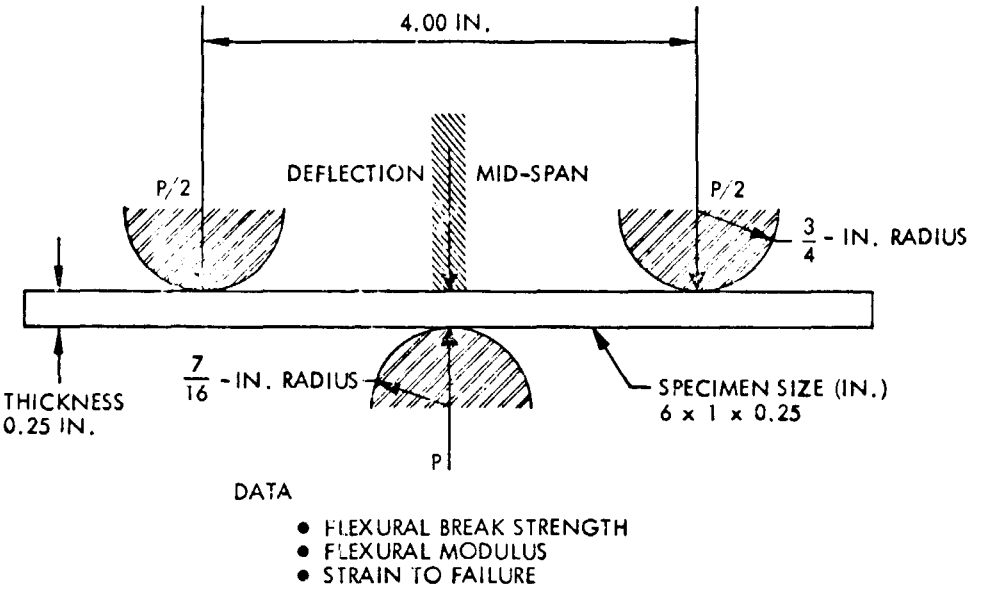

Fig. 3.4.2-2 Flexural Test Method

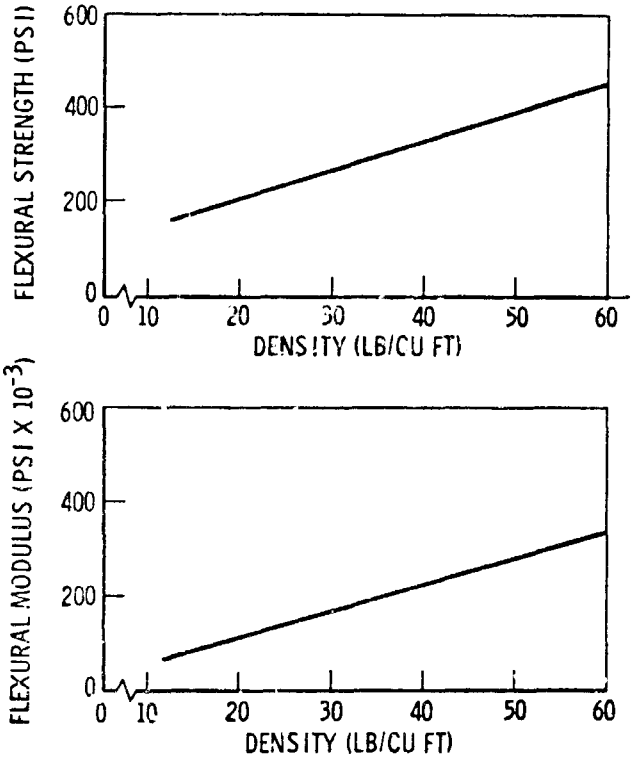

Fig. 3.4.2-3 Flexural Properties as a Function of Density

An analytical study of the integral coating concept was performed under the TPS Development Contract NAS 9-12083 to determine the effects of density gradients on the RSI and silicone rubber bonding. Computer modeling for two profiles, thick and thin, is shown as dotted lines in Fig. 3.4.2-1. Utilizing this computer modeling, comparative results for a beryllium subpanel with the LI-1500 material (Table 3.4.2-1) show that there is virtually no difference in stress levels for thin or thick profile except for the integrated coating layer stress. The integral coating concept results in lower coating stresses due to its lower modulus than the add-on concept such as LI-0025 coating. Since the thin profile integral coating concept (hyperbolic type gradient of Fig. 3.4.2-1) indicated significantly lower stress levels with a minimum weight penalty, this concept was utilized in all the subsequent final coating improvement work.

3.4.2.2 Integral Coating Concept Evaluation. The integral coating evaluation represented formulations of three general coating systems. These systems were chromia-silica, silicon carbide-silica, and other silica systems with various emissivity agents added. The formulations and the results of the tests are summarized in Table 3.4.2-2.

For rapid screening of potential integral coating formulations, the LMSC Radiant Heat Facility was used extensively. For preliminary evaluations 3 in. × 3 in. × 1 in. thick LI-1500 specimens were utilized. The radiant heat pulse used was ambient to 2500°F in 300 sec, held at 2500°F for 200 sec, and cooled to 800°F in 400 sec. The thermal response evaluation was principally by visual examination and physical measurements.

The initial integral coatings tested in the thermal environments were basically chromia or cobalt oxide in a silica matrix. These emissivity agents were introduced either as a dispersed powder or as a salt solution which was subsequently decomposed into oxides. Although possessing low modulus porous structure characteristics, these types of specimens failed by surface cracking when exposed to the 2500°F environments. Subsequent controlled experiments indicated that these cracking failures may have been caused by the emissivity agents impregnated into the LI-1500 test model. On test models impregnated with the emissivity agents and models with the emissivity agent applied as a surface wash, the thermal test showed

Table 3.4.2-1

STRUCTURAL COMPARISON OF COATING CONCEPTS

	MAXIMUM STRESS (PSI)	ADD-ON COATING	INTEGRAL COATING THIN PROFILE	INTEGRAL COATING THICK PROFILE
LI-1500	SHEAR	51.5	49.2	49.2
	IN-PLANE COMPRESSIVE	68.9	69.4	69.5
	PEEL	11.1	10.3	10.8
RTV-560	PRINCIPAL TENSILE	48.0	48.6	48.2
	PRINCIPAL COMPRESSIVE	145.5	114.6	116.0
	SHEAR	50.8	47.6	47.6
	IN-PLANE TENSILE	32.5	32.3	32.4
	PEEL	11.5	10.4	10.9
COATING	THICKNESS (IN.)	t = 0.010	t = 0.010	t = 0.150
	PRINCIPAL TENSILE	11.3	14.4	6.1
	PRINCIPAL COMPRESSIVE	1761.2	230.0	161.4

PRESSURE	= 6.75 PSI COLLAPSE
$t_{e\ BERYLLIUM}$	= 0.4312 IN.
$t_{RTV-560}$	= 0.020 IN.
$t_{LI-1500}$	= 2.3 IN.
$t_{COATING}$	= AS SHOWN
LI-1500 TILE LENGTH	= 12 IN.

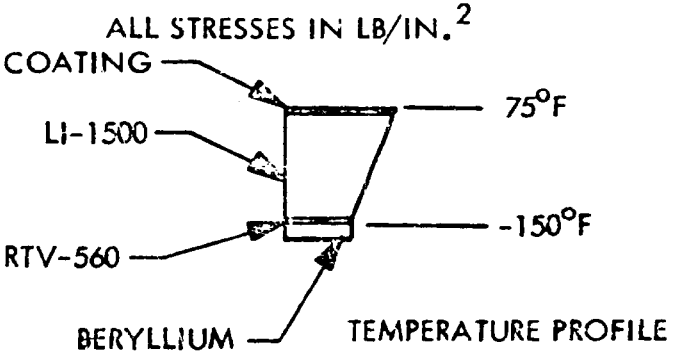

Table 3.4.2-2

INTEGRAL COATING CONCEPT EVALUATION

Formulation				Gradient* Profile	Gradient* Depth	Results (2500°F Thermal Exposure)
Chromia-Silica System						
NO.	12-126	50:50	Single application	H	(a)	High porosity
	25-25	40:60	Single application	H	(b)	High porosity
	25-27	40:60 50:50	Double application	H	(b)	Mud cracks
	25-31	40:60	Double application	H	(c)	Hairline cracks
	25-13E	90:10	Solution-impregnated	L	(b)	Mud cracks
	25-32A	100:00	Solution-impregnated	L	Cr_2C_3 GRADIENT	Cracks in LI-1500
	25-32C	100:00	Powder-infiltrated	H	Cr_2O_3 GRADIENT	Cracks in LI-1500
	23-95A	Cr_2O_3	Powder over silica-graded surface	L	(c)	Hairline cracks
	23-95B	Cr_2O_3	Powder over silica-graded surface	L	(a)	Slight cracks
	23-95C	Cr_2C_3	Powder over silica-graded surface	L	(b)	No visible failure
	23-96C	50:50	Over SiO_2-graded surface	L	(b)	No failure; porous
	23-96F	50:50	Over SiO_2-graded surface	L	(c)	No failure; porous

*See footnote at end of table.

Table 3.4.2-2

INTEGRAL COATING CONCEPT EVALUATION (Con't)

Formulation				Gradient Profile	Depth	Results (2500°F Thermal Exposure)
Silicon Carbide-Silica System						
NO.	23-96B	50:50	SiC/SiO_2 over silica-graded surface	L	(c)	No cracks; looks good
	25-36A	50:50	SiC/SiO_2 over silica-graded surface (scale-up)	L	(c)	No cracks; looks good
	25-36B	50:50	SiC/SiO_2 over silica-graded surface (scale-up)	L	(b)	No cracks; looks good
	23-96H	50:50	SiC/SiO_2 over silica-graded surface (heavy application)	L	(b)	Mud cracks
	23-98A	33:66	Directly on LI-1500 SiC in gradient	L	(a)	Mud cracks
	23-98B	18:82	Directly on LI-1500 SiC in gradient	L	(a)	Hairline cracks
	23-98C	10:90	Directly on LI-1500 SiC in gradient	L	(a)	No cracks
	23-99B	66:30	Directly on LI-1500 followed with dilute SiO_2	L	(a)	No cracks
	23-99E	66:33 33:66	Application followed with application; SiC in gradient	L	(a)	Cracks
	23-99C	66:30	Over heavy silica-graded surface	L	(c)	Poor adhesion
	23-99D	40:60	Over silica-graded surface	L	(a)	No cracks

Table 3.4.2-2

INTEGRAL COATING CONCEPT EVALUATION (Con't)

Formulation				Gradient Profile	Gradient Depth	Results (2500°F Thermal Exposure)
Silicon Carbide-Silica System						
NO.	23-99F	33:66	Over silica-graded surface	L	(b)	No cracks
	23-100B	33:66	Over silica-graded surface	H	(a)	Microcracks
	23-101A	50:50	Over silica-graded surface	L	(a)	Microcracks at corners of holes
	23-101B	50:50	Over silica-graded surface	H	(a)	Cracks
	23-101C	50:50	Over silica-graded surface	L	(b)	Cracks
	23-101D	50:50	Over silica-graded surface	H	(a)	Cracks
	23-104	50:50	Multiple coated over silica-graded surface	L	(a)	No cracks - occasional cracking
	23-114A	50:50	600 grit SiC over silica-graded surface	H	(a)	No cracks; looks good
	23-114B	50:50	800 grit SiC over silica-graded surface	H	(a)	No cracks; looks good
	23-114C	50:50	Double application over silica-graded surface. 1st coat 600 grit 2nd coat 1200 grit	H	(a)	No cracks; looks good
	23-114D	50:50	Same as above except 1st coat 1200 grit 2nd coat 600 grit	H	(a)	Looks good
	23-115A	50:50	800 grit SiC over steeply graded silica	H	(a)	No cracks
	23-115B	50:50	1000 grit SiC over steeply graded silica	H	(a)	Microcracks

Table 3.4.2-2

INTEGRAL COATING CONCEPT EVALUATION (Con't)

Formulation				Gradient Profile	Gradient Depth	Results (2500° F Thermal Exposure)
Other Systems						
NO.	23-96A	50:50	CoO/SiO_2 over silica-graded surface	L	(c)	No failure; non-uniform color
	23-96E	50:50	CoO/SiO_2 over silica-graded surface	L	(b)	Slight cracking
	23-94C	50:50	CoO Single application	L	(a)	Mud cracks
	23-101	50:50	NiO/SiO_2 over silica-graded surface	L	(a)	Cracks
	23-101A	50:50	Si_3N_4/SiO_2 over silica-graded surface	L	(a)	Cracks
	25-41A	50:50	Ni-Cr spinel/SiO_2 over silica-graded surface	L	(a)	Rough surface - non-uniform appearance
	25-41B	50:50	$FeTiO_3/SiO_2$ over silica-graded surface	L	(a)	Rough texture, poor appearance
	23-96G	50:50	CoO-Fe-Cr_2O_3/SiO_2 over silica-graded surface		(c)	No failure; looks good
	23-96D	50:50	CoO-Fe-Cr_2O_3/SiO_2 over silica-graded surface		(b)	No failure; looks good

(a) Density Gradient <50 mils depth
(b) Density Gradient 50-100 mils depth
(c) Density Gradient >100 mils depth
L Linear Type Density Gradient
H Hyperbolic Type Density Gradient

cracking into the impregnated material while the surface washed material exhibited minor mud cracking detectable under microscopic examination. Further examination of reaction of candidate emissivity agents indicated that both chromia and cobalt oxide, when used in sufficient quantities, in intimate contact with silica fibers, and in high temperature environments such as 2500°F, may promote crystallinity in the fibers and cobalt silicate. This reaction at 2500°F does not seem to occur with the silicon carbide emissivity agents. This reaction also does not occur with the chromia or the cobalt oxide at the lower temperature environments. These characteristics of the emissivity agents were discussed in Section 3.4.1.

Further evaluations of the integral coating concept utilized only the silica solution for achieving graded densification. The emissivity agent was confined chiefly with a silica matrix to the densified top surface of the LI-1500 specimen. The specimens containing the silicon carbide material exhibited higher thermal performance capabilities than the specimens prepared with chromium oxide or cobalt oxide. On repeated thermal cyclic testing, the latter types of specimens exhibited a greater propensity for cracking.

The numerous thermal testings of integral coatings with silicon carbide/silica densified surface indicated that the thermal performance was not appreciably affected by the integral coating profile or the coating depth. The controlling variable appeared to be the emissivity coating layer. Excessive emissivity coating surface thickness (over 4 mils) tended to cause the formation of microscopic "mud" cracking on the coating surface.

The smaller particle size of the silicon carbide also seems to contribute to the microscopic mud cracking tendency. However, this mud cracking did not appear to affect the thermal performance. On progressive thermal cycling further propagations of the microcracks were not evidenced; they remained confined to the surface and did not extend into the LI-1500 insulation.

Two test models of the integral coating concept with the silicon carbide emissivity agent added were subjected to 100 cycles of thermal testing at 2500°F in the LMSC

Radiant Heat Facility. These tests conducted with the new improved LI-0042 coating system (discussed in Section 3.4.3) are described in Section 3.7. Results of the tests showed that the integral coated specimens exhibited some surface cracking and minor distortions in certain areas of the LI-1500 material. However, the cracking did not propagate or extend into the LI-1500 material.

3.4.2.3 Surface Hardening and Sealing of Integral Coating. Although the surface hardness of integral coating thickness did not appreciably affect the thermal performance of the LI-1500 material, handleability and resistance to water considerations made it necessary for increased surface hardness and water imperviousness of the coating. Several techniques for sealing and hardening were investigated. The techniques were various applications such as spray, brush, dip at varying temperatures and with varying controlled concentrations of the silica impregnation solution. Complete surface sealing for water imperviousness with the densified silica coating was not achieved. Examination of the SEM photographs of 500 and 2000 magnification presented in Fig. 3.4.2-4 indicates that although a major portion of the surface appears to be sealed with the densified silica material, some porosity of the surface still remains. The 2000 magnification photo indicates the presence of the silica impregnant at a lower depth and under the porous surface openings. The technical information and application techniques investigated under this phase of the program were utilized in the improved coating phase being conducted concurrently and described in Section 3.4.3.

500X

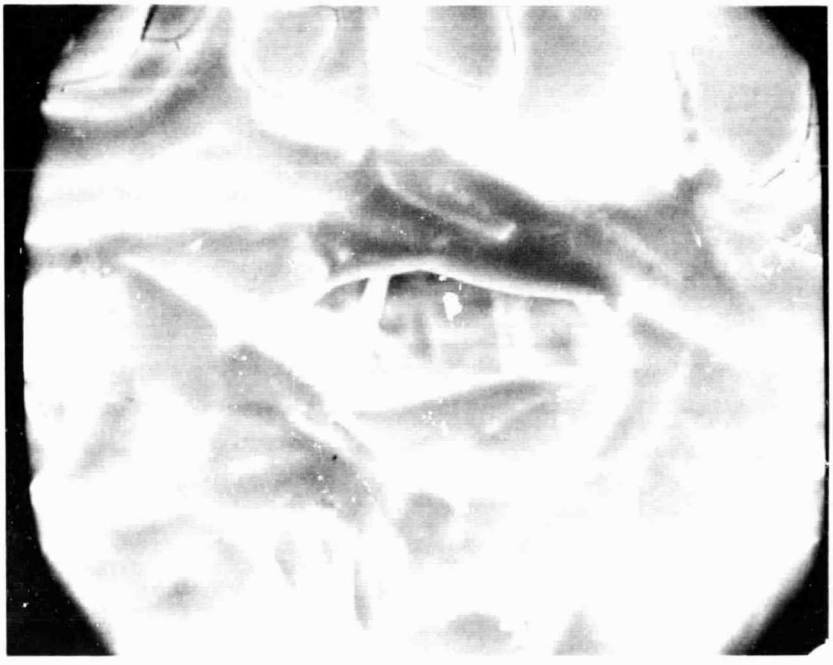

2000X

Fig. 3.4.2-4 SEM Photograph (500X & 2000X)
Silica Densified LI-1500 Surface

3.4.3 Improved Coating

The baseline coating for this Material Improvement Program was the LI-0025 borosilicate coating system with chromium oxide emissivity agent as previously described in Section 3.1. Although performing successfully in many of the shuttle environmental tests, it was desirable to obtain a more reliable, higher performance coating system to meet the requirements of the thermal, mechanical, and other environmental parameters for the shuttle operation. The LI-0025 coating system appeared to be highly sensitive to processing techniques and resulted in erratic performance during simulated reentry and environmental evaluations. The lower emissivity characteristics of the coating at elevated temperatures contributed to higher surface operating temperatures than desired. The coating also was not water impervious as processed because of the restricted thermal treatment. The objective of this phase of the program was to achieve an improved coating system through investigation and evaluations of modification of the baseline coating, inclusions of new higher performance emissivity agents, integral coating concepts (previously described in Section 3.4.2), new coating systems, and surface texturing or coating discontinuities techniques.

3.4.3.1 Modification of Baseline LI-0025 Coating. The LI-0025 coating consisted of a chromia emissivity agent dispersed in a borosilicate matrix of 82.2-percent silica by weight. Although somewhat erratic, the coating system performed successfully in many thermal exposures such as test model No. TT-5D which was submitted under Contract NAS 9-11222 to NASA/MSC. The specimen was tested successfully for thirty-two 10-min cycles at 2,300° F in the MSC Arc Jet Facility. No degradation of the coating surface attributable to the arc jet testing was noted after the thermal exposures. Although the coating surface was of a semi-porous nature prior to the thermal testing, when checked at completion of the tests the coating had evidently "matured" from the thermal exposures and proved to be water impervious. Because of the cracking propensity of the old silica fiber materials (as described in Section 3.2), the previous LI-0025 coating system was not heat treated to a sufficiently high temperature to ensure maturing of the surface to achieve a water-impervious ceramic coating. With availability of the improved fiber material, also described in Section 3.2, higher heat treatment temperatures were allowable for the coating systems on the improved LI-1500 material. With higher processing temperatures, up to 2,500° F,

the LI-0025 coating resulted in water-impervious surfaces. However, the apparent processing sensitivity still existed. Because of this processing sensitivity and the unsatisfactorily low emissivity characteristics, modification of the LI-0025 coating system was discontinued.

3.4.3.2 Strain Relief Techniques. In an attempt to circumvent the problems relatable to mismatch of thermal expansion and mechanical properties between the dense high modulus surface coating and the much lower density lower modulus substrate LI-1500 material, strain relief techniques directly in the coating system were investigated. Three concepts investigated were texturing, coating discontinuities, and microsphere inclusions.

Texturing. A signwave form surface was prepared prior to surface coating. An example of the concept is shown in the photograph in Fig. 3.4 3-1. Analytical studies performed on this concept (described in the companion TPS Development Program NAS 9-12083) indicated that in the particular case studied, approximately 10-percent decrease in maximum coating stress was achieved. Computer modeling and its results are shown in Fig. 3.4.3-2. This type of concept is highly directional in its properties and may be undesirable in certain stress loading conditions.

Coating Discontinuities. Several patterns of the strain relief concept were investigated. These included the cross hatch, stippled effect, fine grids, and honeycomb patterns. Examples of some of these patterns are presented in Fig. 3.4.3-1. Analyses performed in Contract NAS 9-12083 are presented in Fig. 3.4.3-3. Indications are that the overall effect on coating stress is essentially the same as that achieved by texturing techniques. However, the stresses in the LI-1500 at the discontinuities are magnified approximately five times over those corresponding to a continuous coating system.

Microsphere Inclusion. This inclusion technique was investigated using available high purity silica microspheres. The microsphere inclusion was an attempt to lower the apparent modulus of the coating to be more compatible with the substrate LI-1500 material. However, the relatively large quantity of impurities contained in the "high purity" microspheres in this form was not compatible with the silica fiber system.

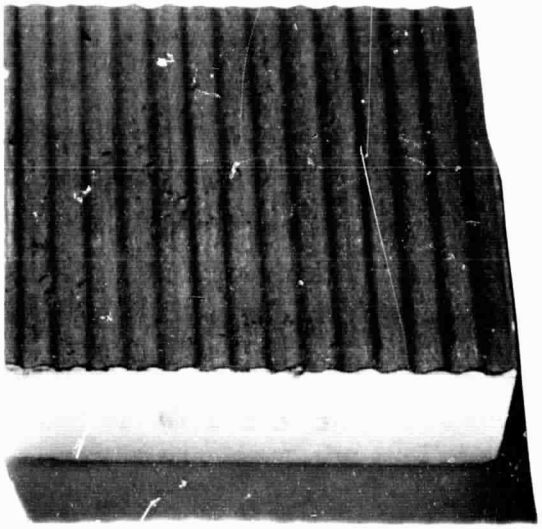

SINE WAVE TEXTURED PATTERN

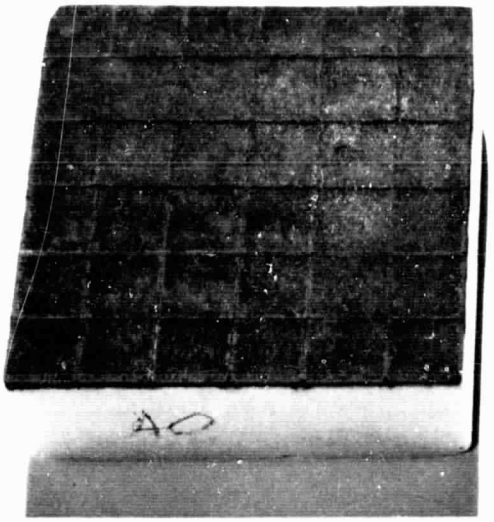

CROSS HATCH PATTERN

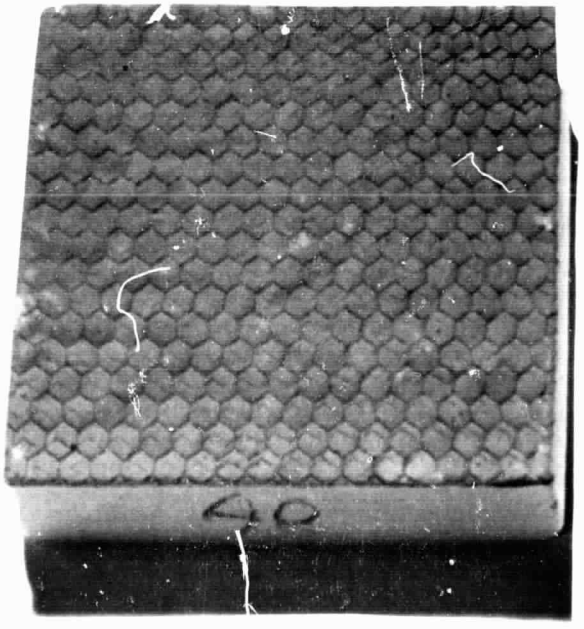

HONEYCOMB PATTERN

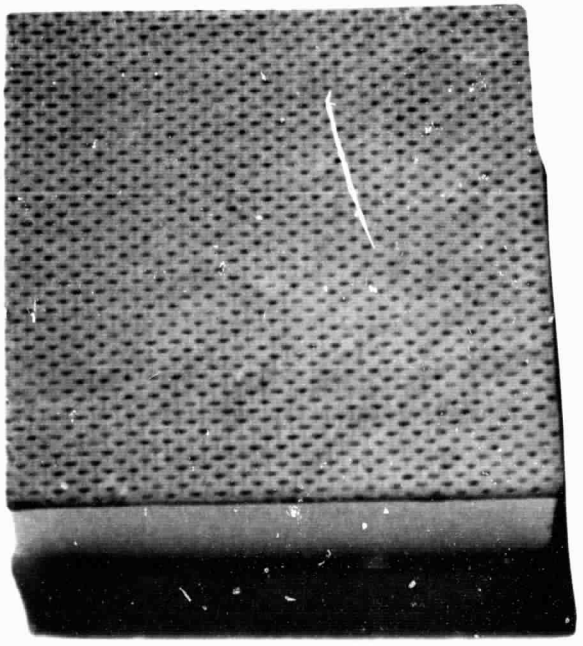

FINE GRID PATTERN

Fig. 3.4.3-1 Strain Relief Coating Surface Patterns

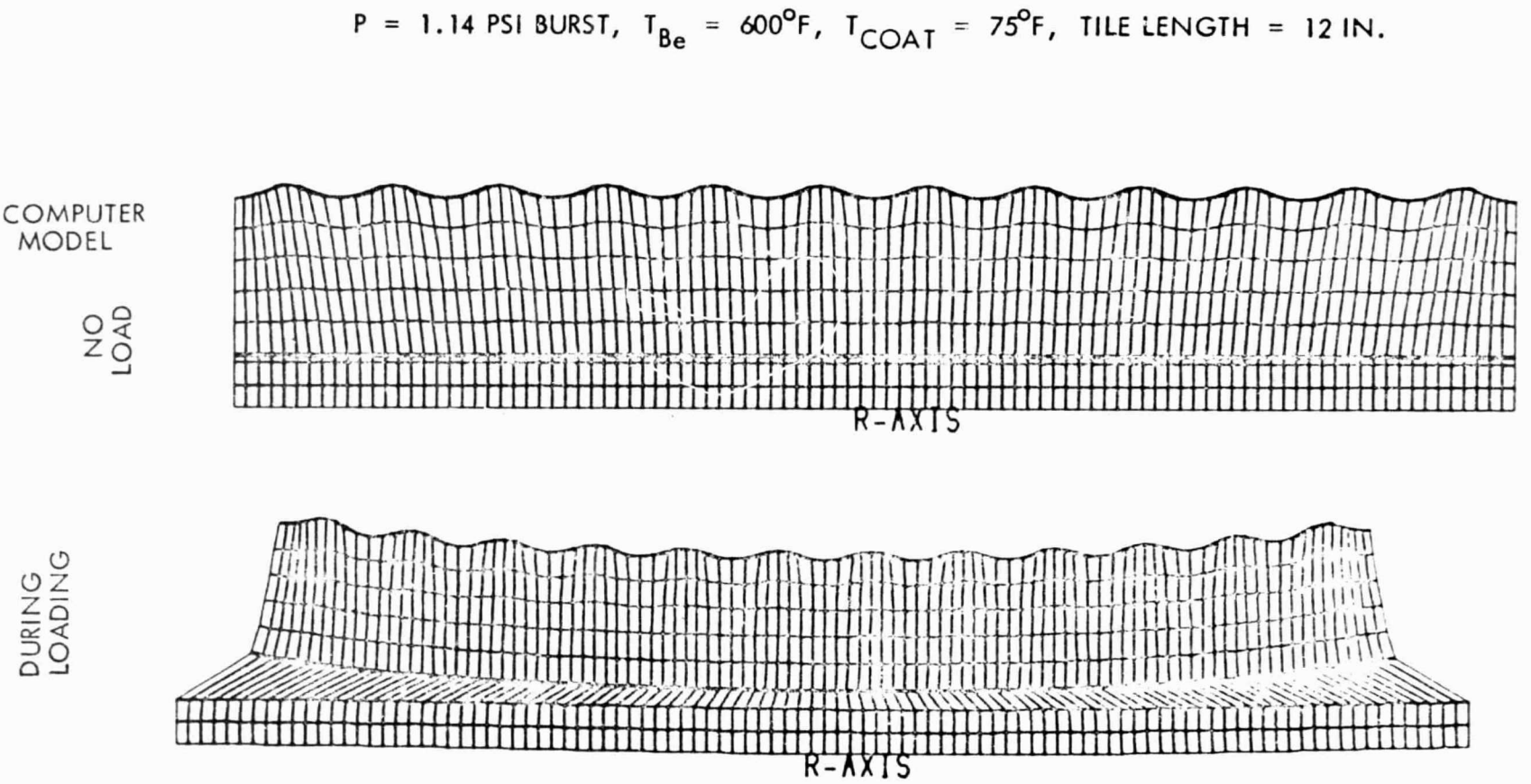

Fig. 3.4.3-2 Texture Coating Study – Computer Modeling

$P = 1.14$ PSI BURST, $T_{Be} = 600^{\circ}F$, $T_{COAT} = 75^{\circ}F$, TILE LENGTH = 12 IN.

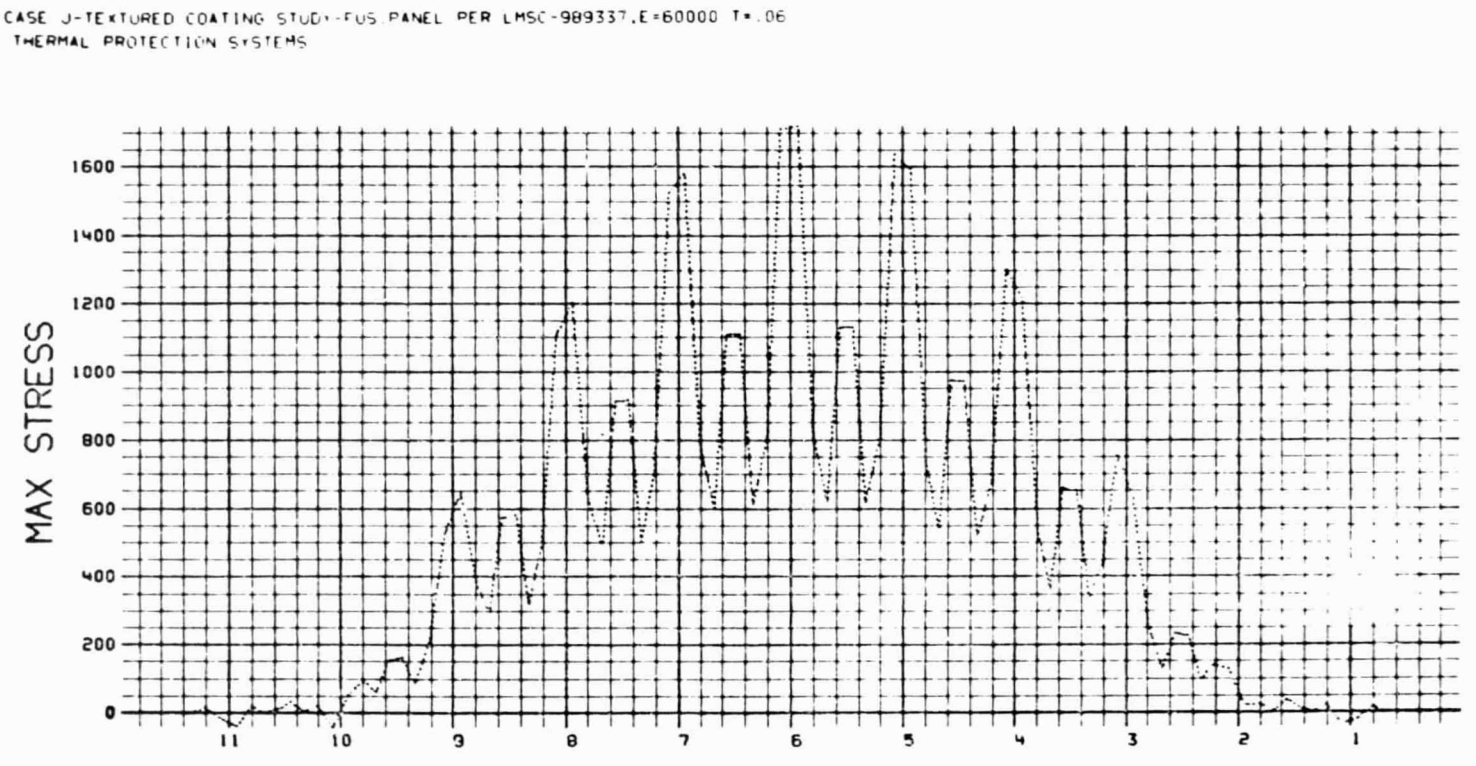

MAX TEXTURED COATING STRESS = 1718 PSI (TENSION)
MAX STRAIGHT COATING STRESS = 1950 PSI (TENSION)

Fig. 3.4.3-2 Texture Coating Study – Computer Modeling (Cont'd)

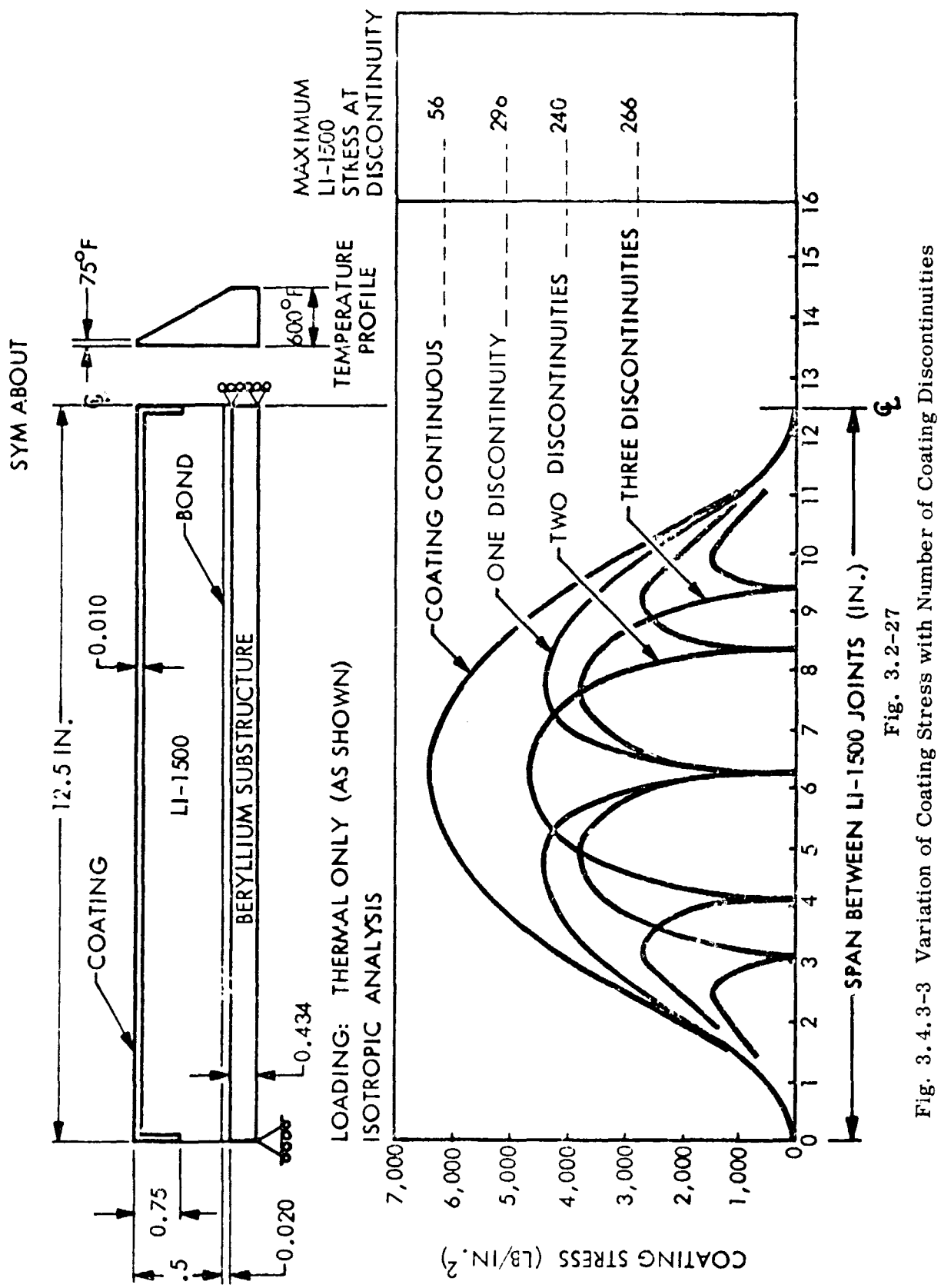

Fig. 3.4.3-3 Variation of Coating Stress with Number of Coating Discontinuities

Fig. 3.2-27

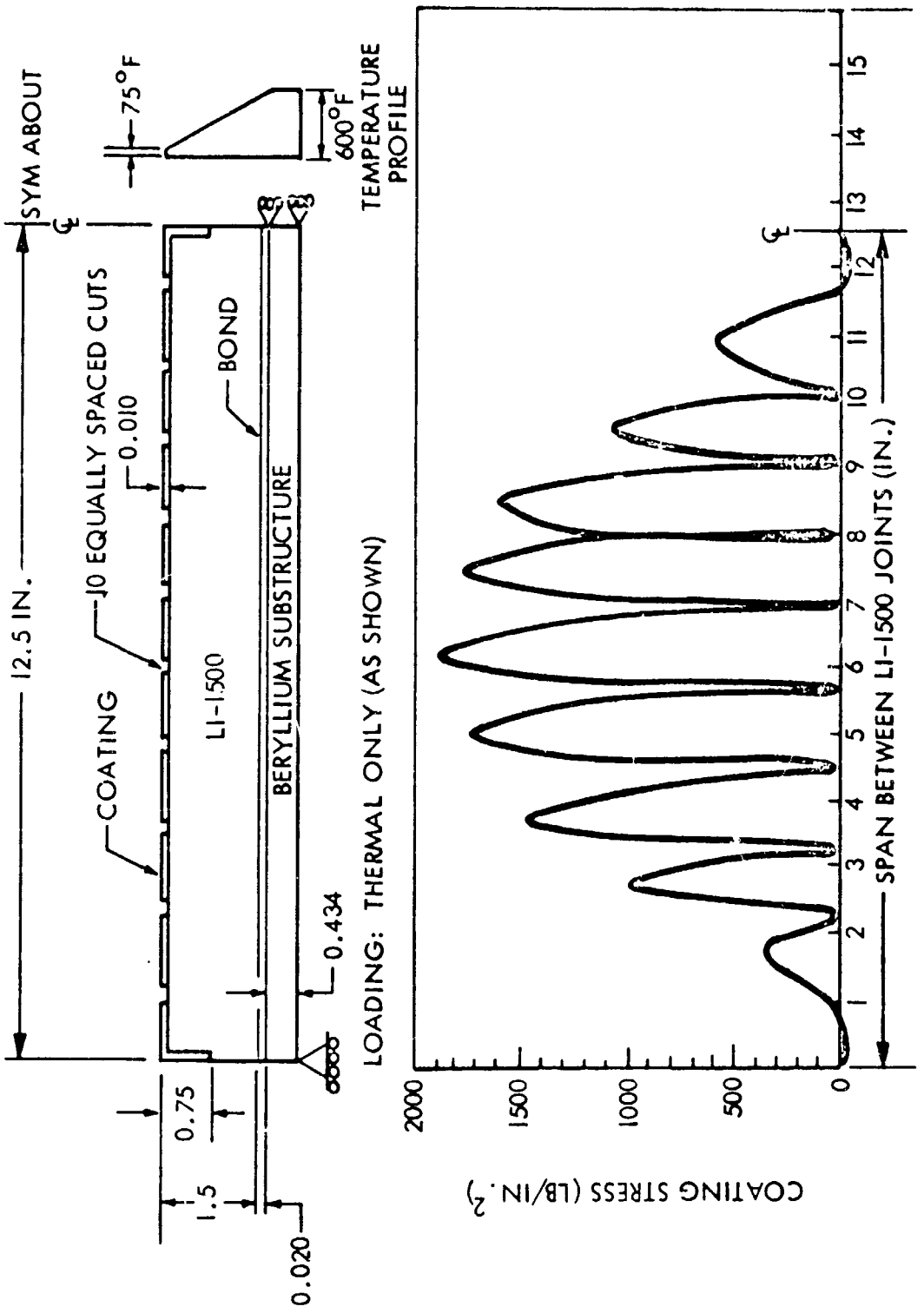

Fig. 3.4.3-3 Variation of Coating Stress with Number of Coating Discontinuities (Cont'd)

3.4.3.3 New Coating Formulations. Development of new coating formulations was pursued concurrent with developmental efforts directed toward improved LI-0025 integral coating and textured effects. The same problems continued of finding candidate material systems which offered a hope of matching the thermal expansion of the base composite without incurring chemical attack. The general basic families of glass-forming constituents are listed in Table 3.4.3-1 which compares the expected thermal expansions and fusion temperature ranges with amorphous silica.

Table 3.4.3-1

THERMAL EXPANSION AND FUSION RANGES FOR VARIOUS GLASS FORMING COMPOSITIONS AS COMPARED WITH AMORPHOUS SILICA

Family Type	Thermal Expansion Range	Fusion Range
$PbO-B_2O_3-SiO_2$	$6\text{-}9\times10^{-6}$ °C	1000-1300° F
$PbO-SiO_2$	$9\text{-}10\times10^{-6}$	1300-1500° F
K_2O, CaO, $PbO-Al_2O_3-B_2O_3-SiO_2$	$5\text{-}8\times10^{-6}$	1300-1600° F
CaO, MgO - Al_2O_3 - SiO_2	$4\text{-}5\times10^{-6}$	1900-2400° F
Li_2O - Al_2O_3 - SiO_2	3×10^{-6}	1900-2500° F
ZnO - B_2O_3 - SiO_2	$6\text{-}9\times10^{-6}$	800-1000° F
PbO - Al_2O_3 - SiO_2	$6\text{-}8\times10^{-6}$	1800-2200° F
Amorphous Silica	0.8×10^{-6}	2900-3200° F

Cursory testing showed that commercial frits based upon these materials produced glaze coatings which were totally incompatible physically and chemically with LI-1500. Exploratory investigations identified only two systems which offered a hope for developing compatible coatings for amorphous silica – i.e., lithium aluminosilicates and borosilicates. The latter had been identified in the development of the LI-0025 formulation which did match the thermal expansion of the base composite material. These two systems were explored in concurrent investigations to develop a new and improved coating formulation.

3.4.3.4 Lithium Aluminosilicates. The lithia-alumina-silica system has several crystalline phases having low-to-negative thermal expansions. The composition and common mineral names include the following:

$Li_2O \cdot Al_2O_3 \cdot 2SiO_2$	Eucryptite
$Li_2O \cdot Al_2O_3 \cdot 3SiO_2$	
$Li_2O \cdot Al_2O_3 \cdot 4SiO_2$	Spodumene
$Li_2O \cdot Al_2O_3 \cdot 6SiO_2$	Lithium feldspar
$Li_2O \cdot Al_2O_3 \cdot 8SiO_2$	Petalite
$Li_2O \cdot Al_2O_3 \cdot 10SiO_2$	

A series of thermal expansions were reported for these materials by Hummel* in 1951 and are compared to amorphous silica in Fig. 3.4.3-4. These data show lithium aluminosilicates in the range of 1:1:4 (spodumene) to 1:1:10 are very similar to silica with 1:1:2 (eucryptite) having an extreme negative thermal expansion. The common method of preparation requires first melting as a glass at above 2,000° F, then followed by a heat soak in the 1,450-1,700° F range for at least 30 minutes. The second heat treatment converts the glass to a crystalline aggregate usually consisting of beta-eucryptite or beta-spodumene bound by an undefined amount of undevitrified glass phase. The crystalline phases and/or glass-ceramic materials exhibit low thermal expansions.

The prime candidate source materials for investigation of the lithium aluminosilicate systems included a Lockheed-Georgia Company frit patented for glazing fused silica; two commercially available frits and a granular beta-spodumene material developed by Lockheed-California Company for low expansion high temperature ceramic tooling. The Lockheed-Georgia material formulation shown in Table 3.4.3-2 was prepared in small quantity by LMSC in crucible melts to 2,500° F. A commercial "fritter" was employed for larger quantities. The Lockheed-California material was processed by rotary calcination of spodumene and kaolin and showed a thermal expansion of 4.5×10^{-7}° C.

*F. A. Hummel, "Thermal Expansion Properties of Some Synthetic Lithia Minerals," J. Am. Ceram. Soc. 34 (8) 235-239 (1951)

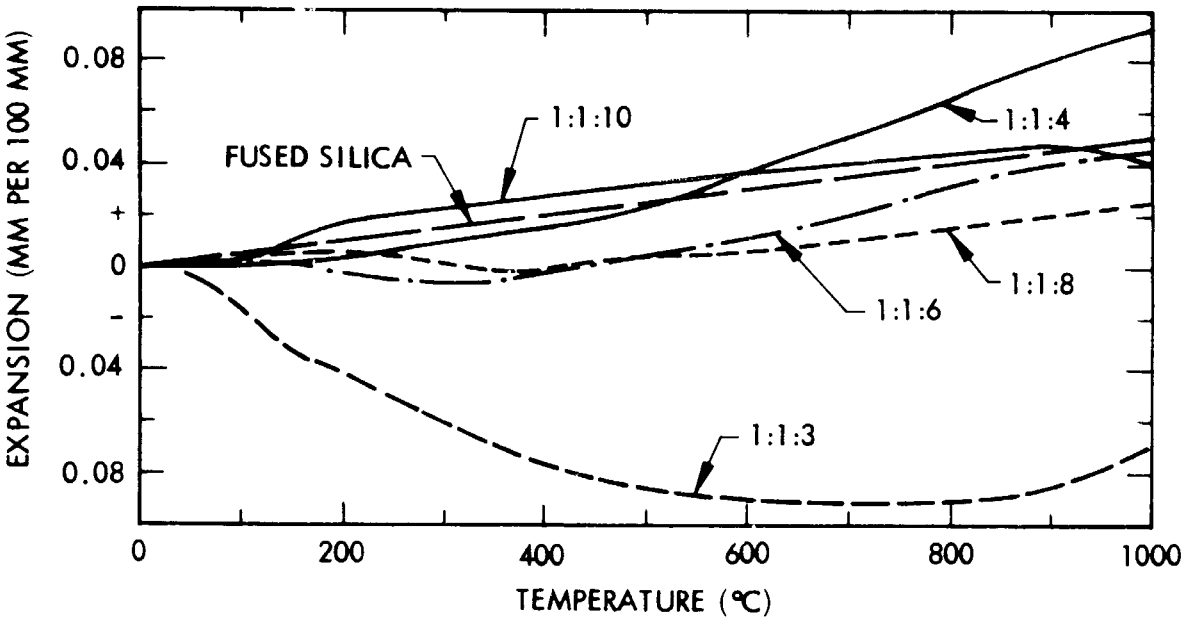

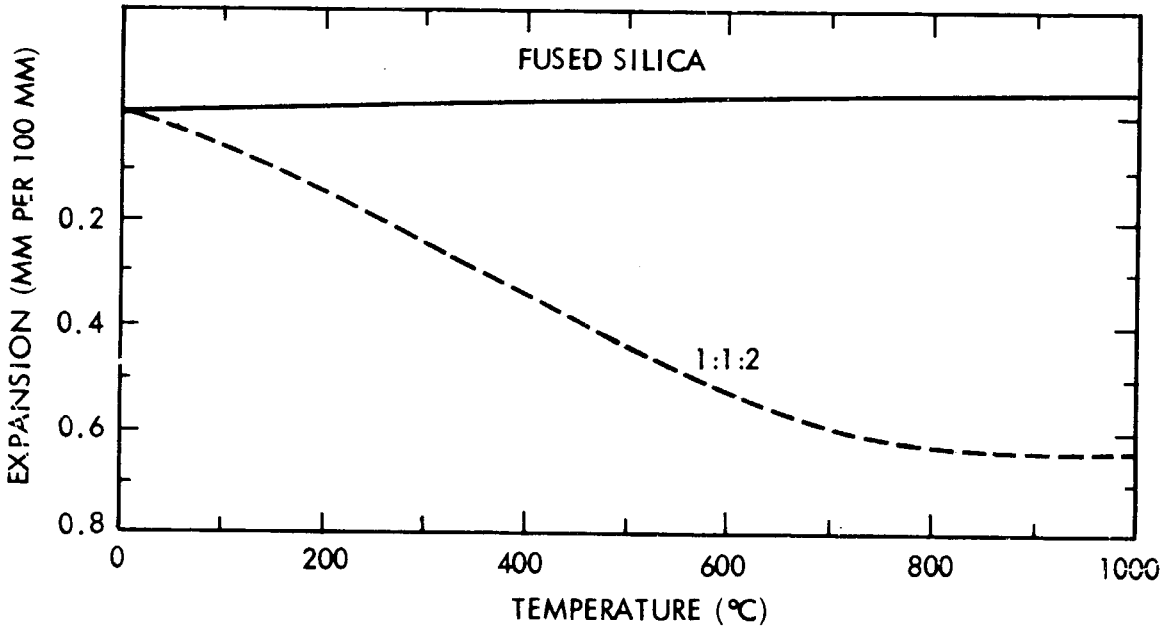

Fig. 3.4.3-4 Thermal Expansion of Lithium Aluminosilicate Systems

Table 3.4.3-2
LITHIUM ALUMINOSILICATE FRIT (PATENT 3,498,804)

Weight Composition		Oxide Composition	
Litharge	18.0%	PbO	29.8%
Potash Spar	20.1	K_2O	2.8
Boric Acid	13.2	Li_2O	0.9
Silica	18.6	Al_2O_3	3.1
Lithium Carbonate	1.0	B_2O_3	12.6
Chrome Oxide	0.4	Cr_2O_3	0.6
Zircon	5.6	SiO_2	44.7
		ZrO_2	6.2

Over forty samples were evaluated in exploratory work which included varied mixtures of these source materials, application techniques, and LI-1500 surface preparations and interface materials. Although encouraging mixtures and results were noticed, at no time did the coatings evidence the thermal shock resistance desired. The mixtures displayed erratic behavior at 2,500°F. The best coatings series might be crack free and moisture tight for a few cycles at 2,500° F. However, repeat samples or continued cycling would crack and spall the coating from the insulation material surface.

In general, investigations clearly indicated the need for a dense silica surfacing as an interface between the glass melt phases and the base material. As shown in Fig. 3.4.3-5, severe reactivity occurred where no interface material was used. Cracking and lift-off would occur on 2,500° F cycling with thick coat applications, while thin coatings would be absorbed at 2,500° F.

The incorporation of beta-spodumene type granules into formulations improved coating results, reducing the tendency toward crazing. This addition insured the presence of low-expansion crystalline phases in the coating systems. Results were also improved by including a heat-soak period after the initial firing of the glaze, allowing further crystal nucleation of the parent glass phase. This finding and the inability to duplicate

Fig. 3.4.3-5 Identical Coatings With and Without Dense Silica Substrate

2,500° F cyclical results were attributed to the physical characteristics of the material system. The solidus-liquidus phase separation temperature for the beta-spodumene end of the phase diagram is at 1,356° C (2,470° F), Fig. 3.4.3-6. Under 2,500° F testing, the concentration of the various crystalline phases can change, leading to change in crystalline content with resultant variance of thermal expansion characteristics. The potential presence of silica devitrification may also have some bearing on the unreproducible performance of formulations, for x-ray diffractions in general showed an increase in cristobalite content when admixed with silica, but no silica crystalline phases when fired alone. The increase in cristobalite percentages may be caused by the presence of free Li_2O uncombined in the glass phase.

With these findings and evidence of real progress in the experimental work with new borosilicate formulations, this work was curtailed and emphasis was shifted to the B_2O_3-SiO_2 glass glaze system.

3.4.3.5 Borosilicate Coatings. As in the parallel effort on lithium aluminosilicates, a dense silica layer was found to be desirable between the coating system and base material. Coatings of interest were evaluated with heat cycling at 2,300 and 2,500° F. Isothermal evaluation for 3-1/2 hr, the time equivalent of over 100 cycles of reentry, was primarily used as initial screening tests before use of radiant heat cycling, because of time factors. Isothermal evaluation was considered to be a more severe condition on both insulation and coating than expected on space shuttle reentry. Coating development depended heavily on emissivity and morphology studies to define constituent properties and as an aid in directing coating development.

Borosilicate formulations investigated are summarized in Table 3.4.3-7. In general, a wide range of compositions showed good opacity, reproducibility of color appearance, craze-free surfaces and moisture-tightness prior to isothermal testing. Coating refractoriness was particularly sensitive to the B_2O_3 content. Best results were generally obtained with B_2O_3 contents in the range of 3.5 to 12.6 percent. Coatings with B_2O_3 content below 3.5 percent remained porous and did not fully mature when fired at 2,500° F. Increasing the B_2O_3 content above 13 percent significantly lowered the sintering range of the coating. However, a corresponding reduction in the temperature capability of the resultant coatings was evidenced. On thermal exposure testing

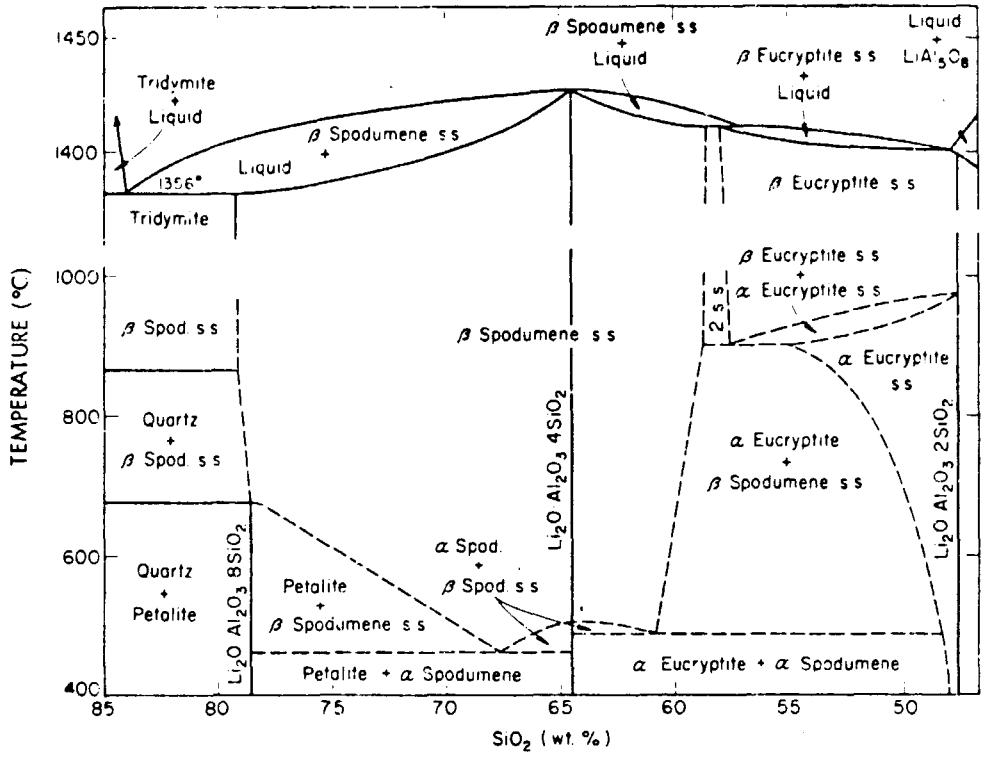

Fig. 3.4.3-6 System Li_2O-Al_2O_3-$2SiO_2$ (Eucryptite)–SiO_2*

*R. Roy, D. M. Roy, and E. F. Osborn, J. Am. Ceram. Soc., 33 (5) 156 (1950).

Table 3.4.3-3

BOROSILICATE COATINGS

Sample	Thickness (Mils)	Coating Major Constituents (percent)							Comments
		SiO_2	B_2O_3	Cr_2O_3	SiC	$CoO-Cr_2O_3$ Fe_2O_3	$NiO\cdot Cr_2O_3$	CoO	
111-4	5	91.0	3.8		4.8				Moisture tight after 3-1/2 hr @ 2,300°F
122-3	8	91.0	3.8			4.8			Unsatisfactory color tonality; moisture tight, no coating defects
121-1	11	91.0	3.8		4.8				Porous after thermal exposure at 2,300°-2,500° F
118-2	6	90.3	4.3		4.8				Silica - SiC integral coating; crack, craze defects
112-1	7	90.3	4.3		4.8				Porous after thermal exposure at 2,300°-2,500° F; crack, craze defects
109-1B	4	90.3	4.3	4.8					Moisture tight, no coating defects
113-4	8	90.3	4.3					4.8	Unsatisfactory color tonality; moisture tight, no coating defects
110-3	6	90.3	4.3		4.8				Porous after thermal exposure at 2,300°-2,500° F
110-4	6	90.3	4.3		4.8				Porous after thermal exposure at 2,300°-2,500° F
118-B	4	89.2	4.8			4.8			No barrier coating; attacks underlying fiber
114-3	6	89.2	4.8			4.8			Porous after thermal exposure at 2,300°-2,500° F
118-A	4	88.0	5.7			4.8			No barrier coating; attacks underlying fiber
109-1A	4	88.0	5.7	4.8					Moisture tight, no coating defects

Table 3.4.3-3

BOROSILICATE COATINGS (Cont)

Sample	Thick-ness (Mils)	Coating Major Constituents (percent)							Comments
		SiO_2	B_2O_3	Cr_2O_3	SiC	$CoO-Cr_2O_3$ Fe_2O_3	$NiO\cdot Cr_2O_3$	CoO	
121-3	8	87.0	3.6		4.5	4.5			Porous after thermal exposure at 2,300-2,500° F
113-2	5	86.2	4.1			9.1			Moisture tight after 3-1/2 hr @ 2,300° F
114-1	6	86.2	4.1				9.1/NiO		Unsatisfactory color tonality; moisture tight, no coating defects
114-2	6	86.2	4.1		9.1/ Si_3N_4				Unsatisfactory color tonality; moisture tight, no coating defects
113-3	10	86.2	4.1	4.5				4.5	Crack, craze defects
113-1	7	90.3	4.3				4.8		Unsatisfactory color tonality; moisture tight, no coating defects
114-4	5	84.1	5.4			9.1			Porous after thermal exposure at 2,300-2,500° F
121-2	9	83.2	3.5		4.3	8.7			Porous after thermal exposure at 2,300-2,500° F
121-4	10	82.6	3.9		4.3	8.7			Porous after thermal exposure at 2,300-2,500° F
121-5	6	81.2	9.7		4.3	8.7			Moisture tight after 3-1/2 hr @ 2,300° F
108-3B	5	80.4	10.3	4.8					Porous after thermal exposure at 2,300-2,500° F; crack, craze defects
108-3A F.S.	5	76.5	12.6	4.8					Porous after thermal exposure at 2,300-2,500° F; crack, craze defects

Table 3.4.3-3

BOROSILICATE COATINGS (Cont)

Sample	Thick-ness (Mils)	Coating Major Constituents (percent)							Comments
		SiO_2	B_2O_3	Cr_2O_3	SiC	$CoO-Cr_2O_3$ Fe_2O_3	$NiO \cdot Cr_2O_3$	CoO	
109-2	5	18.5	1.2		80.0				Crack, craze defects
122-1	8	82.6	3.9		4.3	8.7			Moisture tight, no coating defects

at 2,300° to 2,500° F, the best results generally were indicated by coatings containing the lowest amount of B_2O_3 required to produce water imperviousness at 2,500° F.

For emissivity considerations of the borosilicate coating system, silicon carbide was used singularly and as admixtures with other agents. Calcines of cobalt chrome and iron oxides provided a deep black at 9.1 percent concentrations. A range of gray-to-black tones could be achieved when this was used in conjunction with varying silicon carbide. Other potential emissivity agents examined included nickel-chrome spinel, iron titanate, cobalt compounds, nickel oxide and silicon nitride. Of all these compounds, the cobalt family gave the strongest opacity. Silicon nitride and nickel oxide both gave weak coloration with low opacity. Iron titanate showed potential at high percentages only. Even color tonality was easily achieved with high-cobalt low-chrome calcines and interest was retained in these along with the cobalt, chrome, iron oxide (black) for identification markings of orbiter surfaces for location of fasteners, etc., as suggested in Fig. 3.4.3-7.

X-ray diffraction results for experimental cobalt oxide compounds admixed with silica indicated a high rate of devitrification at 2,500° F. Since rates of devitrification are extremely temperature dependent, cobalt compounds may still be suitable in low-fired coatings designed for use under 2,000° F.

3.4.3.6. Selection of LI-0042 (2,300° F). Midway in the program a selection of the best coatings that had been observed to that point for 2,300° F operation was made and transferred to the NAS 9-12083 contract for intensive evaluation and use on prototype panels. This followed the intent and original objective that improvements would be incorporated into that contract at the earliest possible date. There were two "best" competitive systems at that time – one based upon the use of cobalt, chrome, and iron oxides as an emittance agent and the other upon silicon carbide for that purpose. The SiC was favored because of its superior emittance characteristic and less influence upon transformation. However, there was some concern as to an unassessed possible sensitivity to dissociation by oxidation and vacuum effects. Several tests were run at 2,300° F and 10 Torr vacuum, duplicating the atmospheric conditions expected when maximal surface temperatures would occur on the orbiter surfaces during reentry.

All test samples had a water-impervious surface after four continuous hours of exposure, even though the exposed coating was determined to contain 7 percent cristobalite. Emissivity evaluations indicated that the severity of test conditions had not affected emissivity. Figure 3.4.3-8 shows 3 in. diameter test samples rough-cut from larger 6 in. × 6 in. panels after 4 hr exposure at 2,300° F at 10 Torr vacuum conditions. Also, tests were conducted under isothermal conditions in normal atmosphere furnaces. These tests showed no degradation of the coating imperviousness up to 2 hr at even 2,500° F. With these findings, the coating formulation containing SiC was selected for use at 2,300° F on program NAS 9-12083 test and evaluation hardware. This coating was designated as LI-0042.

3.4.3.7. LI-0042 For Evaluation Test Models and Prototype Panels. For the last 3 months of the program, 0042 was used on over 100 NASA Contract test panels. Little difficulty was found in coating 12 in. × 12 in. panels or coating side surfaces for joint-gap test panels. The coating/material compatibility displayed by LI-0042 was even applicable to right-angled surfaces without the edge-cracking problems observed for other candidate materials. Other materials exhibited high modulus and low strain-to-failure and tended to crack and induce stresses. The ease of coating intricate geometries may possibly be due to the novel pore-filled structure of 0042 and matched thermal-expansion coefficient.

On analyzing LI-0042 under magnification, the microstructure may be characterized by a high volume of closed pores, with a resultant rough-textured surface. A top and side view of the 0042 coating is shown in Fig. 3.4.3-9. The side view shows the dense silica barrier layer and the characteristic vesicular structure of the LI-0042 formulation. These features are even more clearly apparent in Fig. 3.4.3-10 which shows a cross-section of the coating on a flat surface and at a corner. The unique closed pore structure of the LI-0042 was considered to be one of the prime contributors to its apparent ease of withstanding 2,300° F and 2,500° F thermal cycling. This type of structure does not propagate cracks as readily as would be expected of a continuous glassy structure. Added to this is the dispersion ("hardening") of the SiC particles to provide grain boundaries. A fracture initiated at the surface might be stopped by a pore or grain boundary before resulting in complete failure. Crack

Fig. 3.4.3-7 Sintered-on Identification Marking

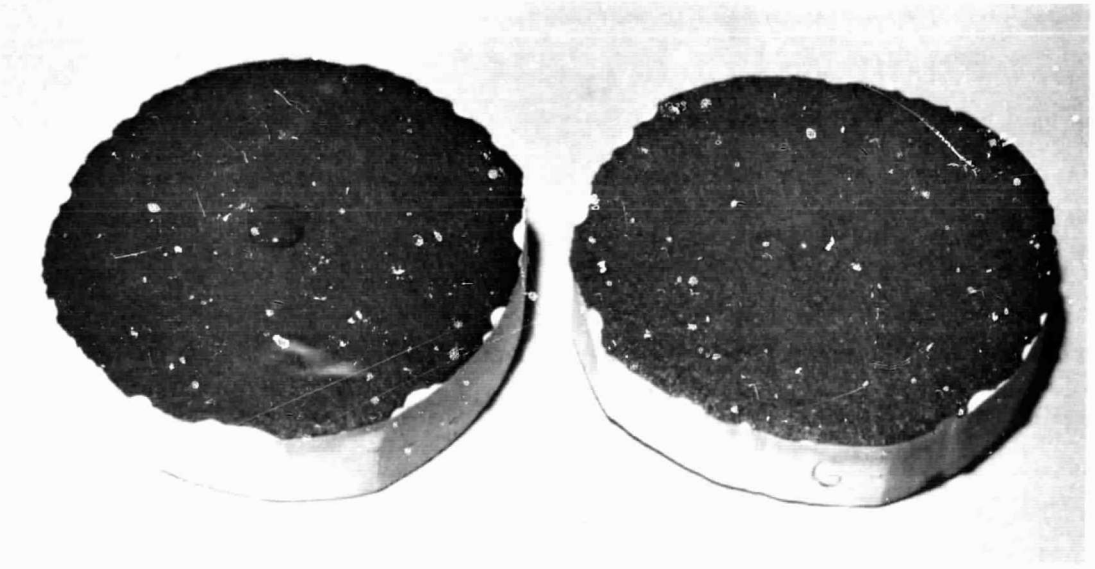

Fig. 3.4.3-8 Borosilicate Coating After 4 hr, 2300° F at 19 Torr Vacuum

a) Top View of 0042 (7X)

b) Side View of 0042 (28X)

Fig. 3.4.3-9 Photomicrographs of LI-0042 Surface Coating

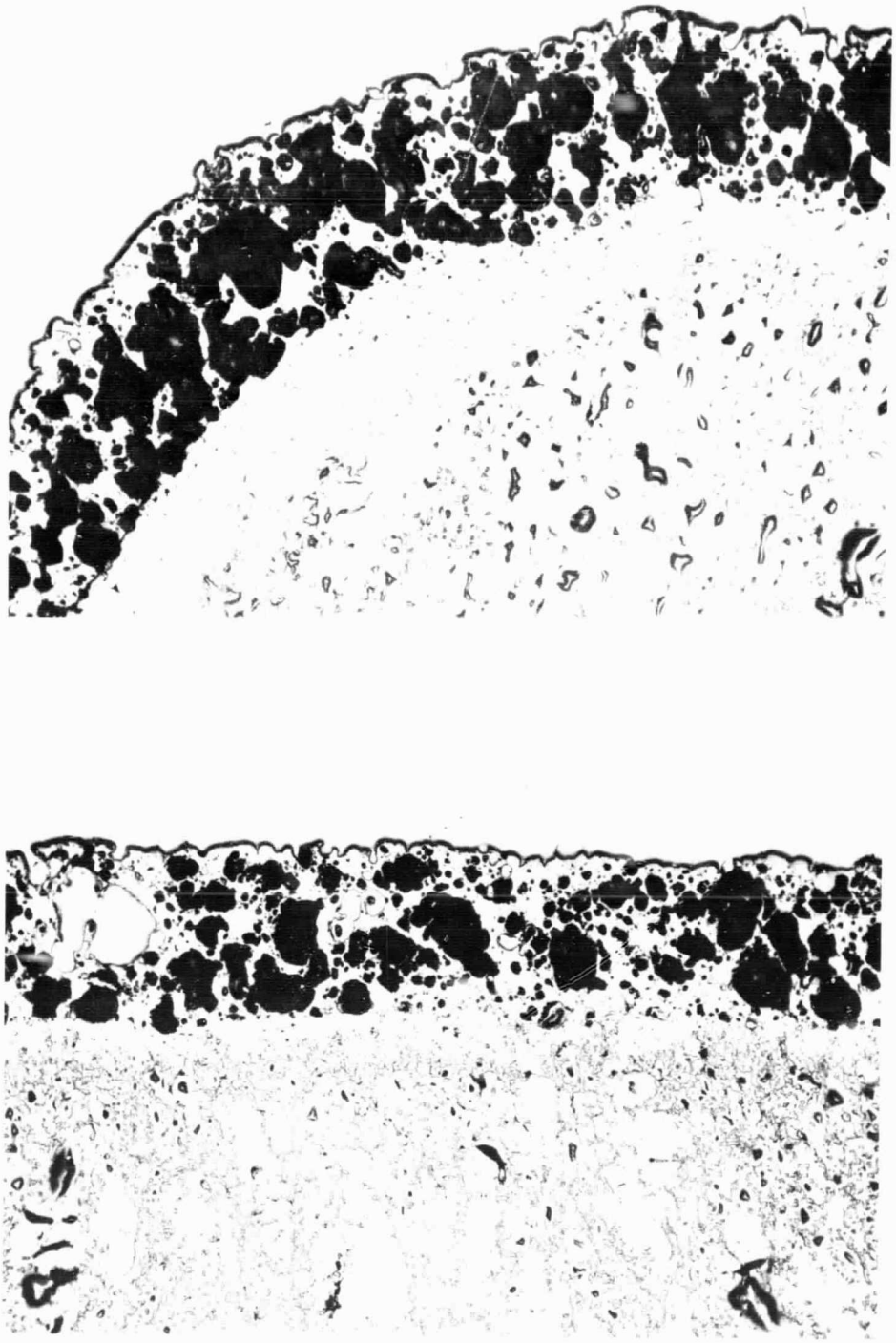

Fig. 3.4.3-10 Photomicrographs (100X) Illustrating Cross Section of LI-0042 Surface Coating

propagation would be hindered by the pores so that surface checking might result rather than complete catastrophic failure. However, during the testing phase, particularly while being subjected to 100 cycles at 2,500° F in radiant heat tests, it was noted that this coating gave sporadic results with respect to retention of water tightness during prolonged over-heating above 2,400° F. While this was an adequate coating for operation up to 2,300° F, it was apparent that slight modification would be required to attain equal reliability for water tightness during many cycles to 2,500° F. It is interesting that water tightness was apparent in overtests of LI-0042 up to 3,000° F. The only changes noted in these evaluations was an increase in the vesicular cell size to provide what might be visualized as a foam overcoat insulator.

3.4.3.8. Development of LI-0045 (2,500° F). With acceptability of LI-0042 confirmed for 2,300° F environments, development efforts were concentrated on optimization of the borosilicate system for utilization in the 2,500° F regime. Two areas of coating improvement were investigated:

1. Develop an additional borosilicate glass layer.
2. Improve the barrier coating to reduce interaction.

Approximately 30 coatings and techniques were evaluated in this phase of development work. Isothermal/furnace firings at 2,500° F were conducted on significant formulations as a means of identifying best developmental areas. Initial studies were in application of a glass overcoating applied directly over the normal LI-0042 coating. At lower top coating refractoriness (Fig. 3.4.3-11), boiling of the top coat was experienced. Best compatibility was achieved with the more refractory coatings having less B_2O_3. On isothermal firing at 2,500° F, all such overcoatings tended to show improved results over the normal LI-0042, retaining moisture tightness for 2-1/2 hr, but none were capable of remaining moisture impervious for 3-1/2 hr or longer. No crazing, spalling, or delamination problems developed throughout the compositional test matrix. The overglaze would tend to lose gloss during extended firings, the surface would roughen and the overglaze would tend to be absorbed into the LI-0042 sublayer, leaving the surface open to the absorption of moisture. Further attention then was given to the base coating matrix to attain greater density and refractoriness. This modification, along with the build-up of application technique experience, eventually led to the

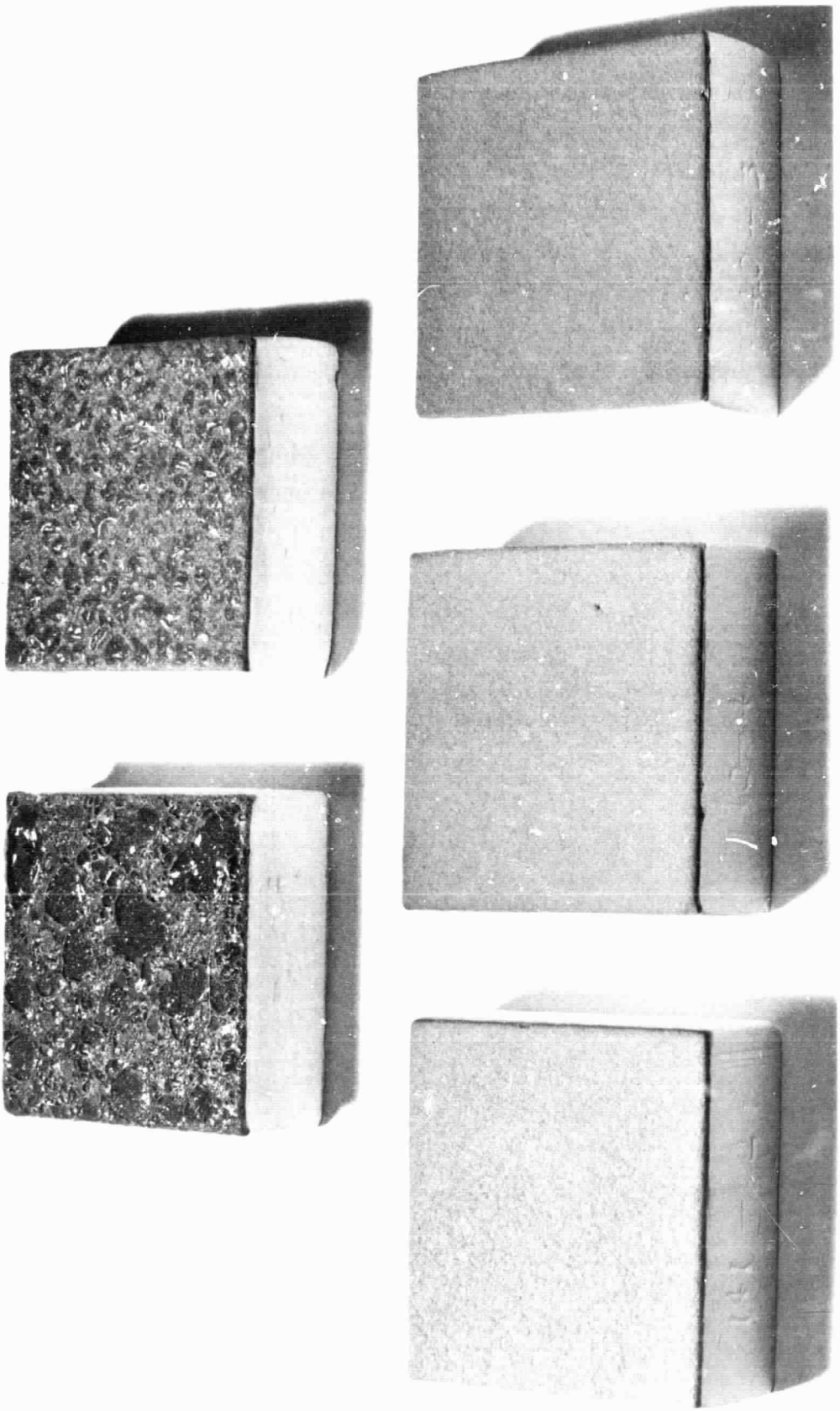

Fig. 3.4.3-11 0042 Oversprayed With Coatings of Various Refractoriness

development of a system which consistently withstood laboratory isothermal firings at 2,500° F for 3-1/2 hr without developing porosity and with a smoother surface than LI-0042. The smooth surface of the coating was maintained throughout isothermal tests. The coating was applied to both 8 and 15 lb/ft^3 insulation materials with the same effectiveness. This new material coating system was designated as LI-0045 and was offered for more comprehensive evaluations to be conducted in Section 3.7. Those evaluations included cyclic exposure at 2,500° F in the LMSC Radiant Heat Facility. The basic properties were similar to LI-0042. A photomicrograph of the LI-0045 cross-section, as processed, is shown in Fig. 3.4.3-12. The barrier coat is now thicker when compared with the 0042 coating. It consists of a dense silica layer and a borosilicate layer with a fine void structure. The top surface is essentially void-free. Figure 3.4.3-13 shows micrograph top views of the 0045 coating after 0.5 hr and 3.5 hr of isothermal cycling at 2,500° F. After 0.5 hr, the top coat has "fined" after initial fusion and has a fine microscopic bubble structure. After 3.5 hr of exposure, the bubble structure has progressed slightly with continued thermal treatment, but a high-gloss and nonporous surface is maintained.

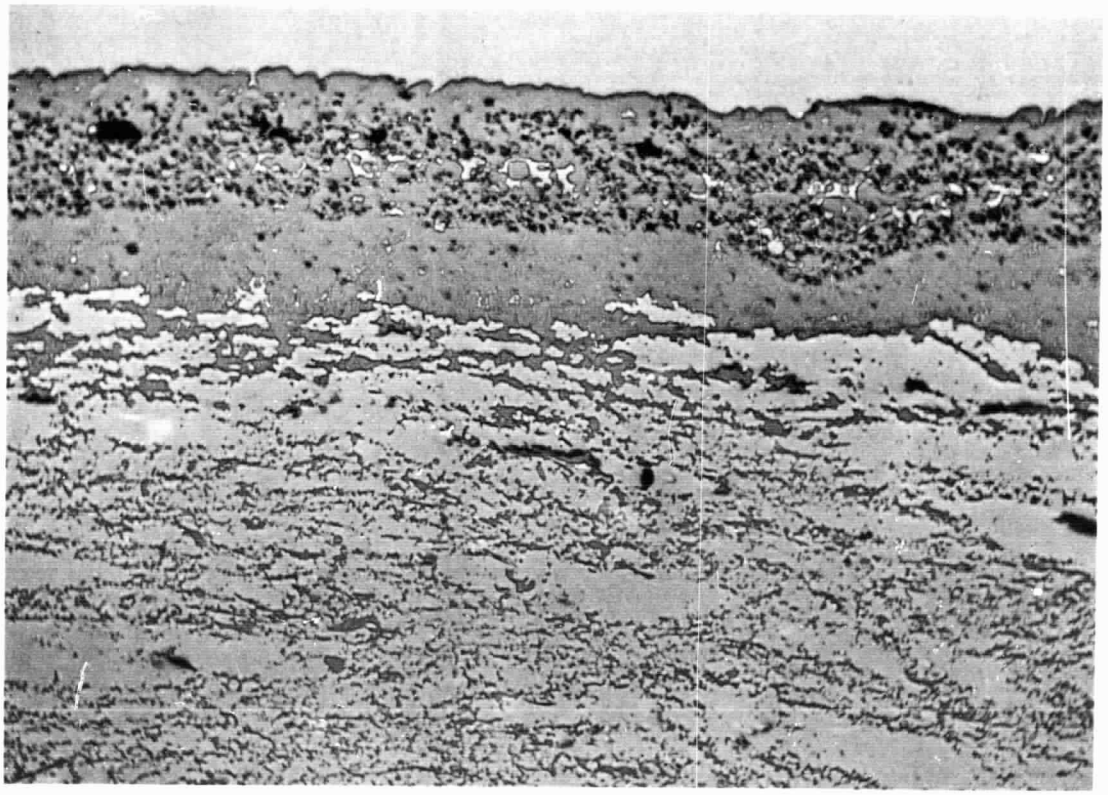

Fig. 3.4.3-12 Cross-Section View of LI-0045 Coating (100×)

After 0.5 hr Exposure

After 3.5 hr Exposure

Fig. 3.4.3-13 Photomicrographs (28X) of LI-0045 Coating After Isothermal Exposures at 2,500°F

3.5 MOISTURE REDUCTION TECHNIQUE AND VEHICLE EFFECTS

Moisture absorption in the RSI system could significantly increase the shuttle weight during launch phase because of the large volume of surface insulation anticipated for use on the space shuttle vehicle. The moisture absorption of RSI material must be minimized during ground storage and earth atmospheric flight trajectories. Although water impervious surface coating systems have been developed for the LI-1500 material (LI-0042 and LI-0045), these surface coatings may not offer fail-safe reliability for absolute barrier to moisture. That is, moisture may be introduced through the substrates, joints, gaps, minor damaged areas, minor processing imperfections, or as condensations. Use of a secondary water repellent system applied to the RSI material appears to be one of the simplest and yet most positive means of minimizing moisture pickup. Many years previous to this contract, a refurbishable secondary water repellent system, LI-003, was developed and successfully applied to the LI-1500 RSI system. The LI-003 formulation was based upon a dimethylsiloxane polymer fluid (Dow Corning DC-200) and the water repellent material was applied to each individual fiber in the insulation material to obtain the hydrophobic properties for the LI-1500 system.

The objective of this phase of the program was to improve and simplify the secondary waterproofing techniques by the investigation and application of water repellent systems to the LI-1500 material. To achieve the required improvement and simplification, the following were necessary:

- Investigate candidate water repellent materials.
- Improve process application techniques and determine techniques for refurbishment after each shuttle mission.
- Determine humidity resistance, rain resistance, and time/temperature limits of useful life.
- Develop a secondary water repellent system that will be compatible with the substructure attachment bonding.
- Determine problems associated with the anticipated environmental conditions.

Although a fully optimized secondary water repellent system has not yet been developed, all prime objectives within the scope of this program phase have been achieved and are summarized as follows:

- Investigation of candidate materials (silicones and tetrafluoroethylene materials) resulted in the selection of the improved LI-007 water repellent system based upon the polydimethylsiloxane polymer (Dow Corning DC-1107).
- The LI-007 system may be readily applied to the LI-1500 material during processing or during the refurbishment operation by various techniques and may be cured in ambient conditions or at moderately elevated temperature environments.
- Water repellency properties have been achieved for humidity and rain environments with a minimum penalty to the overall system weights. Initial time/temperature evaluations have indicated that the water repellency effectiveness may be retained even after certain exposures to 1,000°F environments.
- The LI-007 water repellent system is compatible with the attachment bonding concept. The RSI material with the -007 treatment is readily bonded to the substructure with the silicone bonding material under consideration for the program.
- Space environment considerations for the silicone water-repellent material have indicated that the LI-007 system appears to be suitable for the outgassing in space requirements.
- The silicone water repellent system is a chemically clean material and shows no detrimental effects on the morphology of the fibers during thermal-chemical decomposition.

3.5.1 Investigation of Candidate Materials

Because of their hydrophobic characteristics and previous successful experience at LMSC, the primary materials for investigation were silicone-based water repellent systems. The silicone materials also appeared to exhibit compatible chemistry (basically a silica material minimizing contamination and reducing the possibility of detrimental morphology effects on the fiber system), excellent high- and low-temperature properties, availability in various forms, adaptability to the RSI

system, and an apparently high ratio of water repellency efficiency to the additional weight penalty of the system. In addition to the various silicone materials, the tetrafluoroethylene (teflon) materials, exhibiting many of the attributes of the silicone type material, were also considered for a limited initial evaluation.

Commercial silicone products may be divided into the following five classes: fluids, compounds, lubricants (greases and fluids), resins and elastomers. Silicone synthetic polymers are partly inorganic in nature. They have a polymer structure that comprises alternating silicon and oxygen atoms.

$$\left[-\overset{|}{\underset{|}{Si}} - O - \overset{|}{\underset{|}{Si}} - O - \overset{|}{\underset{|}{Si}}-\right]$$

Typically, the silicon atoms will have one or more organic groups attached. These side groups may be methyl, alkyl or phenyl units. The ultimate physical form is determined by molecular weight, extent of crosslinking between polymeric chains and type and number of organic groups attached to the silicon atoms. The outstanding water repellent property of the silicones has increased utilization in the textiles and electronics fields. The water repellent or hydrophobic properties of the silicone system may be attributable to film forming ability and to the phenomenon of the orientation of the molecules in the silicone polymer. In the classic example of the polyorganosiloxane, the siloxane dipoles point to the phase boundary while the free surface is covered by the methyl groups in close packing as illustrated by the sketch. An increase in the density of the packing of the organic groups raises the hydrophobic effect. This orientation and packing of the organic groups may be accomplished by either heat or catalysts.

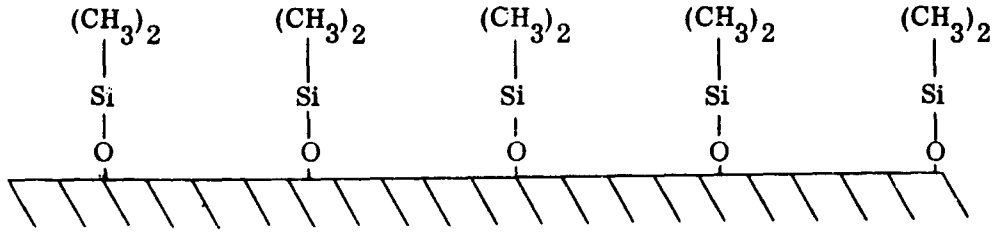

Ref: Chemistry and Technology of Silicones by Walter Noll, Academic Press, 1968

The initial materials selected for the moisture reduction technique evaluation are shown in Table 3.5-1. These materials consisted of four groups of silanes (alkyltrichloro silanes, dialkyldichloro silanes, alkylsilane esters, and organo functional silanes), commercial water repellent formulations, phenyl methyl polysiloxane resins, silicone protective coatings, dimethyl siloxane polymer fluids and a polydimethylsiloxane polymer. In addition, tetrafluoroethylene (teflon) material also is listed in the table. The initial evaluation consisted of applying the various water repellent systems to the basic LI-1500 material and evaluating the water repellent characteristics. The initial screening of the candidate materials consisted of a simple water drop absorption observation evaluation. A controlled drop of water was placed on the surface and time for absorption noted. For more water repellent surfaces, comparative changes in the water droplet form and contact angles were determined at 15 min after introduction of the water drop. Photographic techniques were used to determine the contact angles.

As shown in Table 3.5-1, all of the materials were eliminated except two of the alkyl trichlorosilanes (methyl and ethyl), the phenylmethyl polysiloxane resin (DC-805), the silicone protective coating (DC-630), the dimethylsiloxane polymer fluid (DC-200), the polydimethylsiloxane polymer (DC-1107), and the teflon material. Examples of the photographic techniques used to determine the contact angles of the droplet forms of the more promising candidates systems are presented in Fig. 3.5-1. The most promising materials were selected for further investigation.

3.5.2 Selection of Material for Water Reduction

Selection of the final water reduction technique material for this program was achieved by evaluation and analysis of humidity performance, simulated rain resistance, effect of morphology on the basic fibers, attachment/bonding considerations to the substrate, and the penalty of weight to the overall TPS system.

3.5.2.1. Humidity. The results of the humidity investigation (Table 3.5-2) show the outstanding moisture resistance characteristics of the DC-200 and DC-1107 material to the humidity environments. All specimens except as noted were treated with the equivalent of 4 percent by weight water-repellent material. The relatively rapid

Table 3.5-1

LI-1500 MOISTURE REDUCTION TECHNIQUE INITIAL MATERIALS EVALUATION

Type	Company and Designation		Initial Evaluation Results
• Alkyltrichlorosilanes			
Methyltrichlorosilane	Union Carbide	A-154	(2)
Methyldichlorosilane	Union Carbide	A-155	(1)
Ethyltrichlorosilane	Union Carbide	A-17	(2) Contact Angle 150 Deg
Amyltrichlorosilane	Union Carbide	A-18	(1)
Phenyltrichlorosilane	Union Carbide	A-152	(1)
• Alkoxysilane Esters			
Ethyltriethoxysilane	Union Carbide	A-15	(1)
Methyltriethoxysilane	Union Carbide	A-162	(1)
Amyltriethoxysilane	Union Carbide	A-16	(1)
Methyltrimethoxysilane	Dow Corning	Z-6070	(1)
Diphenyldimethoxysilane	Dow Corning	Z-6074	(1)
Dimethyldiethoxysilane	General Electric	XC-3902	(1)
• Organofunctional Silanes			
Epoxy Substituted Silane	Union Carbide	A-186	(1)
Vinyltricacetoxysilane	Dow Corning	A-6075	(1)
• Water Repellent Formulations (Proprietary)	Union Carbide	R-21	(1)
	Union Carbide	R-22	(1)
• Siloxanes			
Phenylmethylpolysiloxane Resin	Dow Corning	DC-805	(2) Contact Angle 120 Deg
Dimethylsiloxane Polymer Fluid	Dow Corning	DC-200	(2) Contact Angle 140 Deg
Polydimethylsiloxane Fluid	Dow Corning	DC-1107	(2) Contact Angle 145 Deg
Silicone Protective Coating	Dow Corning	DC-630	(2) Contact Angle 135 Deg
Tetrafluoroethylene Spray	Miller Stephenson	MS-122	(2)

(1) Evaluation discontinued. Unsatisfactory response to initial water drop absorption test.

(2) Satisfactory response to initial water drop absorption test. Material considered for further evaluation.

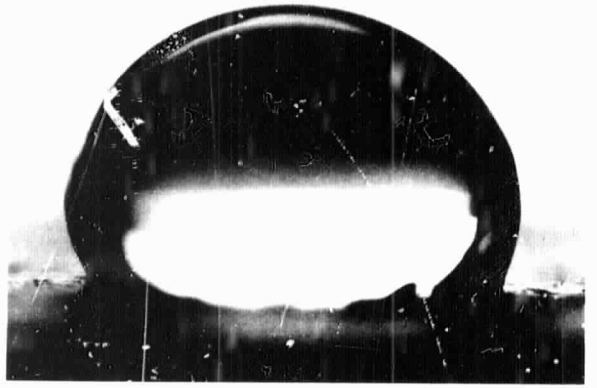

DC 805 METHYL-PHENYL
SILICONE RESIN

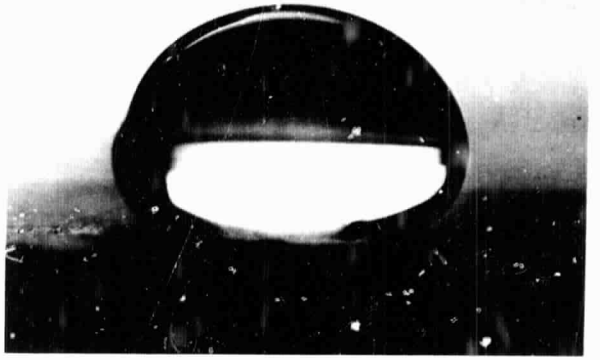

DC 1107 POLYDIMETHYL
SILOXANE RESIN

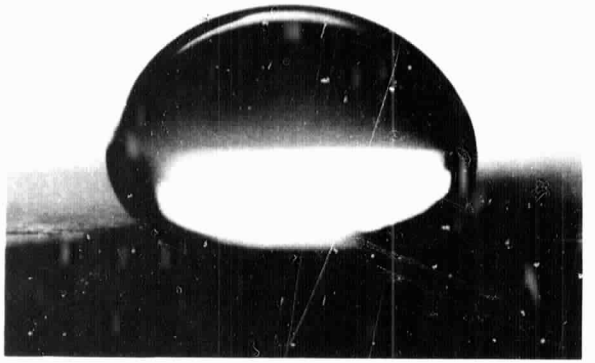

DC 200
SILICONE FLUID

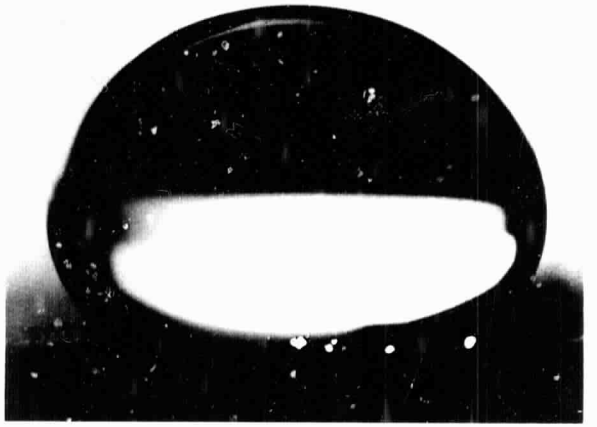

UC A-17
ETHYLTRICHLOROSILANE

Fig. 3.5-1 Water Reduction Technique – Water Droplet Evaluation

Table 3.5-2

WATER REDUCTION TECHNIQUE MATERIALS
HUMIDITY EVALUATION (96% RH at RT)

Water Repellent Material*	Weight (%) Moisture Pick-Up (Days Exposed)					
	3	7	14	21	28	150
DC-1107	0.03	0.09	0.12	0.07	0.09	0.15
DC-200	0.50	0.44	0.51	0.40	0.34	0.55
DC-805	1.15	1.12	1.18	1.08	1.23	-
DC-630	1.23	5.0 ◄	Test Discontinued ►			
A-17 Silane	20.5 ◄	Test Discontinued ►				
A-154 Silane	5.1 ◄	Test Discontinued ►				
Control (no water repellant)	-	7.7	7.8	8.1	7.9	-
**Teflon (Sintered)	4.5	-	-	-	-	-
(Unsintered)	3.8	-	8.6	10.3	-	-

* LI-1500 sample size 1 in. x 1 in. x 1/2 in. impregnated with water repellent material

** LI-1500 sample size 1 in. x 1 in. x 6 in. spray coated.

moisture absorption of the controlled specimen was attributable to the high surface area ratio of the small specimens. The further evaluation of the chlorosilanes was discontinued at this time because of their unsatisfactory response to the moisture absorption test and the liberation of corrosive chemical byproducts resulting from its basic chemistry. Although cured for 4 hr at 260°F, the hydrolysis of the material during the humidity exposure forms HCl acid (evidenced by attacking the aluminum container in which the specimens were placed). The initial high weight gain of the silane specimens was believed to be the result of the moisture affinity to the HCl.

The DC-630 and DC-805 materials under the controlled 4-percent water repellent material addition showed relatively high moisture weight gains when exposed to the humidity environments. Although the DC-805 material appeared to achieve equilibrium conditions after a two-week exposure, equilibrium conditions were not experienced

with the DC-630 coating material after a 2-week exposure period. Further evaluations of these materials were also discontinued at this time. Because of the particular teflon selected, the material was sprayed onto the surface and did not completely impregnate the LI-1500 material. In both the as-sprayed and sintered conditions, the teflon showed excellent response to the water drop test; however, it showed relatively poor moisture absorption resistance when exposed to the humidity environments. Indications are that for this particular application, the material did not coalesce into an impermeable film, but was a series of closely packed small particles exhibiting hydrophobic properties to liquid water, but not to water vapor. Although not fully evaluated under this program, the teflon system showed many attributes and might be developed into a workable over-spray system for the refurbishment operation.

3.5.2.2 Influence on Fiber Morphology. Evaluations conducted showed that there were no morphology changes of the basic LI-1500 silica fibers due to the effect of the selected silicone moisture repellent materials. Silica fiber specimens were impregnated (25 to 50% by weight) with the DC-200, DC-805, and DC-1107 materials, respectively, and were exposed for four hours at 2300° F. The thermally exposed specimens examined by x-ray diffraction techniques determined that there were no crystalline phase changes in the silica fiber material.

3.5.2.3 Attachment/Bonding to the Substrate. Adhesive bonding evaluations showed that adequate attachment with the silicone adhesives (such as the RTV-560) can be achieved to the DC-1107 and the DC-805 resin system. Adhesive attachment evaluations with the DC-630 protective coating, DC-200 polymer fluid, and the teflon materials showed a clean separation from the adhesive to the material and resulted in unsuitable adhesive bonding properties. With the DC-1107 system, adequate bonding to the silicone adhesive can be achieved without priming the water repellent treated surface. Tensile tests showed all failures occurred in the LI-1500 material when utilizing the DC-1107 and the RTV adhesive.

3.5.2.4 Material Selection. The evaluation and analyses selected the DC-1107 as the basic water-repellent material for further evaluation for this program. A water-repellent hydrophobic material system identified as LI-007 was formulated utilizing

the basic DC-1107 silicone material and was used in the further evaluation for this program as well as in conjunction with the deliverable LI-1500 TPS items required under the companion contract NAS 9-12083. For this material improvement, the DC-200 fluid system was also included in certain of the evaluations as a back-up material system.

3.5.2.5 LI-007 Water Repellent System Evaluation. Various evaluations of the LI-007 system have been conducted under investigations supporting this program, IRAD programs, and the TPS development program of Contract NAS 9-12083. All evaluations indicate the suitability of the LI-007 water repellent system for the intended shuttle application and an improvement in a majority of the areas over the previously used LI-003 silicone hydrophobic material. The evaluations included the constituent material investigations, environmental exposures of both the basic LI-1500 material and the surface coated LI-1500 materials, thermal exposures, environmental/thermal cyclic exposures, and analysis of weight considerations to the overall TPS system. A listing and description of evaluations conducted on the LI-007 system are presented in Table 3.5-3.

Table 3.5-3

LI-007 MOISTURE REDUCTION SYSTEM EVALUATION

Freeze/Thaw[1]

- 100% RH, 2 hr → Freeze, 8 hr @ 0°F → Thaw, 8 hr @ 1000°F → 2 Cycles → Wt. Change[2] Nil

Moisture Absorption[1]

- 50% RH, 2 hr min → Thermal 2,300°F → WT. Change[2] Nil

Rain Environment[1]

- 1 in. Per hr Rain Rate 1 hr → Wt. Change Nil → Thermal 2,300°F → Wt. Change[2] Nil

Salt Spray[1]

- Salt Spray 95% RH @ 100°F 4 hr → Wt. Change Nil → Thermal 2,300°F

*See footnote at end of table.

Table 3.5-3

LI-007 MOISTURE REDUCTION SYSTEM EVALUATION (Cont)

→ Wt. Change Nil → Refurbishment 0.01 percent by weight → 5 Cycles[2]

Thermal Cycling/Residual Weight[3]

- Thermal 2,300°F → Refurbishment After Each Cycle → 7 Cycles → Wt. Change[2] 0.03-0.12%

(1) Detailed description and results presented in Section 3.7. All specimens LI-1500 material with 0042 surface coating and the 007 water-repellent treatment.

(2) No visual defects noted after tests.

(3) LI-1500 with 0025 surface coating and 007 water-repellent treatment.

3.5.2.6 Constituent Material Evaluation. Thermal gravimetric analysis conducted on the basic silicone material showed some deterioration as indicated by the start in weight loss at approx. 626° F and with the 10 percent weight loss occurring at 968° F. At 1832° F a total weight loss of 29.8 percent was observed. Relatively good thermal stability of the material was exhibited by this analysis. The analysis was conducted in a helium atmosphere with a heating rate of 6°C/min. As previously reported in Section 3.5.2, the silicone material caused no promotion of crystalline formation in the basic silica fiber material after exposures of 4 hr at 2,300°F.

3.5.2.7 Space Environments and Vehicle Effects. Outgassing and the resulting decomposition products during launch, orbit, and reentry may impose problems on certain experimental and operational phases anticipated for the shuttle vehicle. Because the material selected for the secondary water repellant purpose is applied over the major portion of the vehicle outer surface, it is of prime importance for the selected material not only to perform its primary function as a water repellant system, but to possess minimal outgassing characteristics in the reduced pressure space environments.

A review of the document "The ATM Material Control For Contamination Due to Outgassing," No. 50M02442, Revision 5, Dec. 1, 1971, was directed to acceptable materials

that may be applicable with the needed moisture repellent properties. The acceptable materials reviewed were evaluated for the use parameters of hydrophobic properties, temperature capability, film forming capability, low processing viscosity, curing, compatibility (with RSI attachment bond adhesive and the basic LI-1500 insulation), and other application techniques. For these parameters, the review was concentrated on the silicone and teflon type materials. Both the tetrafluoroethylene and fluorinated ethylene propylene teflon materials are approved, but are problems in the areas of application and compatibility for water repellent utilization. However, these materials have been evaluated and are under consideration for refurbishment purposes. Although many silicone materials are listed, the majority are compounded rubbers, greases, adhesives, laminating resins, compounds with fillers, etc., which are not amenable for the intended water reduction applications. The Sylgard 182 type silicone material listed as acceptable may be adaptable for moisture reduction purposes, but is of a relatively high viscosity (approximately 5000 cp), not compatible with the more commonly used silicone adhesive systems, and may cause processing difficulties in achieving maximum water repellent properties with minimal weight penalties.

Although the DC-1107 material used for the LI-007 water repellent system is not listed, the chemistry is reported by the supplier to be similar to the polydimethylsiloxane Sylgard 182. The volatiles from silicone materials in space environment consist of absorbed and adsorbed gases and moisture, byproducts of the curing reaction, and small amounts of unreacted low molecular weight linear and cyclic polymer. The DC-1107 fluid is reported by Dow Corning* to be a tightly crosslinked polymer when cured and is essentially free of low boiling cyclic and unreacted linear species and should possess low outgassing characteristics.

Evaluations were conducted at LMSC to determine preliminary indications of the effect of simulated reduced pressure and temperatures on the DC-1107 material. After cure, the material was exposed to environments of $260^{o}F$ and 1×10^{-6} Torr

*Dow Corning, Space Grade Silicons for High Vacuum Environments, Aerospace Application, Laboratory Report 261, Midland, Michigan

pressures for a 24-hr period. Material identification, test conditions, and results were as follows:

Product:	DC-1107 Fluid (Dow Corning)
General Name:	Silicone (polydimethylsiloxane)
Cure:	3 hr 150°F, 2 hr 250°F, 3 hr 325°F
Sample Configurations:	thin film
Samp'e Weight:	1.039 gm
Sample Surface Area:	32 cm^2

Weight Loss (%)				Condensable Material, Weight (%)			
6-Hr Exposure		24-Hr Exposure		6-Hr Exposure		24-Hr Exposure	
Total	*	Total	*	Total	*	Total	*
0.28	0.0015	0.28	0.0004	0.13	0.0007	0.13	0.0002

*Calculated as $\%/cm^2/hr$

This preliminary examination indicated relatively low weight loss (outgassing) and low volatile condensable material (VCM) when exposed to the particular test conditions. Weight loss and VCM equilibrium were achieved after the initial 6-hr exposure. Additional evaluations are needed in this area.

During the operation of the shuttle vehicle, the RSI material system may be exposed to intermittent splash-type contact with fuels and oxidizers anticipated for use with the shuttle propellent system. Compatibility of the refurbishable waterproof materials (teflon (FEP), DC-200, and DC-1107) with liquid oxygen (LO_2), nitrogen tetroxide (N_2O_4), and Aerozine 50 was investigated by total immersion of prepared specimens. Results of the tests were as follows:

Material		Teflon	DC-200	DC-1107
LO_2:	Splash	← No visible change →		
	6 hr	← No visible change →		
	24 hr	← No visible change →		

Material		Teflon	DC-200	DC-1107
N_2O_4:	Splash	← No visible change →		
	6 hr (10°C)	No change	Few bubbles	No change
	24 hr	No change	50% viscosity change	Color change
Aerozine 50:	Splash	← No visible change →		
	6 hr (22°C)	No change	No change	Bubbles
	24 hr	No change	No change	Cloudy liquid

The teflon material was compatible with all the oxidizers and/or fuels. The DC-200 and DC-1107 were slightly attacked by the N_2O_4 and Aerozine 50, but no violent reaction was noted. Based on this preliminary evaluation, the water repellent materials under consideration appear to be satisfactory for the splash and limited exposures anticipated for the shuttle application.

3.5.2.8 LI-007 Application. To achieve minimum weight penalties to the RSI system, the basic silicone material must be diluted by a suitable solvent in a controlled and predetermined quantity to achieve the needed water repellency characteristics with minimum weights. It is intended that prior to the installation of the RSI onto the shuttle vehicle, the individual tiles would be impregnated with the LI-007 coating to render each fiber in the RSI hydrophobic. Solvents such as naphtha have been successfully utilized for controlled laboratory and pilot line operations. However, for large quantity production and for refurbishment considerations it would be desirable, and necessary in many cases, to utilize nonflammable, nonexplosive, and relatively non-toxic compounds for this solvent application. Laboratory evaluations and analysis have shown the freon carriers completely compatible with the LI-007 system together with the other requirements. The high vapor pressure of the freons would be more amenable to automation and would simplify the entire processing system. The freon carrier is amenable to controlled spraying techniques as well as brush coating or complete impregnation processing. Laboratory testing has shown that the quantity of the LI-007 material can be controlled readily on the LI-1500 material by proper adjustment of the silicone fluid ratio to the freon solvent. Using either spray or

immersion techniques with the freon solvent, the treated LI-1500 specimens exhibited equivalent moisture repellency as compared to the use of naphtha solvent when evaluated by the water drop test method.

3.5.2.9 Simulated Rain Exposure. Samples of LI-1500 material were exposed to simulated rain conditions of 1-in./hr for 1 hr with a 4 in. x 4 in. surface exposed. Control specimens, specimens with 007 treatment (4 percent by weight), specimens with 0042 surface coating, and specimens with 0042 surface coating and 007 treatment (4 percent by weight) were exposed. Results of the tests were as follows:

LI-1500 Sample	Average Moisture Gain Wt. (gms)	Wt. (%)
Control (no treatment)	27.8	66.7
With 007 Treatment	0.09	0.15
With 0042 Surface Coating	4.5	6.0
With 0042 Surface Coating and 007 Treatment	0.01	0.04

The results showed the very effective water reduction capability of the 007 hydrophobic water repellent system. It is noted that a portion of the weight gain of the 0042 surface coated sample may be attributable to residual moisture remaining "wetting" the sample surface after the exposure.

3.5.2.10 Moisture Reduction Systems Evaluation. All of the systems evaluations described in Table 3.5-3 showed the efficient water repellant capability of the -007 material. A description and detailed result of the tests are presented in Section 3.7. The thermal/residual weight evaluations indicated a minor residual weight gain attributable to the thermally decomposed products of the -007 material. These evaluations utilized 3 in. x 3 in. x 1 in. thick LI-1500 material coated with the 0025 system on the top surface only. The water repellent material was applied to the top surface in sufficient quantity for the surface to reject a water droplet without wetting. The specimen was then exposed to a 2300° F cycle (a 200-sec soak at 2,300° F) in the LMSC Radiant Heat Facility. The specimen was reweighed to determine weight gain caused

by residual remaining material, refurbished with the -007 water repellent material, and exposed to the thermal cycle. Both the DC-1107 and DC-200 moisture reduction materials indicated significantly small residual weight gain after 7 thermal cycles (0.12 percent and 0.03 percent, respectively). The weight increase appears to plateau between the 4th and 6th cycles. This plateauing appears to be a surface phenomenon of increased sealing. The results of this evaluation were as shown in the presented curve.

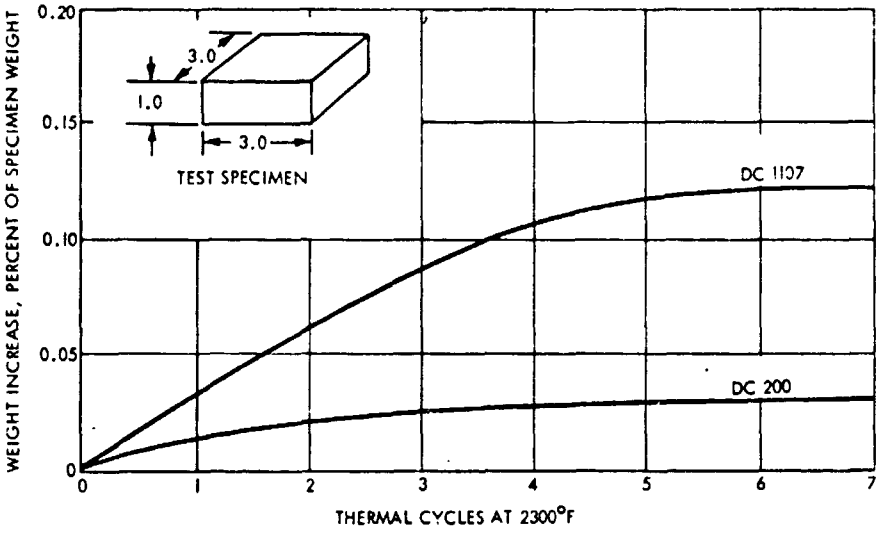

Effect of Thermal Cycling on Moisture Reduction Materials

3.5.2.11 Time/Temperature Effect on Water Repellancy. The initial tests to determine the time/temperature effect on the water repellency properties of the 007 treatment for the LI-1500 material were compared by isothermal furnace exposures up to 900°F. LI-1500 specimens 2.75 in. x 1.75 in. x 0.6 in. treated with the 007 system (4 percent by weight) were subjected to various time/temperature furnace exposures and then evaluated for water repellency retention by total water immersion. Results of the initial tests were as follows:

Temperature (° F)	Exposure Period (hrs)	4-hr Water Immersion Weight Gain (%)
R.T.	Control (with 007)	0.6
700	1.5	0.6
800	2	1.1
900	2	2.4

The initial tests indicated excellent retention of water repellency properties up to 900° F for relatively long exposure periods. Additional evaluations were conducted to determine the effect of isothermal treatments at higher temperature environments. LI-1500 specimens 3 in. x 3 in. x 1 in. treated with 4 percent by weight of the 007 system were used. Water repellency retention was evaluated by simulated rain exposure of the front surface of 1 in./hr for 1 hr. Results of the tests were as follows:

Temperature (° F)	Exposure Period (min)	1-hr Rain Exposure Weight Gain (%)
R.T.	Control (no 007)	67.5
R.T.	Control (with 007)	0.2
900	15	1.2
	30	6.1
	45	5.0
950	15	6.5
	30	0.6
	45	7.2
1000	15	4.8
	30	5.4
	45	0.3

The simulated rain exposures indicated retention of water repellency properties through the 1,000° F exposure.

To further establish the time/temperature effect on water repellency, a previously thermally cycled test model (a 4 in. x 4 in. x 2-1/2 in. thick LI-1500 simulated joint model) was utilized. The model was completely refurbished with the -007 treatment and thermocouples located at various sections on one side of the model as illustrated by the photograph of Fig. 3.5-2. The thermocouple closest to the top heated surface was 0.4 in. from the surface. The model was installed into the Radiant Heat Facility, masked-off with insulation fibers (exposing only the top surface to direct radiant heat), and subjected to a 2,300° F heat pulse. The temperature traces obtained indicate the 0.4 in. location reached a peak temperature of 1,900° F and remained above 1,000° F for 2330 sec. Water repellency was then evaluated by the water drop technique. The photograph in Fig. 3.5-2 was taken 20 min after application of the droplets. As observed, the droplets in the 0.4 in. thermocouple region remained, demonstrating water repellency in that particular region. Droplets in the near vicinity of the top surface were absorbed into the LI-1500 model. It appears that,under the type of heating expected in shuttle environments, in-depth loss of water repellency may not be experienced after each flight.

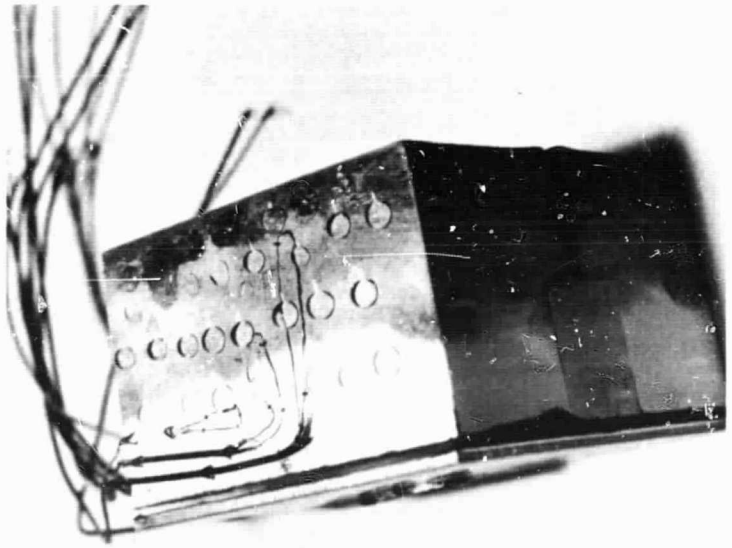

Fig. 3.5-2 Time/Temperature Water Repellency Evaluation

3.6 THERMAL CONDUCTIVITY INVESTIGATIONS

The major factors influencing LI-1500 thermal conductivity are gaseous conductivity, solid structure conductance, and transparency to infrared radiation. Although past investigations have assumed that gaseous conductance may be a significant factor, it is now realized that the intensive heating of the orbiter vehicle occurs at reduced gas pressures. The dependence of thermal conductivity on pressure was taken into account in the sizing of the LI-1500 orbiter TPS under NAS 9-12083 contract. With the gaseous conductivity reduced, the possible areas for improvement of composite thermal conductivity were opacification of the composite internal structure to infrared radiation and reduction of solid conductance by material removal or reduced density. Investigations to explore the potential for improvement of these two factors were conducted concurrently. The significance of the influences of temperature opacification was established. Opacifying agents were identified and low-density materials were developed. The ability to incorporate an opacifier in the reduced-density material was demonstrated during characterization of the new composite structure (Section 3.7).

3.6.1 Infrared Transparency Reduction

Under transient conditions at temperatures above 2,000° F and at the reduced pressures encountered during reentry, the predominant mode of heat transfer is by transmission of radiation through the structure from the heated insulation surface. To gain better insight into the nature of infrared transmission through LI-1500 insulation, spectral transmittance measurements were conducted on several LI-1500-type specimens and on some specially prepared opacified specimens. The composite structures were examined in three thicknesses [illegible], 80, and 160 mils.

Two different methods were used to measure either the total transmission (i.e., normal plus scattered components of incident radiation) through the sample or normal transmission (i.e., normal component only of incident radiation) through the sample. Figure 3.6.1-1 is a schematic layout of the optical system used for the total transmission measurements. The radiation source was a tungsten-strip lamp from

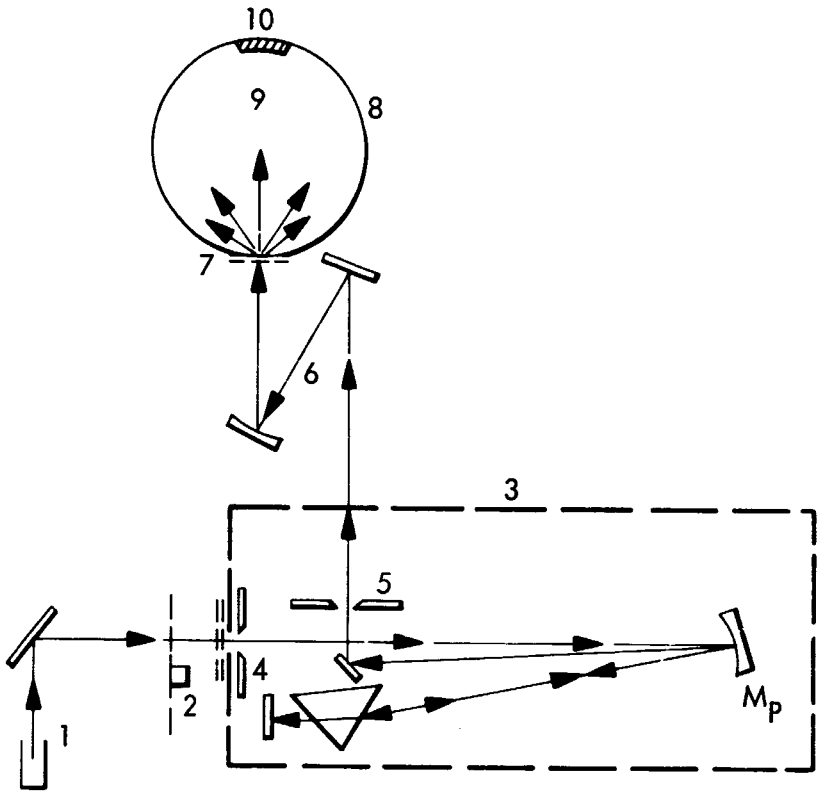

1. Tungsten lamp source
2. Chopper
3. Perkin Elmer Model 98 monochromator with SiO_2 prism
4. Monochromator entrance slits
5. Monochromator exit slits
6. Transfer optics between monochromator and integrating sphere
7. Sample location entrance port to integrating sphere
8. Gier-Dunkle Model SP-210 integrating sphere
9. MgO-coated shield between entrance port and detector
10. Detectors – IP28 photomultiplier or PbS

Fig. 3.6.1-1 Optical System Schematic for Spectral Total Transmittance Measurements

which monochomatic radiation at wavelengths between 0.3 and 2.4 μ was obtained with a Perkin-Elmer Model 98 monochromator with an SiO_2 prism. From the monochromator, the radiation was directed into an MgO-coated integrating sphere that contained an IP28 photomultiplier tube and PbS detector. After measuring the incident radiation energy level with the entrance port open, the sample was positioned in front of the entrance port and the resulting signal ratio was a measure of the total transmittance of the sample at that wavelength. The energy incident on the sample was monochromatic and the angle of incidence was normal (i.e., perpendicular to the sample surface) to within ±2 deg. The integrating sphere collected all of the radiation transmitted through the sample into the 2π steradians of hemispherical space at the backface of the sample. Measurements of spectral total transmittance by this method were restricted to wavelengths between 0.36 and 2.4 μ.

Spectral normal transmission measurements were also made in this wavelength region using the same optical system as shown in Fig. 3.6.1-1 but by positioning the sample in front of the entrance slits of the monochromator instead of in front of the entrance port to the integrating sphere. In this case the total energy spectrum of the tungsten lamp struck the sample at a normal angle of incidence and the spectral normal component of energy at a particular wavelength transmitted by the prism from the total spectrum of transmitted energy through the sample. Furthermore, only that energy that was transmitted in a near-normal direction through the sample was collected by the paraboloid mirror (Mp) in the monochromator for dispersion and detection. This solid angle was approximately 0.03 sr for the Model 98 monochromator, or about 1/200th of the 2π sr hemispherical solid angle that was collected by the integrating sphere. For scattering-type specimens, normal transmittance values were observed to be between 2×10^2 to 5×10^2 times smaller than the corresponding total spectral transmittance values. Spectral normal transmission measurements at infrared wavelengths longer than 2.4 μ were made in a similar manner, but with the following exceptions:

- A 1,450° F heated cavity was used as the radiation source instead of the tungsten lamp.
- A NaCl prism was used in the monochromator instead of the SiO_2 prism.

- A vacuum thermocouple detector, housed inside the monochromator, was used instead of the integrating sphere detectors.

A schematic layout of the optical system for the infrared spectral normal transmission measurements is shown in Fig. 3.6.1-2.

Discrepancies between normal transmittance values obtained with the tungsten lamp source and with the heated cavity source at wavelengths between 2.0 and 2.4 μ were presumed to be caused by stray radiation effects, i.e., the detection of radiation at wavelengths other than the selected measurement wavelength.

Spectral transmittance data for 0.040-in.-thick specimens of LI-1500 and LI-1500 containing various opacifiers are shown in Fig. 3.6.1-3. These curves illustrate the variations in spectral transmittance of the LI-1500 control material (curves 1a, 1b, and 1c) caused by differences in measurement methods and also illustrate the opacifying effects of various candidate materials. Measurements of the LI-1500 control sample at wavelengths between 0.36 and 2.4 μ indicate that the normal transmittance of this material was no greater than 0.04 percent (curve 1c); however, measurements of the total transmittance of the sample were found to average about 9 percent throughout the visible portion of the spectrum and to increase beyond 1 μ to a maximum value of 16 percent at 2.4 μ. The large ratio between the total and normal transmittance values indicates that the LI-1500 material is essentially a perfect scatterer so that the radiant intensity of the transmitted energy emerging from the backface of the sample was the same in all directions. The infrared normal transmittance data (curve 1b) indicate that this property, and presumably the total transmittance also, remains essentially the same at wavelengths to about 4.5 μ and then drops off sharply to immeasureably low values between 4.5 and 5 μ. A transmitting "window" was observed to occur to 7.25μ where a normal transmittance value of 7 percent was measured. This relatively high normal transmittance value indicates that transmitted energy at this wavelength must be primarily in the normal direction rather than being highly scattered as at the shorter wavelengths. This window at 7μ may be of little significance in terms of radiant heat energy. As indicated in Section 3.4.1, very little heat energy is radiated at long wavelengths.

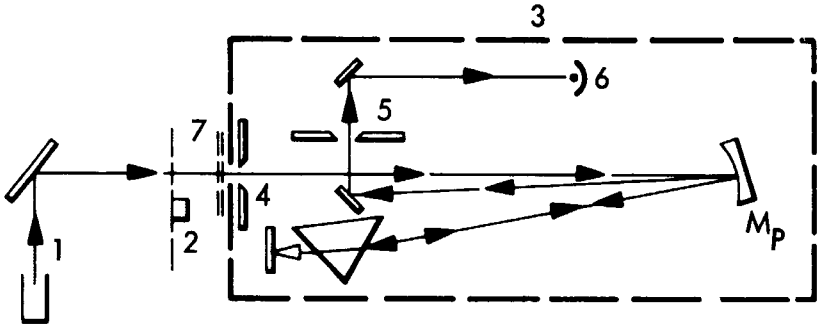

1. Heated cavity source
2. Chopper
3. Perkin-Elmer Model 98 monochromator with NaCl prism
4. Monochromator entrance slits
5. Monochromator exit slits
6. Vacuum thermocouple detector
7. Sample location in front of entrance slits to monochromator

Fig. 3.6.1-2 Optical System Schematic for Spectral Normal Transmittance Measurements in Infrared

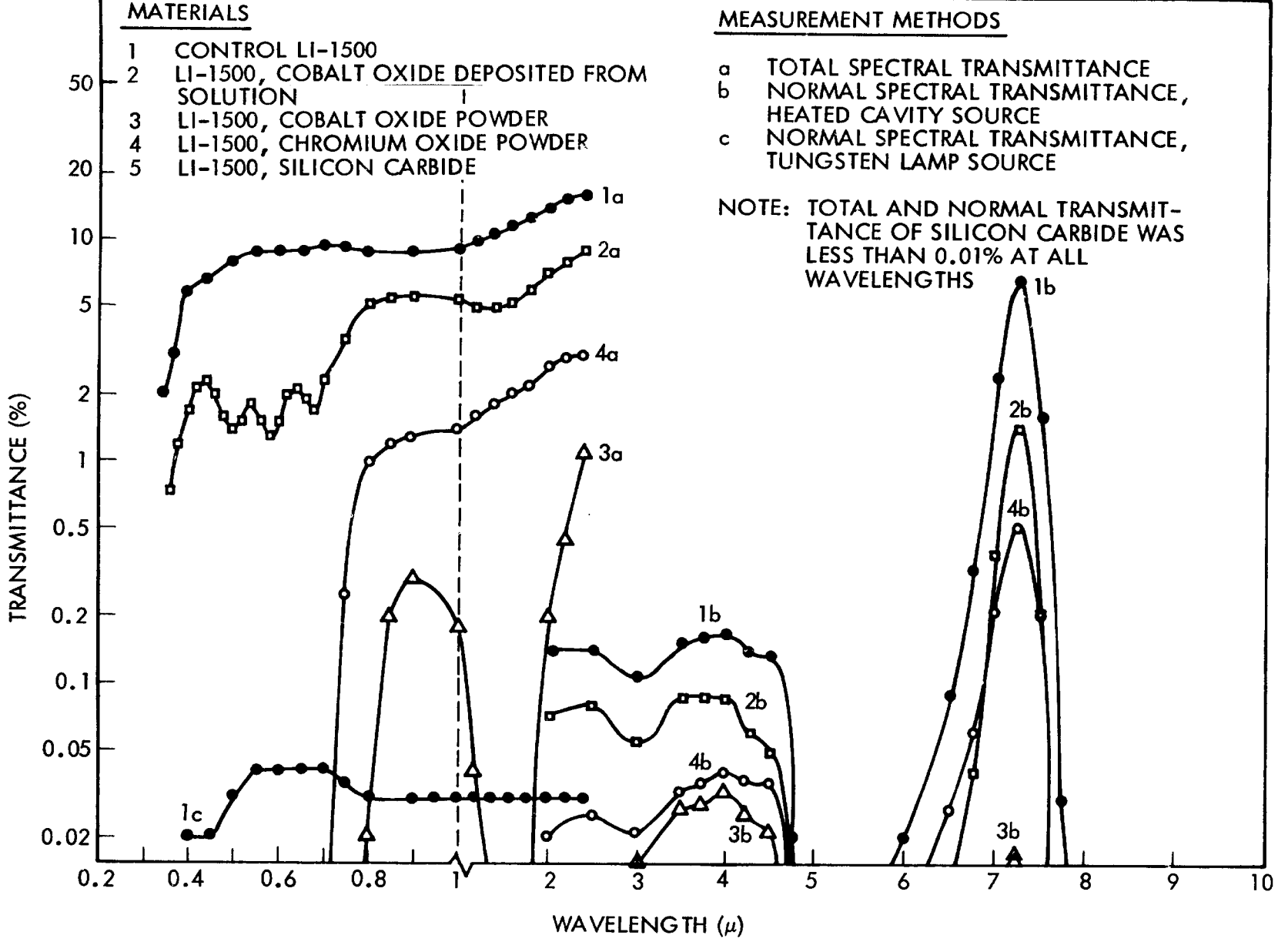

Fig. 3.6.1-3 Spectral Transmittance of LI-1500 With Various Opacifiers (0.040-in. Thickness)

The value of 7μ corresponds to the wavelength for maximum spectral radiant intensity at approximately 260° F. The wavelengths of interest for elevated temperature transmittance of radiant heat energy are primarily between 1 and 5 μ, according to the laws for blackbody radiation. For example, the wavelengths for maximum spectral radiation at temperatures of 1,520, 1,700, 2,060, and 2420° F are 2.7, 2.4, 2.1, and 1.8 μ, respectively.*

Transmittance data for the various opacified samples indicate that the most effective of the materials examined was the silicon carbide. No measurable transmission was detected at any wavelength through the 0.040-in.-thick sample of this material. The next most effective material was cobalt oxide powder, then chromium oxide powder, and, finally, cobalt oxide deposited from solution.

The attenuating effect on total transmittance of increasing the thickness (40, 80, and 160 mils) of LI-1500 is illustrated in Fig. 3.6.1-4. (The somewhat lower transmittance for the 40-mil-thick sample from that shown in Fig. 3.6.1-3 may be attributed to specimen differences.) Normal transmittance values for all of the 80- and 160-mil-thick samples were immeasureably low (less than 0.01 percent) at all wavelengths except at the 7.25-μ "window." The attenuation effect of thickness was the same for all specimens tested. In all cases, the transmittances were indicated to be approximately inversely proportional to the thickness. Included in this transmittance test matrix were LI-1500 specimens that had been thermally cycled (twenty 30-min cycles at 2,300° F) and showed no change in spectral transmittance characteristic.

Figure 3.6.1-5 presents the spectral total transmittances (0.160-in. thickness) as influenced by density for LI-1500 silica insulations and compared to a low-density mullite insulation (investigated under IRAD). As expected, these data indicate that lowering the density of silica insulation tends to increase the infrared transparency. Whether this increase will actually result in significantly higher thermal conductivity cannot be determined by this test alone, as the solid conductivity should have an opposing effect. The significance of this change was determined by thermal conductivity measurements performed (Section 3.7) on the lower density composite (LI-900)

*Harrison, Radiation Pyrometry, John Wiley & Sons, 1960, p. 23.

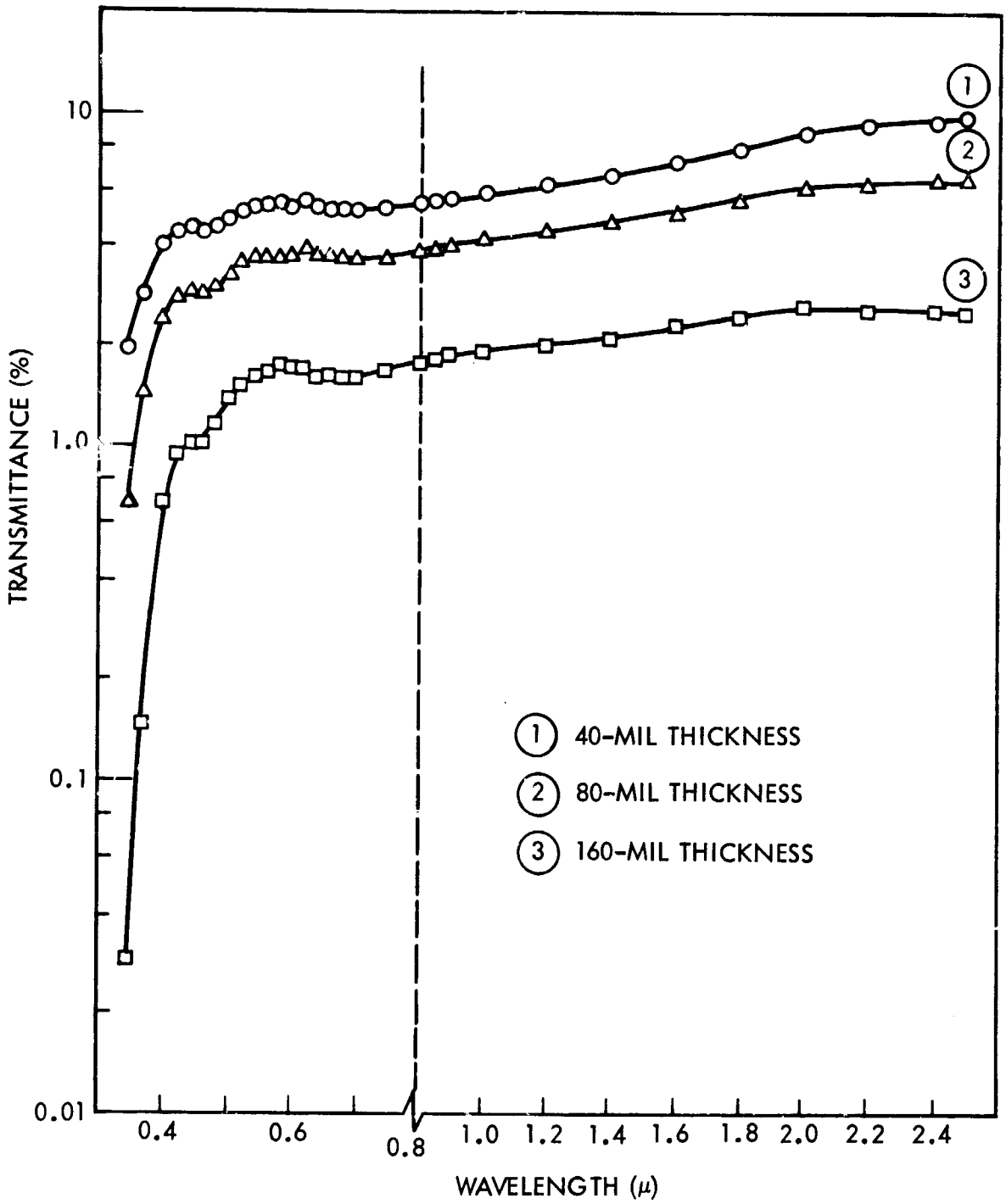

Fig. 3.6.1-4 Influence of LI-1500 Thickness on Spectral Transmittance (Total)

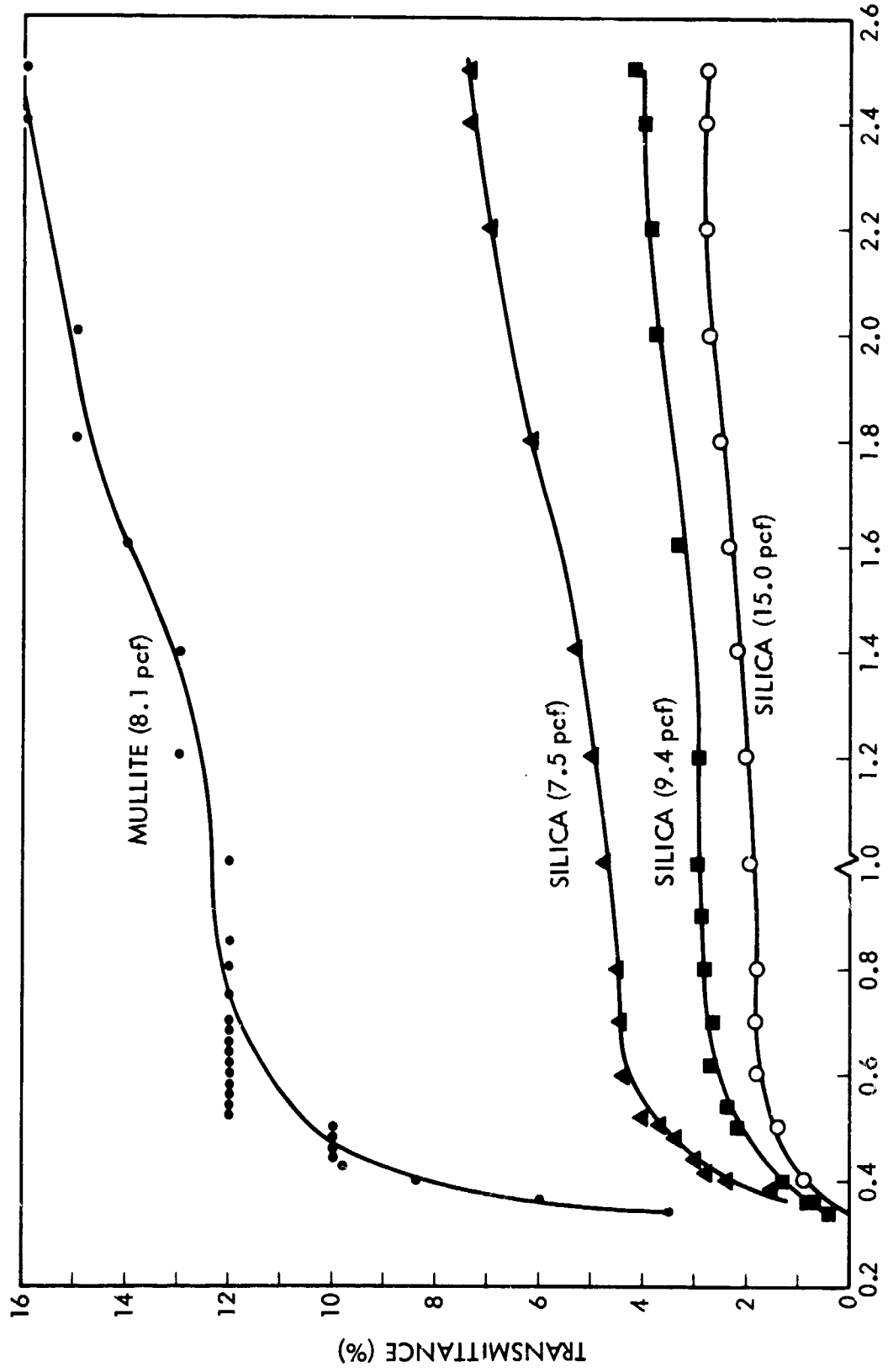

Fig. 3.6.1-5 Spectral Total Transmittance of Low-Density Fibrous Insulations at 0.160 In.

with and without an opacifier. Also of importance is the fact that the slightly higher IR transmittance of lower density silica material primarily affects the thermal conductivity in the higher temperature regimes. This was reflected in the data for FI-600 (Section 3.2), where the thermal conductivity of the 6-lb/ft^3 material was equivalent to LI-1500 at 1,500° F or below. The reason for the transmittance characteristic of all the silica composites being lower than the mullite composite may be attributable chiefly to the finer fiber diameter. The fiber diameters used in these composites were as follows:

- Silica: $0.76 \sim 1.6\,\mu$ (Average $1.2\,\mu$)
- Mullite: $1.00 \sim 8.0\,\mu$ (Average $4.0\,\mu$)

In coatings technology, optimum particle size of a pigment for maximum opacity has been the subject of numerous studies. One such result is the following equation:*

$$d = \frac{0.9\lambda}{N_b \pi}\left[\frac{N^2 + 2}{N^2 - 1}\right]$$

and $N = \frac{N\lambda}{N_b}$

where

N = refractive index, pigment
N_b = refractive index, medium
d = particle diameter in microns
λ = wavelength in microns

Calculation for silica—assuming it to be spheres and that it has a refractive index of 1.45 at wavelengths of $1\,\mu$ and 1.42 at $3\,\mu$ — indicate that the optimum particle diameter would be 1.0 and $4.0\,\mu$ for these respective wavelengths. Although it appears that the particular diameters of the silica fiber used are more desirable for opacification considerations, further analysis is needed to determine the configuration (spherical-fiber diameter) relationship as applicable to opacity.

*W. Jaenicke, "Lightstreuung und Aufhellungsvermogen Weiser Pigmenten " Electrochemie, Vol. 60, 1956, p. 163-74. H. Weber, "Deckfahigkeitsmessungen an Weispigmenten," Forbe und Lock, Vol. 63, 1957, pp. 586-94

From the evaluations conducted, it appears that the addition of opacifiers may not significantly improve the high opacity of the LI-1500. However, with much lower density versions of this RSI, added opacification may be necessary. In these tests only absorbers were investigated, but reflectors such as the following high refractive-index material also should be effective.

TiO_2 (anatase)	2.52
TiO2 (rutile)	2.71
Zirconia	2.20
Zirconium silicate	2.00
High-purity silicon carbide	2.00
Diamond	2.40

Two major requirements for good opacification by light scattering are particle size and refractive index.

During these evaluations spectral normal transmission measurements were also conducted on the new LI-0042 coating (silicon carbide/borosilicate formulation). It was found that the transmittance was less than 0.1 percent between the wavelengths of 1.5 to 20μ. The LI-0045 coating is expected to display the same characteristics.

3.6.2 Lower Density Material

Reduction of the density of a silica composite is a simple task. To meet varied requirements of other applications, LMSC had fully demonstrated the ability to vary the density over the range of 5 to 60 lb/ft^3, primarily by control of the fiber/binder ratio and compaction. However, to reduce the density to a target value as low as 10 lb/ft^3 as intended here, without significantly degrading the thermal or mechanical properties as used in TPS designs, was a major undertaking. Previous process development work (LMSC IRAD Program Report,LMSC-D153908) established feasibility and techniques for producing lower density silica composite materials for RSI applications.

The LI-1500 formulation had displayed in extensive evaluations an excellence thought to be optimum in overall balance of thermal/mechanical characteristics. It was obvious that in such a balanced system some property characteristics would change if the density were reduced. However, the task was undertaken with the thought that

improved TPS material of lower density might be achieved even if some properties changed, provided the prime properties defining design could be held to desirable values.

For example, in the case of thermal characteristics, a reduction in solid conductance and an increase in transparency to infrared radiation would be expected with density reduction. However, it is possible that one change might offset the other so that the thermal conductivity might not be altered significantly. If this were not found to be the case, then the radiant heat transfer component might be reduced sufficiently by use of opacifiers to yield satisfactory, if not improved, overall conductivity values for designs.

In the case of mechanical characteristics, LI-1500 was highly anisotropic, and thus the designs would not be dependent upon each absolute mechanical property value. Instead, the design points were set on properties in the weaker direction more than the strong one. Again, reduced weight material could be developed even if some property changes occurred, provided the prime values dictating designs remained essentially unchanged. Also, a change in other design features, such as attachment material and/or methods, might make material usable even with reduced property values.

In evaluations described in Section 3.3.1, it was determined that the major drivers in the design and sizing of TPS panels under NAS 9-12083 were the shear and tensile properties in the transverse or weak direction of the composites. As expected, these values in the strong direction were much higher than necessary and did not control the design. This being the case, it might be possible to reduce the density without impacting the mechanical design by "borrowing" some of the strength in the overly strong directions to maintain sufficiently high critical values as material is removed to lower the density. It was decided that the shear characteristics in the transverse direction would be utilized as a guide in the laboratory development work directed toward reducing the density while maintaining adequate mechanical properties. It was hoped that this would be a sensitive indicator of utility and that general property relations for tension would remain unchanged. This property characteristic had been

established under NAS-9-12083 for LI-1500, as indicated in Section 3.7.1 . It was planned that this property would be measured for the final improved lower density material developed under this task by the same test method described in that section, utilizing the same facilities and personnel to ensure a point for true comparison. However, a simpler, more rapid test method was desirable for preliminary screening and evaluations during the laboratory investigations. A review was made of possible test methods for determining composite shear values. A compression interlaminar shear test, which had been used on other programs to examine interlaminar shear characteristics of resin/fiber laminates, was quite attractive because of simplicity of specimen requirements and test procedures. In use on plastic laminates the deficiencies had been noted to be that high values for interlaminar shear might be indicated (as compared to four-point flexure test values), composite stiffness was not measured, test values were susceptible to composite local imperfections, and the strength data were somewhat dependent upon specimen support for thin laminates. In developing this method for evaluating shear in RSI-type composites, the shear-loading geometry shown in Fig. 3.6.2-1 was established by trial.

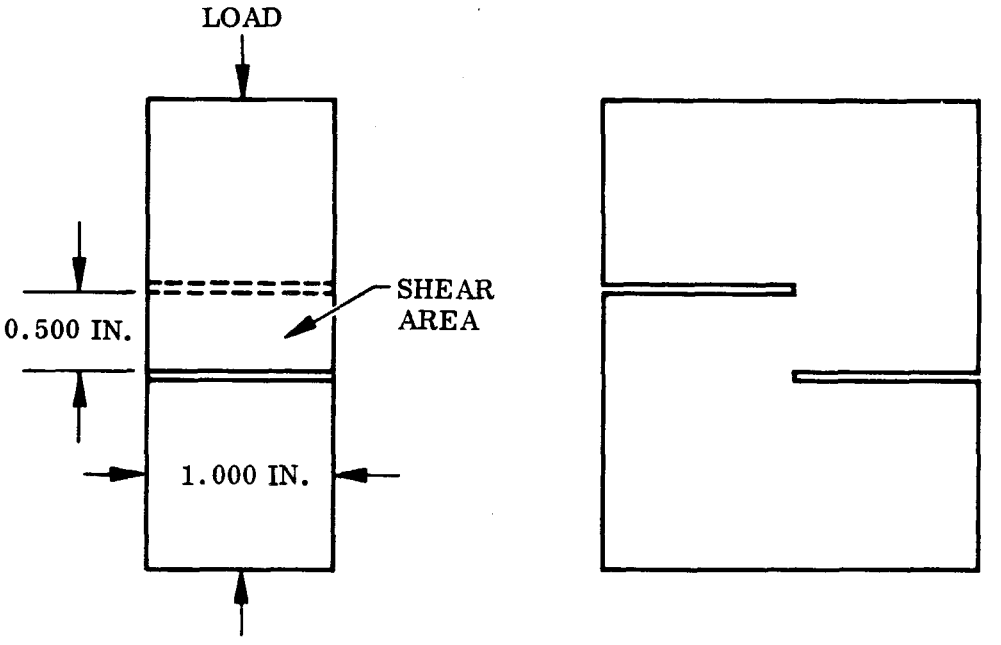

Fig. 3.6.2-1 Shear-Loading Geometry

C.4

For this geometry, the RSI could be cut in large enough thicknesses to eliminate the need for any specimen-supporting fixture that might add to the complication of the set-up or influence the results. Tests of the LI-1500 comparing this method with that to be used for final shear characterization (Section 3.7) yielded average transverse shear of 24 psi and 27 psi, respectively. These results were sufficiently close for the compression shear test to be used for laboratory screening. Time and scope for this task did not allow for comprehensive testing other than the screening for this one value. It was found that this test would not produce the proper types of breaks for evaluations of strong direction shear.

Potential material improvements that were hoped for – such as an improved fiber developed under the NASA/Lewis contract to Johns-Manville (NAS 3-15566) or the use of fibers of increased fiber aspect ratio – did not materialize during this short program. These possibilities still exist and might be considered in any future work addressed to further improvements.

Laboratory material investigations primarily considered the parameters associated with:

- Dispersion
- Fiber/Binder Ratio
- Binder Application
- Binder Distribution
- Improved Composite Microstructure
- Sintering Schedules

The investigations involving variable binder distribution and surface densification indicated improvement of mechanical property versus bulk composite density with results quite similar to those generated under Section 3.4.2 in the development of integral coatings. While encouraging, this method was not emphasized as a means for accomplishing this task as the improvement was only marginal when weighed against increased complication of manufacturing techniques. However, the other major

variables indicated were examined in producing material over the density range of 6.5 to 14.9 lb/ft.^{3} Transverse compression shear evaluations of materials over this range of densities indicated values of 10.5 to 78.9 psi. The material variants produced in these investigations did not display the mechanical-property-to-density relationship associated with past materials characterized under other programs (NAS 9-11122 and NAS 9-12083). As judged by the laboratory shear test, these materials exhibited properties significantly higher at reduced densities. This is evident in values derived for a series of composites exhibiting a range of densities accomplished by altering the fiber/binder ratio.

Density (pcf)	Transverse Shear (psi)	Compression (psi)
8.2	28.5	18.5
9.1	38.0	51.6
14.0	44.9	77.2
15.4	57.3	95.3

Factors that undoubtedly contributed to this improvement were improved microstructures of the composite, elimination of large void common in the standard material, improved fiber property, more isotropic fiber orientation, more effective use of bonding ingredients, and sintering conditions adjusted for fiber/binder components. There was not enough time to ensure that optimum process variables and composite disposition were developed, for this totaled to a comprehensive matrix. However, the limited evaluations indicated that one set of compositing variables yielding composites of 9 lb/ft^3 would reproducibly display more than 20-psi transverse shear properties in the laboratory screening tests. This composite was selected for more extensive property characterization (Section 3.7), as it appeared to meet the study critical objectives of composite density reduction to at least 10 lb/ft^3 without severe degradation of the transverse shear properties. It was thought that if these property determinations showed that the tensile properties in the weak direction were equally preserved, the new RSI material, LI-900, could be readily incorporated into the current designs

established for LI-1500. If not, then the attachment/tile size relation might have to be altered to accommodate this material improvement. The thermal conductivity of this new composite was determined and is reported in Section 3.7.3.

3.7 MATERIAL PROPERTY DETERMINATION

The objective of the evaluation conducted during this phase of the program was to determine physical, mechanical, and thermophysical properties of the improved LI-1500 and surface coating materials. Properties were determined and are reported herein for both the improved LI-1500 and the 0042 surface coating (Section 3.7.1) and the improved lower density LI-0900 and the 0045 surface coating (Section 3.7.2) materials. Mechanical, thermophysical, and environmental response behavior properties are described in the following sections. In addition, batch-to-batch reproducibility surveillance and analysis of the single fabrication process used to produce the LI-1500 material required for Contract NAS9-12083, as well as the analysis of the more limited production of the LI-0900, are presented in Section 3.7.3.

3.7.1 LI-1500/0042 Material Properties

The mechanical, thermophysical, and environmental response properties of the improved LI-1500 and 0042 materials are described in the following sections.

3.7.1.1 Mechanical Properties

The mechanical properties of improved LI-1500 were determined under Contract NAS 9-12083. Tests were conducted under varied conditions at room and elevated temperatures. Configurations used for the mechanical property test specimens are shown in Fig. 3.7.1-1. A brief description of the test procedures and a summary of results are given in this report. Detailed information and data on these tests will be found in the final report for Contract NAS 9-12083.

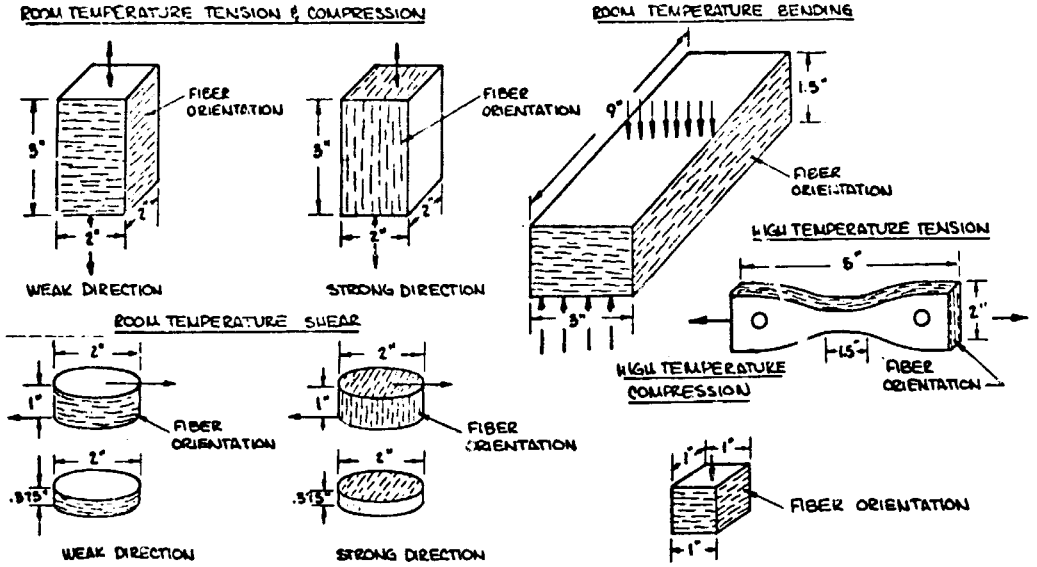

Fig. 3.7.1-1 Sketch of Mechanical Property Test Specimens

3.7.1.1.1 Test Methods

Room Temperature Tension Tests. The tensile tests were run on 2-in. cubes, using the fixture shown in Fig. 3.7.1.1-1. Cross-head motion was set for an approximate strain rate of 0.2 percent per minute. Load and strain were recorded continuously on an X-Y plotter.

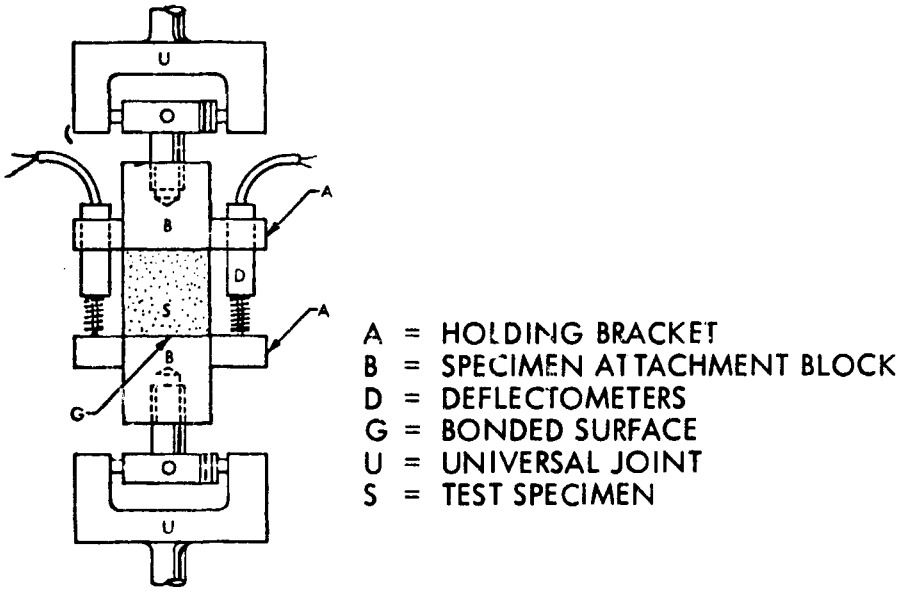

Fig. 3.7.1.1-1 Test Fixture for Tensile Tests of LI-1500
(Room Temperature and -150°F)

Elevated Temperature Tensile Tests. Elevated temperature tensile tests were performed in a platinum-wound tube furnace with a 3-in.-diam. by 15-in.-long hot zone. The temperature within the gage section was held to ± 15° F of the test temperature. Dynamic tests were made at a constant cross-head rate of 0.02 in./min. Loads were applied in 2-lb increments in static tests. A detailed test description is given in the Space Shuttle Thermal Protection System Development Final Report, LMSC-D152738.

Room Temperature Compression Tests. The compression tests were run in a test setup as shown in Fig. 3.7.1.1-2. Test rates were the same as for the tensile tests.

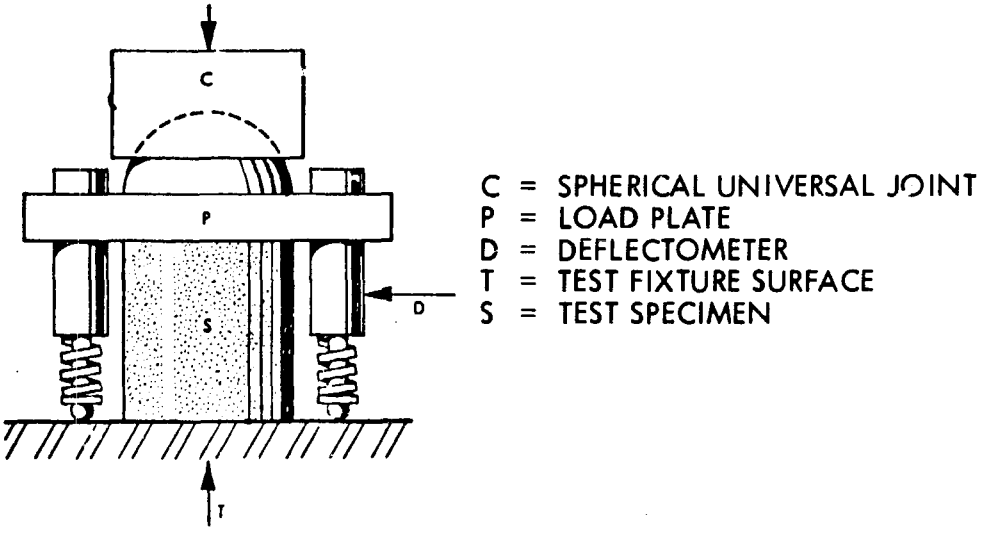

Fig. 3.7.1.1-2 Test Fixture for Compression Tests of LI-1500

Elevated Temperature Compression Tests. The elevated temperature compression tests were run in the same apparatus as the elevated temperature tension tests at a constant cross-head rate of 0.02 in./min.

Bend Tests. The bend tests were run on a Four-Point loading fixture with upper and lower spans of 4 in. and 8 in., respectively. The loading rate was about 0.25 percent strain per min. The load and deflection were continuously recorded on an X-Y plotter.

Disc Shear Tests. The shear tests were performed in a fixture as shown in Fig. 3.7.1.1-3. Relative fixture plate movement versus load (torque) was recorded on an X-Y plotter.

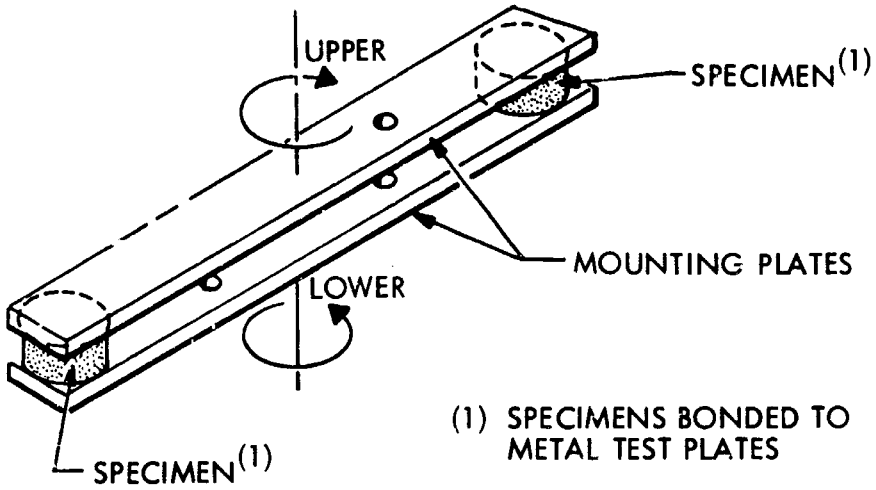

Fig. 3.7.1.1-3 Shear Test Specimens and Mounting Plates

Coating Cantilever Test. The mechanical properties of LI-1500 surface coating were determined by applying a cantilever bending movement on a rectangular plate specimen of the coating. The apparatus used is shown in Fig. 3.7.1.1-4.

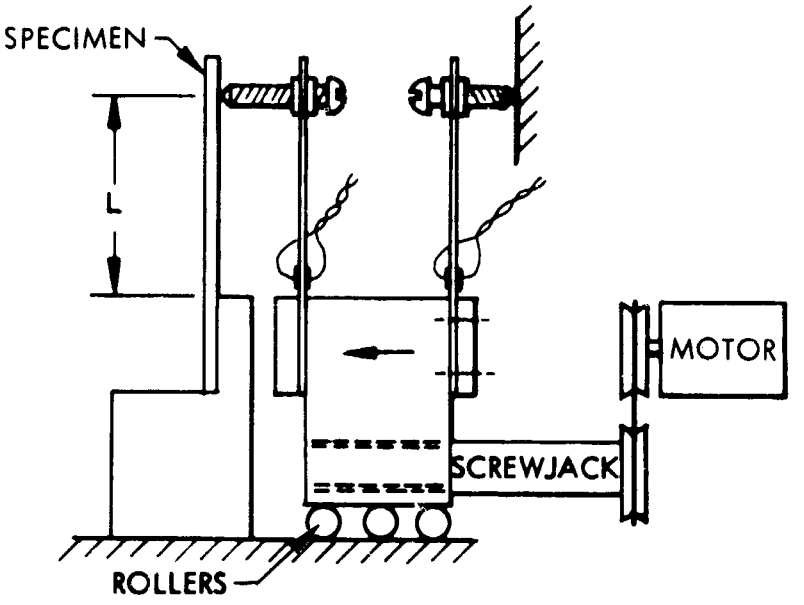

Fig. 3.7.1.1-4 Schematic of Coating Test Apparatus

Test Conditions. Besides tests at room and elevated temperatures, tests were run on LI-1500 with prior thermal and acoustic cycling as shown in Figs. 3.7.1.1-5 and 3.7.1.1-6, respectively. The total exposure for specific tests is shown with the summary of test results in Table 3.7.1.2-1.

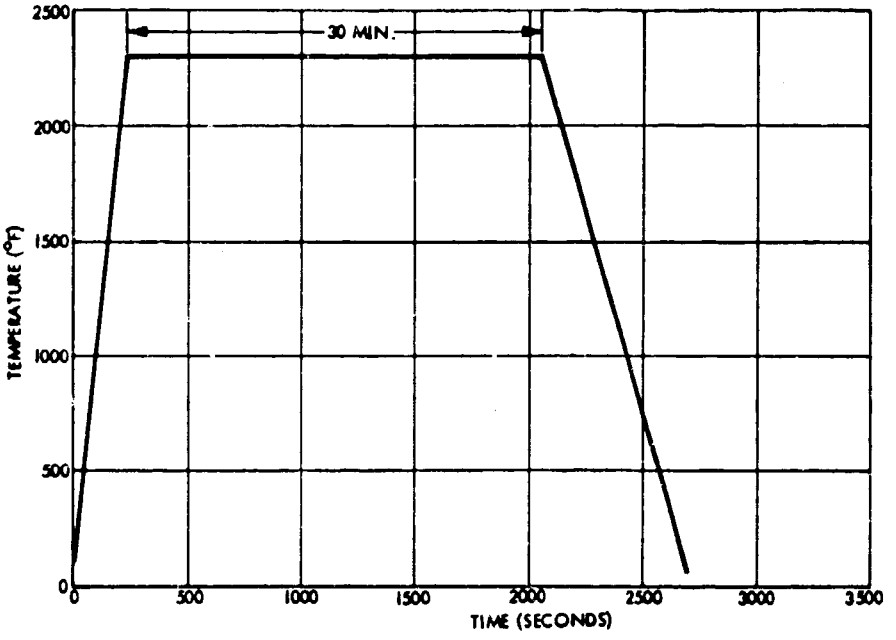

Fig. 3.7.1.1-5 Oven Thermal Cycle for Thermal Degradation Tests

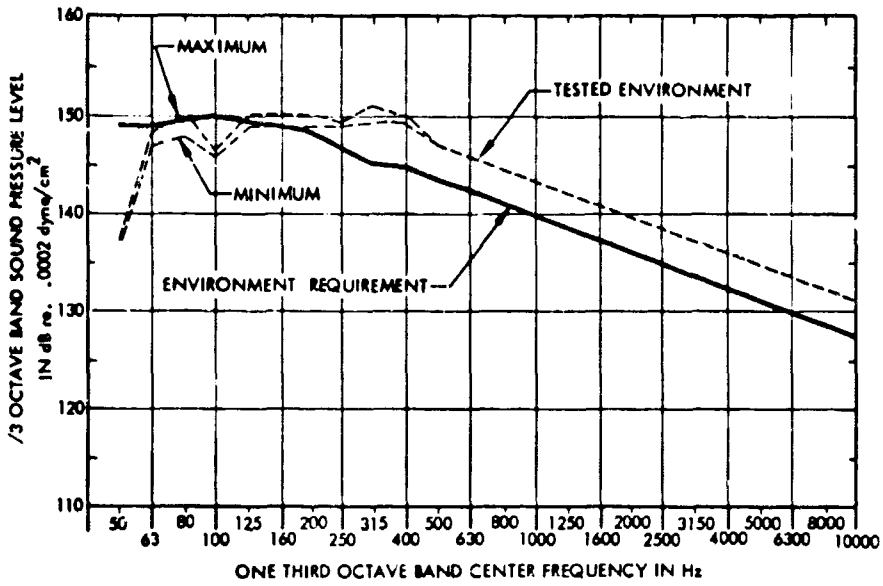

Fig. 3.7.1.1-6 Comparison of Applied Acoustic Test Environment with Requirement

3.7.1.1.2 Test Results

The summary of test results for the improved LI-1500 and 0042 coating is given in Table 3.7.1.1-1. In addition to the tests listed in the table, limited tensile testing was performed at 2,100°F, 2,200°F, and 2,300°F. The results indicated that the improved LI-1500 undergoes a brittle-ductile transition at around 2,100°F with elongation of 150 percent at 2,300°. Up to 2,000°F the results showed an increase in tensile strength and decrease in modulus. A complete description and results of the tests have been reported.*

The strength decreased as the ductility increased with increasing temperature in the ductile range. The behavior was noted to be characteristic of glasses at high temperature and of many plastic materials. It is possible, considering the structure and density of LI-1500, that sliding between fibers may be the primary deformation mode.

The need for further studies is indicated to gain more complete knowledge of the high-temperature characteristics of the improved LI-1500.

*Space Shuttle Thermal Protection System Development Final Report, LMSC-D152738.

Table 3.7.1.1-1

SUMMARY OF IMPROVED LI-1500 MECHANICAL PROPERTY TEST RESULTS

Type of Test	Test Direction	Temp. (F)	Number of Thermal and Acoustic Cycles	Time at 2300°F (hr)	Average Strength ($lb/in.^2$)	Average Modulus ($lb/in.^2$)
Tension	Parallel*	RT	0		78	56,400
	Parallel	RT	0		70	57,450
	Normal **	RT	0		15	5,780
	Normal	RT	0		14	9,518
	Normal	RT	10	5	14	10,073
	Parallel	-150	0		91	40,575
	Parallel	1500	0		101	46,700
	Parallel	2000	0		165	16,000
	Parallel	RT†	0		77	60,850
	Parallel	RT	10	5	47	91,300
	Parallel	RT	20	10	56	89,500
Compression	Parallel	RT	0		174	39,700
	Normal	RT	0		42	4,070
	Normal	2300	0		4	219
	Parallel	2300	0		40	2,140
	Parallel	RT	10	5	234	84,700
	Parallel (Coated)	RT	0		167	60,300
	Normal	RT	10	5	77	10,615
Shear	Parallel	RT	0		28	6,605
	Normal	RT	0		75	31,900
	Parallel	RT	10	5	39	-
Bending	Parallel	RT	0		115	53,780
	Parallel	RT	10	5	179	83,195
Coating (0042)		RT	0		2,000	1,900,000

* Parallel to the fiber orientation direction
** Normal to the fiber orientation direction
† Control specimens for tests in elevated temperature fixture

Thermal and Acoustic Cycle Conditions

Type of Test Specimens	No. of Thermal Cycles (2300°F)	No. of Acoustic Cycles	Total Time (thermal) (hr)	Total Time (acoustic) (min)	Missions Equivalent to
Tension	10	10	5	10*	120
	20	20	10	20	240
Compression	10	10	5	10**	120
Shear	10	-	-	-	-
Bending	10	10	5	10	120

* One specimen exposed to 45-min total time
** One specimen exposed to 35-min total time

3.7.1.1.3 LI-1500 Insulation System Design Properties

The design criteria for the use of LI-1500 in TPS Systems have been revised to reflect the properties of improved LI-1500. These are shown in Table 3.7.1.1-2.

Table 3.7.1.1-2

LI-1500 INSULATION SYSTEM DESIGN PROPERTIES

(ROOM TEMPERATURE UNLESS OTHERWISE NOTED)

PROPERTY (ULTIMATE)		LI-1500 STRONG DIRECTION	LI-1500 WEAK DIRECTION	RTV-560 BOND	LI-0042 COATING	LI-0025 COATING
TENSION (PSI)		70	15	800	> 2000	600
TENSILE MODULUS (PSI)		60,000	6,000	300	$<9.1 \times 10^6$*	3.5×10^6
COMPRESSION (PSI)		150	40	–	> 2000	>>600
COMPRESSION MODULUS (PSI)		50,000	5,000	–	$<9.1 \times 10^6$*	3.5×10^6
SHEAR (PSI)		40	25	400	–	
SHEAR MODULUS (PSI)		20,000	4,000	100	$<3.7 \times 10^6$	1.4×10^6
		PARALLEL TO FIBER	PERPENDICULAR TO FIBER			
THERMAL EXPANSION (IN./IN./°F)		3.0×10^{-7}	3.0×10^{-7}	1.14×10^{-4}	2.0×10^{-7}**	2×10^{-7}
HEAT CAPACITY (BTU/LB-°F)	(RT)	0.15	0.15	0.30		
	(2000°F)	0.32	0.32	–		
THERMAL CONDUCTIVITY (BTU-IN./FT^2-HR-°F) ~1 ATMOSPHERE	(RT)	0.58	0.35	2.16	6.5	
	(2000°F)		1.56	–	14.2	
THERMAL CONDUCTIVITY (BTU-IN./FT^2 HR-°F) ~VACUUM	(RT)	0.31	0.17	–	6.5	
	(2000°F)		0.67		14.2	
EMITTANCE	(RT)	-	-	–	0.89	0.85
	(2000°F)	-	-	–	0.93	0.63

* LATEST TEST DATA INDICATE MODULUS VALUES OF APPROXIMATELY 1.9×10^6 PSI. VALUES IN TABLE USED IN ANALYSIS.

**LATEST TEST DATA INDICATE THERMAL EXPANSION COEFFICIENT OF APPROXIMATELY 4.0×10^{-7} IN./IN./°F VALUES IN TABLE USED IN ANALYSIS, EXCEPT WHERE NOTED.

3.7.1.2 Thermophysical Properties

Detailed thermophysical properties of the improved LI-1500/0042 RSI system were obtained. Most of these data were generated by the companion Contract NAS 9-12083 program. Detailed descriptions have been reported.*

The thermophysical properties are summarized in Table 3.7.1.2-1.

Table 3.7.1.2-1

IMPROVED LI-1500/0042 SYSTEM THERMOPHYSICAL PROPERTIES

Material Property	LI-1500		LI-0042 Coating
	Parallel Direction	Normal Direction	
Thermal Expansion (in./in.-°F) 80 ~ 2000°F	$2.8 \sim 3.8 \times 10^{-7}$	3.4×10^{-7}	2.0×10^{-7}
Specific Heat (Btu/lb-°F)			
RT	0.15	0.15	
2000°F	0.32	0.32	
Thermal Conductivity (Btu-in./ft^2-hr-°F)			
RT 1 atm	0.58	0.35	6.5
2000°F 1 atm		1.56	14.2
RT vacuum	0.31	0.17	6.5
2000°F vacuum		0.67	14.2
Emittance			
RT			0.89
2000°F			0.93
Solar Absorptance			
As fabricated			0.773
After 5750 ESH			0.815
After 20 cycles			0.763
α/ϵ			
As fabricated			0.93
After 20 cycles			0.915

*Space Shuttle Thermal Protection System Development Final Report, LMSC-D152738.

Thermal Expansion. The linear thermal expansion of the improved LI-1500 remains essentially unchanged from the previously reported baseline data (NAS 9-11222). The expansion also demonstrated stability after thermal cyclic exposure at 2,300°F. Comparisons of the expansion data are presented in the following table.

Comparison of Linear Thermal Expansion Before and After Cyclic Exposure Testing in Parallel and Normal to Fiber Orientation Direction

Temperature (°F)	As Fabricated (in./in.)		After 20 cycles (30 min at 2300° F (in./in.)	
	Normal	Parallel	Normal	Parallel
400	9.7 to 13.5×10^{-5}	10.3 to 13.6×10^{-5}	8.6×10^{-5}	12.4×10^{-5}
650	20.1 to 25.1×10^{-5}	10.3 to 19.6×10^{-5}	15.1×10^{-5}	21.2×10^{-5}
900	30.3 to 33.8×10^{-5}	22.3 to 25.9×10^{-5}	22.5×10^{-5}	30.2×10^{-5}
1300	39.4 to 47.0×10^{-5}	37.7 to 42.3×10^{-5}	33.3×10^{-5}	41.0×10^{-5}
1650	54.6 to 62.7×10^{-5}	50.4 to 56.0×10^{-5}	37.6×10^{-5}	53.6×10^{-5}
2000	64.0 to 69.8×10^{-5}	53.0 to 73.0×10^{-5}		58×10^{-5}
2200	-40.0 to 200×10^{-5}	$+52.0$ to -25.0×10^{-5}		5×10^{-5}

The linear thermal expansion of the LI-0042 coating is presented in the following figure. At temperatures above 2,000° F, there is an "apparent shrinkage." This contraction was due to softening and yielding of the coating material specimen tested in rod form. At temperatures above 2,000° F, the coating is somewhat pyroplastic.

However, at temperatures below 2,000°F, the linear expansion closely matches that of the basic LI-1500 material. The expansion values are:

Temperature (°F)	Thermal Expansion (in./in. °F)
70	5.6×10^{-7}
900	5.6×10^{-7}
1050	4.3×10^{-7}
1400	2.5×10^{-7}
1600	2.5×10^{-7}
1900	0

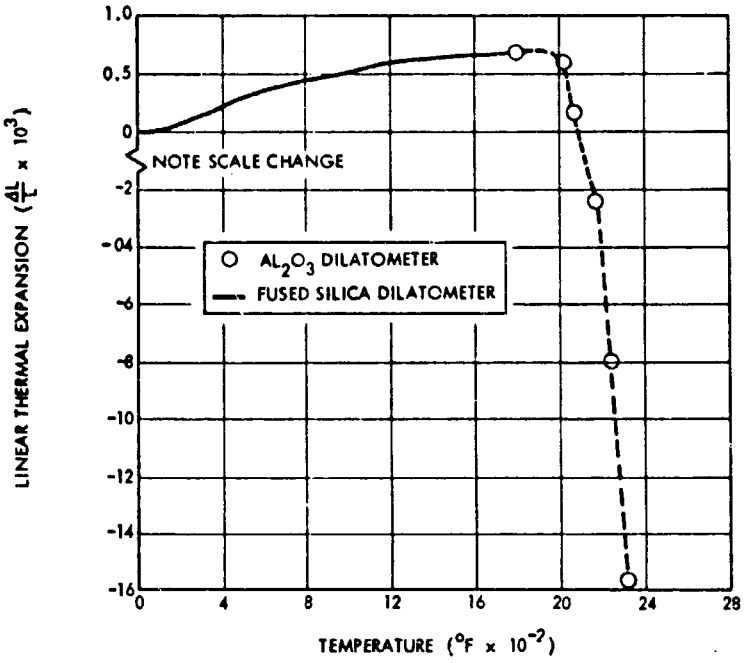

Thermal Expansion of 0042 Coating

Specific Heat. The specific heat of the improved LI-1500 material remained essentially unchanged from the values reported previously for the baseline material (NAS 9-11222) as well as from values obtained after 20 thermal cycles (30 min at 2,300° F). The variation of LI-1500 specific heat with temperature is shown in the following figure.

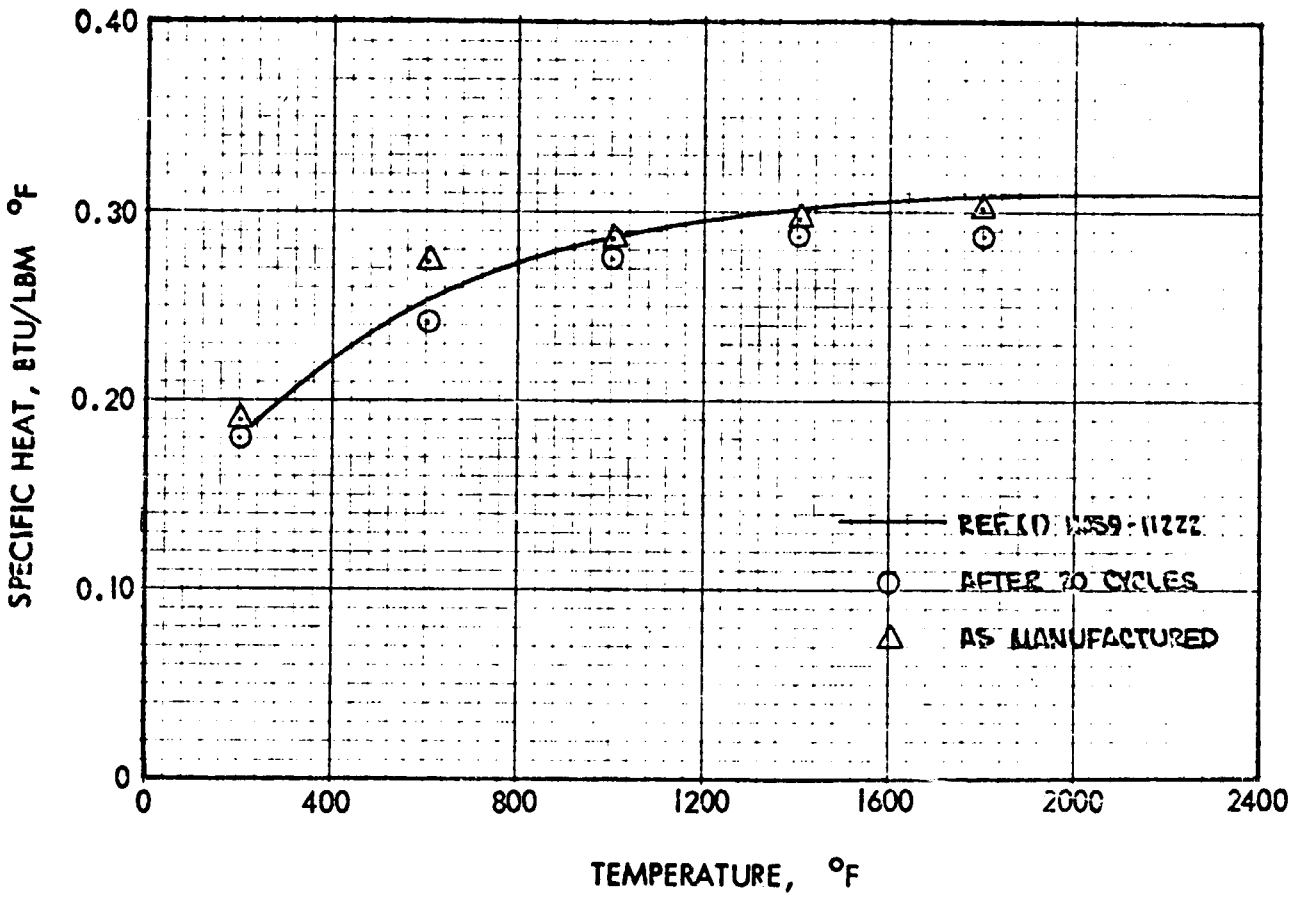

Variation of LI-1500 Specific Heat With Temperature

Specific interim design values are as follows:

Temperature (°R)	Cp (Btu/lb-°R)
360	0.0716
540	0.151
720	0.198
900	0.234
1080	0.263
1260	0.280
1440	0.287
1800	0.294
2160	0.306
2520	0.316
2890	0.320

Thermal Conductivity. The thermal conductivity of the improved LI-1500 also remains essentially unchanged from the previous values (NAS 9-11222) and after thermal cyclic exposure as shown in Fig. 3.7.1.2-1. Variation of thermal conductivity with temperature and pressure is presented in Fig. 3.7.1.2-2. The interim conductivity design values are as follows:

Interim Design Values – Thermal Conductivity
(Btu-in./ft^2-hr-°R)

Temp (°R) \ Pressure (mm Hg)	0.1	1.0	10.0	100.0	760.0
460	0.17	0.19	0.28	0.32	0.35
760	0.21	0.23	0.31	0.34	0.37
1160	0.27	0.29	0.35	0.47	0.52
1860	0.45	0.47	0.60	0.90	1.00
2460	0.67	0.69	1.02	1.40	1.56
2960	0.92	0.94	1.35	1.88	2.09

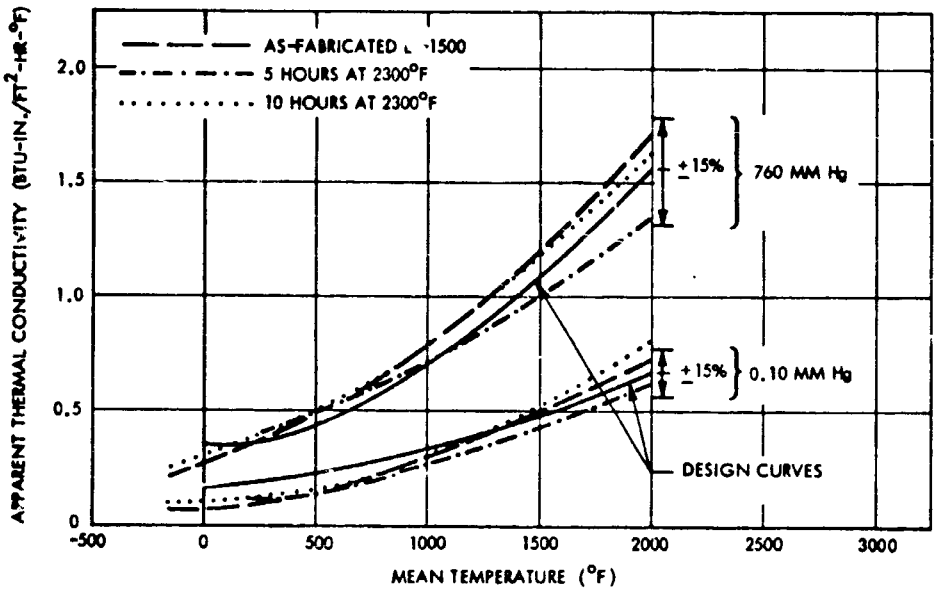

Fig. 3.7.1.2-1 Comparison of Design Curves With Recent Thermal Conductivity Data

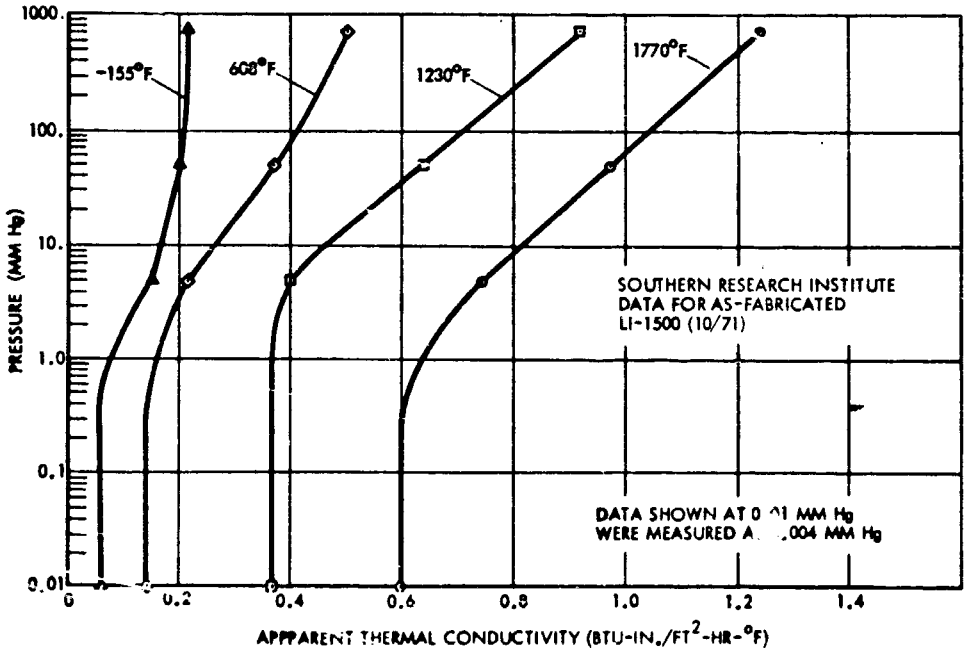

Fig. 3.7.1.2-2 Variation of LI-1500 Thermal Conductivity With Temperature and Pressure

The thermal conductivity of the 0042 coating was obtained from thermal diffusivity measurements by use of pulse techniques. Since measurements are made only to 500°F, the higher temperature values were extrapolated on the basis of coating constituents. The resulting values are as follows:

Thermal Conductivity of 0042 Coating

Temperature (°F)	Conductivity, K (Btu/ft-sec-°F)
0	0.15×10^{-3}
400	0.15×10^{-3}
1000	0.25×10^{-3}
2000	0.33×10^{-3}
2500	0.39×10^{-3}

Specimen density = 104 lb/ft^3

Emittance. The emittance values of the 0042 coating presented in Table 3.7.1.2-1 are based on measurements conducted at TRW. These values were previously discussed in Section 3.4.1.

3.7.1.3 Environmental Response Behavior

During this Material Improvement Program and the companion TPS Development Program Contract NAS 9-12083, various evaluations were conducted to demonstrate the capability of the LI-1500 RSI system to withstand the critical environmental conditions to be encountered in shuttle operations. LMSC developed a comprehensive test program and performed the required testing to simulate the critical environments encountered by the TPS for the various shuttle mission phases. The test program included temperature and pressure tests of small TPS panels and tests of design detail models with gaps, joints, and steps, in MSC's Arc-Plasma facilities. Thermal testing was also performed in programs sponsored by NASA/ARC. In addition, specialized environmental tests were performed on small specimens to fully demonstrate the suitability of the LI-1500 for the space shuttle TPS. The tests and results of the evaluation reported in this section utilized the improved LI-1500 and the 0042 coating system.

3.7.1.3.1 Simulated 100 Cycle (2500° F) Thermal Tests

The improved LI-1500 material with the 0042 surface coating was successfully subjected to an accelerated 100-cycle test evaluation under simulated shuttle reentry thermal environments and demonstrated the reusability and integrity of the improved RSI material system. The 4-in. x 4-in. x 2.4-in. thick test models were exposed to a perturbed reentry environment up to 2,500°F in the LMSC Radiant Heat Facility for 100 simulated shuttle missions. The thermal test cycle used remained at 2,500°F for 2.5 min. and was above 2,300°F for 8.3 min. The test cycle used is compared with the surface temperature histories of various design trajectories as shown in the following figure.

Evaluation of the tests showed that the 0042 coating was intact after 100 cycles. No open cracks or coating failures were detectable. Plan-view shrinkage was within the accuracy of the vernier caliper measurement tools, and thickness shrinkage after 100 cycles was 1.4 percent on one test model and 3 percent on the second model.

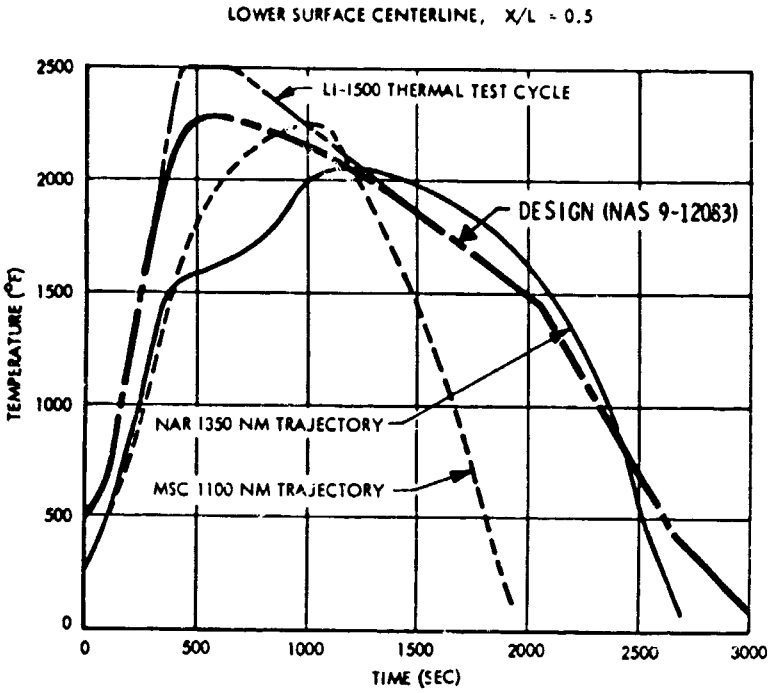

040A Orbiter Surface Temperature History Comparison

The improved LI-1500/0042 surface coated material demonstrated the capability of withstanding 83.3 hr of accumulated thermal exposure with 14 hr at temperatures greater than 2,300°F and 4 hr at 2,500°F. The environment corresponds to 100 consecutive overshoot reentries representative of an 1,100-nm crossrange mission. Complete details of this thermal evaluation have been reported.*

3.7.1.3.2 Material/Substrate Evaluation

LMSC has fabricated a prototype structural panel consisting of a 6- x 24-in. aluminum "Z" stiffened panel (one-quarter of a regular vehicle panel) with one 6- x 12- x 2.5-in. and two 6- x 6- x 2.5-in. LI-1500 tiles with joints and bonded to the panel with a 0.090-in. thickness of RTV-560. Complete descriptions of the test panel, conditions, and the results obtained are presented in Section 5.1 of the work cited in the footnote. In preliminary testing, the panel was subjected successfully to two simulated reentry heat pulses to peak temperatures of 2,300°F in the LMSC Radiant Heat Facility. A preliminary comparison of the predicted and measured temperatures is presented in the following curve.

*Space Shuttle Thermal Protection System Development Final Report, LMSC-D152738.

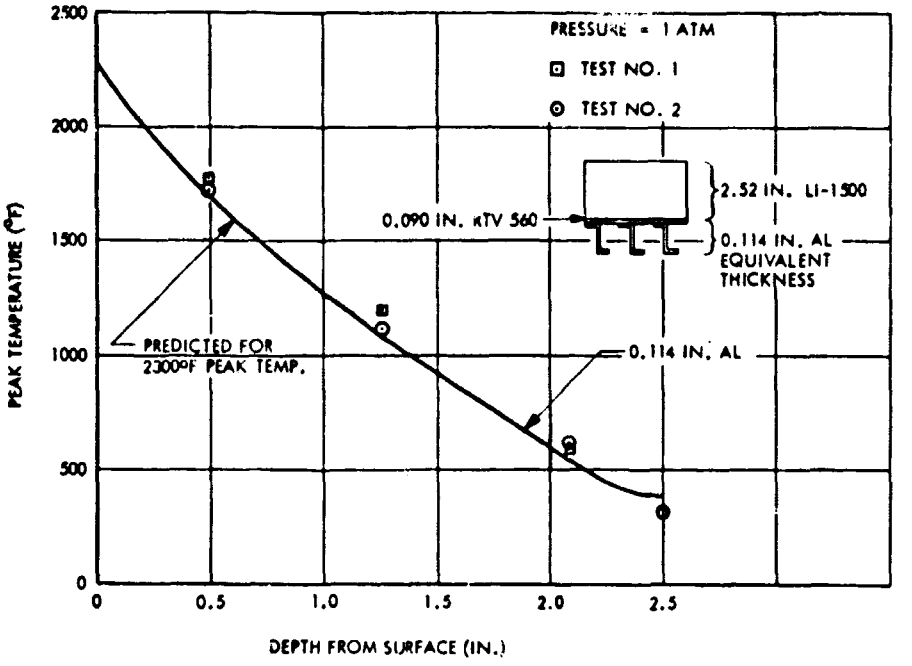

Preliminary Comparison of Measured and Predicted Temperatures for Prototype Panel Tests

3.7.1.3.3 Design Details Evaluation

Subscale instrumented test models were designed and fabricated for the evaluation of critical design details such as gaps, joints, and steps to determine the degree to which they may cause potential heating and/or stress problems. Complete descriptions of the test results, conditions, and test models have been reported.*

Joint comparison tests. Radiant heat tests were performed on three joint configurations (lap joint, bevel joint, and strip joint) to compare in-depth and substrate temperature responses. The specimens were tested in LMSC's 1-atm radiant heat facility for five cycles to a peak surface temperature of 2,300°F. The data shown (with the configuration and thermocouple locations) in the following figures were representative of all five cycles.

The results of the radiant test indicated no obvious thermodynamic advantage in any of the three joints. In flight application, where the LI-1500 tiles will be subjected to hot boundary layer gases during reentry, the existence of gaps extending into the substrate

*Space Shuttle Thermal Protection System Development Final Report, LMSC-D152738.

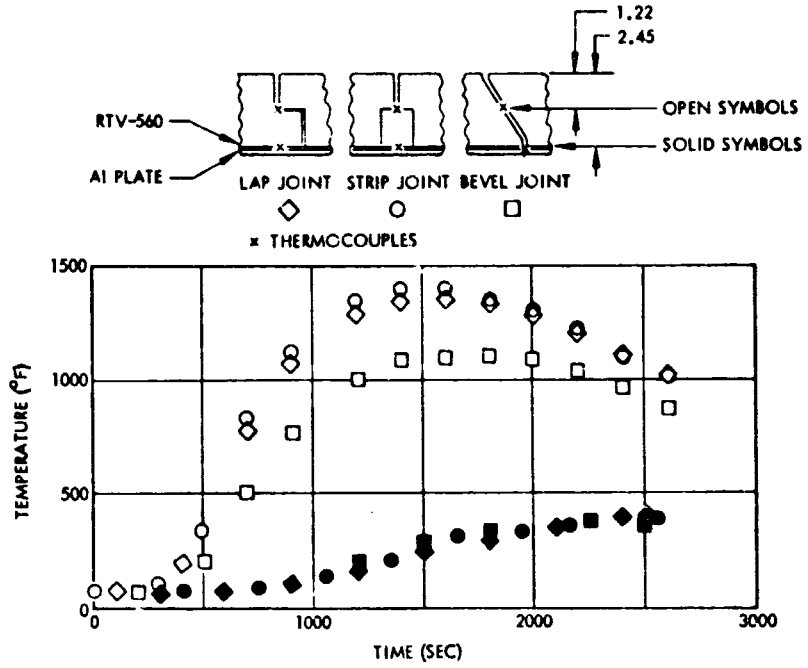

Temperature Response of Various Joint Configurations to a Radiant Heat Test

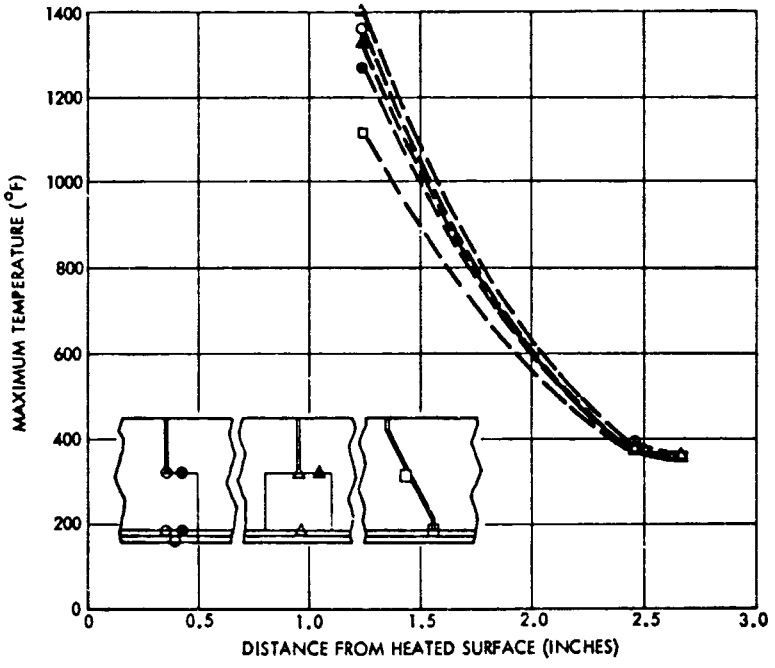

Comparison of Measured Peak Temperatures for Three Joint Configurations

will probably be prohibitive. Hence, the bevel-type joint is undesirable, and a lap or strip joint is preferable since any gases that penetrate the joint will probably not reach the substrate. LMSC currently favors the strip-joint approach because of its easier individual tile replacement and its inherent design feature of preventing boundary layer gases from reaching the substrate.

3.7.1.3.4 Specialized Environmental Tests

Test evaluations intended to establish the effects of various environmental conditions on the RSI material and coating were conducted. These evaluations included infrared transmission, hard vacuum, solar radiation, freeze/thaw, rain erosion, moisture absorption, cold soak, temperature overshoot, and salt spray.

Infrared Transmission. Spectral transmissions of LI-1500 and also of the coating material were determined at room temperature in a range of wavelengths. Test methods, conditions, and complete results have been reported.* The test matrix is as follows:

Infrared Transmission Test Conditions

Specimen Type	Thermal Cycles	Test Temperature (°F)	Measurement Range (μ)
LI-1500	0	Ambient	1.0 to 15.0
LI-1500	20	Ambient	1.0 to 15.0
Coating	0	Ambient	1.0 to 15.0

The following curve shows room temperature data for a range of LI-1500 material thicknesses over a wavelength range from 0.35 to 2.5 μ. For the LI-1500 thickness proposed for the space shuttle (0.5 to 2.5 in.), transmission is expected to be negligible.

*Space Shuttle Thermal Protection System Development Final Report, LMSC-D152738.

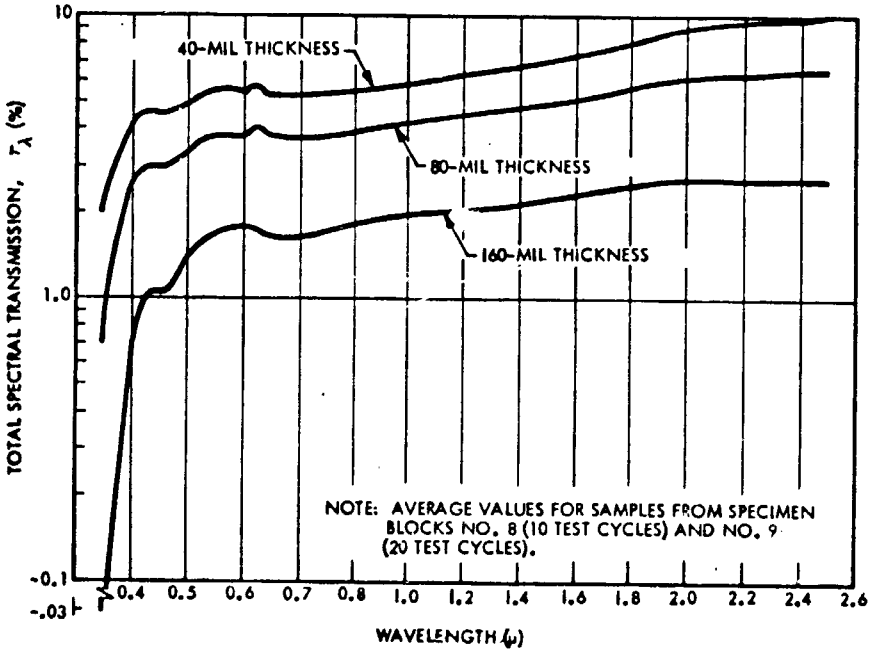

Total Spectral Transmittance Data for Three Thicknesses of LI-1500

Normal transmission measurements are shown in the following table.

Spectral Normal Transmittance of LI-1500

Wavelength (~ microns)	% Transmission for Thickness (mils)		
	40	80	160
1.5	0.12	0.07	0.03
2.0	0.13	0.07	0.03
2.5	0.11	0.04	0.01
3.0	0.06	0.005	< 0.001
4.0	0.17	0.05	0.008
5.0	0.01	0.001	< 0.001
6.0	0.02	< 0.001	< 0.001
7.0	1.93	0.03	0.001
7.5	1.27	0.02	0.001
8.0	0.01	< 0.001	< 0.001
10.0	0.006	< 0.001	< 0.001
12.0	0.002	< 0.001	< 0.001
14.0	0.002	< 0.001	< 0.001
16.0	< 0.001	< 0.001	< 0.001
20.0	0.01	< 0.001	< 0.001

With exception of the transmission band at 7.5 μ, the material appears to behave as an isotropic scatter. In this band, it appears that the energy is principally transmitted in a normal direction rather than scattered hemispherically. Post-cycling specimens

did not show any significant variation in the spectral transmission for 40 and 80-mil thicknesses. The spectral normal transmission measurements on the 0042 coating showed no transmission greater than 0.1 percent from 1.5 to 20μ. For the basic LI-1500 material, no significant change in transmission is expected at 1,000° F.

Hard Vacuum Test. A 30-day vacuum exposure test was performed to evaluate any long-term vacuum-induced effects on dimensional stability of LI-1500 material. The tests were conducted in a vacuum chamber operated at a pressure of 1×10^{-6} Torr and ambient temperatures (75 ± 5° F). Complete descriptions of the tests have been reported.* The weight and dimensional measurements (shown in the following table) and visual observation concluded that long-term exposure of LI-1500 to vacuum conditions results in no significant degradation of the material.

LI-1500 Vacuum Exposure Test Results

Sample	Thermal Cycles	Specimen Weight (gm)		
		Initial	After 20 days	After 30 days
1	0	21.812	21.834	21.845
2	0	21.832	21.853	21.858
3	20	4.240	4.240	4.240
4	20	4.697	4.697	4.697
5	20	4.512	4.512	4.512
6	20	4.321	4.321	4.321

Solar Radiation Tests. Tests were performed to determine coating degradation as a function of ultraviolet (UV) exposure duration and number of reentry heating exposures. The tests were conducted in a static ultraviolet exposure chamber with typical chamber pressures of 2×10^{-7} Torr. Solar absorption (α_s) determined by measuring the spectral reflectance was determined prior to and subsequent to specific equivalent sun hours (ESH) of UV exposure. Complete descriptions of test conditions, test methods, and results are cited in the footnote. The effects of extended UV radiation on the solar absorptance of the coated LI-1500 and the effects of UV exposure on emittance are shown in the following tables.

*Space Shuttle Thermal Protection System Development Final Report, LMSC-D152738.

Effect of UV Exposure on Solar Absorptance

SET	SAMPLE	α_s (PRETEST)	α_s (2900 ESH)	α_s (5750 ESH)	$\Delta\alpha_s$ (FINAL)
1*	1	0.774	-	-	-
	2	0.773	0.829	0.825	0.052
	3	0.775	0.831	0.818	0.043
	4	0.766	-	0.803	0.037
2**	5	0.768	0.781		0.013
	6	0.759	0.772		0.012
	7	0.761	0.777		0.016

* UNCYCLED SAMPLES
** 20 THERMAL CYCLES

Effect of UV Exposure on Emittance

SET	SAMPLE	ϵ (PRE-TEST)	ϵ (2900 ESH)	ϵ (5750 ESH)
1*	1	0.859	0.858	0.859
	2	0.866	0.867	0.867
	3	0.862	0.862	0.861
	4	0.865	0.866	0.865
2**	5	0.856	0.856	
	6	0.864	0.862	
	7	0.865	0.866	

*UNCYCLED SAMPLES
**20 THERMAL CYCLES

Extended UV exposure of uncycled coated LI-1500 causes an increase in α_s of 0.04–0.06. The material subjected to multiple simulated reentry cycles degrades somewhat less ($\Delta\alpha = 0.01-0.02$). In all cases, however, the measured values of emittance were unchanged as a result of UV exposure. It was concluded that extended exposure to solar UV radiation will not alter the room temperature emittance of the coated LI-1500. The solar absorption of the material appears to increase by 0.04-0.06 after 2,900 ESH and remains essentially unchanged after an additional exposure of 2,850 ESH. The material previously subjected to reentry conditions appears to degrade somewhat less. The change in solar absorptance is of sufficiently small magnitude to consider the effects of UV radiation negligible to the overall thermal performance of the material.

Freeze/Thaw Tests. Evaluation tests were conducted to determine whether cyclic temperature conditions that would cause alternate freezing and thawing of the RSI may cause degradation of the basic LI-1500 material and/or coating. Detailed descriptions of the test conditions, test methods, and results have been reported.*

A "worst case" approach was taken in exposing the test specimens to the various temperature conditions. Actual ambient temperature changes occur gradually, instead of abruptly as in the tests. However, this represented a most severe test condition, and it was felt that acceptable behavior for these conditions will assure integrity for any less severe conditions. In addition, a range of thaw temperatures was chosen to determine thaw temperature level effects that may be encountered for both prelaunch and ascent conditions.

The specimens were 1- by 4- by 4-in. LI-1500 tiles coated on one 4- by 4-in. surface with the 0042 coating system. All the specimens were treated with the LI-007 silicone hydrophobic water-repellent material prior to the initial test series. Each test for a particular specimen consisted of exposure to a specific moisture environment, followed by a freeze/thaw cycle. Each specimen was subjected to a series of three tests, each test being at a different thaw temperature. Test conditions and results are presented in the table on the following page.

The resulting dimension and weight changes were considered negligible. No visual degradation of either the basic LI-1500 material or 0042 coating was observed.

Additional tests were performed to determine the influence of elevated temperature on the effectiveness of the water-repellent material. Specimen TT541, which had been previously cycled at ambient, 500, and 1,000°F thaw temperatures, was subjected to 100 percent humidity conditions, frozen, and then thawed at 1,000°F. Specimen TT545, which was treated with the LI-007 silicone hydrophobic water-repellant material, was tested under the same conditions to obtain a direct comparison. The test results are

*Space Shuttle Thermal Protection System Development Final Report, LMSC-D152738.

Specimen No.	Moisture Environment		Freeze Environment		Thaw Environment		Pre-Test	Post-Test
	% RH	Time (hr)	Temp (°F)	Time (hr)	Temp (°F)	Time (hr)	Weight (gm)	Weight (gm)
TT 544	(1) 50	2	0	14	70	8	69.9	69.4
	(2) 50	2	0	64	500	8	69.4	69.4
	(3) 50	2	0	18	1000	8	69.4	69.3
TT 542	(1) 95	2	0	8	70	8	74.0	73.9
	(2) 95	2	0	66	500	8	73.9	73.7
	(3) 95	2	0	16	1000	8	73.7	73.8
TT 541	(1) 100	3	0	12	70	8	70.6	70.7
	(2) 100	2	0	68	500	8	70.7	70.3
	(3) 100	2	0	14	1000	8	70.3	70.5

(1), (2), (3): Each specimen subjected to three sequential cycles.

shown in the table on the following page. Although the untreated specimen absorbed more moisture than the treated one, the amount is considered negligible (<1.0 percent). No visual degradation of either the basic LI-1500 material or 0042 coating was observed.

Based on these tests, it is concluded that freeze/thaw cycles, even under conditions of high humidity or rain, do not cause any degradation of LI-1500 material or 0042 coating.

3.7.1.3.5 Moisture Absorption Tests: Humidity and Rain Environments

Seven test models, 4- by 4- by 2.4-in. thick, were prepared utilizing the improved LI-1500/0042 material system and were subjected to various humidity and simulated rain environments. Configurations of the tests models were as shown in Table 3.7.1.3-1. One of the models was of a typical joint configuration. On the tile configurations the test models were surface-coated on top and half-way down the sides, leaving portions of the sides uncoated and exposed. Each test model was subjected to a specific moisture environment, followed by a simulated ascent/entry combined heating and pressure

Specimen No.	Moisture Environment		Freeze Environment		Thaw Environment		Results	Sequence
	% RH	Time (hr)	Temp (°F)	Time (hr)	Temp (°F)	Time (hr)	Weight (gm)	
TT 541*	–	–	–	–	–	–	70.2	Pre-Humidity
	100	2	–	–	–	–	70.8	Post-Humidity
	–	–	0	62	–	–	70.7	Post-Freeze
	–	–	–	–	1000	8	70.3	Post-Thaw
TT 543**	–	–	–	–	–	–	63.4	Pre-Humidity
	100	2	–	–	–	–	63.7	Post-Humidity
	–	–	0	62	–	–	63.6	Post-Freeze
	–	–	–	--	1000	8	63.3	Post-Thaw

*TT 541 was previously cycled to 1000 °F

**TT 543 was treated with LI-007 silicone hydrophobic water repellent material but uncycled prior to this test.

environmental cycle. The cyclic sequences of the 007 treatment, moisture environments and the thermal exposures, as well as the resulting test data, are described in Table 3.7.1.3-1.

The four test models subjected to the humidity environments (with or without the 007 treatment) showed essentially no moisture weight pickup after the exposure. Subsequent 007 refurbishment and thermal testing showed essentially no weight changes attributable to the test environments. In the simulated rain environments both the tile and joint test models, when treated with the 007 system, showed little or no weight differences attributable to the test environments. The high weight gain (195.9 grams) of the test model (without the 007 treatment) in the simulated rain environment was caused by water intrusion into the model through the uncoated and untreated exposed side sections of the model and not through the LI-0042 surface coating material. This model, with the high water content, when subjected to thermal test environments, indicated no visual deterioration except for minor coating flaking.

Table 3.7.1.3-1

MOISTURE ABSORPTION TESTS: HUMIDITY AND RAIN ENVIRONMENTS

Test Model No.	Config-uration	Moisture Environ-ment (ME)	Test Sequence								
			Initial Model WT (GM)	Thermal Test Cycles(1)	Weight After 007 Treat. (GM)	Weight After ME	Weight After 007 Treat. (GM)	Weight After Thermal Test (GM)(1)	Weight After 007 Treat. (GM)	Weight After ME (GM)	Weight After Thermal Test (GM)(1)
TT49A-1	Tile*	50% RH 2-hr (min)	275.0	0	283.0	283.0	–	283.0	283.1	283.1	283.0
TT49A-2	Tile*	50% RH 2-hr (min)	277.1	0	–	277.25	293.6**	293.6	293.7	293.7	291.9
TT49B	Tile*	75% RH 2-hr (min)	281.6	0	–	281.6	–	281.6	295.85**	295.85	294.2
TT49C	Tile*	95% RH 2-hr (min)	264.3	0	–	264.5	280.3**	280.3	280.85	280.85	278.9
TT49D-1	Tile*	Rain 1 in./hr 1 hour	277.8	5	283.3	282.5	–	282.1	282.3	282.5	282.1
TT49D-2	Tile*	Rain 1 in./hr 1 hour	283.2	5	–	479.1	–	343.95	–	–	–
TT44E	Joint*	Rain 1 in./hr 1 hour	281.1	0	282.6	290.7	–	290.0	296.5	297.2	295.3

*Tiles: 0042 coated top surface and one-half down sides. Joint 0042 coated top surface and into joint.
**Improper application of 007 treatment necessitated rebonding and added weight.
(1)2300° F radiant heat exposure.

These particular tests showed that the LI-1500 material with 0042 surface coating and the 007 water repellant treatment, resulted in minimal moisture weight gains when exposed to the humidity and simulated rain environments. Visual examination of the tested specimens also showed that the LI-1500 system is not affected by exposure to various moisture environments; nor do subsequent simulated ascent/entry pressure and heating environments degrade the material.

Rain Erosion Tests

Rain conditions may be encountered by the space shuttle orbiter during cruise; to enable establishment of system constraints for these environmental conditions, the erosion resistance of the TPS must be determined. A test program was conducted to evaluate coated LI-1500 material to demonstrate its ability to survive anticipated rain and environmental conditions during flight. The tests were performed in the Edler Industries, Inc., high-speed rain-erosion test facility located in Newport Beach, Calif. The tests subjected 3- by 3-in. LI-1500 surface area coated with the LI-0042 surface coating. Complete descriptions of the test facility, test conditions, environments, and the test results are presented in Section 5.3.5 of the Contract NAS 9-12083 Final Report.* The conditions and results of the rain-erosion tests conducted are indicated in the following table. Test Nos. 1 through 4 were conducted sequentially on the same test specimens.

The degradation and damage to the test specimens noted in the rain-erosion test were caused by the severe mechanical loads imposed on the test specimens by the facility equipment. The failures were attributed to the high mechanical loads (approximately 6,000-g radial acceleration) developed by the facility on certain test conditions. Based on the tests conducted, it was concluded that at a 10-deg angle of attack and velocities up to 350 mph, degradation of the 0042 coating due to rain erosion is insignificant. Recommendations are that additional tests be conducted at 20-deg angle of attack in a facility that imposes less severe mechanical loads on the test specimens.

*Space Shuttle Thermal Protection System Development Final Report, LMSC-D152738.

RAIN EROSION TEST CONDITIONS AND RESULTS

Test No.	Specimen No.	Specimen Angle of Attack (deg)	Velocity (mph)	Rain Intensity (in./hr)	Test Duration (min)	Results
1	1	10	200	0	2	No change
	2	↑	↑	0	2	No change
	3	↑	↑	0	2	No change
	4	↑	↑	0	2	No change
2	1	↑	↑	1.3	5	No change
	2	↑	↑	1.3	5	No change
	3	↑	↓	1.3	5	No change
	4	↑	200	1.3	5	No change
3	1	↑	350	0	2	No change
	2	↑	↑	0	2	Coating cracked and chipped
	3	↑	↑	0	2	Coating cracked
	4	↑	↑	0	2	No change
4	1	↑	↑	1.05	5	No change
	2	↑	↑	1.05	5	No change
	3	↑	↑	1.05	5	Coating and material loss
	4	↓	↑	1.05	5	No change
5	5	20	↑	0	2	No change
	6*	20	↑	0	2	Lost specimen
	7	20	↓	0	2	No change
	8	20	350	0	2	No change

*Specimen 6 had cracked coating prior to testing.

3.7.1.3.6 Cold Soak Tests

Testing was conducted to determine whether RSI degradation will occur when the TPS experiences an entry temperature history following an initial -150° F temperature condition. Complete descriptions of the test methods, test models, and results have been reported.* Two specimens 4- by 4- by 2.45-in. thick were exposed to low-temperature environments until an equilibrium temperature of -150° F was obtained. These specimens were removed from the temperature environment and subjected to simulated entry heating environments with peak temperatures of 2300° F. After testing, no visual degradation or measurable change in dimensions or weight was observed. Typical measured temperature profiles are shown in the following figure. Difference in midpoint temperature (specimens A and B) is believed to be the result of excessive contact resistance between thermocouple A and the surrounding material.

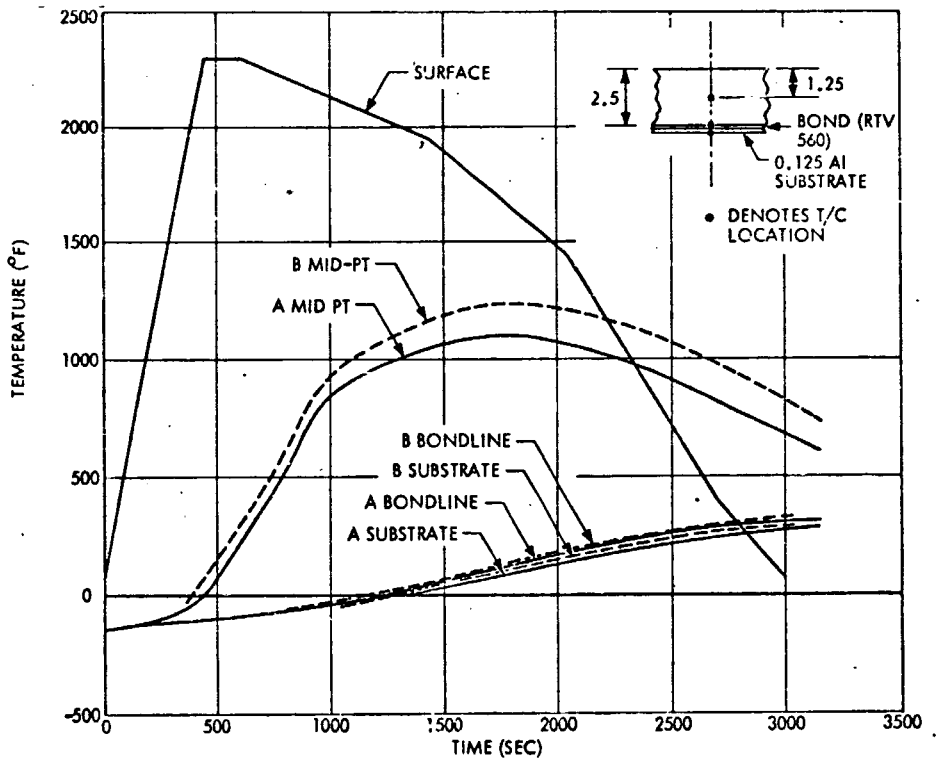

Cold Soak Test Data (Test No. 2)

*Space Shuttle Thermal Protection System Development Final Report, LMSC-D152738.

3.7.1.3.7 Temperature Overshoot Tests

The effect of exceeding the design heating profile was examined by subjecting specimens to surface temperatures greater than the 2300° F design limit. Two specimens were used for these tests. Specimen No. 1 was a 4- by 4- by 1-in. thick coated tile with no baseplate or instrumentation. Specimen No. 2 was a 4- by 4- by 2.45-in. coated tile bonded to a 0.114-in. -thick aluminum plate with a 0.090-in. thickness of RTV 560 adhesive. This particular specimen had been previously used in the cold-soak test. Specimen No. 1 experienced a series of five tests (with surface temperature profile as shown in the following figure) with maximum surface temperature progressively increased from 2600 to 2950° F. At the conclusion of the tests, small open pores were observed in the coating. No coating cracking was observed, and the water repellency was retained. When subjected to a 3000° F heat pulse, the coating of specimen No. 2 remained uncracked and water repellent, although some local surface slumping was noted. The temperature profiles for these tests are shown in the following figures:

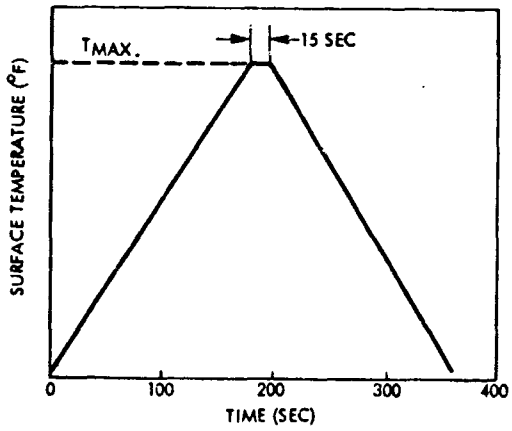

RUN	$T_{MAX.}$ (°F)
1	2600
2	2700
3	2800
4	2900
5	2950

Temperature Overshoot Profile – Specimen No. 1

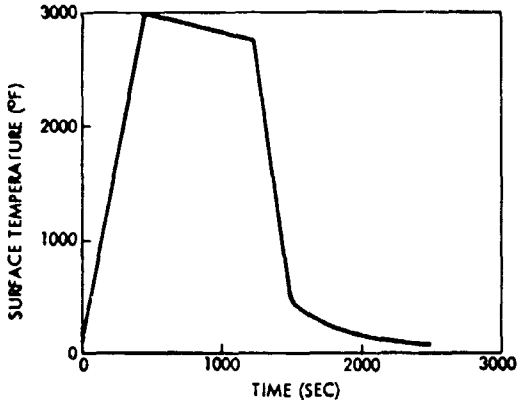

Temperature Overshoot Profile – Specimen No. 2

The effect of maximum surface temperatures greater than designed value on bondline temperature is shown in the following figure. Although the 300° F maximum design temperature of the aluminum structure is exceeded (410° F for a 3000° F maximum surface temperature), the structure would remain intact and the vehicle could be landed safely.

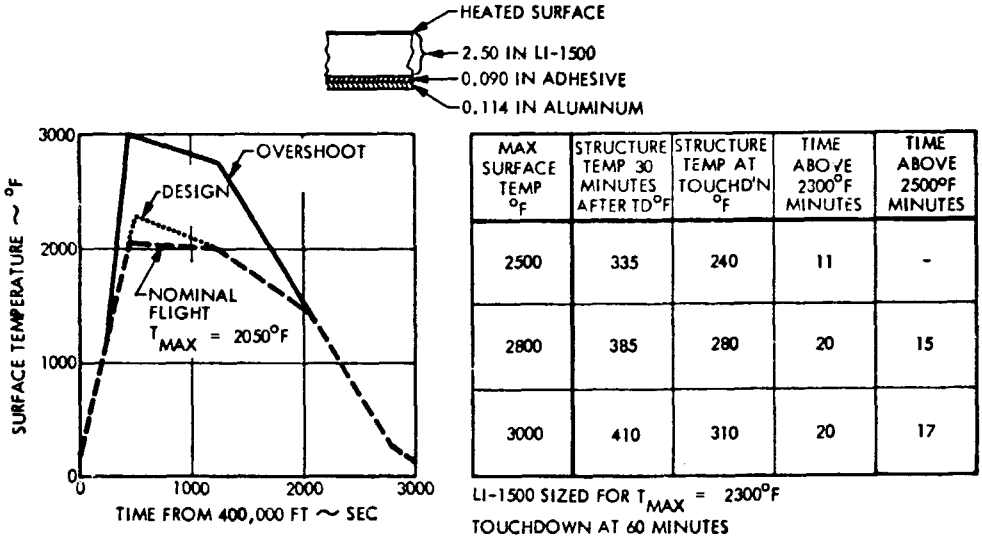

MAX SURFACE TEMP °F	STRUCTURE TEMP 30 MINUTES AFTER TD°F	STRUCTURE TEMP AT TOUCHD'N °F	TIME ABOVE 2300°F MINUTES	TIME ABOVE 2500°F MINUTES
2500	335	240	11	-
2800	385	280	20	15
3000	410	310	20	17

LI-1500 SIZED FOR T_{MAX} = 2300°F
TOUCHDOWN AT 60 MINUTES

Effect of Temperature Overshoot on Structure Temperature

3.7.1.3.8 Acoustic Environment Tests

FI-600, a low-density, flexible silica composite material was used for the seal strips in prototype panel joints delivered under Contract NAS 9-12083.* This material fabricated into a joint model was subjected to acoustic environment, as shown in the following figure, for a total exposure duration of 30 min. Visual inspection of the model after test showed no observable damage or degradation of the LI-1500 or the FI-600 material.

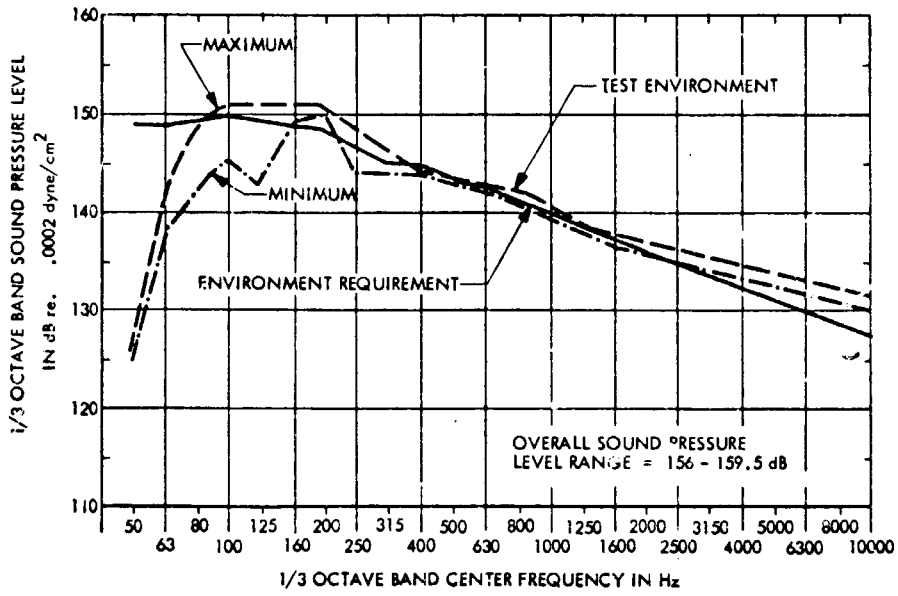

Comparison of Applied Acoustic Test Environment With Requirement

Salt Spray Tests. LI-1500 test models were subjected to cyclic exposures of salt spray environments and thermal testing in the LMSC Radiant Heat Facility. Two test models 4- by 4- by 1-in. thick coated top surface with the 0042 surface coating, previously used in the Freeze/Thaw testing, were evaluated in the salt spray tests. The models were treated with a refurbishment type (approximately 0.1 gm of 007 on the top surface) application, exposed to a simulated salt spray environment, subjected to a radiant heat cycle of 300 sec at peak temperatures of 2300° F, and recycled for a

*See "Space Shuttle Thermal Protection System Development Final Report," LMSC-D152738.

total of five cycles. The salt solution was per MIL-STD 810B, method 509, Procedure I, at a ratio of 5 gm salt to 95 gm water with a pH of 6.7 at 35° C. The salt spray environmental exposure was at 95 percent RH for a period of 250 min. per cycle with the model masked-off, allowing exposure of only the top surface area. Weights, visual examination, and water impervious evaluations were conducted after each cycle. Results of the tests were as follows:

SALT SPRAY TESTS

Sample No.	Cycle	Weight (gm) After 007 Treatment	Weight (gm) After Salt Spray	Weight (gm) After Thermal Test
TT53-2	1	51.9	51.8	51.60
	2	51.65	51.81	51.71
	3	51.60	51.65	51.65
	4	51.60	51.60	51.55
	5	51.50	51.55	51.45
TT54-2	1	75.70	75.75	75.35
	2	75.40	75.36	75.31
	3	75.40	75.60	75.35
	4	75.40	75.50	75.35
	5	75.40	75.50	75.45

The weight differences during the salt spray tests were negligible. Although the surface coating changed to a frosty mottled appearance, no detrimental effects were apparent, and the coating retained its water impervious characteristics when evaluated by the water drop test.

3.7.2 LI-0900/0045 Material Properties

The LI-0945 system (silica insulation of 9 lb/cu ft density, and 0045 borosilicate/silicon carbide coating) was evaluated during the latter part of this contract period. Much of the data accumulated for the improved LI-1500 system is believed to be applicable to the new LI-0900 material (e.g., thermal expansion, specific heat, emittance, environmental behavior, etc). Therefore, selective property determinations should enable assessment in preliminary design considerations of the feasibility and desirability of using this new material in place of LI-1500.

3.7.2.1 Mechanical Properties

Mechanical properties of LI-0900 were determined using the methods previously described in Section 3.7.1. Tension, compression, and shear data determined at room temperature are presented in Table 3.7.2.1-1. For comparison, data obtained on the improved LI-1500 material are also presented in the table.

The data indicate that the mechanical strength of LI-0900 is lower than that of LI-1500 material. However, strength in the design critical transverse direction is comparable. Property characteristics in this case are actually the "controlling" factors in the designs. Of significance is that the modulus of the LI-0900 material is substantially reduced from that of the LI-1500 material. This is an important change, as it should diminish the buildup of stress concentration in use.

3.7.2.2 Thermal/Physical Properties

Since LI-0900 and LI-1500 are essentially composed of identical chemical constituent species, the thermal expansion and specific heat properties are expected to be essentially identical. Of prime interest was the thermal conductivity characteristics of the lighter weight LI-0900. The thermal conductivity data were generated utilizing the guarded hot plate method. The data obtained are as follows:

Table 3.7.2.1-1

LI-0900 MECHANICAL PROPERTIES

Property		LI-0900		LI-1500(1)	
		Stress (psi)	Modulus (psi)	Stress (psi)	Modulus (psi)
Shear					
Longitudinal (Strong Direction):	Ave	43.0(8)*	7,180(8)*	75.0(8)*	31,880(8)*
	Min	41.9	6,800	56.1	25,900
	Max	44.9	7,440	97.8	43,100
Transverse (Weak Direction):	Ave	23.3(6)*	3,320(6)*	27.5(4)*	6,610(4)*
	Min	20.4	2,970	25.4	6,370
	Max	25.4	3,650	29.6	6,840
Tension					
Longitudinal (Strong Direction):	Ave	44.6(3)*	15,900(8)*	73.7(8)*	56,930(8)*
	Min	41.5	13,400	56.2	27,600
	Max	47.4	19,300	90.8	68,000
Transverse (Weak Direction):	Ave	11.7(5)*	2,450(5)*	14.3(8)*	7,650(8)*
	Min	8.8	1,450	12.5	4,890
	Max	15.3	3,200	18.0	9,870
Compression					
Longitudinal (Strong Direction):	Ave	49.9(4)*	15,800(4)*	174(6)*	39,700(6)*
	Min	46.3	14,700	148	30,800
	Max	54.0	16,500	190	47,000
Transverse (Weak Direction):	Ave	34.2(4)*	3,400(4)*	42.1(4)*	4,070(4)*
	Min	31.5	3,100	39.4	3,470
	Max	36.5	3,740	44.2	5,120

*Numbers in parentheses indicate number of specimens tested and averaged.

(1)Data from Space Shuttle Thermal Protection System Development Final Report, LMSC-D152738.

Condition	Thermal Conductivity (Btu-in./ft^2-hr-° F)
RT, 1 atm	0.91
580° F, 2×10^{-5} Torr	0.17
1050° F, 2×10^{-5} Torr	0.25
1290° F, 2×10^{-5} Torr	0.34
1600° F, 2×10^{-5} Torr	0.52

The generated thermal conductivity data points are shown plotted in Fig. 3.7.2.2-1 on the LI-1500 Thermal Conductivity Design Curve developed in the NAS 9-12083 contract.* The data indicate the thermal conductivity of LI-0900 to be slightly lower than that of LI-1500 in temperature regions below 1600° F. Since radiation becomes a predominant mode of transmission at elevated temperatures, the possible reduced light-scattering characteristics of the lower density LI-0900 may result in somewhat higher conductivities at the elevated temperatures. Further evaluations should be conducted to determine the influence of the lower density on conductivity at the elevated temperatures. If needed, it is believed that the opacifiers discussed in Section 3.6.1 would have a beneficial influence on high-temperature conductivity of the LI-0900 material.

Optical properties of the 0045 coating were very similar to those of the 0042 coating reported in Section 3.4.1, Emissivity Investigations. Comparative emissivity computed from room-temperature spectral data are presented as follows:

	0042 Coating	0045 Coating
Solar Absorptance (α_s)	0.79	0.75
*Total RT Emittance (DB-100 Data)	0.85	0.89
Normal Emittance* At: 70° F	0.85	0.90
500° F	0.87	0.91
1000° F	0.88	0.90
1500° F	0.87	0.88
2000° F	0.86	0.86
2500° F	0.86	0.86

*Predicted normal emittance values from spectral reflectance data.

*Space Shuttle Thermal Protection System Development Final Report, LMSC-D152738.

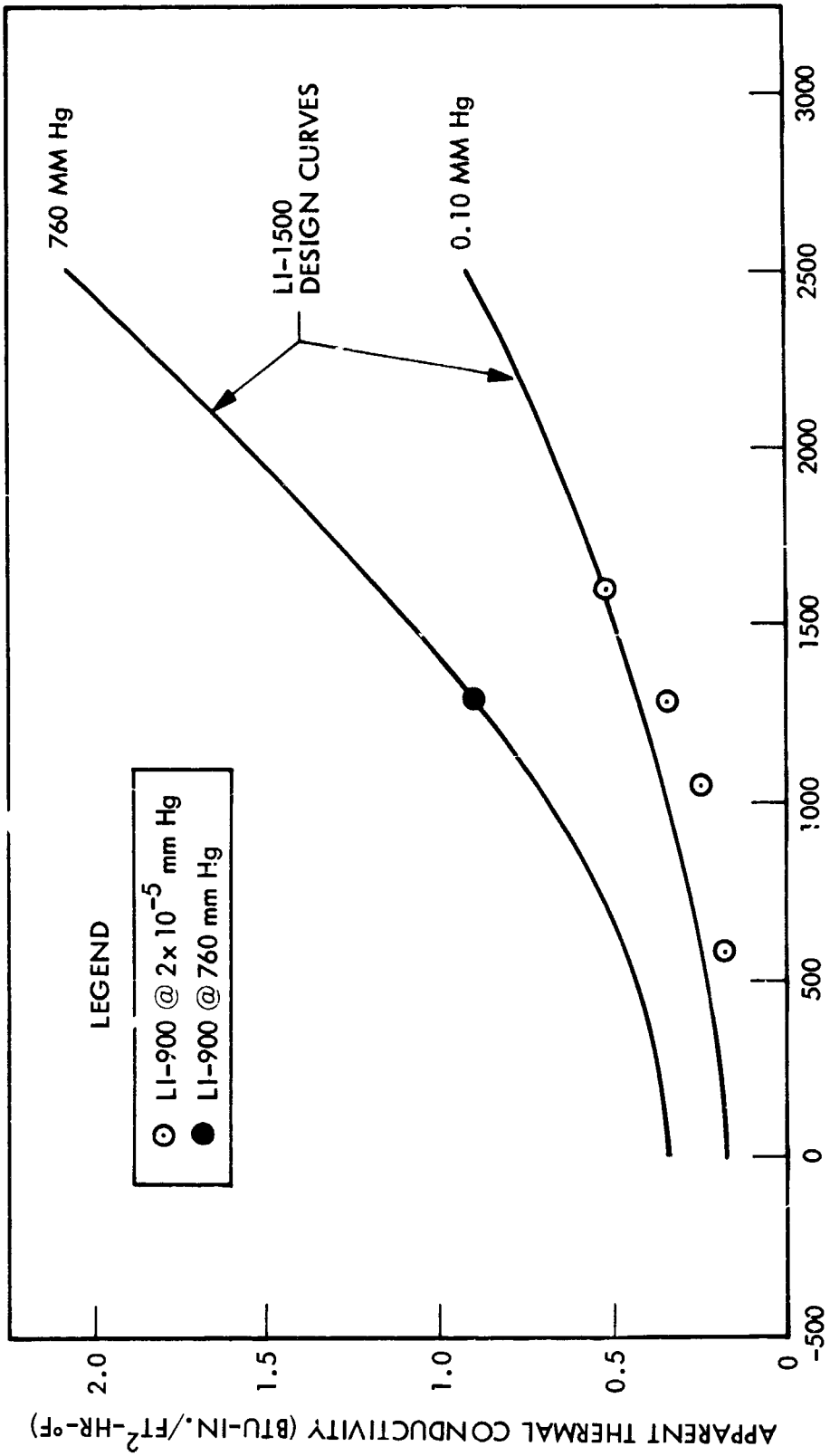

Fig. 3.7.2.2-1 LI-0900 Thermal Conductivity Test Data

3.7.2.3 Environmental Response Behavior

During this phase of the material improvement program, simulated environmental thermal and rain-resistance testing was conducted on the LI-0900 and the 0045 surface coating systems. In addition, thermal evaluations were conducted on the LI-0900 material with the 0042 surface coating and on the LI-1500 material with 0045 surface coating.

Five test models of LI-0945 (LI-0900 with 0045 surface coating) were successfully subjected to 32 cycles of simulated shuttle reentry heating. These models, 3-1/2 in. by 3-1/2 in. by 2 in. thick, were exposed to a perturbed reentry environment (up to 2500° F surface temperature) in the LMSC Radiant Heat Facility. The thermal test cycle remained at 2500° F for 2.5 min and was above 2300° F for 8.3 min. The complete test cycle was previously described in Section 3.7.1.3. Evaluation of the tests showed that all five specimens remained intact and water-impervious after the 32-cycle exposure. No cracking or coating failures were detectable. The maximum plan-view shrinkage was measured to be 0.5 percent. The identification of the five models and the test results are as shown below:

Model No.	Material	Shrinkage (%)
TT101-1	LI-0945	–
TT101-2	LI-0945	<0.1
TT101-3	LI-0945	0.5
TT101-4	LI-0945	0.5
TT101-8	LI-0945	<0.1

On specimen TT101-8, the 0045 coating was intentionally applied to twice the required thickness (approximately 22 mils versus 10 mils). The comparative performance of this model was identical with the other tested models. The results indicated that this type of coating thickness variation did not adversely affect the thermal performance of the material.

In addition, three test models 3-1/2 in. by 3-1/2 in. by 2 in. thick, representing the LI-1545 (LI-1500 with 0045 coating) and the LI-0942 (LI-0900 with the 0042 coating) materials, were exposed to identical 32-cycle thermal testing at 2500° F. Results of these tests showed that the test models performed equally as well as did the LI-0945 test models. The evaluation indicates that LI-0900 and LI-1500 materials with either 0045 or 0042 coating systems perform satisfactorily in simulated thermal cyclic environments. The model identification and the results are presented as follows:

Model No.	Material	Shrinkage (%)
TT101-9	LI-1545	0.1
TT101-13	LI-0942	<0.1
TT101-30	LI-1545	–

Water-resistant properties of LI-0900 with 0045 coating were determined under simulated rain environments. Two specimens of LI-0900 3-1/2 in. by 3-1/2 in. by 1 in. thick were coated on five sides with 0045 coating. These specimens were bonded to an aluminum substrate with RTV-560 silicone adhesive. The samples were exposed to simulated rain of 1 in./hr for a period of 1 hr, to determine the imperviousness of the coating. The 0045 coating system demonstrated excellent water-repellent characteristics in the simulated rain environment. The results of the testing are as follows:

Specimen No.	Original Weight (gm)	After-Rain Exposure Weight (gm)	Weight Change (%)
1	49.10	49.13	0.06
2	49.80	49.83	0.06

3.7.3 LMSC RSI Batch-to-Batch Reproducibility

Since a comparatively limited final production run for this Material Improvement Program was made, the 6-month production of the LI-1500 material for the companion Contract NAS 9-12083 (TPS Development) was monitored and analyzed for reproducibility. Utilizing this analysis as a comparison medium, similar surveillance and analysis of the limited final production of LI-0900 for the Material Improvement Program, as well as for material produced for the LMSC IRAD program, were also conducted.

The material for Contract NAS 9-12083 was produced in the LI-1500 manufacturing facility devoted exclusively for the fabrication of RSI materials. The LI-1500 manufacturing sequence is illustrated by the following flow diagram. Each manufacturing sequence is carefully monitored, controlled and documented.

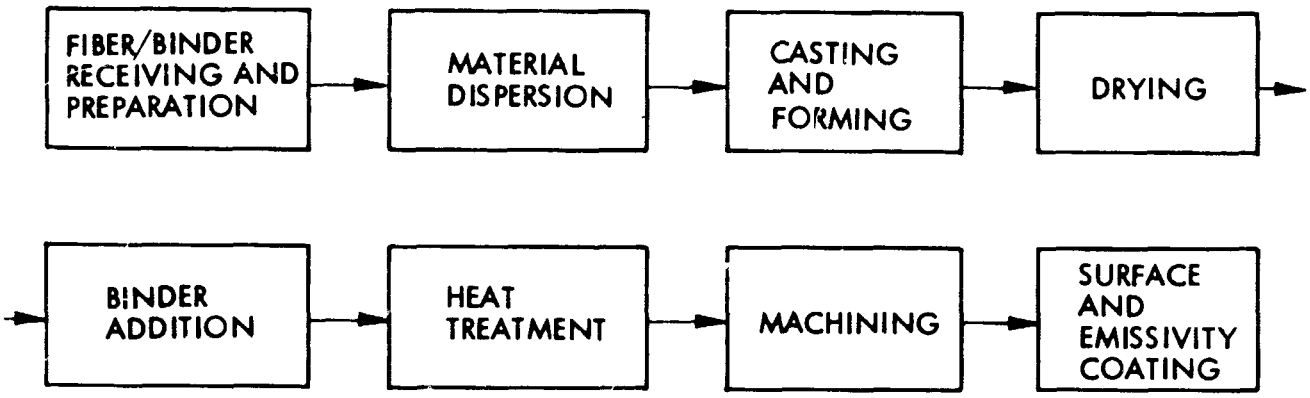

LI-1500 Manufacturing Sequence

For Contract NAS 9-12083, 82 standard (12- by 12- by 2-in.) LI-1500 panels were used from 7 process lots manufactured. Results of the monitoring and analysis are as follows:

Process Lot No.	2085	2087	2088	2091	2096	2097	2098	Avg.
Fiber Analysis								
Percent SiO_2	99.54	99.62	99.54	99.50	99.33	99.55	99.49	99.51
Percent Ash	0.46	0.38	0.46	0.50	0.67	0.45	0.51	0.49
Hot Stage X-Ray Diffraction	← See Fig. 3.7.4-2 →							
LI-1500 Panel								
Density, lb/ft^3	14.2 ±1.2	14.0 ±0.5	13.0 ±0.6	13.9 ±0.5	14.7 ±0.3	14.5 ±0.4	14.7 ±0.6	14.1 ±0.6
Avg. Density of 82 Panels	← 14.1 lb/ft^3 →							
Δ Dimensions, % (a)	±2.5	±2.7	±2.6	±1.8	±1.9	±2.9	±2.4	±2.1
Crystallinity (b)	← None →							

(a) 2500° F Furnace Control Tests; Deviation from the Lot mean shrinkage value.

(b) X-Ray Diffraction Analysis after 4 hr at 2300° F exposure

Results of the Hot Stage X-Ray Diffraction Analysis are presented in Fig. 3.7.4-1. The test procedures were previously described in Section 3.2.1. The analyses for Lot Nos. 2084, 2086, and 2089 are also included.

To fulfill contractual requirements, various specimens were prepared from the individual fabricated LI-1500 panels. During this preparation, the densities of the individual machined specimens were monitored as relatable to the particular manufactured LI-1500 panel from which they were machined. Typical results were as follows:

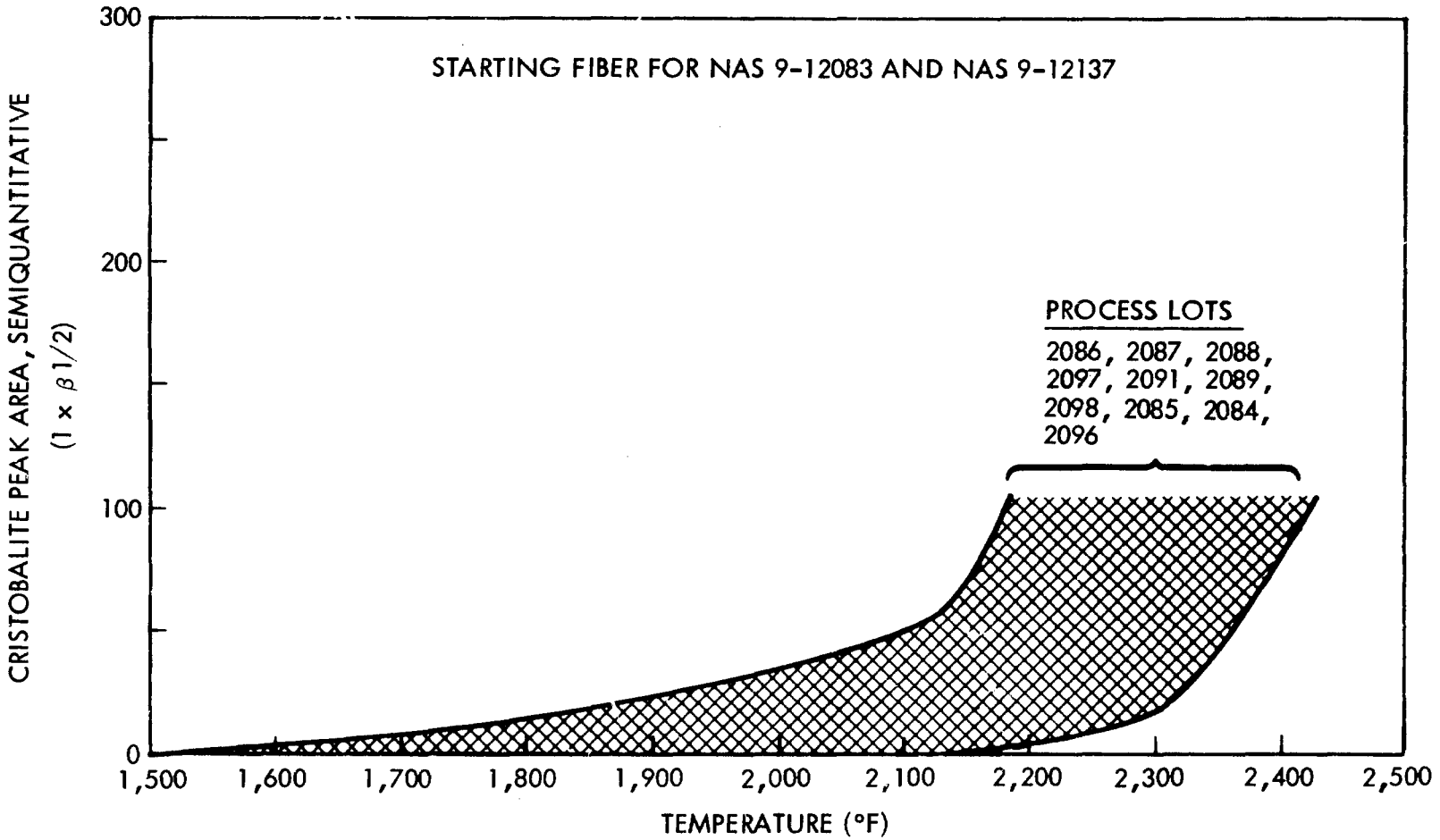

Fig. 3.7.4-1 Hot-Stage X-Ray Diffraction Analysis

No. of Specimens [a]	Density (lb/cu ft)
65	14.0 ±0.6
45	13.8 ±0.4
42	14.2 ±0.6
38	14.2 ±0.6
26	13.6 ±0.6
12	14.7 ±0.1
12	14.9 ±0.1

(a) Number of specimens machined from one panel

For the NAS 9-12083 program, 15 12- by 12- by 2-in. thick LI-1500 tiles coated with the LI-0042 surface coating and treated with the LI-007 water-repellent system were prepared and delivered. The density range of these finished tiles was 16.3 ±1.2 lb/cu ft.

Monitoring and analysis of production for the NAS 9-12083 Contract has indicated that batch-to-batch, as well as within-individual-panel, reproducibility of the LI-1500 material can be achieved.

For this Material Improvement Program and also to determine the reproducibility of LI-0900 and the material needs to support LMSC IRAD programs, production of 23 panels produced from three process lots was monitored. Results of the analysis are as follows:

Process Lot No.	2084	2086	2089	
Fiber Analysis				
Percent SiO_2	99.71	99.52	99.62	Avg. 99.62
Percent Ash	0.29	0.48	0.38	Avg. 0.38
Hot Stage X-Ray Diffraction	See Fig. 3.7.4-1			
LI-0900 Panel				
Density, lb/ft^3	8.5 ±1.4	8.8 ±0.2	8.5 ±1.0	
Average Density of Panel	← 8.6 lb/ft^3 →			
Crystallinity (4 hr 2,300°F)	← None →			

The various specimens were also prepared from the individual fabricated LI-0900 panels to support the evaluation efforts. During this preparation, the densities of the individual machined specimens were monitored as they related to the particular manufactured LI-0900 panel from which they were machined. Typical results were as follows:

No. of Specimens[(a)]	Density (lb/cu ft)
8	9.4 ± 0.1
8	9.0 ± 0.5
32	8.9 ± 0.6
3	7.9 ± 0.2

(a) Number of specimens machined from one panel

Monitoring and analysis of the material produced has indicated that batch-to-batch, as well as within-individual-panel, reproducibility of LI-0900 material may be achieved.